TOPICAL LIPOSOME FORMULATIONS OF HYDROXYZINE AND CETIRIZINE: EVALUATION OF THE PHYSICOCHEMICAL CHARACTERISTICS AND STABILITY, AND THE PERIPHERAL H_1-ANTIHISTAMINIC ACTIVITY AND SYSTEMIC ABSORPTION IN A RABBIT MODEL

By

ABEER ELZAINY

A THESIS SUBMITTED TO THE FACULTY OF
GRADUATE STUDIES
IN PARTIAL FULFILLMENT OF THE REQUIREMENTS FOR THE
DEGREE OF
DOCTOR OF PHILOSOPHY

FACULTY OF PHARMACY
UNIVERSITY OF MANITOBA
WINNIPEG, MANITOBA, CANADA

October 1st, 2004

THE UNIVERSITY OF MANITOBA

FACULTY OF GRADUATE STUDIES

*****

COPYRIGHT PERMISSION

TOPICAL LIPOSOME FORMULATIONS OF HYDROXYZINE AND CETIRIZINE: EVALUATION OF THE PHYSICOCHEMICAL CHARACTERISTICS AND STABILITY, AND THE PERIPHERAL H_1-ANTIHISTAMINIC ACTIVITY AND SYSTEMIC ABSORPTION IN A RABBIT MODEL

BY

ABEER ELZAINY

A Thesis/Practicum submitted to the Faculty of Graduate Studies of The University of Manitoba in partial fulfillment of the requirement of the degree

Of

DOCTOR OF PHILOSOPHY

ABSTRACT

The objectives of this study were to evaluate peripheral H_1-antihistamine efficacy, and systemic absorption after application of liposome formulations containing hydroxyzine or cetirizine to the skin of a rabbit model and to evaluate the physicochemical stability of these liposome formulations containing hydroxyzine or cetirizine. Using L-α-phosphatidylcholine (PC), L-α-phosphatidylserine (PS), and L-α-phosphatidylcholine hydrogenated (HPC) and hydrating buffers pH 5.0-7.0, small unilamellar (SUV), HPC-SUV and multilamellar (MLV) vesicles containing hydroxyzine or cetirizine were produced by ethanol injection, extrusion, and thin-lipid film hydration methods, respectively. PC-MLV were subjected to hydration times of 1h, 24h, and 48h as well as five cycles of freeze-thawing. Liposomes freshly prepared and stored for up to 24 months at 10±2°C, 25±3°C, 37±0.1°C were evaluated by determining percent entrapment of hydroxyzine (PETH) or cetirizine (PEC), by checking the physical appearance, by determining particle size, and by taking transmission electron micrographs (TEM) and optical micrographs (MOM). For *in vivo* evaluation each liposome formulation and Glaxal Base (GB), the control, containing 10 mg of hydroxyzine or cetirizine was applied to the shaved backs of rabbits (3.08 ±0.05 kg) then intradermal tests with 0.05 ml histamine phosphate (1mg/ml), and blood sampling were performed before application, and at pre-selected times for 24 h. Wheal suppression was calculated and hydroxyzine and cetirizine plasma concentrations were measured. Based on the percent entrapment of 90%, physical appearance and TEM, HPC-SUV, and HPC-MLV at pH 6.5, were the most stable liposomal formulations. Hydroxyzine or cetirizine SUV and MLV for *in vivo* testing were prepared at pH 6.5 using PC and HPC. Compared with baseline, hydroxyzine from all formulations significantly suppressed histamine-induced wheal formation by 75% to 95% for up to 24 hours. The areas under the plasma hydroxyzine concentration versus time curve (AUC) from PC-SUV and PC-MLV, 80.1 ± 20.8 and 78.4 ± 33.9 ng.h/mL, respectively, were lower than that from GB, 492 ± 141 ng.h/mL, $P \leq .05$, over 24 hours, while concentrations of cetirizine from hydroxyzine in all formulations were similar. After 24h, only 0.02% to 0.06% of the initial hydroxyzine dose remained on the skin. Compared to baseline, histamine-induced wheal formation was suppressed by cetirizine in PC-SUV and PC-MLV from 0.5-24 h in HPC-SUV only at 24 h, in HPC-MLV from 0.5-24 h and by cetirizine in GB from 0.5-8 h, $p \leq 0.05$. Maximum wheal suppression by cetirizine in PC-SUV and PC-MLV ranged from 90.6 ± 4.9 % to 89.0 ± 3.8 % and 98.0 ± 1.3 % to 94.0 ± 2.3 % respectively from 6-8 h and in HPC-SUV at 24 h, 91.7±5.2 %, and in HPC-MLV from 1 to 24 h, 93.8±2.2 to 76.2±6.5 %, greater than in GB, 36.5±7.4 to 60.6±14.2 %, from 1h to 24 h, $p \leq 0.05$. The plasma cetirizine AUC from HPC-SUV, 67± 5.2 ng.hr/mL, was lower than from PC-SUV, 201± 24.2 ng.hr/mL, from PC-MLV, 334.6 ± 65.1 ng.hr/mL, from HPC-MLV, 221.2 ± 42.3 ng.hr/mL, and from GB, 248.3 ± 34.6 ng.hr/mL. After 24 h, the percent of the cetirizine dose remaining on the backs of the rabbits from HPC-SUV was significantly lower than from both HPC-MLV and GB, $p \leq 0.05$. In this rabbit model, hydroxyzine or cetirizine from PC-SUV, PC-MLV, and cetirizine from HPC-MLV result in excellent topical H_1-antihistamine effects with accompanying low plasma concentrations. These results suggest that the liposome formulations appear to localize hydroxyzine or cetirizine in the skin thus reducing the potential for systemic adverse effects. These results will need to be confirmed in patients with allergic skin conditions.

ACKNOWLEDGEMENTS

I would like to thank Dr. Keith J. Simons for assistance in designing this research and for his patience, encouragements, and supervision during the completion of my thesis. I am also grateful to Dr. Estelle Simons, Department of Pediatrics, and Faculty of Medicine for kindly reading several publications from my thesis and offering many helpful criticisms.

I would like to express my thanks also to Dr. X. Gu at the Faculty of Pharmacy, University of Manitoba, for his help during the completion of this thesis, and my advisory committee Dr. Estelle Simons, Dr. A. McIntosh, Dr Colin Briggs, Dr. Frank Burczynski at the Faculty of Pharmacy for their scientific suggestions. I would like to express my thanks to Dr. Marianna Foldvari, Professor at College of Pharmacy, University of Saskatchewan for reading my thesis.

I owe my profound gratitude and special thanks to my husband A. Halim Elamy, M.Sc., (Computer Engineering) for his assistance with the computer analysis and my parents and my children who have been a source of moral support throughout the course of this research work. I would like to thank Viventia Biotec Inc., for measuring the particle size of the liposomes.

My graduate research training would not have been possible without the award of University of Manitoba Fellowship and the Manitoba Health Research Council Graduate Studentship. I would like to extend my thanks to Success Skills' Center for Altrusa International of Winnipeg award and Parke-Davis Company for the valuable award that I have received during my study. This study was funded by a grant from Pfizer USA.

CONTENTS

LIST OF TABLES

LIST OF FIGURES

GLOSSARY

AUC	Area under the plasma concentration versus time curve
C.V.	Coefficient of variation
CH	Cholesterol
GB	Glaxal Base
HPC	Egg L-α-phosphatidylcholine hydrogenated
HPC-MLV	Multilamellar vesicles prepared using egg L-α-phosphatidylcholine hydrogenated
HPC-SUV	Small unilamellar vesicles prepared using egg L-α-phosphatidylcholine hydrogenated
HPLC	High performance liquid chromatography
J028	[(2-{2-[4-(diphenylmethylene)-1-piperidinyl] ethoxy} ethoxy) acetic acid chorhydrate] used as the internal standard for HPLC analyses of cetirizine
MLV	Multilamellar vesicles
MOM	Micrographs from an optical microscope
PC	Egg L-α-phosphatidylcholine
PC-MLV	Multilamellar vesicles prepared using egg L-α-phosphatidylcholine
PC-SUV	Small unilamellar vesicles prepared using egg L-α-phosphatidylcholine
PEC	Percent entrapment of cetirizine

PETH	Percent entrapment of hydroxyzine
PL	Phospholipids
PS	L-α-phosphatidylserine (brain- sodium salt)
PS-MLV	Multilamellar vesicles prepared using L-α-phosphatidylserine (brain- sodium salt)
PS-SUV	Small unilamellar vesicles prepared using L-α-phosphatidylserine (brain- sodium salt)
S.D.	Standard deviation
SEM	Standard error of the mean
SUV	Small unilamellar vesicles
TEM	Transmission electron micrograph

CHAPTER 1. INTRODUCTION

In the scientific and medical literature, percutaneous absorption usually refers to the local effects produced by medications applied topically to the skin to treat skin disorders (1, 2). Transdermal absorption is generally defined as the mass movement of substances from the skin surface to the systemic circulation in order to treat systemic diseases (3).

The percutaneous route for medication administration has many advantages over other pathways. The hepatic first-pass effect, a systemic complicating factor of oral absorption for treatment of skin disorders, is avoided. There is also reduced potential for adverse effects and medication interactions often observed between medications in the systemic circulation.

The selection of the optimal percutaneous formulation or medication delivery system is important because it must overcome the barrier functions of the skin which inhibit the penetration of most medications while allowing the medications to be retained in the dermal layers (4). The delivery of medications by percutaneous absorption for the relieving allergic skin disorder symptoms using liposomes as a medication delivery system will be evaluated.

1.1. PERCUTANEOUS ABSORPTION

Factors affecting percutaneous absorption and distribution include: the relationship between the structure and the barrier function of the skin; the mechanisms and route of skin penetration of medications applied to the skin and; the major physiological, physicochemical and formulation factors influencing percutaneous absorption (4).

1.1.1. Structure and Function of the Skin

The human skin provides an excellent barrier both for controlling the loss of water and body constituents, and for preventing the entry of noxious substances from the external environment. Human skin is a heterogeneous membrane, which consists of three distinct layers: the epidermis, the dermis, and the subcutaneous fat (5).

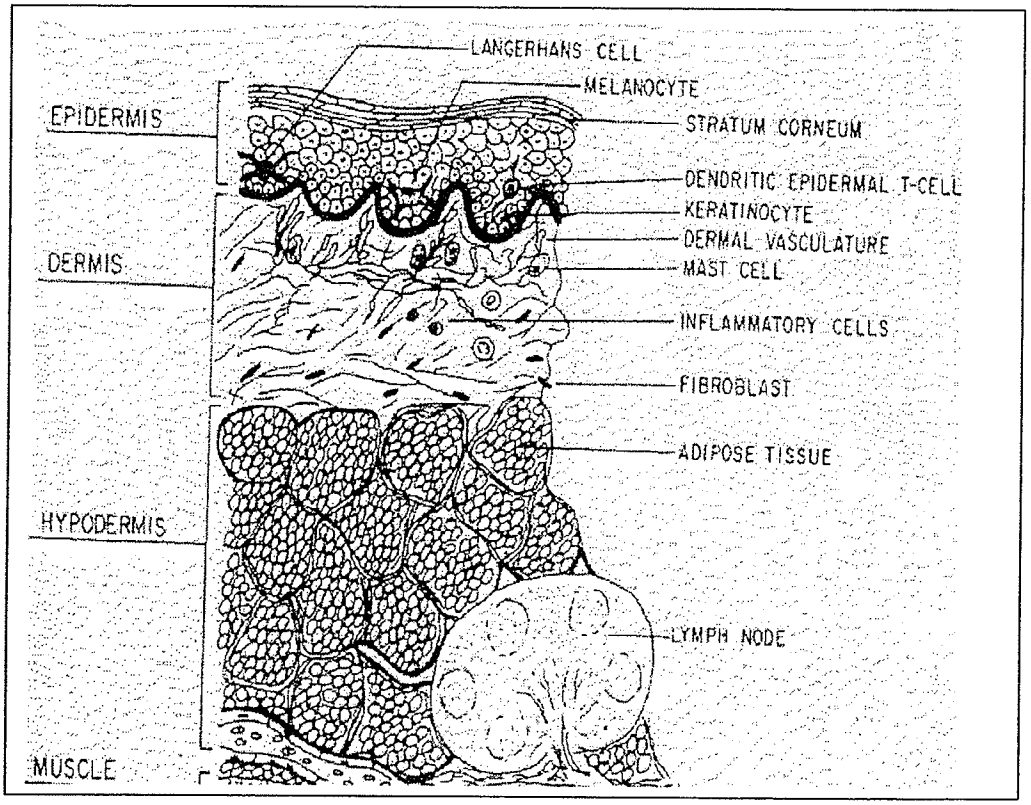

Figure 1: Schematic representation of histological cross-section of the skin. (From Ref. 6)

1.1.1.1. Epidermis

The epidermis consists of the stratum corneum and the viable epidermis layers. The stratum corneum, the non-viable epidermis, is the outermost layer of the skin and is recognized as the principal barrier to water loss and to entry of external environmental agents. It is a multicellular, metabolically inactive cornified dead tissue layer derived from previously viable epidermal cells. Each stratum corneum cell, called a corneocyte, is composed of 70% insoluble bundles of keratines, and 20% lipids encased in a cell envelope. The intercellular spaces, comprised mainly of lipids including ceramides, cholesterol, cholesterol esters, and free fatty acids, are structured in multilamellar bilayers at the physiological temperature of 37°C, which is below the gel–to-liquid crystalline phase transition temperature for these compounds. Desmosomes for corneocyte adhesion are also present. The stratum corneum layer is described as the rate–limiting barrier of the skin protecting the viable epidermis and the dermis (5, 7). The viable epidermis, below the stratum corneum, includes the stratum granulosum, the stratum lucidum, the stratum spinosum, and the stratum germinativum. It is different from the stratum corneum since it is physiologically more closely akin to other living cellular tissues and contains many metabolizing enzymes.

The viable epidermis has many functions including the generation of the stratum corneum and the metabolism of many foreign substances, and it also contains the Langerhan's cells, which are involved in the immune response of the skin (5, 7).

1.1.1.2. Dermis

The dermis is composed of a semi-gel matrix of mucopolysaccharides. This matrix is a dense network of structural protein fibers containing mainly collagen, elastin, and reticulum. The dermis is penetrated by hair follicles with the sebaceous glands, and eccrine and apocrine sweat glands and has a very rich nerve fiber and blood supply which provides the entire body with temperature, pressure and pain regulating mechanisms (5).

1.1.1.3. Subcutaneous Fatty Tissue

The subcutaneous fatty tissue located below the dermis, is composed of cells that contain large quantities of fat, making the cytoplasm lipoidal in character. The collagen between the fat cells provides the linkage of the epidermis and the dermis with the underlying structures of the skin. The main function of subcutaneous fatty tissue is to act as a heat insulator and a shock absorber (8).

1.1.1.4. Reservoir and Barrier Functions of the Skin

The stratum corneum is considered to be the main reservoir for many medications applied topically to the skin, due to its morphological structure and the resulting barrier function (9-11). Sheth *et al.*, (12) have evaluated the medication reservoir function of the stratum corneum to predict the therapeutic efficacy of topical iododeoxyuridine for herpes simplex virus infections.

1.1.1.5. Enzymes and Metabolic Functions in the Skin

The skin is an important portal of entry for xenobiotics or foreign substances, either applied intentionally or as a result of exposure to the

environment. The metabolizing enzymes in the skin convert xenobiotics into polar metabolites, facilitating their body clearance. The skin contains many metabolizing enzymes similar to those initially identified in the liver. The transferase activities in the skin can approach 10 % of that found in the liver, while in comparison, the relative activity of cytochrome P-450 enzymes in the skin may be only 1-5 % of the liver's capacity (13). The metabolizing enzymes in the skin can catalyze Phase-I reactions including oxidation, reduction, and hydrolysis and Phase-II reactions such as glucuronidation, and sulfation.

Cytochrome P-450 enzymes in the skin have been shown to metabolize a broad range of compounds such as corticosteroids and theophylline (14-16). As well, the hydrolase enzyme found in the skin contributes to the metabolism of benzoyl peroxide, diflucortolone valerate and vidarabine (13).

Glucuronidation and sulfation require the presence of the cofactors, uridine diphosphate-glucuronic acid and adenosine 3'-phosphate 5'-phosphosulphate respectively, which are also present in the skin (13). Higo *et al.*, (17, 18) have studied the cutaneous metabolism of nitroglycerin to 1,2-glyceryl di-nitrate and 1,3- glyceryl di-nitrate in the skin. This metabolism was heavily dependent on the presence of glutathione, the cofactor for the transferase enzyme.

1.1.2. Mechanism and Route of Skin Penetration

The process of percutaneous absorption of medication molecules applied to the skin surface consists of an initial distribution or partitioning of the molecules into the stratum corneum and subsequent passive diffusion through

the different layers of the skin. Three routes of medication penetration across the stratum corneum have been proposed (Figure 2).

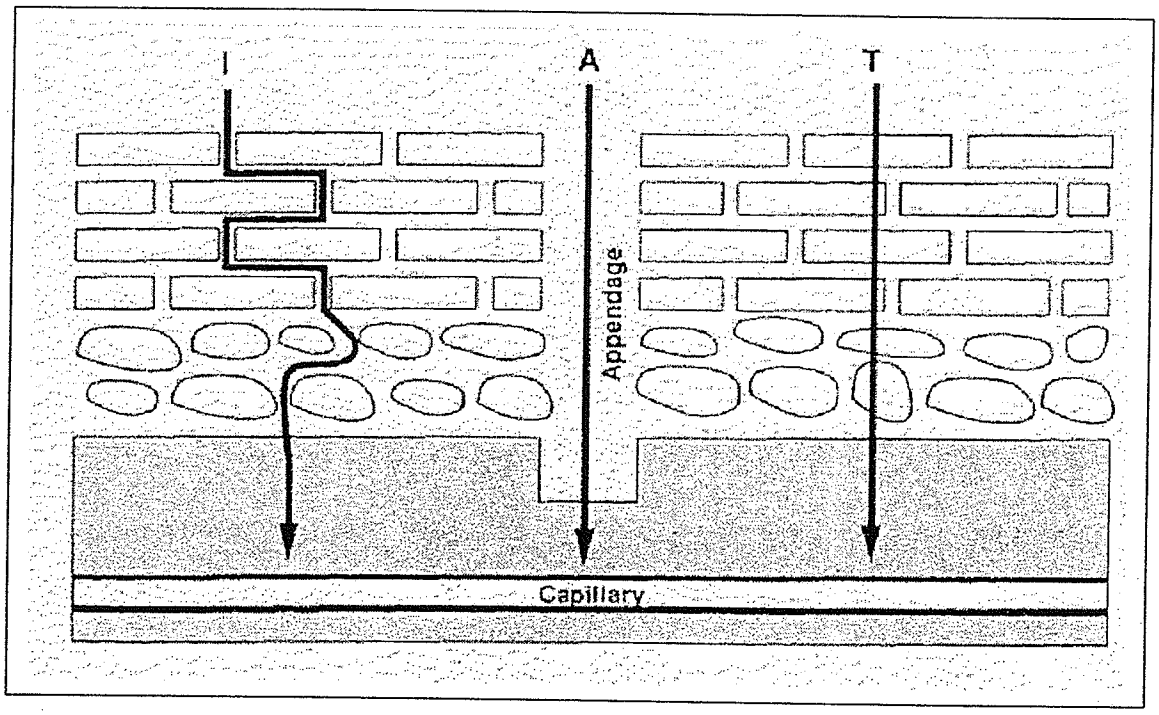

Figure 2: Schematic diagram of the potential routes of medication penetration through the stratum corneum of human skin. I= intercellular, T=transcellular, A=appendageal. (From Ref.19)

The first route of medication penetration is the transcellular route by which the permeant molecules cross the epidermis by the most direct routes of diffusion or partition, and then repeatedly partition between, and diffuse through, the cornified cells of the stratum corneum and the intercellular bilayers. This route is considered the most difficult route of medication penetration because the molecules have to pass from hydrophilic to hydrophobic layers across the epidermis and dermis.

The second route of medication penetration is the intercellular route where the solute remains in the lipid domains and permeates via a tortuous pathway between the cornified cells of the stratum corneum, the viable epidermis and dermis. Within this lipid domain, the medication has to repetitively cross complete multilamellar bilayers of lipids. This route is considered the primary route of medication penetration because the hydrophobic molecules easily pass through the hydrophobic layers of the intercellular bilayers.

The third route of medication penetration is the appendages route. Here, the penetrant substances traverse the stratum corneum via a "shunt" pathway by using the hair follicles or sweat glands. It has been suggested that the contribution of the hair follicles to percutaneous absorption considerably outweighs that of the sweat gland because of the relatively higher density of hair follicle distribution (19). In contrast, it has been stated that the extent of medication absorption via the "shunt" pathway, although it may occur, is insignificant, because the absorption is against the outward flow of the sweat and body secretions. In addition these orifices occupy only 1% of the body skin surface area (20). Other authors (21) reported that the available surface area for follicular transport is limited on most sites of the body, to approximately 0.1 % of the total skin area. However it has also been demonstrated that the "shunt " pathway contributed significantly to the initial phase of stratum corneum permeation (21) and furthermore, results from recent experiments using an afollicular animal model have shown a significant role for the follicular route of transport (21). The extent of the role of the "shunt" pathway is still controversial.

1.1.3. Factors Affecting Percutaneous Absorption

The diverse chemical composition of the skin makes the percutaneous absorption of xenobiotics or medications into the skin a series of complex biological processes. The skin is a multi-layered bio-membrane with each layer demonstrating unique absorption properties. There are three major factors that have been shown to influence the percutaneous absorption of medications or substances applied to the skin. These factors are the physiology of the skin, the physicochemical properties of medications applied to the skin, and the individual components of the formulations used to deliver medications applied to the skin.

1.1.3.1. Physiology of the Skin

The role of the skin physiology is very important when studying the percutaneous absorption of medications applied to the skin. The most important physiological factors influencing the percutaneous absorption of medications applied to the skin are: the degree of skin hydration and skin temperature, skin integrity, the participants' age, and the location of the skin site on the body.

The degree of skin hydration and skin temperature are inter-dependent factors. Any situation or treatment that increases the skin temperature also increases skin hydration. For example, the application of occlusive dressings or oleaginous ointment bases increases both the skin temperature and the degree of skin hydration, which subsequently enhances the penetration of many medications into the stratum corneum (22, 23). It was found that a hydrocolloid

patch occlusion increased the penetration of triamcinolone acetonide through skin in man 3-4-fold relative to that when no occlusive patch was used (24). The rate of percutaneous penetration of different medications into the skin may also increase as the environmental temperature and humidity increase (25). The increase in environmental humidity was observed to increase the degree of skin hydration and dramatically increase the total percutaneous absorption of the pesticide propoxur from 33 % to 63 % (26).

The stratum corneum layer of the epidermis is a major barrier to percutaneous medication absorption. Any conditions such as inflammation or dermatitis of the skin that alter the structure or function or damage the integrity of the stratum corneum result in an increase in percutaneous absorption (25).

Participants' age is an important factor that controls the body surface area to weight ratio, as well as the hydration, permeability, thickness and texture of the skin. The body surface area to weight ratio of a neonate is three to four times that of adults. The greater degree of skin hydration and the neutral skin surface pH of infants might contribute to the increased permeability of neonatal skin compared to adult skin (27-29).

Morphological and physiological changes in aged skin may affect the percutaneous absorption of compounds and thus their potential for localized as well as systemic activity. The stratum corneum, the least permeable layer of the skin, is well developed in a normal adult, and forms the rate-limiting barrier to most medications applied topically to the skin. The thickness of the stratum corneum of elderly individuals, over the age of 60, remains unaltered compared

with young adults, although there are reports of a slight decrease in the thickness of the viable epidermis. There are, however, alterations in the dermo-epidermal junction, in the blood vessels, and in other parts of the skin, which suggest that dermal clearance of the medication is more likely to be decreased with age (30).

The extent of percutaneous absorption largely depends on the thickness and permeability of the intact stratum corneum at the absorption site (30). Percutaneous absorption in man and animals varies depending on the area of the body surface to which the chemical has been applied. This is called *regional variation*. Scopolamine transdermal systems are designed to be applied to the post-auricular area, because the percutaneous absorption of this skin region is suitable to permit effective quantities of the medication to be absorbed (31). It was found that the highest total absorption of topical steroids in an ointment vehicle was through skin of the scrotum while the lowest absorption was through the nails (25).

1.1.3.2. Physicochemical Properties of the Medication

Passive percutaneous delivery of medications depends on several factors, including medication lipophilicity, charge, and molecular size. The molecular size of medications that can be absorbed percutaneously without penetration enhancer has to be less than 500 Dalton.

The percutaneous absorption of medications also depends on many physicochemical characteristics of medication molecules applied to the skin, including molecular weight, the degree of ionization, and the particle size and

shape of the medication powder. Ionized molecules do not have sufficient free energy for transfer from the aqueous phase of the vehicle to the lipid phases of the membrane. Thus, the fraction of medication in the unionized state existing in the topical dosage formulation may determine the effective membrane gradient for ionizable medications. (32-34).

The physicochemical properties of medications influence solubility, partition coefficients and stratum corneum-water partition coefficients, and permeability constants. These parameters may affect the rate and extent of medication penetration into the skin (32-34).

The physicochemical properties of medications influence the interactions between the medications and the vehicle that contains and delivers these medications, and the interactions between the medications and the skin. Subsequently, these interactions may influence the rate and extent to which medications penetrate the skin (32-34).

The solubility of a medication in a vehicle determines the amount of medication which can be presented to the absorption site per mass of delivery system. The octanol-water partition coefficient of the medication strongly influences the rate at which the medication is released from the vehicle and controls the rate of diffusion of the medication into the stratum corneum. The octanol-water partition coefficient by itself will give only a limited indication as to whether or not a compound will be absorbed into the human skin. For example, the percutaneous absorption is essentially the same for testosterone, 13.2 %,

and for haloprogin, 11 %, although these compounds have completely different partition coefficients of 1.81 and 45.4 respectively (32-34).

Consideration of both the octanol-water partition coefficient and the permeability coefficient of a compound applied to the human skin provide a better prediction of the rate and extent of percutaneous absorption. For example, in a series of polyhalogenated aromatic hydrocarbons, as permeability coefficients decreased, the octanol-water partition coefficients and the stratum corneum-water partition coefficients decreased (32-34).

The medication-vehicle interaction may enhance or restrict the rate of diffusion of the medication from the vehicle onto the skin surface. This in turn will affect the rate of diffusion of the medication across the stratum corneum. The influence of various lipophilic and hydrophilic vehicles on the epidermal permeation of benztropine free base and its mesylate salt were studied *in vitro* using human cadaver skin membranes. The lipophilic vehicles were a mixture of mineral oil and isopropyl myristate and hydrophilic vehicles were alkanol-isopropyl myristate mixtures. Alkanol was one of the following solvents ethanol, isopropyl alcohol, tertiary butanol, propylene glycol, or polyethylene glycol 400. Benztropine base was found to be highly permeable through human cadaver skin membranes *in vitro* when delivered from lipophilic solvents such as isopropyl myristate and mineral oil. Benztropine mesylate was found to be highly permeable through human cadaver skin membranes by the alkanol- isopropyl myristate mixtures or binary vehicles. This was probably as a result of a combination of decreasing barrier ability of the stratum corneum by the binary

vehicles and moderately partitioning benztropine mesylate through the viable epidermis/dermis (35).

1.1.3.3. Formulation of Topical Dosage Forms

The composition of topical dosage formulations applied to the skin may affect the degree of skin hydration, skin temperature, and the integrity of the stratum corneum.

1.1.3.3.1. Effect of Medication Vehicle

The medication vehicle is the carrier used to deliver the medication into the skin (36). In Table 1 are listed the theoretically expected effects of common vehicles on skin hydration and subsequently, on skin permeability.

Table 1: Theoretically Expected Effects of Common Vehicles on Skin Hydration and Skin Permeability. (From Ref. 37).

VEHICLE	EXAMPLES/ CONSTITUENTS	EFFECT ON SKIN HYDRATION	EFFECT ON SKIN PERMEABILITY
Occlusive dressing	Imperforated waterproof plaster	Prevents water loss; full hydration	Marked increase
Lipophilic	Paraffin, oils, fats, waxes, fatty acids, alcohol, esters, silicones	Prevents water loss; may produce full hydration	Marked increase
Absorption base	Anhydrous lipid material and water/oil emulsifiers	Prevents water loss; marked hydration	Marked increase
Emulsifying base	Anhydrous lipid material and oil/water emulsifiers	Prevents water loss; marked hydration	Marked increase
Water/oil emulsion	Oily creams	Retards water loss; raised hydration	Increase
Oil/water emulsion	Aqueous creams	May donate water; slight hydration increase	Slight increase
Humectants	Water-soluble bases, glycerol, glycols	May withdraw water; decreased hydration	Can decrease or act as penetration enhancer (38)
Powder	Clays, organics, inorganics, "shake" lotions	Aid water evaporation; decreased excess hydration	Little effect on stratum corneum

1.1.3.3.2. Effect of Penetration Enhancers

Penetration enhancers, also called sorption promoters or accelerants, play an important role in reducing the skin barrier integrity of the stratum corneum. Penetration enhancers have the ability to increase medication permeability into the skin by causing reversible damage to the stratum corneum at many potential sites and by many mechanisms. Some of the penetration enhancers act on the intercellular lipid matrix and may cause disruption of the packing motif of the intercellular lipid matrix. The drastic penetration enhancers act on the intracellular keratin domains of the stratum corneum corneocytes or damage desmosomal connections between the corneocytes. Further potential mechanisms of action, include the enhancers acting on or altering metabolic activity within the skin, or the enhancers exerting an influence on the thermodynamic activity/solubility of the drug in its vehicle, or the enhancers acting as a cosolvent. The cosolvent effects increase the thermodynamic activity of medications applied to the skin and increase their partition coefficients into the tissue by acting as a solvent for the permeant within the membrane thus promoting their release from the vehicle into the skin (38, 39).

Numerous types of penetration enhancers which have been evaluated include sulphoxides (such as dimethylsulphoxide, DMSO), Azones (such as laurocapram), pyrrolidones (such as 2-pyrrolidone, 2P), alcohols and alkanols (ethanol, or decanol), glycols (such as propylene glycol, a common excipient in topically applied dosage forms), surfactants (also widely used in dosage forms), and terpenes (38, 39).

Those penetration enhancers which have the ability to damage or alter the barrier nature of the stratum corneum in such a way that the diffusion resistance is reduced, possibly due to removal of intercellular lipids, produce holes or artificial shunts. These artificial shunts in the stratum corneum allow the medications or compounds to penetrate at a faster rate than through the intact stratum corneum. These drastic penetration enhancers such as acids, and phenols have an irritating effect on the skin. Also some organic solvents, such as benzene, ether, alcohol, cyclohexane and a mixture of cyclohexane and ethanol, which have been reported to increase the permeability of a number of water- and lipid-soluble medications by alteration of the barrier resistance of the stratum corneum, subsequently enhance the percutaneous absorption of both types of medications (40-43).

The most common, mildest penetration enhancer is water that enhances the permeation of most polar and nonpolar compounds. Water has the ability to increase the absorption of medications by increasing the hydration of the skin consequently improving the penetration of the medication through the stratum corneum.

Some recent "biochemical enhancers" specifically inhibit enzymes that synthesize the stratum corneum lipids. Inhibition of the enzymatic process causes the barrier of the stratum corneum to be opened for relatively long periods of time, and increases the permeability of medications such as lidocaine applied topically to the human skin (44-47).

Phospholipids can occlude the skin surface and thus can increase tissue hydration, which, as shown above, can increase drug permeation. When applied to the stratum corneum as vesicles, phospholipids can fuse with stratum corneum lipids. This collapse of structure liberates permeant into the vehicle in which the drug may be poorly soluble and hence thermodynamic activity could be raised, facilitating drug delivery. Phospholipids, may become incorporated into the intercellular matrix of the stratum corneum modifying its fluidity and permeability and altering the lipid crystallinity. It was reported that liposomes prepared using phospholipids facilitated the penetration of many medications such as insulin, diclofenac and melatonin (46- 49).

1.2. Liposomes:

1.2.1. Definition of Liposomes

Liposomes are closed vesicles of phospholipid bilayers or lamellas with an entrapped aqueous core that are able to encapsulate medications. They consist of single or multiple lamellas and can range in size from as small as 20 nm to as large as 20 μm. Liposomes are divided into two major classes based on the number of lamellas in their structure. Multilamellar vesicles (MLV) consist of five or more lamellas, and their size ranges from 100 nm to 20 μm. Unilamellar vesicles, containing a single bilayer, are subdivided into small unilamellar vesicles (SUV, <100 nm) and large unilamellar vesicles (LUV, 100-1000 nm) (50). These liposomes can encapsulate water-soluble drugs in their aqueous spaces and lipid-soluble drugs within the lamellas themselves (51).

1.2.2. Liposomes as Skin Delivery Systems

Liposomal encapsulation of drugs represents a method of drug delivery that appears to offer important therapeutic advantages over existing methods of drug delivery. There are many advantages to the use of liposomes to administer medications topically to the skin for the treatment of peripheral medical conditions. Liposomes, as a medication delivery system, have been shown to facilitate the transport and localization of the medications into the skin (52 - 54). The application of medication-loaded liposomes onto the skin may yield higher peripheral therapeutic effects from the medications and permit less frequent application, consequently lowering systemic toxic effects or adverse effects. Liposomes cause minimal or no irritation to the skin compared to other penetration enhancers, act as moisturizing agents, and form occlusive films, which lead to increased skin hydration and subsequently, increased medication penetration (55-57). Liposome-encapsulated ursolic acid increases ceramides and collagen content in human skin cells (58). Liposomes moisturize and hydrate the skin by contributing lipids to the stratum corneum (55, 59).

Price *et al.*, (60, 61) found that the liposomes of aminoglycoside antimicrobials for treatment of infectious burns, and tobramycin containing liposomes for treatment of soft tissue wounds, sustained tissue levels and permitted less frequent application.

A number of investigators (62-67) reported that dermal drug delivery by liposome encapsulation altered the structure of the human stratum corneum and favorably enhanced penetration of topically applied medications on the skin.

Ferreira *et al.*, (68) found that the application of liposomal entrapped paromomycin resulted in localization of the medication at the site of application with low systemic availability. El-Rudy and Khalil (69) found that encapsulation of lignocaine in liposomes localized and prolonged the local anesthetic activity compared to an equivalent conventional topical application.

Bonowitz *et al.*, (70) found that a liposomal formulation containing povidone iodine (PVP-I) targeted the medication to the fungal surface but not to human cells and resulted in a greater amount of active ingredient in the vicinity of pathogens when compared to a conventional ointment formulation. This approach yielded less systemic toxicity and better therapeutic effects. Li and Hoffman (71) found that entrapment of lacZ reporter gene in liposomes yielded selective targeting of the gene therapy to the hair follicle. Perugini *et al.*, (72) reported that the loading of glycolic acid, which exfoliates and moisturizers the skin in cosmetic products, into liposomes resulted in a slowing down of the release of glycolic acid and more control of its irritant side effects.

1.2.3. Liposome Preparation Techniques

Betageri and Kulkarni (73) described five basic techniques for the preparation of liposomes: mechanical agitation, detergent removal, replacement of organic solvents by aqueous media, size transformation by fusion, and pH adjustment. The method of preparation affects the liposome type, size, size distribution, encapsulation capacity and retention of liposomal contents. The three most important factors to be considered for preparation of medication-loaded liposomes are trapping efficiency, medication/lipid ratio, and

medication retention (73). The other factors that affect encapsulation of drugs in liposomes are charge on the liposome surface, bilayer rigidity, method of preparation, remote loading, addition of ion pairing, and complexing agents and characteristics of the drug to be encapsulated (50).

An ideal method of liposome preparation should have the following attributes: avoid or minimize the use of organic solvents and detergents, avoid long exposure to heavy mechanical stress, employ low temperature and pressure, be reproducible and economical, yield a high medication/lipid ratio, and be adaptable to large scale production (73).

1.2.4. Materials Used for Liposome Preparation

1.2.4.1. Phospholipids

Phospholipids (PL) are the principle ingredients in the preparation of liposome formulations. The PL molecules are amphipathic, have a hydrophobic tail and a hydrophilic 'polar head'. The hydrophobic tail consists of two free fatty acid chains on a glyceryl bridge molecule connected to a polar head group containing phosphate esters. When phosphate is esterified to choline or serine, phosphatidylcholine (PC) or phosphatidylserine (PS) are generated respectively (51, 73, 74). The degree of saturation of the free fatty acid chains affects the transition temperature (Tc) of the PL which is the temperature at which the lipid changes from a gel state to a fluid state (51, 75). The transition temperature of the PL is a result of the balance between a decrease in the packing density in the gel phase and a decrease in the rotational

freedom of the chains in the liquid crystal phase, both affected by the number of double bonds in the free fatty acid chains (76).

Egg phosphatidylcholine (PC) is a naturally occurring mixture of diglycerides of stearic, palmitic, and oleic fatty acids, linked to the choline ester of phosphoric acid. It is found in plants, animals, and egg yolk. In naturally occurring PC, the phosphoric acid is attached to the glycerol at the α–position, however, the phosphoric acid can also be attached in the β– position. PC is a neutral phospholipid and is oxidized readily on exposure to air (77-80). Upon complete hydrolysis, each molecule of PC yields two molecules of fatty acid, one molecule of each of glycerol, phosphoric acid and choline ester (78). Unless there is an egg allergy, PC is generally a nonirritating and nonsensitizing compound when applied to animal and human skin (79, 80). PC is used in cosmetic industry to formulate lipstick, foundation creams etc. and in food industry as additive in cake mix etc. (79, 80). The structure of PC is shown in Figure 3 (78).

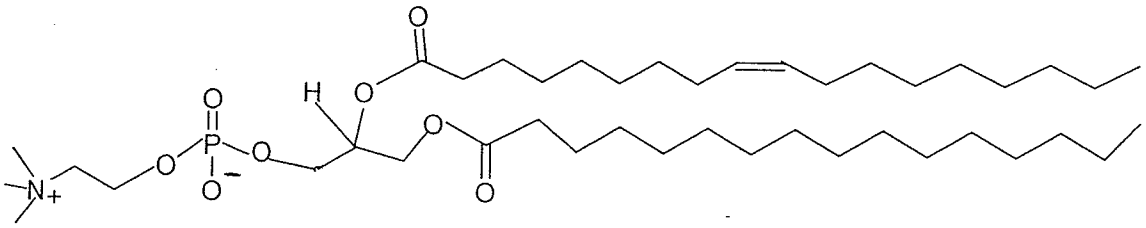

Figure 3: Structure of Egg Phosphatidylcholine. (From Ref. 78),

1,2-diacyl-*sn*-glycero-3- phosphatidylcholine

Egg Phosphatidylcholine hydrogenated (HPC) is a neutral, saturated PL and the end product of the controlled hydrogenation of PC (lecithin) (78). Unless there is an egg allergy, HPC is generally nonirritating and nonsensitizing when applied to animal and human skin (80).

Phosphatidylserine sodium salt is a negatively charged PL and prepared from pork brain extracts and transphosphatidylation of soybean lecithin. Unless there is any allergy, PS is generally nonirritating and nonsensitizing when applied to animal and human skin (78). The structure of PS is shown in Figure 4 (78).

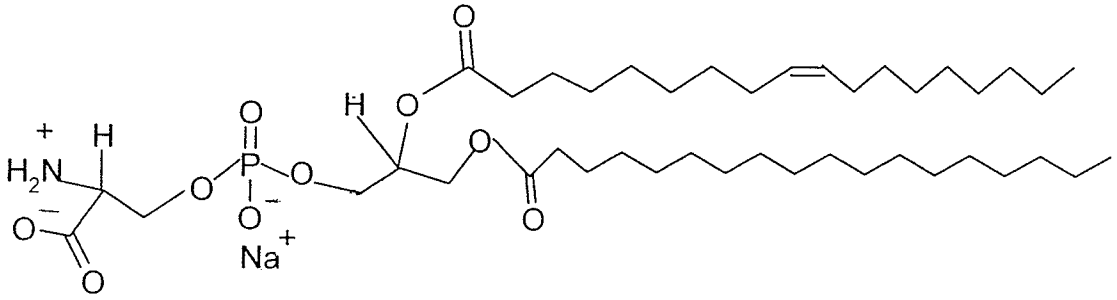

Figure 4: Structure of Pork-Brain Phosphatidylserine. (From Ref. 78)

1,2-diacyl-*sn*-glycero-3- phosphatidylserine sodium salt

1.4.1.1.2. Cholesterol (CH)

Cholesterol shown in Figure 5, is an additive material used in the preparation of liposomes. Cholesterol molecules are amphipathic, have a hydrophobic tail and a hydrophilic 'polar head'. Cholesterol molecules stack themselves at the outer half of the lipid region of the bilayer membrane of the liposomes with its polar hydroxyl group located at the level of the bridge region,

where hydrogen bonding can take place (81). This arrangement reduces the leakage of medications through the bilayer membranes of the liposomes and increases the stability of the liposomes (81 - 86). The CH molecules change the fluidity and consequently the permeability of the bilayer membranes of the liposomes. Below the transition temperature of phospholipids, the CH molecules push apart the PL molecules resulting in weakening of the packing of head groups of the PL and increasing in the fluidity of the order of the gel phase of the bilayer membranes of the liposomes (73). Above the transition temperature of phospholipids, the CH molecules reduce the rotational freedom of the acyl chains in the liquid crystal phase resulting in closer and more condensed packing of the PL molecules and decrease the fluidity of the bilayer membranes of the liposomes (73). Other natural sterols such as sitosterol, stigmasterol, and ergosterol were found as major membrane components in plants or fungi, and display similar CH-like behavior (81).

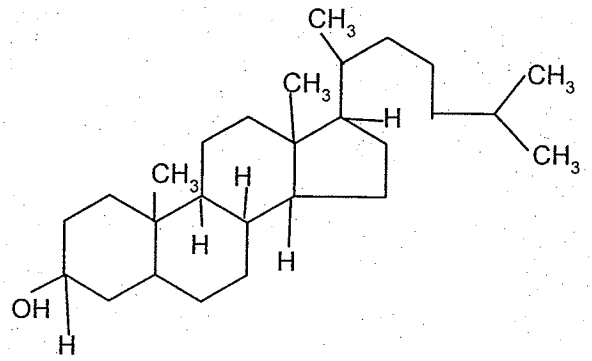

Figure 5: Structure of Cholesterol, Cholest-5-en-3β-ol (From Ref. 79)

In addition to sterols as additive materials, α-tocopherol and α-hydroxy acids are often used as an antioxidant to reduce lipid oxidation (73).

1.3. Percutaneous Treatment of Symptoms of Allergic Skin Disorders

1.3.1. Cutaneous Allergic Responses and Specialized Immune Defense Cells in the Epidermis

After exposure of the skin of an allergic subject to allergen, the early cutaneous allergic responses (ECAR) occurs within five minutes and may persist for up to 1 to 2 hours. This is followed by the late cutaneous allergic response (LCAR) which gradually evolves after the ECAR, peaks at 6 to 12 hours, and may persist for up to 24 hours. The mediators that initiate ECAR are histamine and the cysteinyl leukotrienes, LTB_4, LTC_4, LTD_4, and LTE_4. The development of LCAR is IgE-dependent and involves a complex interaction of T cells and other inflammatory cells. The mediators of the LCAR are theTh2-type cytokines including interleukin-5, granulocyte-macrophage colony stimulating factor (GMCSF), interleukin-4, interleukin-13, vascular cell adhesion molecule (VCAM), as well as other mediators of inflammation (87, 88).

In normal skin, mast cells, primarily of the MC_{TC} subtype, are present in the greatest density in the superficial dermal zone. Like all other mast cells, human skin mast cells bind IgE with high affinity to specific FCεRI receptors. The skin mast cells are different from those found in lungs, tonsils, adenoids, or intestine, because skin mast cells also express the CS_a receptors (CD88) and

activation sites for substance P, vasoactive intestinal polypeptide (VIP), somatostatin, and compound 48/80 (89).

In addition to the mast cells, there are some specialized immune defense cells found in the epidermis such as keratinocyte cells, Langerhans cells, Granstein cells, and T cells. Each cell has specific roles in the immune defense system (90, 91).

Keratinocytes, which are responsible for generating hair and nails, are also important immunologically. They secrete interleukin-1, which influences the maturation of T cells that tend to localize in the skin. Apparently, some post-thymic steps in T cell maturation take place in the skin under keratinocyte guidance. Langerhans cells that migrate to the skin from the bone marrow, process and present antigen to T_H cells (helper T cells), and facilitate responses to skin-associated antigens. Granstein cells, which serve as antigen presenting cells, process and present antigen to suppressor T cells and put the "brake" on the skin activated immune responses. T cells, the sensitized T lymphocytes, recognize antigen by macrophages and are converted to activated T cells. These activated T cells release cytokines that attract other cells, which cause tissue inflammation and the delayed hypersensitivity reaction (90, 91).

1.3.2. Role of Sensory Nerve in Cutaneous Allergy

Vasodilator fibers are present in peripheral sensory nerves so that when such nerves are stimulated by several stimuli such as heat, firm pressure, or certain chemicals, they cause blood vessels, primarily located in the skin, to become dilated. The blood vessel dilatation is due to release of substance P

(SP) or other neuropeptides. Substance P is about 100 times more potent on a molar basis than histamine in producing wheal and flare reactions. The neuropeptides, SP and neurokinin A then mediate the effects of inflammation either directly or indirectly by inducing release of the histamine from the mast cells. The generation of certain types of inflammation, and reflexes in sensory neurons operate to cause vasodilatation and increased vascular permeability in both the skin and lung (92).

1.3.3. Common Skin Allergic Disorders

Among the common allergic skin disorders that can be treated with H_1- antihistamines are urticaria, often combined with dry skin, and also possibly atopic dermatitis.

1.3.3.1. Urticaria

Urticaria, or hives, may develop in response to a number of stimuli such as allergic reactions, medications, cold, pressure, stings, sunlight and neuropsychological events. Urticaria and angioedema share similar pathologic mechanisms, may appear together or separately, but are distinguishable. Acute urticaria is a self-limiting disorder, usually disappearing within six weeks. The symptoms are cutaneous eruption of transient, erythematous pale papules or wheals, usually pruritic. However, chronic urticaria, characterized by episodes lasting longer than six weeks, and which may persist for years, may be due to specific causes never fully identified. Acute urticaria is often a manifestation of the Type I IgE-mediated allergic reaction. The release of

histamine and other mediators contained in the granules of basophils and mast cells plays a central role in the pathogenesis of urticaria (93-96).

Dry skin or xerosis which often accompanies urticaria, is the result of dehydration of the stratum corneum. There are many causes of dry skin including aging, and environmental factors, such as exposure to cold drying winds in winter. It may also be present with other dermatoses such as atopic dermatitis. Symptoms of dry skin include roughness, flaking, scaling and chapping, which usually occurs on the front of the lower legs, the back of the hands and on the forearms. The dry skin may be accompanied by inflammation, pruritus and fissuring (97).

1.3.3.2. Atopic Dermatitis

Atopic dermatitis or eczema is a chronic inflammatory pruritic dermatosis of the skin. It is characterized by severe pruritus that often starts during infancy. It is usually associated with other allergic conditions such as asthma and allergic rhinitis. The distinctive clinical indications of atopic dermatitis are intense pruritus, flexural involvement, and several clinical, immunologic, and biochemical alterations. The most obvious symptoms of atopic dermatitis are pruritus, lesions resulting from scratching which may include weeping erosions, vesicles and excoriated, reddened, scaling papules or plaques. In chronic dermatitis, the skin may be thickened with the appearance of pigmentation. Activated T cells, eosinophils, and Langerhans cells are present in the skin lesions of atopic dermatitis. The plasma IgE level is usually high in most of the chronic atopic dermatitis patients (98, 99).

1.3.4. Treatment of Allergic Symptoms

Oral and/or topical antihistamines, with or without topical corticosteroids, are medications of choice for the treatment of the symptoms of urticaria and possibly atopic dermatitis.

1.3.4.1. Topical Corticosteroids

Topical corticosteroids are the most potent agents used to treat the symptom of urticaria and possibly atopic dermatitis due to the anti-inflammatory effects. Topical corticosteroids in the appropriate strengths should be applied two to four times per day (100). Corticosteroids are used alone or possibly in combination with other agents such as salicylic acid, antibiotics, urea and zinc oxide (101). The adverse effects of topical corticosteroids due to some systemic absorption include the possibility of adrenal suppression, epidermal and dermal thinning due to skin and subcutaneous tissue atrophy, changes in skin pigmentation, abnormal excessive growth of hair or telangiectasia, acne on the face and secondary infections (102, 103). Brown *et al.*, (104) reported that corticosteroids after 8 days of ophthalmic application led to depression and mania.

1.3.4.2. Oral H_2- antihistamines

H_2- antihistamines have been used alone or in combination with H_1- antihistamines in the treatment of urticaria. The role of H_2- antihistamines in neuro-immunology and treatment of urticaria could be explained by the ability of these agents to block H_2- receptors on vasculature and prevent angioedema, to block histamine release in response to neuronal stimulation, to block the

neuronal release of neurotransmitters or neuropeptides if H_2- receptors were present on neurons, to block the neuronal effects on blood vessels, and to block the release of catecholamines from the adrenal medulla whether in response to acetylcholine or histamine (105).

Cimetidine alone was found beneficial in treatment of acute allergic skin reactions, and chronic idiopathic urticaria and angiodema and also demonstrated inhibition of suppressor T lymphocytes (106-109).

1.3.4.3. Oral H_1-antihistamines

H_1- antihistamines are nitrogenous bases containing an aliphatic side chain that structurally shares with histamine the common core structure of an ethylamine chain linked to an the unsubstituted amino terminal group. H_1-antihistamines are classified into first generation sedating and second generation non- or slightly sedating compounds (110, 111). Classically, separated into the six major groups of first generation H_1- antihistamines are: ethylenediamines (pyrilamine), ethanolamines (diphenhydramine), alkylamines (chlorphenhydramine), phenothiazines (promethazine), piperazines (hydroxyzine) (110), and piperidines (azatadine). The most widely used second generation H_1- antihistamines include cetirizine, loratadine, desloratadine (111, 112), and fexofenadine (113). Levocabastine and azelastine are only used topically in ophthalmic and nasal formulations. Hydroxyzine and cetirizine are two H_1-antihistamines widely used for relief of pruritus, urticaria and allergic skin disorders (110, 111).

Hydroxyzine dihydrochloride, a first generation piperazine class

H_1- antihistamine, is one of the most potent compounds that is still used to treat symptoms of allergic skin disorders. Hydroxyzine is well absorbed after a single oral dose of 50 mg in healthy young adults, with maximum plasma concentrations (C_{max}) occurring within 1-2 h of administration, and mean terminal elimination half-life values of 14-20 h. After an oral dose of 0.7 mg/kg, in children with atopic dermatitis, the mean elimination half-life was 7 h (114). In elderly adults, the mean half-life was 29 h, and in adults with hepatic dysfunction secondary to primary biliary cirrhosis, a mean half-life of 37 h has been reported (115). The mean apparent oral volume of distribution was 16 L/kg. In an animal model, the pharmacokinetics of hydroxyzine administered daily for 150 days did not change over time. There was no evidence for auto-induction of hepatic enzyme systems, more rapid clearance of the medication, or lower serum concentrations of the medication over time (115).

Following oral administration, hydroxyzine enters the skin rapidly and results in sustained high concentrations in the skin after single or multiple doses. This may contribute to its high efficacy in the treatment of skin disorders in which histamine plays a role (115). Hydroxyzine, like other first generation antihistamines, results in the adverse effects of central nervous system sedation, urinary retention, dry mouth, loss of appetite, constipation or diarrhea, weakness, and anorexia (116).

Balen *et al.*, (117) determined the ionization constant (pK_a) and the lipophilicity (log P = partition coefficient and log D= distribution coefficient) parameters of hydroxyzine in isotropic systems (n-octanol/water) and anisotropic

systems (liposomes/water). In the isotropic systems hydroxyzine has two pK_a which are 1.75, and 7.49; two log P, for the cationic form (log P^C_{oct} =0.93), and for the non-ionized form (log P^N_{oct} =3.5), and one log D value of 3.1. In the anisotropic systems, hydroxyzine has two log P, for the cationic form (log P^C_{lip} =2.8) and for the non-ionized form (log P^N_{lip} =3.4) indicating that the cationic form gained in lipophilicity when passing from the isotropic systems to the anisotropic systems. Log D of hydroxyzine was increased by increasing the pH; the values were 2.76, 3.13, and 3.46 at pH range of 3.1 to 4.9, at pH 7.4, and at pH 9 respectively indicating that the cationic form converted into non-ionized form and gained in lipophilicity when pH increased. Hydroxyzine structure is shown in Figure 6.

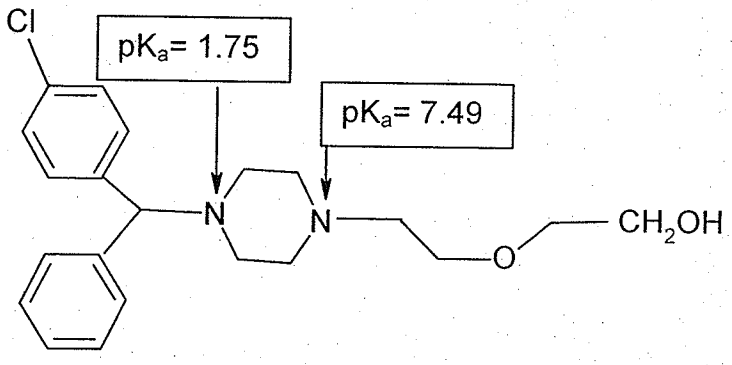

Figure 6: Hydroxyzine Structure

Cetirizine, the active carboxylic acid metabolite of hydroxyzine and a safe, effective second-generation H_1- antihistamine, is widely used to treat the symptoms of allergic diseases in patients of all ages (118).

Cetirizine is a potent H_1- antihistamine, has high specific affinity for H_1- receptors and has anti-inflammatory properties. Cetirizine is rapidly absorbed after oral administration with peak plasma concentrations (C_{max}) of 257 μg/L to 460 μg/L occurring approximately at 1 h following a 10-mg dose in adults. After multiple-doses of cetirizine, 10 mg daily for 10 days, to healthy adults, a mean C_{max} of 311 ng/mL is observed. Cetirizine is present in a zwitterionic form at the physiological pH with marked hydrogen-bonding capacity. This property explains the low penetration through the blood brain barrier and the very small apparent volume of distribution (Vd/F) of 0.56 L/kg. The plasma protein binding of cetirizine is about 93 %, independent of medication concentration over the range of 25-1000 ng/mL (119-122).

The mean elimination half-life in healthy volunteers is 8.3 h and from 40 % to 80 % of the unchanged medication is identified in the urine (115). In children, the cetirizine terminal elimination half-life is 7 h and in elderly subjects 11.8 h, in whom it is dependent on the renal function rather than age. In subjects with renal dysfunction the terminal elimination half-life is prolonged to about 20 h. In healthy adults, the total body clearance of cetirizine (Cl/F) is 0.04 to 0.05 L/h/kg (119-122).

Cetirizine does not interact with concomitantly administered medications, has no cardiac adverse effects, and does not appear to be associated with teratogenicity. Any sedation attributed to oral cetirizine is dose-dependent and generally mild. In dermatology, cetirizine has proven to be effective in the

treatment of various forms of urticaria and it reduces the pruritus of atopic eczema (119-122).

Cetirizine has three pK_a which are 2.19, 2.93, and 8.00; three log P for the cationic form (log P^C_{oct} =1.12), the zwitterionic form (log P^Z_{oct} =1.55) and for the anionic form (log P^A_{oct} =-0.19), and one log D =1.5. In the anisotropic systems, cetirizine, has three log P for the cationic form (log P^C_{lip} =3.2), the zwitterionic form (log P^Z_{lip} =2.3) and the anionic form (log P^A_{lip} =2.3) indicating that all forms gained in lipophilicity when passing from the isotropic systems to the anisotropic systems. The log D value of cetirizine averages 2.3 at the pH range from 3.1 to 9. This indicates that the lipophilicity of cetirizine does not change when the pH is increased from 3.1 to 9 (117). Cetirizine structure is shown in Figure 7.

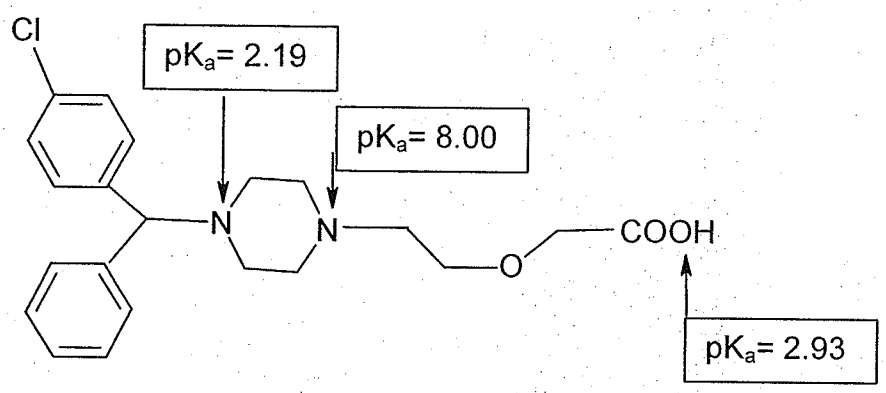

Figure 7: Cetirizine Structure

1.3.4.4. Topical Antihistamines

Except for fexofenadine, there are no H_1-antihistamines totally free from adverse CNS effects under all circumstances (113, 123). The approach of applying antihistamines topically to the skin is to produce a local effect in the skin tissue itself while minimizing any systemic absorption and the accompanying adverse effects. The topical application of H_1-antihistamine creams for treatment

of allergic symptoms of skin disorders has been in use for over 50 years. Diphenylpyraline hydrochloride has been used for the treatment of the eczematous and other itching dermatoses but the major adverse effects include symptomatic psychosis and psychomotor restlessness, disorientation, and optic and acoustic hallucinations. Promethazine has been used for generalized eczema but its adverse effects are disorientation, hallucinations, hyperactivity, convulsion, and coma. Doxepin was recently introduced for oral and topical use as an antipruritic but clinical sedation frequently occurs (123, 124).

Damage to the stratum corneum by scratching the skin due to itching, or the presence of an allergic skin disease such as atopic dermatitis, increased skin permeability, and consequently increased the systemic absorption of the medication applied topically on the skin. Three children with varicella-zoster lesions developed bizarre behavior including visual hallucinations and auditory hallucinations following frequent topical applications of large amounts of diphenhydramine cream to the majority of the skin surface area (125).

Topical H_1-antihistamines, formulated in conventional ointment and cream bases, have been used for over 50 years for the treatment of allergic skin disorders. However, extensive absorption leading to toxicity has been reported when these formulations are applied liberally to skin damaged by allergic skin conditions (125).

It has been found (126) that liposomes act as topical carrier systems for hydroxyzine delivery into the skin for therapeutic effects while resulting in lower systemic absorption of the medication. From this previous preliminary study, it

was found that hydroxyzine from liposome formulations had a better suppression of skin wheal areas than from Glaxal Base cream. These preliminary results provided some information to design this study.

1.4. STUDY PROPOSAL

1.4.1. Purpose of the Study

The primary purpose of this study was to design and prepare liposome formulations containing the H_1-antihistamines hydroxyzine and cetirizine and to use these products to determine the peripheral H_1-antihistaminic activity and extent of systemic absorption of these antihistamines following application to the depilated skin in a rabbit model. The secondary purpose was to characterize the liposome formulations prepared using different PL with different transition temperature (127) by evaluating the percent entrapment of hydroxyzine and the percent entrapment of cetirizine. Also the percent entrapment of the H_1-antihistamines was used to monitor the long term stability of the liposome formulations. Other *in vitro* techniques used included particle size analyses and the use of transmission electron micrographs and micrographs from an optical microscope of the liposome formulations.

1.4.2. Study Hypothesis

The molecular arrangement of the phospholipid and cholesterol in the liposome bilayers is similar to the molecular arrangement of the ceramides, triglycerides, fatty acids, and cholesterol in the intercellular bilayers of the stratum corneum, with the polar head directed to the aqueous layer and the

non-polar tail to the lipid layers (7, 10, 51, 73). This arrangement may help the movement and localization of the liposomes within the lipid tail region of the intercellular bilayers of the stratum corneum (49, 59).

It is anticipated that H_1-antihistamines in liposome formulations applied to the skin would provide equivalent peripheral H_1-antihistaminic blockade as similar doses of these H_1-antihistamines administered by IV-route in rabbit model (110) and orally to humans (114, 128, 129) with considerably lower plasma H_1-antihistamine concentrations, which could potentially result in reduced systemic adverse effects of the H_1-antihistamines.

It is hypothesized that:

Liposome formulations when applied to the skin would be excellent delivery systems for the topical application of H_1-antihistamines to the skin for relieving of allergic skin disorder symptoms.

H_1-antihistamines in liposome formulations when applied to the skin, would provide faster onset, more prolonged and greater peripheral H_1-antihistaminic activity than H_1-antihistamines in conventional ointment or cream formulations.

The liposome formulations would concentrate the H_1-antihistamines in the skin and reduce their systemic absorption thus decreasing the potential for systemic adverse effects compared to conventional ointment or cream formulations.

The liposome formulations containing hydroxyzine or cetirizine would have physicochemical stability for at least one year, and the results from these studies

would provide preliminary data required as a basis for the stability of commercial formulations.

1.4.3. Specific Aims

The peripheral H_1-antihistamine efficacy of hydroxyzine and cetirizine in liposome formulations will be evaluated by measuring the onset, extent and duration of wheal suppression induced by intradermal injection of histamine. These results will be compared with the suppression of the wheals from hydroxyzine or cetirizine in Glaxal Base, the control topical o/w cream formulation.

The rate and extent of systemic absorption after application of liposome formulations containing hydroxyzine or cetirizine on the depilated skin of a rabbit model will be evaluated by measuring the hydroxyzine or cetirizine plasma concentrations. This will be compared with the hydroxyzine or cetirizine plasma concentrations from Glaxal Base.

The formulation and physicochemical stability of the liposome formulations containing hydroxyzine or cetirizine for at least one year will be assessed by determination of the percent entrapment of hydroxyzine or the percent entrapment of cetirizine.

In addition, the liposome formulations containing hydroxyzine or cetirizine will be characterized by measuring the particle size using the submicron particle-sizer, and by measuring the largest diameter of liposomes containing hydroxyzine or cetirizine using the transmission electron micrographs, and

micrographs displayed on the screen of the computer monitor of an optical microscope.

CHAPTER II. METHODS

2.1. Chemicals, Supplies, and Equipment

2.1.1. Chemicals

1. Acetone: Fisher Scientific, Fair Lawn, NJ, USA.
2. Acetonitrile: Fisher Scientific, Fair Lawn, NJ, USA.
3. Ammonium phosphate monobasic: Fisher Scientific, Fair Lawn, NJ, USA.
4. Antazoline hemisulfate salt ((M.W. 314.4): Sigma Chemical, St. Louis, MO, USA.
5. Cetirizine dihydrochloride (M.W. 461.8): UCB-Pharmaceutical Sector R&D, Braine-L' Alleud, Belgium.
6. Chloroform: Fisher Scientific, Fair Lawn, NJ, USA.
7. Cholesterol (M.W. 386.7): Fisher Scientific, Fair Lawn, NJ, USA.
8. Citric acid: Fisher Scientific, Fair Lawn, NJ, USA.
9. Egg L-∝-Phosphatidylcholine (95%) (M.W. 760): Avanti Polar Lipids, Alabaster, AL, USA.
10. Egg L-∝-Phosphatidylcholine hydrogenated (95%) (M.W. 762): Avanti Polar Lipids, Alabaster, AL, USA.
11. L-∝-Phosphatidylserine (Brain sodium salt) (95%) (M.W. 812): Avanti Polar Lipids, Alabaster, AL, USA.
12. Ethanol: Fisher Scientific, Fair Lawn, NJ, USA.
13. Ethyl acetate: Fisher Scientific, Fair Lawn, NJ, USA.
14. Ethyl Ether: Fisher Scientific, Fair Lawn, NJ, USA.
15. Evans-blue: Fisher Scientific, Fair Lawn, NJ, USA.

16. Glaxal Base: Roberts Pharmaceutical Canada, Oakville, ON, Canada.
17. Heparin Sodium Injection B.P. (100 i.u./mL): Leo Laboratories Canada, Ajax, ON, Canada.
18. Histamine phosphate: (U.S.P. 1mg/mL): Glaxo Smithkline Canada,Toronto, ON, Canada.
19. Hydroxyzine dihydrochloride (M.W. 447.8): Sigma Chemical, St. Louis, MO, USA.
20. J028: (2-{2-[4-(diphenylmethylene)-1-piperidinyl] ethoxy} ethoxy) acetic acid chorhydrate (MW 431.960) ($C_{24}H_{29}NO_4$). UCB 20028, Pharmaceutical Sector R&D, Braine-L' Alleud, Belgium.
21. Nitrogen: Praxair Canada, Mississauga, ON, Canada.
22. Outdated Human Plasma, Canadian Blood Services, Winnipeg, Manitoba.
23. Phosphoric acid: Fisher Scientific, Fair Lawn, NJ, USA.
24. Potassium hydroxide: Fisher Scientific, Fair Lawn, NJ, USA.
25. Sodium 1-decanesulfonic acid: Sigma Chemical, St. Louis, MO, USA.
26. Sodium chloride (0.9): AstraZeneca Canada, Mississauga, ON, Canada.
27. Sodium citrate dihydrate: Mallinckrodt Specialty Chemical Canada Inc., Mississauga, ON, Canada
28. Sodium hydroxide: Fisher Scientific, Fair Lawn, NJ, USA.

2.1.2. Supplies

1. Alcohol swabs: Becton Dickinson & Company Franklin Lakes, NJ, USA.
2. Nair (Depilatory): N.CS: Carter-Wallace, Mississauga, ON, Canada.

3. Disposable syringes (1cc, 5cc, 10cc): Becton Dickinson & Company Franklin Lakes, NJ, USA.
4. Disposable test tubes (16x100 mm): Baxter Healthcare, Valencia, CA, USA.
5. I.V. Catheter Placement Units: 22G, Critikon, Tampa, FL, USA.
6. Male Adapter Plug-short: Abbot Hospital, N. Chicago, IL, USA.
7. Needles (22G x $1_{1/2}$", 23G x $1_{1/2}$", 27G x $1_{1/2}$"): Becton Dickinson & Company Franklin Lakes, NJ, USA.
8. Steri-Pad: Johnson & Johnson, Montreal, Canada.
9. Sure Sep-II Serum Plasma Separator: Organon Teknika, Durham, N. CA, USA.
10. Utrafiltration membranes (YM100 62 mm): Amicon, Beverly, MA, USA.

2.1.3. Equipment

1. Axioskop Routine Microscope fitted with a Video Camera (Sony power HAD 3ccD color) connected to a PC-computer: Zeiss Gruppe, Jena, Germany.
2. Balance (Mettler AE 160): Mettler Instrument AG, Switzerland.
3. Centrifuge (IEC HN-sII): International Equipment Company, Needham Hts, MA, USA.
4. Epson Perfection (1250 Scanner, G820A), Epson Corp, Indonesia.
5. Extruder, 2 syringes 1 μL (Hamilton), 200 and 0.03 μm-polycarbonate membranes, and hold/heating block: Avanti Polar Lipids, Alabaster, AL, USA.
6. Hair Clipper (Oster A5® size 40, 1/10mm): Cryotech ™, Fort Madison, IA, USA

7. High Performance Liquid Chromatography System: Waters Corporation, Millford, Massachusetts, USA.

   7.1. 510 Solvent Delivery System

   7.2. 712 WISP Injector.

   7.3. 480 UV Detector, LC spectrophotometer (Lambda-Max, model 480).

   7.4. Column: C_{18} μ-Bondapak 10μ, 0.4x30 cm stainless steel

   7.5. Varian Star Integration System

8. Milli-Q water System: Millipore, Mississauga, ON, Canada.
9. Submicron Particle Sizer (NICOMP 370): Particle Sizing Systems, Santa Barbara, CA, USA.
10. Northern Eclipse software 6.0: Impix Imaging, USA.
11. PCSAS® 8.2e software: SAS Institute, Cary, NC, USA.
12. WinNonlin Standard Edition, version 1.1: Scientific Consulting Inc., Apex, NC, USA
13. pH meter (Accumet® AP62): Fisher Scientific, Fair Lawn, NJ, USA.
14. Sigma Scan® 5.0 Software: Jandel Scientific, San Rafael, CA, USA.
15. Syringe Pump (22-Ealing): Scientific, St. Laurent, Quebec, Canada.
16. Transmission Electron Microscope (Hitachi H-7000), Hitachi Scientific Instruments, Tokyo, Japan.
17. THELCO® General Purpose Incubator (2DG): Precision Scientific Corporation, Chicago, IL, USA.
18. Ultra-filtration Apparatus: Amicon, Beverly, MA, USA.

19. Vortex Mixer (Multi-tube vortexer, VX-2500): VWR Scientific Products, Bridgeport, NJ, USA.
20. Wrist-Action Shaker: Burrell Corporation, Pittsburgh, PA, USA.

2.2. *In vitro* Studies of Hydroxyzine and Cetirizine in Liposome Formulations

These studies were conducted using liposome formulations SUV and MLV prepared using three phospholipids, and the H_1-antihistamines, hydroxyzine and cetirizine, as medications. The phospholipids used were Egg L-∝-Phosphatidylcholine (PC), Egg L-∝-Phosphatidylcholine hydrogenated (HPC), and L-∝-Phosphatidylserine (Brain sodium salt) (PS) with transition temperature (Tc) of –15°C, 50°C, and 24°C respectively (127). The control formulation was Glaxal Base (GB), an oil/water emulsion base widely used in Canadian pharmacies for extemporaneous compounding of topical formulations.

2.2.1. HPLC Analysis of Hydroxyzine and Cetirizine in Aqueous Liposome Filtrates

The HPLC instrument was a Waters™ component system comprised of a 510 Solvent Delivery System, a 712 WISP Injector, and a 480 UV Detector. This system was connected to a computer with Varian Star Integration Software for data analysis. All chromatography was performed on Waters C_{18} μ-Bondapak 10μ, 0.4x30 cm stainless steel columns.

2.2.1.1. Calibration Curves of Hydroxyzine

All stock solutions and dilutions were prepared using 0.05% w/v phosphoric acid (H_3PO_4). A stock solution of hydroxyzine 1 μg/mL was used to prepare serial dilutions of hydroxyzine in concentrations ranging from 100 to 800 ng/mL. One mL of antazoline solution 24 μg/mL as the internal standard was added to each sample. From these samples, 50 μL aliquots were injected directly into the HPLC system.

The following HPLC conditions were used. The mobile phase was acetonitrile: phosphate buffer (0.075 M $NH_4H_2PO_4$, adjusted with H_3PO_4 to pH 2.5) 37:63 V/V. The flow rate was set at 1.5 mL/min. The detector wavelength was fixed at 229 nm with sensitivity setting at 0.2 to 0.005 a.u.f.s (128). Under these conditions the retention times of hydroxyzine and the internal standard were 6 min and 8 min respectively and their corresponding peaks were well resolved. The value 2.5 ng was considered as the quantification limit. All stock solutions and dilutions were prepared and analyzed 8 times on 8 different days then the calibration curve was prepared by plotting mean peak area ratios of hydroxyzine to antazoline versus concentrations of hydroxyzine. Appendix A, Figure 1 shows a representative HPLC chromatogram.

2.2.1.2. Calibration Curves of Cetirizine

All stock solutions and dilutions were prepared using 0.05% w/v phosphoric acid (H_3PO_4). A stock solution of cetirizine 1 μg /mL was used to prepare serial dilutions of cetirizine in concentrations ranging from 100 to

1000 ng/mL. One mL of J028 solution, [(2-{2-[4-(diphenylmethylene)-1-piperidinyl] ethoxy} ethoxy) acetic acid chorhydrate] 25 μg/mL as the internal standard, was added to each sample. From these samples, 50 μL aliquots were injected directly into the HPLC system.

The following HPLC conditions were used. The mobile phase was acetonitrile: phosphate buffer (0.01 M KH_2PO_4, 0.02 M 1-decanesulfonic sodium salt, adjusted with H_3PO_4 to pH 2.9) 46:54 V/V. The flow rate was set at 2 mL/min. The detector wavelength was fixed at 229 nm with sensitivity setting at 0.2 to 0.005 a.u.f.s (129). Under these conditions the retention times of cetirizine and the internal standard were 5 min and 7 min respectively and their corresponding peaks were well resolved. The value 2.5 ng was considered as the quantification limit. All stock solutions and dilutions were prepared and analyzed 8 times on 8 different days then the calibration curve was prepared by plotting mean peak area ratios of cetirizine to the internal standard versus concentrations of cetirizine. Appendix A, Figure 2 shows a representative HPLC chromatogram.

2.2.2. Preparation of Small Unilamellar Vesicles (SUV)

2.2.2.1. Ethanol Injection Method

Ethanol solutions of 7 mL volumes were prepared containing 406 mg PC or 433 mg PS and 61.5 mg cholesterol (CH) and designated as the lipid phases. Exactly 80 mg of hydroxyzine or 82 mg of cetirizine were dissolved in 100 mL of phosphate buffer (0.2 M K_2HPO_4) pH 6.5, and designated as the aqueous phases. The lipid phases were injected into the rapidly stirred aqueous

phases at a rate of 0.5 mL/min using a 22G needle and a calibrated syringe pump (130-133).

2.2.2.2. Extrusion Method

To prepare SUV using HPC (HPC-SUV), multilamellar vesicles (MLV) (HPC-MLV) containing hydroxyzine or cetirizine were prepared first using the lipid film hydration method as described in Section 2.2.3. In this method chloroform solutions of 5 mL volumes were prepared containing 407 mg HPC and 61.5 mg CH and designated as the lipid phases. Exactly 80 mg of hydroxyzine or 82 mg of cetirizine were dissolved in 100 mL of phosphate buffer (0.2 M K_2HPO_4) pH 6.5 and designated as the aqueous phases. In a 250 mL round bottom flask, the solvent was removed from the lipid phases at 40°C under vacuum by using the rotary evaporation apparatus, resulting in thin lipid films on the walls of the flasks. The lipid films were hydrated at 60°C well above the transition temperature of 50°C (134), using the rotary evaporation apparatus then by continuous wrist shaking for 1 h in a water bath at 60°C. The liposome suspensions produced were concentrated to 10 mL using an Amicon Ultrafiltration Apparatus and an ultrafiltration membrane with a greater than 100,000 M.W. cut-off. This was accomplished with rapid stirring under a nitrogen pressure of less than 10 psi. HPC-SUV of hydroxyzine or cetirizine were prepared by extruding 10 mL concentrated, freshly prepared HPC-MLV 11 times through polycarbonate membranes of 200 μm followed by an additional 11 times through polycarbonate membranes of 0.03 μm using a mini-extruder. During the extrusion procedure the temperature of the liposome suspensions was

maintained at 60°C well above the HPC transition temperature of 50°C (134). The separated filtrates resulted from concentrating the HPC-MLV batches were added back to the HPC-SUV suspensions after extrusion. The percentage entrapment of hydroxyzine or cetirizine was determined by measuring the hydroxyzine or cetirizine content in the clear filtrate and washings, obtained by filtration of HPC-SUV suspensions using the Amicon Ultrafiltration Apparatus as described in Section 2.2.6.1.

2.2.3. Preparation of Multilamellar Vesicles Using Lipid Film Hydration Method

Chloroform solutions of 5 mL volumes were prepared containing 406 mg PC or 433 mg PS or 407 mg HPC and 61.5 mg CH and designated as the lipid phases. Exactly 80 mg of hydroxyzine or 82 mg of cetirizine were dissolved in 100 mL of phosphate buffer (0.2 M K_2HPO_4) pH 6.5 and designated as the aqueous phases. In a 250 mL round bottom flask, the solvent was removed from the lipid phases at 40°C under vacuum by using the rotary evaporation apparatus (130, 135-137), resulting in thin lipid films on the wall of the flasks. The lipid films for PC or PS were hydrated with the buffer containing the medications by continuous wrist shaking for 1 h at room temperature (25±5°C) using the wrist shaker. The lipid films for HPC were hydrated at 60°C well above the transition temperature of 50°C (134, 138), using the rotary evaporation apparatus then by continuous wrist shaking in a water bath for 1 h at 60°C.

The preparation technique was optimized with regard to a number of formulation factors that are described in Section 2.2.4.

2.2.4. Factors Evaluated During Liposome Formulation

2.2.4.1. Effect of Using Different Methods of Preparation of MLV

The MLV were prepared using the lipid film hydration method as described in Section 2.2.3. Chloroform solutions of 5 mL volumes were prepared containing 406 mg PC and 61.5 mg CH and designated as the lipid phase. Exactly 80 mg of hydroxyzine were dissolved in 100 mL volumes of phosphate buffer (0.2 M K_2HPO_4) pH 7 and designated as the aqueous phase. The formulation technique was evaluated using various hydration times and periods of freezing and thawing as described below (73).

Hydration Time (h)	Freezing and Thawing (5 cycles after Hydration)	
	No	Yes
1	Control batch	Batch A
24	Batch B	Batch C
48	Batch D	Batch E

The hydration of the lipid film formed on the wall of the flask was carried out at different lengths of time 1 h, 24 h, or 48 h by continuous shaking at room temperature with the aqueous phase containing 80 mg hydroxyzine using the wrist shaker. One freezing and thawing cycle of the liposomes was performed by

freezing the liposome suspensions for 24 h in the freezer at -20°C. Then the liposome suspensions were thawed at room temperature for approximately 3 h. After thawing, the liposome suspensions were frozen again at -20°C for 24 h. The freezing and thawing cycle was repeated five times.

2.2.4.2. Effect of Using Buffer of Different pH Values

The PC-SUV and PC-MLV were prepared using the ethanol injection and the lipid film hydration methods, respectively as described in Sections 2.2.2 and 2.2.3 using buffer at pH values of 5.0, 5.5, 6.0, 6.5 and 7.0.

2.2.4.3. Effect of Using Different Phospholipids

The SUV, HPC-SUV and MLV were prepared by the ethanol injection, the extrusion, and the lipid film hydration methods as described in Sections 2.2.2.1, 2.2.2.2, and 2.2.3. respectively.

2.2.5. Stability Studies of Hydroxyzine and Cetirizine Liposomes

To perform the stability studies of hydroxyzine or cetirizine liposomes, all batches were purged with nitrogen to remove atmospheric oxygen while placed in opaque containers. The containers were sealed air-tight, then stored in desiccators. Each batch was prepared three times.

In the long-term stability studies of hydroxyzine liposome batches at various storage temperatures, samples were evaluated every month for up to 24 months. The hydroxyzine liposomes formulated using different methods of preparation were stored at 10±2°C in a refrigerator and at 37±0.1°C in an incubator for up to 24 months. The hydroxyzine liposomes prepared using buffers of different pH values were stored at 10±2°C in a refrigerator for up to 24 months.

The hydroxyzine liposomes prepared using different phospholipids were stored at 10±2°C in a refrigerator, at room temperature 25±3°C, and at 37±0.1°C in an incubator and evaluated monthly for up to 24 months. In the stability studies of all cetirizine liposome batches stored at 10±2°C in a refrigerator, samples were evaluated at 12 and 24 months.

The short-term evaluation of the percent entrapment of hydroxyzine (PETH) or percent entrapment of cetirizine (PEC) as described in Section 2.2.6.1 for all batches of PC-SUV and PC-MLV stored at 37±0.1°C in an incubator, was determined every day for up to 7 days, and every week for up to one month.

2.2.6. Evaluation of Hydroxyzine and Cetirizine Liposomes

Each liposome formulation was prepared three times on three different days. The integrity of these liposome formulations both immediately after the preparation and after storage for various periods of time at several temperatures was evaluated by: determining the percent of the drug entrapment, observing any change in the physical appearance of the liposome suspensions, measuring the mean particle size of the liposome batches prepared using buffer (0.2 M K_2HPO_4) pH 6.5, and subjectively assessing the transmission electron (TEM) and optical microscope micrographs of the liposome formulations (MOM).

2.2.6.1. Percent Entrapment of Hydroxyzine and Cetirizine

The liposome suspensions of each batch, immediately after preparation, and after storage for various periods of time at several temperatures, were filtered using an Amicon Ultrafiltration Apparatus and an

ultrafiltration membrane with a greater than 100,000 M.W. cut-off. Then the liposomes were washed 2 times with 10 mL each of phosphate buffer (0.2 M K_2HPO_4) pH 6.5. This was accomplished with rapid stirring under a nitrogen pressure of less than 10 psi. The initial filtrate and the two 10 mL wash volumes were combined. The amount of hydroxyzine or cetirizine that was not entrapped into the liposomes (F) was determined by measuring the hydroxyzine or cetirizine content in the clear filtrate obtained from concentrating and washing the liposome formulations using the Amicon Ultrafiltration Apparatus. Hydroxyzine or cetirizine in the clear filtrate were analyzed using the HPLC methods described in Section 2.2.1. Each experiment was repeated three times. The mean percent entrapment of hydroxyzine (PETH) and cetirizine (PEC) were calculated using Equation 1:

Equation 1: Percent Entrapment= ((I – F) x 100) / I

Where:

I = Initial amount of hydroxyzine or cetirizine added during preparation

F = mean amount (n=3) of hydroxyzine or cetirizine in the filtrate, not entrapped into the liposomes.

The extent of adsorption of hydroxyzine or cetirizine to the filtration membrane was evaluated by filtration of aqueous solutions of hydroxyzine or cetirizine at various concentrations. The amount of hydroxyzine or cetirizine in the aqueous solutions was determined before and after filtration and any loss by adsorption to the filtration membrane was calculated.

2.2.6.2. Physical Appearance

The physical appearance of the liposomes was examined periodically to monitor any discoloration or change in appearance of the liposome suspensions. The samples were evaluated subjectively, and in some cases photographs of the samples were taken.

2.2.6.3. Transmission Electron Micrograph (TEM)

To examine the morphology of PC-SUV, HPC-SUV, PS-SUV, PC-MLV, HPC-MLV and PS-MLV of hydroxyzine and cetirizine, the liposome samples were negatively stained (139) and TEM were taken using a transmission electron microscope (TEM) by technicians in the Electron Microscope laboratory. The negative staining procedures were conducted using the following steps (140).

A sample of each batch of liposomes was diluted 1:5 directly on a copper or nickel formvar-coated grid using 1 μL of liposome formulation and 5 μL of water. The dilution was conducted using cold, double-distilled, Millipore-filtered, freshly boiled and cooled water. The excess fluid of the sample was withdrawn by touching a filter paper triangle to the edge of the grid. The grid was not allowed to dry completely, but a film of moisture was retained on the surface of the grid.

The staining was achieved by adding 5 μL of 1% phosphotungstic acid (pH 7.4) to the sample on the grid for 30 sec. Then the excess fluid was withdrawn by touching a filter paper triangle to the edge of the grid. The grid was then placed into a petri dish lined with filter paper and allowed to totally air dry.

The stained liposomes were then examined using the electron microscope. Three fields of view of each grid were chosen at random and photographed at 40,000X. Electron microscope negatives were developed using standard procedure. An 8" x10" print was then made of each negative on glossy paper, enlarging the negative 3 times and balancing the white edges. Some prints showed more contrast than the others, although a number one filter was used for all prints and a light setting of about 38 units on the rheostat. Test strips of 1-8 sec intervals were used to determine the exposure time. The final magnification was calculated to be 112,200X. Prints were allowed to dry overnight and were labeled. From each TEM, the largest diameters of at least 10 liposomes or whatever number was available in the micrograph were measured. The mean diameter of the liposomes and the standard error were calculated. The TEM are shown in Appendix B, Figures 1-14.

2.2.6.4. Micrographs from an Optical Microscope (MOM)

Samples from each batch of the liposomes containing hydroxyzine or cetirizine were examined under Axioskop Routine microscope which was fitted with a video camera connected to a computer. Northern Eclipse Software 6.0, was previously installed onto the computer and calibrated using a micrometer slide. A captured picture of the slide was displayed on the screen of the computer monitor in the scale of 1μm= 1.5 cm. The samples of the liposomes were diluted 1:2 directly on glass slides using 1 μL of liposome formulation and 2 μL of water. Photomicrographs of the liposomes were taken, saved and displayed on the screen of the computer monitor. Using the micrographs and the line measuring

tool and mouse, the largest diameters were measured of 10 liposomes from each of 6 samples of the same batch of SUV or MLV formulations. The mean±SEM diameter of the 10 liposomes in each sample was calculated (141).

2.2.6.5. Particle Size Analysis

The liposome vesicle sizes in the SUV and MLV formulations were determined using a submicron particle sizer (NICOMP370, 3 nm-5000nm) and by measuring the largest diameter of the liposomes from TEM and MOM as described in section 2.2.6.3, and 2.2.6.4 respectively.

The particle size analysis of the liposomes in suspension were conducted by Viventia Biotec Inc., using Submicron Particle Sizer (NICOMP370, 3-5000 nm) and the following method.

The Submicron Particle Sizer consists of two subunits, the light scattering assembly and the controller/analyzer. The light scattering signal was obtained from the samples described later by focusing the beam from a laser diode (5 mw, 632.8 nm) into a temperature-regulated scattering cell. A fraction of the scattered light was captured at a 90-degree angle and transmitted by optical fiber to the photomultiplier detector in the central controller/analyzer subunits. These subunits controlled the light scattering assembly and performed the dedicated continuous analysis of the particle size distribution. An IBM- compatible personal computer operating under DOS was used for data collection from the controller/analyzer subunits (126).

The parameters for The Submicron Particle Size Analyzer were set as follows: temperature at 23°C, viscosity at 0.933 cp, and index of refraction at

1.333. The Samples of PC-SUV, HPC-SUV, PS-SUV, PC-MLV, HPC-MLV and PS-MLV of hydroxyzine or cetirizine liposome batches freshly prepared and after storage at 20 months at 10°C were diluted with phosphate buffer 0.2 M K_2HPO_4 (pH 6.5) until a count rate of 200-300 KHZ was achieved. Volume-weighted Gaussian analysis was used for unimodal distribution, or volume-weighted instrument-generated non-Gaussian analysis for multi-modal distribution. The run time stopped automatically when a fitting error of 1, or when a Chi-squared value of less than 1 was achieved. Appendix C, Figures 1-6, shows representative histograms and data of the particle sizes analysis of the most stable liposomes containing hydroxyzine and cetirizine, which are HPC-SUV and HPC-MLV.

2.3. *In vivo* Evaluation of Hydroxyzine and Cetirizine Liposomes

The onset, extent and duration of the peripheral H_1-antihistamine effects of hydroxyzine or cetirizine applied to rabbits' skin in freshly prepared liposome formulations was evaluated using suppression of the histamine-induced wheal formation following the intradermal injection of histamine, and compared with hydroxyzine or cetirizine from the control Glaxal Base (GB) o/w formulations. The amount of the H_1-antihistamines absorbed into the systemic circulation was determined by measuring plasma hydroxyzine or cetirizine concentrations at predetermined times after application of the liposomes and the control formulation, Glaxal Base (GB) containing the H_1-antihistamines to the rabbits' skin.

2.3.1. HPLC Analysis of Hydroxyzine and Cetirizine in Plasma

The determination of hydroxyzine and cetirizine concentrations in plasma required extraction of the drug from plasma prior to analysis using the HPLC conditions identical to those described in Sections 2.2.1.1 and 2.2.1.2 for hydroxyzine and cetirizine respectively.

2.3.1.1. Extraction of Hydroxyzine

All stock solutions and dilutions of hydroxyzine were prepared using 0.05% w/v phosphoric acid (H_3PO_4). A stock solution of hydroxyzine 1 μg/mL was used to prepare serial dilutions of hydroxyzine in concentrations ranging from 20 to 100 ng/mL. Frozen plasma was thawed at room temperature and 0.5 mL was added to each of the100 μL serial dilutions of hydroxyzine. Test plasma samples from rabbit studies were thawed and 0.5 mL was used for each analysis. To each of these samples were added 15 μL of antazoline solution, 1 μg/mL, as internal standard, 250 μL of 10% potassium hydroxide solution (KOH), and 5 mL freshly distilled ether. The samples were mixed by vortex for 30 sec, then centrifuged for 5 min. The aqueous phases of these samples were frozen in a dry ice/acetone bath. The ether layers were transferred to clean dry 16 x 100 mm test tubes, followed by the addition of 200 μL of 0.5 % w/v phosphoric acid. The contents of each test tube were mixed again on a vortex mixer for 30 sec then centrifuged for 5 min. As before, the aqueous layers were frozen in a dry ice/acetone bath, then the ether layers were discarded. The frozen aqueous layers were left to thaw under a stream of nitrogen gas to remove any remaining traces of ether. The sample tubes were stored at room

temperature for 24 h. From these samples a 150 μL aliquot of phosphoric acid extract of hydroxyzine was injected directly into the HPLC system (128).

Using the method described below in section 2.3.1.2., cetirizine, as *in vivo* metabolite of hydroxyzine, plasma concentrations were extracted and analyzed where there were sufficient plasma samples remained after hydroxyzine analysis.

2.3.1.2. Extraction of Cetirizine

All stock solutions and dilutions of cetirizine were prepared using 0.05% w/v phosphoric acid (H_3PO_4). A stock solution of cetirizine 1 μg/mL was used to prepare serial dilutions of cetirizine in concentrations ranging from 20 to 100 ng/mL. Frozen plasma samples were thawed at room temperature and 0.5 mL was added to each of the 100 μL of serial dilutions of cetirizine. Test plasma samples from rabbit studies were thawed and 0.5 mL was used for each analysis. To each of these samples were added 50 μL aliquot of J028 solution, 3 μg/mL, as the internal standard, 0.5 mL of sodium citrate buffer (1M, pH 5.0) and 3 mL of ethyl acetate. The samples were mixed by vortex for 60 sec, then centrifuged for 15 min. The aqueous phases of these samples were frozen in a dry ice/acetone bath. The ethyl acetate layers were transferred to clean dry 16 x 100 mm test tubes. The frozen aqueous layers were allowed to thaw, then these samples were re-extracted as before using another 3 mL of ethyl acetate. The ethyl acetate layers from the second extraction were combined with the ethyl acetate fractions from the first extraction. To the combined ethyl acetate layers of these samples of cetirizine, 200 μL of 1.7 % w/v phosphoric acid was added. The contents of each test tube were mixed on a vortex mixer for 60 sec then

centrifuged for 15 min at. The aqueous layers were frozen in a dry ice/acetone bath, and the ethyl acetate layers were discarded.

The frozen aqueous layers were left to thaw under a stream of nitrogen gas to remove any remaining traces of ethyl acetate. The sample tubes were stored at room temperature for 24 h. From these samples a 150 μL aliquot of phosphoric acid extract of cetirizine was injected directly into the HPLC system (142).

Calibration curves were prepared following the analysis of hydroxyzine or cetirizine extracts by plotting mean peak area ratios of the drug to the internal standard versus the concentrations of the drug.

The extraction efficiency was carried out using the same procedure as described above and the following two steps. First, the "spiked" plasma samples with each containing serial dilutions of hydroxyzine or cetirizine in concentrations ranging from 20 to 100 ng/mL, in the presence of internal standard, were extracted. Second, the "spiked" plasma samples with each containing serial dilutions of hydroxyzine or cetirizine, without the presence of internal standard, were extracted. The internal standard was added to the phosphoric acid extract of hydroxyzine or cetirizine in those samples where it was not added prior to extraction. From these phosphoric acid extracts of hydroxyzine or cetirizine, a 150 μL aliquot was injected directly into the HPLC system. The efficacy of the extraction was calculated as a ratio of the peak area ratio of the extract in the first step to the peak area ratio of the extract in the second step.

To test the selectivity of the assay, one sample, pre-dose, of rabbit plasma was obtained from six rabbits before applying the test formulations. These

samples were treated and analyzed using the validated HPLC methods described in Sections 2.2.1.1 and 2.2.1.2 for hydroxyzine and cetirizine respectively.

To check the linearity at the day of analysis, calibration curve samples were extracted and run always before analyzing the extracted plasma samples

2.3.2. Preparation of the Dosage Forms

The PC-SUV and PC-MLV of hydroxyzine or PC-SUV, PC-MLV, HPC-SUV and HPC-MLV of cetirizine were prepared as described in Sections 2.2.2 and 2.2.3. The liposome suspensions were concentrated by the filtration, as described in section 2.2.2.2, so that 1 mL contained 10 mg of hydroxyzine or cetirizine. To confirm that the non-medicinal ingredients of liposomes such as the phospholipids and cholesterol did not have any peripheral antihistaminic activity, non-medicated SUV were also prepared using PC.

The concentrated liposome suspensions were sufficiently viscous in consistency to be applied without incorporating into an ointment or cream base. All liposome suspensions were stored at 10±2°C until the day of the study.

The GB cream formulation containing 10 mg/g of hydroxyzine or cetirizine was prepared by dissolving the H_1-antihistamine in 1 mL of water before levigation into the GB by geometric dilution using a spatula on an ointment slab.

The final product was placed in a plastic ointment jar and stored in the refrigerator at 10°C until the day of *in vivo* evaluation.

2.3.3. *In vivo* Study Design

The animal research study, approved by University of Manitoba Fort Garry Campus Protocol Management and Review Committee (PMRC), was conducted according to current guideline published by the Canadian Council on Animal Care (CCAC).

2.3.3.1. Study Design

The animal research study was a randomized cross over design. This study required 1 gm of GB formulations, as a control, containing 10 mg hydroxyzine or 10 mg cetirizine. In addition, the freshly prepared 1 mL PC-SUV and 1mL PC-MLV containing 10 mg hydroxyzine, 1 mL PC-SUV, 1mL PC-MLV, 1mL HPC-SUV and 1 mL HPC-MLV containing 10 mg cetirizine. All formulations were stored at 10±2°C until the day of *in vivo* evaluation.

2.3.3.2. Animal Model

Six New Zealand white rabbits, mean weight ± standard error of the means (SEM) is 3.2 ± 0.05 kg, obtained from the Department of Zoology, Faculty of Science, University of Manitoba were studied. Rabbits were not studied until after a one-week treatment of antibiotic therapy followed by a two-week environmental adjustment period. Before and between investigations, each rabbit was housed individually in metal cages, with a wire floor to reduce coprophagy. Food and water were supplied *ad libitum*. Rabbits were allowed time to exercise and play each day according to CCAC guidelines. During initial catheterization and dosing, each rabbit was placed briefly in a restrainer cage

and then returned to its own holding cage. Studies were scheduled 3 or more weeks apart for each animal, to allow recovery from previous studies (143 -145).

2.3.3.3. Procedure

2.3.3.3.1. Preparation of the Rabbits

The preparation of the rabbits was conducted with the help of trained technicians and under the supervision of the university veterinarian. Two days before each study, the hair was cut from a 12cmx12cm area on the back of each rabbit using a hair clipper. One day later, the day before each study, a depilatory (Nair) was applied for 15 min to the 12cmx12cm area on the back and both ears, then the depilatory was removed. To prevent any irritation to the rabbits' skin, the back and ears were thoroughly washed with lukewarm water to ensure all remaining depilatory and hair residues were removed from the hairless areas and proximal hair. The rabbits were dried with clean towels and held in a warm area until completely dry. During the preparation of the rabbits' backs and on each study day before each study commenced, the university veterinarian inspected the rabbits carefully. No visual signs of skin irritation were observed using this hair-removal procedure.

2.3.3.3.2. Wheal Circumference

The peripheral H_1-antihistamine activity of hydroxyzine or cetirizine was assessed by evaluating suppression of the wheals produced by an intradermal injection of 0.05 mL of histamine phosphate, 1.0 mg/mL. A different site on the designated area 10cmx10cm after hydroxyzine or cetirizine application on the back was used for each test. The skin test was performed,

once before application of hydroxyzine or the cetirizine formulations to determine the baseline wheal area, then after the application of hydroxyzine or cetirizine formulations each time a blood sample was taken. Before the first skin test only, 1 mL of Evans blue dye, 10 mg/mL, was injected into the opposite ear vein to facilitate identification of the histamine-induced wheal circumferences.

The pre-dose wheal area and wheal areas observed at each test time 0.5, 1, 2, 3, 4, 5, 6, 8,10, 24 h were traced 10 min after each histamine injection, transferred to transparent paper and scanned into a computer using an Epson Scanner. The wheal areas were calculated using 5.0 Sigma Scan® Software (146).

Before the beginning of the animal studies, a pilot study to determine the reproducibility of wheals produced by intradermal injections of 0.05 mL of histamine phosphate, 1.0 mg/mL was conducted. The mean ±SEM and coefficient of variations of these wheal areas induced on the prepared backs of several rabbits were calculated.

To confirm that the non-medicinal ingredients of liposomes such as the phospholipids and cholesterol did not have any peripheral antihistaminic activity, non-medicated SUV were also prepared. The histamine skin tests, intradermal injections of 0.05 mL of histamine phosphate1.0 mg/mL were performed at one-hour intervals, for up to 4 hours after application of non-medicated SUV.

2.3.3.3.3. Blood Sampling

For blood sampling, the ear artery of each rabbit was dilated by rubbing with a swab wetted with 70% isopropyl alcohol before insertion of the

22 G-catheter into the ear artery. Then a male adaptor plug filled with heparin sulfate, 100 IU / mL, was inserted into the head of the catheter. After 0.5 mL of the blood was withdrawn and discarded, a 1.5 mL blood sample was collected as the pre-dose control and placed in a vacutainer with no additives. The catheter was flushed with 2 mL of 0.9 % sodium chloride followed by 0.2 mL heparin solution.

For dosing, 1 mL SUV, 1 mL MLV, or 1 gm GB each containing 10 mg of hydroxyzine or cetirizine was thoroughly applied to the defined area 10cmx10cm on the rabbit's back. The concentrated liposome suspensions were sufficiently viscous to be applied to the defined area without any loss. CCAC approved collars were placed around the neck of each rabbit during the 24-hour study to prevent it from licking its back or dislodging the catheter from the ear artery. The blood sampling was repeated, as previously described for the pre-dose sample, at 0.5, 1, 2, 3, 4, 5, 6, 8, 10 and 24 h. After centrifugation for 15 min with the aid of Sure Sep-II separators, the plasma was separated and stored frozen at –20°C. Later the samples were thawed, and 0.5 mL was used for each analysis. Plasma hydroxyzine and cetirizine concentrations were analyzed using the validated HPLC methods described in Section 2.3.1.

2.3.3.3.4. Dose Remaining on Skin

After 24 h the liposomes applied to the rabbit's skin would be dehydrated and destabilized (147) so any drug remaining on the defined area on the backs of the rabbits would be no longer entrapped in the liposomes. The amount of the dose remaining on the skin was determined by wiping the defined,

treated back area to remove any remaining medication using three gauze sponges wetted with 70 % isopropyl alcohol. The gauze sponges were soaked in 100 mL water and stored under refrigeration for 24h, squeezed to obtain as much of drug solution as possible, and rinsed two times with 50 mL aliquots of fresh water. The water rinses were combined and the sponges were discarded. The 200 mL solution was filtered, then analyzed for hydroxyzine and cetirizine using the validated HPLC method described previously in Sections 2.2.1.1 and 2.2.1.2. respectively. During the 24 h, the CCAC approved collars were placed around the neck of each rabbit to prevent the rabbit from licking the formulations on its back.

2.3.4. Data Analysis

2.3.4.1. Pharmacodynamic Analysis

Pharmacodynamic analysis was conducted by calculating the percent wheal suppression. The wheal areas were calculated using 5.0 Sigma Scan® Software. The percent suppression of the histamine-induced wheals was used as an indication of peripheral H_1-antihistaminic activity or the efficacy of medication (E). E was calculated using Equation 2.

Equation 2: $E = (W_0-W_t)/W_0 \times 100$

Where: E is the efficacy of the medication; W_0 is the baseline wheal area; and W_t is the wheal area after time "t" of medication application.

2.3.4.2. Pharmacokinetic Analysis

Following analysis of the blood samples, the plasma cetirizine concentrations were plotted versus time, then the area under curve (AUC) was calculated using WinNonlin Software.

After 24 h, the percent amount of the dose remaining on the skin was calculated using Equation 3.

Equation 3:

Percent Dose Remaining = $(D_{24} / D_{Initial}) \times 100$

Where $D_{Initial}$ is the original hydroxyzine or cetirizine dose applied and D_{24} is the amount of hydroxyzine or cetirizine remaining after 24 hours

2.3.4.3. Statistical Analysis

Statistical analysis was performed using multi-way ANOVA method (split analysis) and Tukey, Bonferroni methods with the aid of PC- SAS release 8.02e, Software. The following statistical analysis of the data were conducted: (1) the histamine-induced wheal areas obtained at each time for each formulation were compared with the pre-dose values, and with values at all times among the formulations; (2) the extent of medication absorbed into systemic circulation using plasma hydroxyzine and cetirizine concentrations was compared among the 3 formulations; and (3) the percentage of the medication remaining on the backs of the rabbits was compared among the 3 formulations. Differences were considered significant at $p \leq 0.05$.

CHAPTER III: RESULTS AND DISCUSSION

3.1. *In Vitro* Studies of Hydroxyzine and Cetirizine

3.1.1. Calibration Curves of Hydroxyzine in Aqueous Solutions

The data from the mean calibration curves of hydroxyzine using antazoline as internal standard are shown in Table1 and Figure1. The curve was constructed by plotting the mean peak area ratios of hydroxyzine to antazoline versus concentrations of hydroxyzine. Reproducibility was expressed as the percent Coefficient of Variation (% C.V.). The calibration curves were linear over the range 100-800 ng/mL with $R^2 = 0.99$ based on expected hydroxyzine concentrations. The linear equation $y= 0.001x - 0.0112$ derived from average data, was used to calculate the hydroxyzine concentrations in all *in vitro* samples. The peaks of hydroxyzine and antazoline were well-separated yielding retention times of 6 minutes and 8 minutes respectively. The value 2.5 ng was considered to be the lowest limit of quantification. A representative HPLC chromatogram is shown in Figure 1, Appendix A.

3.1.2. Calibration Curves of Cetirizine in Aqueous Solutions

The data from the mean calibration curves of cetirizine using J028 as internal standard are shown in Table 2 and Figure 2. The calibration curve was constructed by plotting peak area ratio of cetirizine to J028 versus concentrations of cetirizine. Reproducibility was expressed as the percent Coefficient of Variation (% C.V.). The calibration curves were linear over the range 100-1000 ng/mL with $R^2 = 0.99$ based on expected cetirizine concentrations. The linear equation $y= 0.0027x - 0.0027$ derived from average

data, was used to calculate the cetirizine concentrations in all *in vitro* samples. The peaks of cetirizine and J028 were well-separated yielding retention times of 5 minutes and 7 minutes respectively. The value 2.5 ng was considered to be the lowest limit of quantification. A representative HPLC chromatogram is shown in Figure 2, Appendix A.

3.1.3. Validation of Percent Entrapment of Hydroxyzine and Cetirizine

The method used to determine percent entrapment of hydroxyzine (PETH) or percent entrapment of cetirizine (PEC) was validated. To determine PETH or PEC, the liposome suspensions were concentrated using the Amicon Ultrafiltration Apparatus and an ultrafiltration membrane with a greater than 100,000 M.W. cut-off to obtain a clear filtrate. The amount of hydroxyzine or cetirizine not entrapped into the vesicles was measured in the clear filtrate.

To account for any loss of hydroxyzine or cetirizine onto the ultrafiltration membrane, the extent of adsorption of hydroxyzine or cetirizine to the membrane was evaluated by separate filtration studies of aqueous solutions of hydroxyzine or cetirizine at various concentrations. The amount of hydroxyzine or cetirizine in the aqueous solutions was determined before and after filtration. There was no detectable hydroxyzine loss by adsorption onto the filtration membrane, and only a small amount of the cetirizine content, 0.6 %, was adsorbed onto the filtration membrane. Any loss of cetirizine by adsorption to the filtration membrane was included in the calculation of PEC results.

3.1.4. Formulation Factors Evaluated During Liposome Preparation

3.1.4.1 Effect of Using Different Methods of Preparation of MLV

Multilamellar vesicles (MLV) of hydroxyzine were prepared using phosphatidylcholine (PC) and cholesterol (CH) and the lipid film hydration method. Phosphate buffer 0.02 M, at pH 7 was used to hydrate the lipid films. This buffer pH was selected because the neutral pH 7 should not irritate the skin. The results were the mean data of at least three experiments and were very reproducible with standard errors of the mean (SEM) ranging from 0.5 to 3 %. Therefore, in stability study samples that resulted in no loss of percent entrapment of hydroxyzine (PETH) over 24 months, intermediate-time PETH values that were > ± 5% of initial PETH values were considered as outliers and not included in the data analysis.

In Table 3 and Figure 3, it is shown that the initial PETH was not affected either by an increase in hydration time of the lipid films for up to 48 h, or by freezing-thawing for 5 cycles. Overall, PETH was about 95%. The variations in the method of preparation using lipid film hydration did not seem to affect the initial percent entrapment of hydroxyzine.

The long-term stability of the liposomes stored at 10 ± 2°C monitored by PETH was not affected either by the increase in hydration time or by the freezing-thawing cycles. Overall, PETH was similar to the initial values even after 24 months of storage at 10 ±2°C.

There was no change in the physical appearance of the liposomes in batch B and the control batch. Some slight discoloration was observed in the

liposomes in batches A, C, D, and E after storing the liposomes for 4 months but the long-term stability of the liposomes, evaluated by monitoring PETH, was not affected. The slight discoloration might be due to some oxidation or hydrolysis of the PC. Antioxidants were not added to the liposome formulations. There was virtually no difference in PETH, and visual appearance between the liposomes of the control batch and batch B. This indicates that the hydration time of the lipid films for 1 h or 24 h without freezing and thawing may yield the most stable formulations.

Batches of liposomes were also stored at 37±0.1°C to evaluate their stability when stored at temperatures above room temperature of 25±3°C. The data in Table 4 and Figure 4 reveal that the PETH of the liposomes stored at 37±0.1°C decreased considerably after just one month. Also following visual inspection, a loss of the liposome structure appeared to occur as evidenced by the appearance of the brown droplets on the surface of the liposome suspensions in all liposome batches, possibly due to hydrolysis of PC. Liposome formulations of the control batch, 26.5%, batch B, 27.6%, and batch D, 43.0%, appear to retain higher PETH than that of batch A, 13.2%, batch C, 12.6%, and batch E, 15.1%. The freezing and thawing of the liposomes after hydration may result in an increase in the fragility of the liposome bilayer membrane and adversely affect the long term stability of the liposomes, especially at the higher storage temperature of 37±0.1°C.

Based on these results, the method used to prepare the control batch, and storage at 10°C may result in the most stable formulations. This preparation

method involved lipid film hydration for 1 h and the liposomes were not subjected to any freezing and thawing processes. This procedure was selected for the preparation of liposomes to study long term stability and to prepare all other liposome batches. These results are in agreement with those of Patel and Misra (148) who found that a hydration time of 2 h was optimum for the preparation of clofazimine-loaded MLV liposomes using PC.

In Table 5 and Figure 5, the data show no difference between the initial PETH, 94.0%, of both PC-SUV and PC-MLV prepared using buffer pH 7. After one month of the liposomes storage at 37±0.1°C, PETH of both SUV and MLV decreased considerably to about 27.0 % relative to the initial 94.0%. This may indicate extensive hydrolysis and oxidation of PC- bilayers and rupture of the most of the liposomes after storage at 37±0.1°C for one month.

In order to determine if the pH could be reduced to be more similar to that of skin pH 4.5-6.5 (149), PC-SUV and PC-MLV liposomes were prepared at pH 6.5 then the liposomes were stored at 37°C. In Table 6 and Figure 6, the data show that the initial PETH of PC-SUV 86.0% and PC-MLV 94 .3% were similar to liposomes prepared using buffer pH 7. PETH of both liposome formulations decreased considerably after one month. Reduction in PETH of PC-SUV to 27.1% was greater than that of PC-MLV to 61.8% after one month. This could be explained by the fact that MLV are multilamellar and the loss of the outer lamella of some liposomes would have less effect on their ability to retain some of the drug entrapped in the inner lamella or aqueous phases. Since SUV are

unilamellar, the loss or rupturing of the single bilayers may result in considerably more drug loss at 37±0.1°C.

The results in Tables 5, 6 and Figures 5, 6 show that at 37±0.1°C, long-term PETH of PC-MLV 61.8% was greater at buffer pH 6.5 compared to that when buffer pH 7, 26.5% was used. This result indicates that using buffer pH 6.5 to hydrate the lipid film might result in more stable formulations at higher temperatures.

Short- term evaluation of the stability of PC liposomes containing hydroxyzine or cetirizine at 37±0.1°C, body temperature, was conducted to evaluate the stability of the liposomes when applied on the skin. PETH of PC-SUV and PC-MLV, prepared using buffer pH 6.5, were determined every day up to 7days.

The data in Table 7 and Figure 7 show that after storage for 7 days, PETH of PC-SUV and PC-MLV, 82.0%, were similar to the initial PETH 86.0% and 94.3% respectively. A slight discoloration of the liposome suspensions relative to the initial formulations was observed after 6 days. This discoloration was more intense in case of PC-MLV than that of PC-SUV. The data in Table 8 and Figure 8 show that after storage for 7 days, percent entrapment of cetirizine (PEC) in PC-SUV and PC-MLV, about 91.0 %, were similar to the initial PEC 92.0 %. A slight discoloration of the liposome suspensions relative to the initial formulations was observed after 6 days.

Overall, these results indicate that the freshly prepared PC liposomes are sufficiently stable for at least 24 h at body temperature and can be used for

in vivo evaluation to assess the efficacy of the formulations applied topically on the skin.

3.1.4.2. Effect of Using Buffers at Different pH Values

Hydroxyzine and cetirizine are reported to have different ionic forms at different pH values that might affect their entrapment and retention within the liposomes and consequently their stability (117). To evaluate the effect of changing the pH of a hydrating buffer on the entrapment of hydroxyzine or cetirizine and the stability of their liposomes, the phospholipid PC and a series of buffer solutions at pH values of 5.0, 5.5, 6.0, 6.5 and 7.0 were used to prepare the liposomes. The results were a mean from at least three experiments and were very reproducible with standard errors of the mean (SEM) ranging from 0.5 to 3 %. Therefore, in stability study samples that resulted in no loss of percent entrapment of hydroxyzine (PETH) over 24 months, intermediate-time PETH values that were > $\pm$ 5% of initial PETH values were considered as outliers and not included in the data analysis.

In Tables 9-12 and Figure 9, the initial PETH and PEC of freshly prepared SUV and MLV liposomes are shown. The PETH of SUV sharply increased from 53.0% to 84.0% when the pH of the buffer used was increased from 5.0 to 5.5. As pH increased from 6.0 to 7.0, PETH continued to increase from 86.0 % to 94.0 %. The lower entrapment of hydroxyzine at a pH 5.0 may be due to the presence of hydroxyzine mainly in the cationic form, which has lower lipophilicity of log P^{C}_{oct} = 0.93, than the non-ionic form with log P^{N}_{oct} = 3.5 (117). This indicates that by increasing the pH of the buffer from 5.5 to 7.0, the cationic form

of hydroxyzine may have gained lipophilicity by conversion into the non-ionic form consequently showing more affinity in the anisotropic system, liposomes/water, resulting in a higher PETH. This explanation is in agreement with the results of Balen *et al.*, (117) who found that the values of log D, distribution coefficient of different forms of hydroxyzine, an indicator of the lipophilicity, were 2.76, 3.13, and 3.46 at the pH range from 3.1 to 4.9, and at pH 7.4, and pH 9 respectively. These data indicate that the cationic form gained lipophilicity by increasing the pH of the buffer used.

The initial PETH of MLV increased slightly from 82 % to 94 % as the buffer pH values increased from 5.0 to 7.0. It is clear that the effect of buffer pH has less impact on the entrapment of hydroxyzine in MLV than SUV. To explain this finding we developed the following model shown below that is also supported by the results of Balen *et al.,* (117), where H-C^+= cation form of hydroxyzine, H-NI= non-ionic form of hydroxyzine, H-SUV= small unilamellar vesicles containing hydroxyzine, H-MLV= multilamellar vesicles containing hydroxyzine.

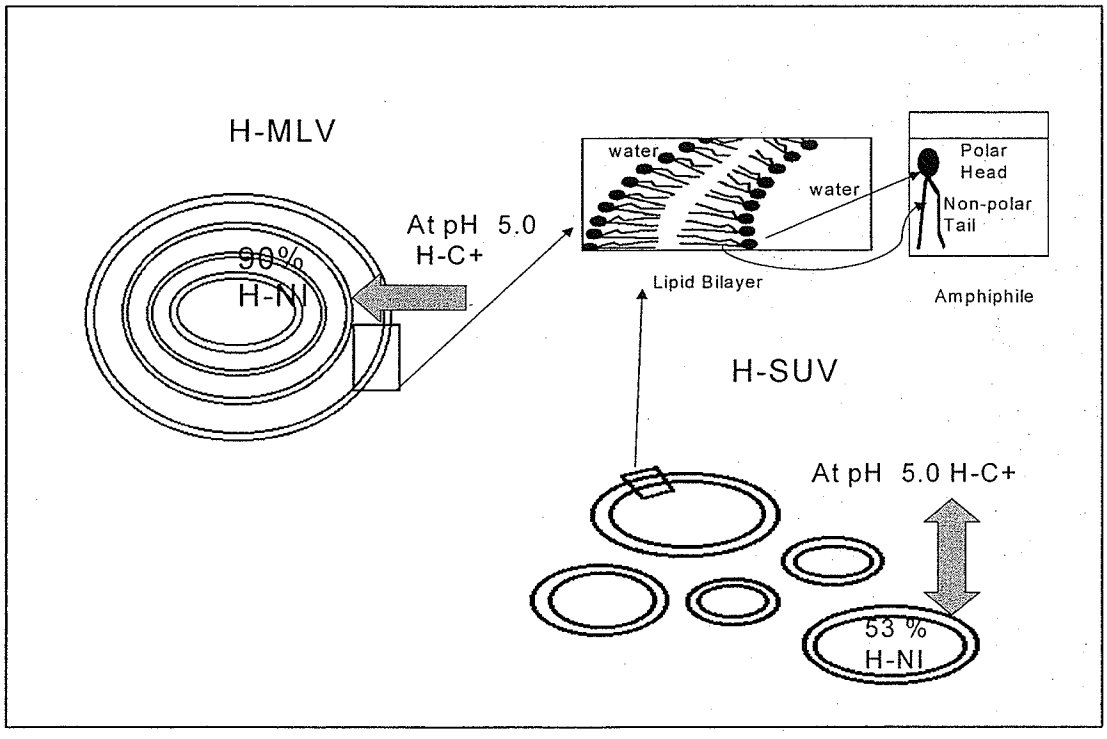

In MLV, we assume that the cationic form of hydroxyzine gained lipophilicity by conversion to the non-ionized form after penetrating into the outer MLV bilayers that maintained drug retention. Then the non-ionic form penetrated into the deeper multilamellar bilayers of the MLV, creating a concentration gradient across the liposome membranes that encouraged more penetration of the non-ionic form of hydroxyzine into the deeper bilayers, consequently enhancing the entrapment. In contrast, this concentration gradient across the liposome membrane did not occur in case of SUV because they are unilamellar. Instead of the concentration gradient, an equilibrium occurs across the single membrane of SUV between the non-ionic forms of hydroxyzine in the aqueous core of the liposomes and the aqueous vehicle surrounding the liposomes, so no further entrapment occurs. This explanation is supported by our finding that only 53.0% entrapment of hydroxyzine occurred at pH 5.0. As more of the non-ionized form of hydroxyzine was present when pH increased from 5.5 to 7 the percent entrapment increased ranging from 84.0% to 94.0% respectively to maintain the equilibrium across the membrane of SUV between the non-ionic forms of hydroxyzine in the aqueous core of the liposomes and the aqueous vehicle surrounding the liposomes.

In contrast to hydroxyzine, for cetirizine there was no effect of pH on PEC in SUV or MLV, which ranged from 92 % to 94 % as buffer pH values increased from 5.0 to 6.5. These findings can be explained by the results of Balen *et al.*, (117) that cetirizine has three forms, which are cationic ($\log P^{C}_{oct}$ =1.12, $\log P^{C}_{lip}$ =3.2), zwitterionic ($\log P^{Z}_{oct}$ =1.55, $\log P^{Z}_{lip}$ =2.3) and anionic ($\log P^{A}_{oct}$ = -0.19,

log P^{A}_{lip}= 2.3). All three forms have a similar distribution coefficient, log D_{oct}= 1.5, log D_{lip} = 2.3, at pH values ranging from 3.1 to 9. This indicates that at pH range from 3.1 to 9, all forms of cetirizine passed equally from the isotropic system, n-octanol/water, compared to anisotropic system liposome/water. Also, all forms of cetirizine gained in lipophilicity when passing from the isotropic system to the anisotropic system creating a driving force that encouraged drug entrapment within the liposomes. From these finding, it is clear that the change in pH from 5.0 to 6.5 had minimal effect on cetirizine entrapment within PC liposomes.

The data in Tables 9,10 and Figures 10,11 show the long-term stability of both SUV and MLV of hydroxyzine. There was no change in PETH in SUV and MLV prepared using buffers at pH 5.0, 5.5, 6.0, 6.5, and 7.0 when stored at 10°C for up to 24 months compared to initial PETH values. Also there was no observed discoloration or change in the physical appearance of the liposomes. No visual mold growth was observed, because all batches were purged with nitrogen to remove traces of atmospheric oxygen while placed in the opaque containers that were well-sealed and air-tight. These findings indicate that using the buffer at pH range from 5.5 to 7.0 to prepare the liposomes results in stable PETH of about 90 % for up to 24 months at 10°C and the retention of hydroxyzine within the liposomes persists for 2 years. This can be explained by the results of Balen *et al.,* (117), who found that at pH range from 5.5 to 7.0, hydroxyzine was mainly in the non-ionic form which had a higher affinity for liposomes than its cationic form, resulting in the drug retention within the liposomes after entrapment and stable long term PETH. It seems that pH value

starting from 6.5 may be the optimum pH for the preparation of liposomes containing hydroxyzine with satisfactory percent entrapment and stability.

The stability data of SUV and MLV of cetirizine are shown in Tables 11,12 and Figures 12,13. Following storage of the liposomes of cetirizine at 10°C, PEC of SUV prepared using buffers of pH values ranging from 5.5 and 6.0 slightly decreased after 24 months while PEC of MLV decreased from about 94% at baseline to 74% after 24 months. There was no visual change in the physical appearance of the SUV liposomes, but the loss of PEC in MLV was accompanied by some slight discoloration indicating minor oxidation of PC. It seems that the use of buffers at different pH did not affect the initial PEC of SUV and MLV. While all MLV formulations lost about 10% to 20% of PEC after 24 months at 10°C. The PEC at pH 5.0, and 6.5 in SUV formulations was unchanged. The decrease in PEC following storage may be due to the formation and leakage of the zwitterionic form of cetirizine, which had minimal binding affinity to the liposomes (117). The maximum PEC after 24 months at 10°C in SUV and MLV of 90.1% and 84% was observed at pH 6.5 and 6 respectively.

In summary, over the pH range of 5 to 6.0, cetirizine entrapment was slightly higher than hydroxyzine entrapment in both SUV and MLV. The change in the pH of buffer from 5.0 to 6.5 had a minimal effect on the entrapment of cetirizine in both SUV and MLV. This pH range also had a minimal effect on the entrapment of hydroxyzine in SUV and MLV, except below pH 5.5 where PETH was reduced in SUV. In all formulations, independent of pH, PETH was stable at 10°C for up to 24 months while PEC decreased slightly.

From these results, it would appear that the buffer of pH 6.5, and 7 is optimal for entrapment and stability of hydroxyzine in SUV and MLV liposomes, while the buffers of pH range from 5.0 to 6.5 are optimal for the initial entrapment and stability of cetirizine in SUV and MLV liposomes. The preparation of both hydroxyzine and cetirizine liposomes using a buffer of pH 6.5 value is recommended for the entrapment and the shelf-life stability of the liposomes. In addition it approximates the pH of the human skin, pH 4.5 to 6.5 (149).

3.1.4.3. Effect of Using Different Phospholipids

Retention of entrapped compounds within the liposomes for a sufficient period of time is the most important factor that has to be evaluated to ensure the stability of the formulations (150). The rate and extent of leakage of the medication molecules from liposomes is governed by the physico-chemical properties of the entrapped molecules and by the type of phospholipids used to prepare the liposomes.

To evaluate the effect of changing the PL on the entrapment of hydroxyzine or cetirizine within the liposomes and the stability of these liposomes, a series of experiments was conducted comparing the unsaturated and neutral PL, phosphatidylcholine (PC) (Tc of -15°C), the unsaturated and negatively charged PL, phosphatidylserine sodium salt (PS) (Tc of 24°C), and the saturated and neutral PL phosphatidylcholine hydrogenated (HPC) (Tc of 50°C) (127). All liposome batches were prepared at pH 6.5. The results were the mean data of at least three experiments and were very reproducible with standard errors of the mean (SEM) ranging from 0.5 to 3 %. In stability study samples

resulting in no loss of percent entrapment of hydroxyzine (PETH) over 24 months, intermediate-time PETH values that were > ± 5% of initial PETH values were considered as outliers and not included in the data analysis.

Regardless of the PL used in the preparation of the liposomes, in all formulations the mean initial PETH and PEC values were similar, ranging from 86% to 94%. It seems that the difference in the Tc or using neutral or negatively charged PL had minimal or no effect on the initial PETH or PEC of SUV and MLV prepared at pH 6.5. Initial PETH of PC-SUV, HPC-SUV, PS-SUV, PC-MLV, HPC-MLV, and PS-MLV were 86.0%, 93.0%, 91.0%, 94.3%, 94.0%, and 93.0% respectively as shown in Tables 13-18 and Figures 14-19. Initial PEC of PC-SUV, HPC-SUV, PS-SUV, PC-MLV, HPC-MLV and PS-MLV were 92.0%, 92.8%, 93.4%, 92.0%, 89.7%, and 90.7% respectively as shown in Tables 19, 20 and Figures 20, 21.

The consistency of PETH in SUV and MLV at different storage temperatures for up to 24 months is also shown in Tables 13-18 and Figures 14-19. At 37°C for up to 24 months, HPC-MLV of hydroxyzine were stable resulting in PETH of 91.0% similar to the initial PETH as shown in Table14 and Figure 15. After one month at 37°C, PETH of PC-SUV and PC-MLV of 27.1% and 61.8% respectively were markedly decreased compared to initial PETH of 86.0% and 94.3% respectively as shown in Tables 13,14 and Figures 14, 15. The instability of PC liposomes and loss of drug entrapment at 37°C is consistent with the data of Betageri (150) which showed that the degree of disorder of the lipid bilayer and consequently the permeability of liposomes is temperature dependent. At the

storage temperature of 37°C, the PC bilayers are in a higher degree of disorder, compared to the other storage temperatures at 10°C and 25°C, resulting in liposomes in the liquid crystalline state. Consequently the bilayer membranes are permeable to entrapped molecules resulting in a major decrease in PETH after one month and the visual loss of liposome structure as indicated by the appearance of brown droplets on the surface of the liposomes. At 37°C for up to 24 months, PETH of PS-SUV of 94.0 % was similar to the initial 91.0 %. At 37°C for up to 13 months, PETH of PS-MLV 92.0% was similar to the initial 94.0% but after 13 months at 37°C PS-MLV lost their liposomal structure and consequently PETH as shown in Tables 13,14 and Figures 14, 15. It seems that PS-SUV were more stable than PS-MLV.

The data in Tables 15-18 and Figures 16-19 show that the storage of the liposomes at 10°C and 25 °C for up to 24 months, regardless of the PL used to form SUV and MLV, had minimal effects on the liposome stability as long-term PETH ranged from 90 % to 97 %. Some discoloration of PC liposomes was observed after 4 months of storage at 25°C, while for PS-SUV some discoloration was observed after 4 months of storage at 10°C and 25°C indicating possible minor hydrolysis and oxidation of the PL. This discoloration increased with time for up to 24 months but was not accompanied by a loss of PETH.

The stability of both HPC-SUV and HPC-MLV may be attributed to the higher Tc of HPC, 50°C. This results in the presence of the liposomes in the gel state, which encourages the retention of hydroxyzine or cetirizine within the

liposomes. Despite the fact that the storage temperatures of 10°C and 25°C were above the Tc of PC, the long-term PETH and the physical appearance indicated that the PC-MLV and PC-SUV formulations containing hydroxyzine were stable. The stability may be attributed to the presence of cholesterol molecules. These molecules are amphipathic, have a hydrophobic tail and a hydrophilic 'polar head', which stack themselves at the outer half of the lipid region of the bilayer membrane of the liposomes with the polar hydroxyl group located at the level of the bridge region, where hydrogen bonding can take place (81). This arrangement increases the stability of the liposomes and reduces the leakage of medications through the bilayer membranes of the liposomes (81 - 86). Above the transition temperature of phospholipids, the CH molecules reduced the rotational freedom of acyl chains in the liquid crystal phase resulting in closer and more condensed packing, thereby decreasing the fluidity of the bilayer membranes of the liposomes (73).

The rapid discoloration of PS liposomes of hydroxyzine at 10°C and 25°C, although the long-term PETH was unchanged, may indicate hydrolysis and/or oxidation of the PS and lower stability relative to PC and HPC from 4 to 24 months.

Storage of cetirizine liposomes at 10°C for up to 24 months as shown in Table 19 and Figure 20 had minimal effects on the long-term PEC of HPC-SUV or HPC-MLV, which ranged from 87% to 92%.

At 10°C for up to 24 months, the initial PEC of PC-MLV and PS-MLV decreased over time from 92.0 % to 74.3% and from 90.7 % to 69.8 %

respectively as shown in Table 20 and Figure 21. Some slight discoloration of the liposomal suspension of PC-MLV and PS-MLV of cetirizine was also observed.

From the PETH results, it appears that HPC-SUV and HPC-MLV liposomes of hydroxyzine were stable upon storage at 10°C, 25°C, and 37°C. The stability of PETH in PC-SUV and PS-SUV liposomes of hydroxyzine was optimal during storage at 10°C and 25°C for up to 24 months. At 10°C for up to 24 months, the PEC of PC-SUV, HPC-SUV and PS-SUV was stable. At 10°C for up to 24 months, the most stable liposomes were HPC-MLV while the least stable liposomes were PS-MLV.

3.1.4.3.1. Particle Size Analysis

The particle size of the liposomes in these hydroxyzine and cetirizine formulations, prepared using all three PL at pH = 6.5, was determined immediately following preparation and after storage at 10±2°C for 20 months using the submicron particle-sizer, and by measuring the largest diameter of the liposomes using the transmission electron micrographs (TEM) (X=112,200), and micrographs displayed on the screen of the computer monitor of the optical microscope (MOM). The data are shown in Table 21, Figures 22a, 22b, 22c, 23a, 23b, 23c, Appendix B, Figures 1-14 and Appendix C, Figures 1-6.

The mean particle sizes of the liposomes, determined using the submicron particle-sizer method for SUV and MLV, were not consistent with the results found by measuring the liposomes from the TEM or MOM. Using the submicron particle-sizer light-scattering technique method, the mean ± SD particle size distribution of all of the liposomes in the test sample was determined. However,

aggregates of liposomes would be recorded as individual liposomes, consequently yielding larger mean particle sizes. Using the TEM or MOM method, individual liposomes were identified from the mounted samples and the largest diameters measured as observed in the photographs, in case of TEM, or on the screen of the computer monitor in case of MOM. The MOM results more likely represent the true sizes of the SUV and MLV. The reproducibility of the MOM measurements was determined by five replicate measurements of representative SUV and MLV liposomes. For SUV the mean±SEM was 113±2.05 nm, % C.V. of 1.8% and for MLV the mean±SEM was 2037±4.44 nm, % C.V. of 0.2%. The MOM results in Table 21, were determined from the measurement of 10 liposomes in each of 6 test samples drawn from each batch of SUV or MLV. These results provide a larger sample size than TEM where often limited numbers of liposomes were located in the photographs.

From the MOM results, it was concluded that the ethanol injection method resulted in liposomes in the size range of SUV (<100 nm) and the lipid film hydration method resulted in liposomes of the size range of MLV (100 nm to 20 μm) as shown in Table 21. The MLV structure could be identified in the TEM. Further studies are needed to identify specific factors that may affect the physical stability of the liposome vesicles containing hydroxyzine or cetirizine. In most cases PETH and PEC results were unchanged following storage.

3.2. *In Vivo* Studies of Hydroxyzine and Cetirizine

The objectives of the *in vivo* studies were to determine the onset, intensity, and duration of the peripheral H_1-antihistamine activity, and the rate and the

extent of systemic absorption of hydroxyzine and cetirizine following the application of liposome formulations to the skin in a rabbit model.

The rabbit has been used for more than two decades as a model to test dermatological products including the topically applied liposomes (151). Also studies have shown that rabbit skin is as reactive as human skin to passive permeability of topically applied substances (152, 153).

The outer layer of the rabbit skin is the epithelium and is known as the epidermis or scarf-skin. It is stratified and composed of several layers of cells. The cells closest to the dermis are formative, growing cells, while those at the surface are flattened squamous cells, which are continuously being discarded. The multiple layers of the rabbit skin, yield a relatively thin membrane covering the entire body. This membrane extends over the entire surface of the rabbit body and connects at certain points with the epithelia of the internal surfaces. The membrane is supported by a thick resistant layer of connective tissue, which forms the true skin or corium (154).

The rabbit as a model to test dermatological medications is suitable because the rabbit body surface area is large enough to permit repeated dermatological tests, and the blood volume is of sufficient size to permit collection of the required number of timed blood samples without significantly affecting the volume of distribution of the medications. The total volume of blood collected from each rabbit was about 22 mL for each study period, always less than 10 % of the total blood volume of each rabbit (155). A recovery period of not less than two weeks was sufficient to allow the blood volume to be restored.

Before the cross-over studies commenced, the reproducibility of the histamine injection test was determined using the histamine-induced wheal area method on the shaved backs of 3 rabbits, 10 injections / rabbit. The mean wheal area obtained was 1.00 ± 0.05 cm^2 with a % C.V. of 8.6%.

To evaluate the possibility of any suppression of the histamine-induced wheals by the non- medicinal ingredients used in the preparation of the liposomes, including phospholipids and cholesterol, non-medicated PC-SUV were prepared and applied to the shaved backs of the rabbits using the same study design as used for hydroxyzine- and cetirizine- containing formulations. The histamine-induced wheal areas on the shaved backs of each rabbit were determined at time intervals of pre-dose, 0.5, 1, 2, 3 and 4 h. There was no significant difference between the pre-dose wheal areas in this study (1.18 ± 0.7 cm^2), and the wheal areas measured after each time interval. The mean values of the wheal areas were 1.11 ± 0.03, 1.33 ± 0.15, 1.46 ± 0.08, 1.3 ± 0.08, and 1.11 ± 0.13 cm^2 at 0.5, 1, 2, 3 and 4 h, respectively. The overall mean from the different time intervals was 1.25 ± 0.06 cm^2 with a % C.V. of 6.80 %. This value is not significantly different from the previously determined validation wheal area study, 1.00 ± 0.05 cm^2, with no application of non-medicated liposomes. These results confirm that phosphatidylcholine and cholesterol did not have any peripheral antihistaminic activity. The results are shown in Table 22 and Figure 24. These results would also be valid for PC-MLV, HPC-SUV and HPC-MLV.

In addition, phospholipids have never been reported to exhibit any antihistaminic activity.

3.2.1. HPLC Analysis of Hydroxyzine in Plasma

Table 23 and Figure 25 show the mean calibration curve of hydroxyzine using antazoline as the internal standard after extracting human plasma "spiked" with hydroxyzine and antazoline. The calibration curve was constructed by plotting the peak area ratio of hydroxyzine to antazoline versus concentrations of hydroxyzine. Reproducibility of the calibration curves were determined by constructing calibration curves each time the analysis of hydroxyzine concentrations were determined in the rabbit plasma samples. The variability is expressed as the percent Coefficient of Variation (% C.V.). The calibration curves were linear over the range selected, 20-100 ng/mL, with R^2 = 0.99. The mean linear equation y= 0.00069x – 0.0057 was used to calculate the concentrations of hydroxyzine in all of the rabbit plasma samples. The value 2.5 ng was considered to be the lowest limit of quantification. The extraction efficiency of hydroxyzine was 95 %. No interfering peaks were found in the chromatograms at the retention times of hydroxyzine or the internal standard.

3.2.2. HPLC Analysis of Cetirizine in Plasma

Table 24 and Figure 26 show the mean calibration curve data of cetirizine using J028 as the internal standard after extracting human plasma "spiked" with cetirizine and J028. The calibration curve was constructed by plotting peak area ratio of cetirizine to J028 versus concentrations of cetirizine.

Reproducibility of the calibration curves were determined by constructing calibration curves each time the analysis of cetirizine concentrations were determined in the rabbit plasma samples. The variability is expressed as the percent Coefficient of Variation (% C.V.). The calibration curves were linear over the range selected (20-100 ng/mL) yielding an $R^2 = 0.99$. The mean linear equation $y= 0.0129x - 0.0045$ was used to calculate the concentrations of cetirizine in all of the rabbit plasma samples. The value 2.5 ng was considered to be the lowest limit of quantification. The extraction efficiency of cetirizine was 85 %. No interfering peaks were found in the chromatograms at the retention times of cetirizine or the internal standard.

3.2.3. *In Vivo* Evaluation of PC Liposomes of Hydroxyzine

Liposomes have been used as a carrier system to deliver medications into the skin in order to achieve topical therapeutic effects with reduced systemic absorption (53, 54, 151). In both the SUV and MLV liposomes prepared for these studies, a high percentage of the amount of hydroxyzine incorporated into the formulations was entrapped within the liposome vesicles.

The liposome batches were prepared using phosphate buffer at pH 6.5. The SUV liposome formulations had a mean ± SD particle size of 0.26±0.2 μm using the submicron particle sizer and a mean ± SEM particle size diameters of 51.7±7.9 nm and 174.0± 82.1 nm using TEM and MOM respectively with 86.0% entrapment of the total amount of hydroxyzine added as shown in Tables 17, 21 and Figures 16, 22a, 22b, 22c. The MLV liposome formulations had a mean ± SD particle size of 4.87±0.65 μm using the submicron particle sizer, and a mean ±

SEM particle size diameters of 264.0±22.3 nm and 1020.0±70.1 nm using TEM and MOM respectively with 94.3% entrapment of the total amount of hydroxyzine added as shown in Tables 18, 21 and Figures 17, 22a, 22b, 22c. The MOM results probably more accurately represent the true sizes of the SUV and MLV prepared in these formulations compared to the submicron particle sizer and TEM results. These findings were discussed in Section 3.1.4.3.1.

The high extent of entrapment of hydroxyzine into the lipid vesicles was probably due to the lipophilicity of the neutral form of hydroxyzine in the liposome system (log P = 3.4), which was similar to that evaluated in an n-octanol/water system (log P = 3.5) (117).

Hydroxyzine peripheral H_1-antihistaminic activity over time is shown in Tables 25-27 and Figure 27 as absolute wheal areas, and in Tables 28 -30 and Figures 28, 28a, as percent suppression of histamine-induced wheals. In comparison with the pre-dose wheal areas, all hydroxyzine formulations significantly suppressed wheal formation for up to 24 h, $P \leq 0.05$. Onset of suppression was rapid, with about 75% suppression occurring as early as 0.5 hour as shown in Tables 28-30, Figures 28, 28a. Maximum suppression, 85% ± 5.6% to 94% ± 5%, was present from 2 to 6 h. There was no significant difference in activity among the formulations PC-SUV, PC-MLV, and GB, the control formulation, containing hydroxyzine, for up to 24 h.

Peripheral H_1-antihistaminic activity did not differ significantly after topical application of hydroxyzine in the 3 formulations tested. This finding may be attributed to the lipophilicity of hydroxyzine, possibly leading to complete skin

penetration of the drug regardless of the formulation. The efficacy of H_1-antihistamines in skin disorders such as urticaria in humans is attributed primarily to their H_1-antihistaminic activity on small unmyelinated afferent C-fibers and reduction of itching. In addition, H_1-antihistaminic activity on neurogenic reflexes reduces erythema/flaring, while H_1-antihistaminic activity on the endothelial cells of the postcapillary venules reduces leakage of the fluid and cells and resultant wheals (156).

The extent of systemic absorption of hydroxyzine was determined from the mean plasma hydroxyzine concentrations measured at the pre-selected times after hydroxyzine application, as shown in Tables 31-33 and Figure 29. Any variability in hydroxyzine plasma concentrations between the individual rabbit was considered during the statistical data analysis. The mean plasma hydroxyzine concentrations after PC-SUV and PC-MLV application were similar to each other, and significantly lower than those after GB application for up to 24 h, $P \leq 0.05$. Compared with both PC-SUV and PC-MLV formulations, which resulted in mean plasma concentrations of only 12.5 ± 12.1 to 0.9 ± 0.4 ng/mL, with an AUC of 80.1 ± 20.8 ng.h/mL, and 78.4 ± 33.9 ng.h/mL, respectively, over 24 h, the mean plasma hydroxyzine concentrations from GB were significantly higher and ranged from 51.7 ± 15.8 to 11.9 ± 4.6 ng/mL, with an AUC of 492 ± 141 ng.h/mL, $P \leq 0.05$.

The hydroxyzine plasma concentrations obtained from GB, when plotted versus time as shown in Figure 29, yield a plasma concentration versus time curve similar in shape to that of oral dosing curve, with a maximum concentration

at 1 h, followed by decreasing concentrations over time as the hydroxyzine was eliminated. These results may be due to the hydroxyzine being released rapidly from the GB and absorbed quickly thorough the skin as a bolus dose. The lipophilic nature of the medication would permit rapid passage through the stratum corneum and the other dermal layers into the systemic circulation. In addition GB, a water in oil emulsion base might improve the penetration of the hydroxyzine through the stratum corneum and increase its plasma concentrations. Hydroxyzine has a relatively large *in vivo* volume of distribution, so it would redistribute rapidly into the skin layers and produce the potent peripheral antihistaminic effects seen in this study, and shown previously in studies in human subjects to whom hydroxyzine was administered orally (146).

The SUV and MLV liposome formulations yielded relatively low and persistent plasma hydroxyzine concentrations in conjunction with rapid onset and duration of significant peripheral H_1-antihistaminic effects, as monitored by suppression of the histamine-induced wheals. These results indicate that the liposomes may be causing the hydroxyzine to be concentrated in the skin. This could be achieved by the liposomes adsorbing to the skin surface intact, before penetrating through the stratum corneum. The smaller SUV may penetrate the skin intact and then release the medication in a modified-release process during the ensuing 24 h. The larger MLV may shed the outer layers, slowly releasing some of the medication, and then penetrate the stratum corneum as oligolamellar vesicles and releasing the medication consistently over the 24 hours. This would

explain the low concentrations of hydroxyzine in the systemic circulation from the two liposome formulations.

The extent of systemic absorption of hydroxyzine from these formulations was also evaluated by measuring the plasma concentrations of cetirizine, the active *in vivo* metabolite of hydroxyzine. Sufficient plasma samples for these analyses were available as shown in Tables 34-36 and Figures 30, 30a. Any variability in cetirizine plasma concentrations between the individual rabbit was considered during the statistical data analyses.

There were no significant differences among mean plasma cetirizine concentrations ranging from 18.4 ± 3.7 to 70 ± 10.5 ng/mL arising from the hydroxyzine absorbed from PC-SUV (AUC of 765 ± 50 ng.h/mL), PC-MLV (AUC of 1035 ± 202 ng.h/mL), and GB (AUC of 957 ± 226 ng.h/mL) over 24 h. It is difficult to account for the fact that plasma cetirizine concentrations arising *in vivo* from hydroxyzine after the SUV and MLV formulations were not significantly different from those obtained after GB. The smaller volume of distribution of cetirizine would partly account for the higher plasma concentrations compared to hydroxyzine (121). If the hydroxyzine is concentrated in the skin from the SUV and MLV doses, then it is possible that it is metabolized to cetirizine in the skin, since the cytochrome P_{450} enzymes that would metabolize it to cetirizine *in vivo*, are definitely present in the skin (157). This requires further study. The cetirizine arising *in vivo* from the hydroxyzine-SUV and -MLV formulations likely also contributes to the suppression of the histamine-induced wheals (129).

The *in vivo* cetirizine concentrations achieved from hydroxyzine after the GB application would be consistent with rapid metabolism of hydroxyzine to cetirizine by the hepatic cytochrome P_{450} system (158). The pattern of suppression of the histamine-induced wheals by hydroxyzine from GB, as shown in Figure 28a, is consistent with the observed hydroxyzine plasma concentrations from GB and from cetirizine as shown in Figure 30a. An initial wheal suppression peak at 2 h caused by the hydroxyzine is followed by a secondary wheal suppression peak at 6 h probably caused by the formation of the active metabolite cetirizine *in vivo*.

At 24 h after topical application of 10 mg hydroxyzine in PC-SUV, PC-MLV, and GB, the amount of the hydroxyzine dose remaining on the skin ranged from $0.02 \pm 0.01\%$ to $0.06 \pm 0.02\%$ of the applied dose, and there was no significant difference among the formulations as shown in Table 37 and Figure 31. The amount of hydroxyzine remaining on the skin was very low compared with the initial dose applied. These results show that the low systemic concentrations of hydroxyzine following the application of the liposome formulations were not due to lack of absorption of the medication. The proposed mechanism of liposome penetration would explain the low concentrations of hydroxyzine in the systemic circulation from the 2 liposome formulations. This would need to be confirmed by measuring hydroxyzine concentrations in the skin in a different animal model. It was not possible to perform biopsy studies in the rabbits since the animals could not be euthanasia due to the crossover study design.

These results are in agreement with those of Mezei (159) and Foldvari *et al.*, (160) who have proposed several mechanisms to explain the liposome skin interactions and/or penetration. Multilamellar and unilamellar liposomes can be adsorbed to the skin surface intact before their penetration into the skin. Although larger liposomes may rupture on the skin surface releasing medication, smaller intact vesicles probably penetrate the skin. It is possible that intradermally localized unilamellar or oligolamellar vesicles are derived from multilamellar liposomes that have lost their outer bilayers by shedding during penetration. Foldvari *et al.*, (160) detected many intact SUV and to a lesser extent MLV liposomes, microscopically in guinea pig skin, by using electron-dense colloidal iron-containing liposomes.

Although skin concentrations of hydroxyzine were not measured in our study, the low plasma hydroxyzine concentrations and the accompanying rapid and persistent suppression of the histamine-induced wheals are also in agreement with Foldvari *et al.,* (160). These investigators found higher concentrations of ^{14}C-lidocaine in the epidermis and dermis of guinea pigs treated with liposome-encapsulated lidocaine compared with lidocaine in Dermabase (o/w) cream. Other investigators (53, 161-163) found that the application of MLV liposomes prepared using phosphatidylcholine and loaded with hydrocortisone resulted in increased drug concentrations in the various layers of the skin epidermis and dermis, with an accompanying decrease in the serum concentrations, potentially leading to an increase in efficacy, while simultaneously decreasing the risk of adverse systemic effects. Foong *et al.,* (54)

concluded that liposomal encapsulation of retinoids by soy phospatide and cholesterol can provide higher drug concentrations in the dermis and epidermis of albino guinea pig skin and lower drug concentrations in plasma and urine, in contrast to cream or gel dosage forms.

In this animal model we found that application of hydroxyzine in liposome formulations significantly reduced systemic exposure to the drug compared to GB, $P \leq 0.05$. In addition, the peripheral H_1-antihistaminic effects evaluated using suppression of the histamine-induced wheal formation were excellent and significant from the liposome formulations compared to pre-dose results, $P \leq 0.05$. These finding support our hypothesis that the liposomes may be causing the hydroxyzine to be concentrated in the skin.

3.2.4. *In Vivo* Evaluation of PC Liposomes of Cetirizine

Liposomes have been used as a carrier system to deliver medications into the skin in order to achieve the therapeutic effect with lower systemic absorption (53). By administering cetirizine in liposome formulations to the skin, the peripheral H_1- antihistaminic activity should be retained, potentially improving the therapeutic effects, while absorption into the systemic circulation should be reduced, minimizing the potential of adverse effects.

The liposome batches were prepared using phosphate buffer at pH 6.5. The SUV liposome formulations had a mean ± SD particle size of 0.17 ± 0.09 μm using the submicron particle sizer and mean ± SEM of 153.5±17.8 nm and 109.0±17.9 nm using TEM and MOM with 92.0% entrapment of the total amount of cetirizine added as shown in Tables 19, 21 and Figures 20, 23a, 23b, 23c. The

MLV liposome formulations had a mean ± SD particle size of 3.47 ± 0.53 μm using the submicron particle sizer, and mean ± SEM of 358.3 ±22.0 nm and 1000.5±100.1 nm using TEM and MOM respectively with 92.0% entrapment of the total amount of cetirizine added as shown in Table 20, 21 and Figure 21, 23a, 23b, 23c. The MOM results probably more accurately represent the true sizes of the SUV and MLV prepared in these formulations compared to the submicron particle sizer and TEM results. These findings were discussed in Section 3.1.4.3.1.

The high extent of entrapment was probably due to the lipophilicity of the cationic form of cetirizine in the liposomal system (log P= 3.2), which was higher than that evaluated in an n-octanol/water system (log P= 1.12) [117]. This may create a concentration gradient that possibly encourages further entrapment of cetirizine into the liposomes to 92 %.

Cetirizine peripheral H_1-antihistaminic activity over time is shown in Tables 38-40 and Figure 32 as absolute wheal areas, and in Tables 41-43 and Figures 33, 33a, as percent suppression of histamine-induced wheals. Throughout 24h, the peripheral H_1-antihistaminic activity of cetirizine, measured as mean (± SEM) percent suppression of histamine-induced wheals versus time was superior to GB, $p \leq 0.05$.

Cetirizine from both SUV and MLV significantly suppressed the wheal formation for up to 24 h, with maximum wheal suppression from 6 h to 8 h ranging from 90.6 ± 4.9 % to 89.0 ± 3.8 % and 98.0 ± 1.3 % to 94.0 ± 2.3 % respectively. Suppression of the wheals by cetirizine from MLV increased linearly

over time from 44.8 ± 9.8 % at 0.5 h to 98.0 ± 1.3 % at 6 h. In contrast, cetirizine from GB resulted in a maximum suppression of only 70.3 ± 3.8 % at 4 h.

The extent of systemic absorption of cetirizine was determined by using mean (± SEM) plasma concentrations at selected times after cetirizine application from SUV, MLV and GB, as shown in Tables 44-46 and Figure 34. Any variability in cetirizine plasma concentrations between the individual rabbit was considered during the statistical data analysis.

Cetirizine plasma concentrations obtained from GB yield a plasma concentration versus time curve similar in shape to oral dosing curve, with a C_{max}, 58.5 ± 5.2 ng/mL at 0.5 h, followed by decreasing concentrations over time as the cetirizine was eliminated, resulting in a mean ± SEM AUC of 248.3 ± 34.6 ng.hr/mL from 0.5 h to 10 h. This may be due to cetirizine being released rapidly from the GB and absorbed quickly through the skin into the systemic circulation as a bolus dose. Cetirizine has a relatively small volume of distribution, but would slowly redistribute into the skin and produce the peripheral antihistaminic effects from GB seen in this study, and as shown previously in oral dosing studies in human subjects (111).

Compared to GB, the SUV may act as a controlled release depot in the skin for cetirizine leading to constant cetirizine plasma concentrations over 24 h with AUC of 201± 24.2 ng.hr/mL from 0.5 h to 10 h. This plasma concentration versus time profile may possibly minimize systemic adverse effects, while resulting in a relatively higher peripheral antihistaminic activity for up to 24 h. SUV liposomes may adsorb to the skin surface and penetrate intact through the

stratum corneum where modified-release of the medication occurs as reflected from constant cetirizine plasma concentrations over 24 h. In a previous study (129), plasma cetirizine concentrations after a 10 mg cetirizine oral dose to children, 25.4 ± 1.9 kg, ranged from 585.6 ng/mL to 1491.6 ng/mL during the 24 h post dose time period. By comparing these results with those obtained after application of SUV containing cetirizine, it is proposed that cetirizine in the liposomes may be concentrated in the skin resulting in a reduction of the histamine-induced wheal reactions (164). This hypothesis would need to be confirmed by measuring cetirizine concentrations in the skin in a different animal model. It was not possible to perform biopsy studies in the rabbits since the animals could not be euthanasia due to the crossover study design.

From 0.5 to 10 h, the AUC of the plasma cetirizine concentrations after application of MLV was 334.6 ± 65.1 ng.hr/mL. The increasing cetirizine plasma concentrations after 3 h from MLV was accompanied by increasing wheal suppression. From 0.5 to 3h, it could be assumed that the peripheral H_1-antihistaminic activity from cetirizine in MLV may be obtained when MLV physically shed the outer lamellas initially releasing some of the medication into the skin. Then after 3 h, MLV could penetrate as oligolamellar vesicles, carrying the drug into the skin, releasing the medication into the skin and the systemic circulation yielding the peripheral antihistaminic effects from MLV. Cetirizine has a relatively small volume of distribution, but would slowly redistribute into the skin and produce the peripheral antihistaminic effects from MLV seen in this study, and as shown previously in oral dosing studies in human subjects (111). These

plasma cetirizine concentrations are still much lower than reported after 10 mg oral doses in children.

This hypothesis may be supported by a previous study conducted by Foldvari *et al.*, (160), who found intact unilamellar liposomes (300-500nm), containing an electron-dense colloidal iron marker, in the dermis of guinea pigs using the electron microscope. These investigators also reported that multilamellar liposomes could be found but less frequently than unilamellar liposomes. In addition the investigators speculated that the unilamellar liposomes (300-500 nm) could penetrate through the 'the lipid channels' of the skin, that is the lipidic material distributed in the intercellular spaces. The investigators also speculated that MLV may shed the outer layers during penetration and could then localize in the skin as uni- or oligolamellar liposomes.

Previous investigators (165-167), found that the sebaceous glands and hair follicles were the major routes of liposome penetration, especially for hydrophilic substances, such as isotretinion, carboxyfluorescein, and betahistine. In contrast, using hairless mice versus shaved normal mice as experimental models, Honzak *et al.,* (168) found that trans-follicular absorption was not a major route of penetration for liposomes into the skin. In their study, the MLV liposomal formulation consisted of phosphatidylcholine plus hydrophosphatidylcholine containing the hydrophilic spin probe GluSL (N-(1-oxyl-2,2,6,6-tetramethyl-4-piperidinyl)-2,3,4,5,6-pentahydroxy-hexane amide). Regardless of the route, in our study, penetration into the skin of cetirizine from

all formulations seemed to be rapid, based on the onset time, 0.5 h, of histamine-induced wheal suppression.

Other investigators have also suggested that the liposome formulations might localize entrapped medications in the skin (53, 54, 68). In addition, Patel (169), reported that [^{3}H]-methotrexate entrapped in liposomes was retained in the skin of nude mice to an extent 2-3-fold greater than drug administered in the free state, was associated with low concentrations of drug in the plasma and with sustained drug effects.

The mean (± SEM) percentages of the 10 mg cetirizine dose remaining on the skin at 24h after the topical application were 9.9 ± 1.5 %, 32 ± 9.2 %, and 17.4 ± 3.6 % for cetirizine from SUV, MLV, and GB respectively as shown in Table 47 and Figure 35. The lowest percent of cetirizine dose remaining was observed from SUV, $p \leq 0.05$. This may be attributed to improved penetration of cetirizine from SUV relative to the other two formulations.

Peripheral H_1-antihistaminic effects evaluated using suppression of the histamine-induced wheal formation were enhanced when cetirizine liposome formulations were applied. The lower plasma cetirizine concentrations from SUV and the lowest percent of cetirizine dose remaining on the skin after the topical application for up to 24 h support our hypothesis that these liposomes would localize cetirizine in the skin and might reduce systemic effects.

3.2.5. *In Vivo* Evaluation of HPC Liposomes of Cetirizine

Various medications have been incorporated into liposomes for topical delivery to enhance the therapeutic effects and reduce the systemic side effects

(170,171). Cetirizine, a potent second-generation H_1-antihistamine, is very effective for the treatment of allergic skin disorders but is slightly sedating when given orally.

The liposome batches were prepared using phosphate buffer at pH 6.5. The SUV liposome formulations had a mean ± SEM particle size of 1.96 ± 0.28 μm using the submicron particle sizer, 40.0 ± 4 nm using TEM, and 180.0±89.0 nm using MOM with 92.8% entrapment of the total amount of cetirizine added as shown in Tables 19, 21 and Figures 20, 23a, 23b, 23c. The MLV liposome formulations had a mean ± SEM particle size of 11.16±1.28 μm using the submicron particle sizer, 296.0 ± 27.1 nm using TEM, and 2300.1±54.2 nm using MOM with 89.7% entrapment of the total amount of cetirizine added as shown in Tables 20, 21 and Figures 21, 23a, 23b, 23c. The MOM results probably more accurately represent the true sizes of the SUV and MLV prepared in these formulations compared to the submicron particle sizer and TEM results. These findings were discussed in Section 3.1.4.3.1.

In both the SUV and MLV liposomes prepared for these studies, a very high percentage of the amount of cetirizine incorporated into the formulations was entrapped within the liposome vesicles. The high extent of entrapment into the lipid vesicles was probably due to the lipophilicity of the cationic form of cetirizine in the liposomal system (log P = 3.2), which was higher than that evaluated in an n-octanol/water system (log P = 1.12) (117). This may create a concentration gradient that possibly encourages further entrapment of cetirizine into the liposomes to the 89.7% and to 92.8% in MLV and SUV, respectively.

Cetirizine peripheral H_1-antihistaminic activity over time is shown in Tables 38, 48, 49 and Figure 36 as absolute wheal areas, and in Tables 41, 50, 51 and Figures 37, 37a, as percent suppression of histamine-induced wheals.

Compared with the pre-dose wheal areas, a rapid onset of H_1-antihistaminic activity was achieved from cetirizine in HPC-MLV. After 1 hour, the suppression was 93.8% ± 2.2% compared with HPC-SUV, 23.6% ± 5.5%, and GB, 36.5% ± 7.4%, $p \leq 0.05$. Compared with pre-dose results, significant wheal suppression from cetirizine in HPC-SUV was achieved only at 24 h, 91.7% ± 5.2%, while in HPC-MLV suppression was significant from 0.5 to 24 h, and in GB from 0.5 to 8 h, $p \leq 0.05$.

Cetirizine from HPC-MLV yielded a prolonged maximum suppression of 97.5% ± 1.4% to 94.4% ± 1.7% from 4 h to 8 h. Cetirizine from GB yielded a maximum suppression of only 70.3% ± 3.8%, at 4 h.

After 24 h, the peripheral H_1-antihistaminic activity of cetirizine from HPC-SUV, 91.7% ± 5.2%, was superior to GB, 36.3 ± 4.3, $p \leq 0.05$. Overall, the peripheral H_1-antihistamine activity of cetirizine from HPC-MLV was superior and prolonged from 4 to 8 h, ranging from 97.5% ± 1.4% to 94.9% ± 1.7% compared with HPC-SUV, 36.5% ± 5.9% to 44.1% ± 11.3%, and GB, 70.3% ± 3.8% to 60.6% ± 14.2%.

The extent of systemic absorption of cetirizine was determined by evaluating the mean plasma cetirizine concentrations at selected times after cetirizine application, as shown in Tables 44, 52, 53 and Figures 38. Any

variability in cetirizine plasma concentrations between the individual rabbit was considered during the statistical data analysis.

Cetirizine plasma concentrations obtained from GB, when plotted vs time as shown in Table 44 and Figure 38, yield a plasma concentration vs time curve similar in shape to the oral dosing curve, with a C_{max} at 0.5 h, followed by decreasing concentrations over time as the cetirizine was eliminated. Cetirizine plasma concentrations from GB were much lower than those obtained from a 10-mg oral dose (129) but higher than those obtained from HPC-SUV and HPC-MLV. This finding may be due to cetirizine being released rapidly from the GB and absorbed quickly through the skin into the systemic circulation as a bolus dose. Cetirizine has a relatively small volume of distribution but would slowly redistribute into the skin and produce the peripheral antihistaminic effects from GB seen in this study, and as shown previously in oral dosing studies in human subjects (111).

The AUC of plasma cetirizine concentrations from 0.5 to 24 h after HPC-SUV, 67 ± 5.2 ng.hr/mL, was significantly lower than after GB application, AUC of 248.3 ± 34.6 ng.hr/mL, $p \leq 0.05$. The mean (± SEM) plasma cetirizine concentrations from 0.5 to 8 h after HPC-SUV were lower but not significantly different compared with cetirizine from HPC-MLV. From 0.5 to 2 h, the mean plasma cetirizine concentrations from HPC-MLV, 24.3 ± 11.7 ng/mL to 25.3 ± 10.8 ng/mL, were significantly lower than from GB, 35.0 ± 3.7 ng/mL to 58.5 ± 5.2 ng/mL, $p \leq 0.05$. The AUC of HPC-MLV was 221.2 ± 42.3 ng.hr/mL.

From 0.5 to 24 h, an increasing linear relationship was observed between the mean percentage suppression of histamine-induced wheal by cetirizine from HPC-SUV vs time. The cetirizine plasma concentrations from HPC-SUV remained relatively low and consistent compared with HPC-MLV and GB, perhaps indicating a zero-order release of medication into the systemic circulation. In contrast, the drug concentrations at the receptor site in the skin may have increased with time resulting in a steady increase in the wheal suppression. These results need confirmation by performing extra skin tests and taking extra blood samples between 10 and 24 h, and further testing after 24 h to determine the duration of the efficacy. It might also be possible to determine skin concentrations of cetirizine in a different animal model.

The MLV liposome formulations yielded relatively low consistent plasma cetirizine concentrations in conjunction with rapid onset and duration of significant peripheral H_1-antihistaminic effects, as monitored by suppression of the histamine-induced wheals, compared with both HPC-SUV and GB. In a previous study (129) after a 10-mg cetirizine oral dose to children (25.4 ± 1.9 kg), plasma cetirizine concentrations ranged from 585.6 to 1491.6 ng/mL during the 24-hour post-dose time period. By comparing these plasma cetirizine concentrations with those obtained after application of liposomes containing 10 mg cetirizine, it is proposed that cetirizine in the liposomes may be concentrated in the skin, resulting in a reduction of the histamine-induced wheal reactions (164).

As was discussed for PC-SUV, this hypothesis may be supported by a previous study conducted by Foldvari *et al.*, (160) who found intact unilamellar liposomes (300-500nm), containing an electron-dense colloidal iron marker, in the dermis of guinea pigs using the electron microscope. These investigators also reported that multilamellar liposomes could be found but less frequently than unilamellar liposomes. In addition the investigators speculated that the unilamellar liposomes (300-500 nm) could penetrate through the 'the lipid channels' of the skin, that is the lipidic material distributed in the intercellular spaces. The investigators also speculated that MLV may shed the outer layers during penetration and could then localize in the skin as uni- or oligolamellar liposomes.

Depending on the above explanations, it could be assumed that a rapid onset of peripheral H_1-antihistaminic activity obtained from cetirizine in MLV may be obtained when MLV physically shed the outer layers, initially releasing some of the medication into the skin. Then MLV could penetrate as oligolamellar vesicles, carrying the drug into the skin and releasing the medication consistently over the 24-hour study period as the skin endogenous phospholipases sequentially degrade the remaining lamellae. The SUV, in contrast, may penetrate the skin as intact liposomes and then release the medication in a modified-release process as the skin endogenous phospholipases degrade the lamellae during the ensuing 24 h. This possible mechanism of liposome penetration would explain the low concentrations of cetirizine in the systemic circulation from the 2 liposome formulations. This hypothesis would need to be

confirmed by measuring cetirizine concentrations in the skin in a different animal model. It was not possible to perform biopsy studies in the rabbits since the animals could not be euthanasia due to the crossover study design.

The higher and faster peripheral H_1-antihistamine activity as well as higher plasma concentrations of cetirizine from HPC-MLV relative to HPC-SUV are similar to the results of Egbaria *et al.*, (172, 173). These researchers found that MLV liposomes of ciclosporin prepared using different phospholipids produced a deeper drug penetration in the skin strata of humans and hairless mice than that found from SUV. After penetration, HPC-SUV may retain the cetirizine until the liposome bilayer membrane is degraded by endogenous phospholipases (174-176) resulting in the slow release of cetirizine over time into the skin, which provides increasing wheal suppression but persistently low plasma concentrations. These results need to be confirmed by measuring cetirizine concentration in the skin and detecting the intact liposomes in the skin.

The mean (± SEM) percentage of cetirizine dose remaining on the skin at 24 h after the topical application of 10 mg of cetirizine from HPC-SUV, 5.9% ± 0.7%, was significantly lower compared with HPC-MLV, 19.2% ± 4%, and with GB, 17.4% ± 3.6%, $p \leq 0.05$ as shown in Table 54 and Figure 39.

The HPC-SUV resulted in the lowest percentage of the cetirizine dose remaining on the skin when compared with the other 2 formulations, $p \leq 0.05$. This finding may be attributed to improved penetration and concentration of the drug into the skin from SUV but delayed release when compared with the other 2

formulations. The relatively low plasma cetirizine concentrations from HPC-SUV are therefore not due to a lack of absorption of the medication. The increasing concentrations of cetirizine in the skin from HPC-SUV hypothesis is supported by the linear increase of peripheral H_1-antihistamine activity over time from 0.5 h up to 24 h.

Peripheral H_1-antihistaminic effects evaluated using suppression of the histamine-induced wheal formation was enhanced from cetirizine MLV liposome formulations compared with cetirizine from SUV and GB. The accompanying lower plasma cetirizine concentrations from liposome formulations, compared with those obtained following GB and when compared with those measured after oral administration to humans (111, 129) support our hypothesis that liposomes would localize cetirizine in the skin and might possibly reduce the incidence of any systemic adverse effects of the medication.

From the above results, the use of liposomes as a delivery system for hydroxyzine or cetirizine appears to improve the penetration and localization of the medication in the skin as reflected from the persistent suppression of the wheals induced by intradermal injection of histamine and low plasma concentrations of hydroxyzine and/or cetirizine. This may increase the peripheral therapeutic antihistaminic effects and minimize the systemic exposure to the medication, thus potentially reducing systemic adverse effects.

CHAPTER IV: SUMMARY AND CONCLUSION

The primary objective of the study was to evaluate the peripheral H_1-antihistamine efficacy and rate and extent of systemic absorption of hydroxyzine or cetirizine from liposome formulations, after topical application on the depilated skin on the back of a rabbit model. The secondary objective was to determine the physicochemical stability of the liposome formulations containing hydroxyzine or cetirizine for at least one year.

Using a randomized, crossover study design, the peripheral H_1-antihistamine efficacy was assessed by measuring the onset, extent and duration of suppression of histamine-induced wheals by hydroxyzine or cetirizine in liposome formulations compared with the suppression from hydroxyzine or cetirizine in Glaxal Base, the control topical o/w cream formulation. The onset and extent of systemic absorption were determined using plasma hydroxyzine and/or cetirizine concentrations measured at predetermined times after application of the liposome and control formulations to the skin.

For all PC-MLV liposome formulations prepared at pH 7, the formulation technique was evaluated using various hydration times and periods of freezing and thawing as described below

Hydration Time (h)	Freezing and Thawing (5 cycles after Hydration)	
	No	Yes
1	Control batch	Batch A
24	Batch B	Batch C
48	Batch D	Batch E

The stability of the liposome formulations was evaluated by measuring the percent entrapment of hydroxyzine (PETH) and percent entrapment of cetirizine (PEC) as well as by particle size analyses.

For all PC-MLV liposome formulations prepared at pH 7, the initial PETH of 94% was consistent and remained stable for up to 24 months at 10±2°C. After one month at 37±0.1°C all batches showed considerable loss of PETH. There was no effect of duration of hydration time on PETH, while the freezing-thawing treatment during the preparation of the liposomes adversely affected PETH.

Using 1 h hydration time and no freezing-thawing treatment, the PETH, 61.8%, of the control batch prepared at pH 6.5, after one month at 37±0.1°C was more stable than the PETH, 27.0%, in the batch prepared at pH 7. It would appear that the buffer of pH 6.5 is better for entrapment and stability of MLV containing hydroxyzine. The pH of buffer range from 5.5 to 7.0 or from 5.0 to 6.5 was optimal for entrapment and stability of hydroxyzine or cetirizine in SUV and MLV liposomes respectively.

From the above results, the preparation of both hydroxyzine and cetirizine liposomes using a buffer of pH 6.5 value was therefore selected for the extent of the entrapment and the stability of the liposomes. In addition it more closely approximates the pH of the human skin (pH 4.5 to 6.5).

For *in vivo* studies, SUV, HPC-SUV and MLV of both hydroxyzine and cetirizine were prepared by ethanol injection, extrusion, and lipid film hydration methods respectively and all batches were kept at 10±2°C until studied using the rabbit model. Phosphatidylcholine (PC) or phosphatidylcholine hydrogenated (HPC) liposomes were prepared as models of "fluid flexible" and "solid rigid" liposomes respectively.

In vivo evaluation of both PC-SUV and PC-MLV containing hydroxyzine revealed that compared with baseline, hydroxyzine from all formulations significantly suppressed histamine-induced wheal formation by 75% to 95% for up to 24 hours, $P \leq 0.05$. Maximum suppression from all formulations, 95%, occurred from 2 h to 6 h. The AUC of plasma hydroxyzine concentration from PC-SUV and PC-MLV, 80.1 ± 20.8 ng.h/mL and 78.4 ± 33.9 ng.h/mL, respectively, were significantly lower than that from GB, 492 ± 141 ng.h/mL over 24 h, $P \leq 0.05$. Plasma concentrations of cetirizine arising *in vivo* as the active metabolite of hydroxyzine, from PC-SUV, PC-MLV, and GB, were similar with AUC of 765 ± 50 ng.h/mL, 1035 ± 202 ng.h/mL, and 957 ± 227 ng.h/mL, respectively. However, the combined plasma concentrations of hydroxyzine and its metabolite cetirizine arising *in vivo* were significantly lower from the liposome formulations than from GB. Only 0.02% to 0.06% of the initial hydroxyzine dose

remained on the skin after 24 h. In this model, hydroxyzine from SUV and MLV had excellent topical H_1-antihistaminic activity, and minimal systemic exposure occurred. Cetirizine formed *in vivo* contributed to some of H_1-antihistaminic activity.

In vivo evaluation of both PC-SUV and PC-MLV containing cetirizine showed that histamine-induced wheal formation was significantly suppressed by cetirizine from PC-SUV and PC-MLV compared to cetirizine from GB, $p \leq 0.05$. Maximum wheal suppression by cetirizine in PC-SUV and PC-MLV ranged from 90.6 ± 4.9 % to 89.0 ± 3.8 % and 98.0 ± 1.3 % to 94.0 ± 2.3 % respectively from 6-8 h. Compared to GB, the PC-SUV may act as a controlled release depot in the skin for cetirizine leading to constant cetirizine plasma concentrations over 24 h. This plasma concentration versus time profile of PC-SUV may possibly minimize systemic adverse effects, while resulting in a relatively higher peripheral antihistaminic activity compared to GB for up to 24 h. After 24 h, the percent of the cetirizine dose remaining on the backs of the rabbits from PC-SUV was lower than from both PC-MLV and GB, $p \leq 0.05$. In this model, cetirizine from both PC-SUV and PC-MLV had excellent topical H_1-antihistaminic effects, while systemic exposure to cetirizine from SUV was reduced, compared to cetirizine from PC-MLV and GB.

In vivo evaluation of both HPC-SUV and HPC-MLV containing cetirizine showed that, compared to baseline, histamine-induced wheal formation was suppressed by cetirizine in HPC-SUV only at 24 h, in MLV from 0.5-24 h and in GB from 0.5-8 h, $p \leq 0.05$. Wheal suppression by cetirizine in SUV at 24 h,

91.7±5.2 %, and in MLV, 93.8±2.2 to 76.2±6.5 %, was greater than cetirizine in GB, 36.5±7.4 to 60.6±14.2 %, from 1 to 24 h, $p \leq 0.05$. Faster onset, as well as greater and more persistent suppression was obtained from cetirizine in HPC-MLV. Plasma cetirizine concentrations from HPC-SUV, AUC of 67± 5.2 ng.hr/mL and from HPC-MLV, AUC of 221.2 ± 42.3 ng.hr/mL, were lower than from GB ,AUC of 248.3 ± 34.6 ng.hr/mL. In this model, cetirizine from HPC-MLV has excellent topical H_1-antihistamine activity while systemic exposure was reduced, compared to cetirizine from GB.

From the above results, it is clear that liposome formulations are excellent delivery systems for the topical application of hydroxyzine or cetirizine to the skin, producing significant peripheral H_1-antihistaminic effects in this rabbit model (177-179). Hydroxyzine or cetirizine in PC-SUV, and PC-MLV and cetirizine in HPC-MLV formulations when applied to the skin, yielded faster onset, more prolonged and greater peripheral H_1-antihistaminic activity than hydroxyzine or cetirizine in a conventional o/w cream formulation. The accompanying plasma hydroxyzine and cetirizine concentrations from liposome formulations were lower than those obtained from GB, and also when compared to those previously described following administration by the IV-route in the rabbit model (110) and orally to humans (114, 128, 129). These results support our hypothesis that liposomes would localize hydroxyzine and cetirizine in the skin and possibly reduce the incidence of systemic adverse effects of these H_1-antihistamines.

The recommended optimum formula that yields excellent long term stability is the liposomes containing hydroxyzine or cetirizine prepared using

L-α-phosphatidylcholine hydrogenated (HPC-MLV). The preparation conditions of HPC-MLV that provide high percent entrapment and the long term stability are hydrating the lipid films with phosphate buffer, 0.02M at pH 6.5, for one hour without using freezing-thawing treatment of the liposomes.

The HPC-MLV physicochemical stability results may be used to support the primary required stability data for pilot studies of commercial formulations. In addition, HPC-MLV containing cetirizine have prolonged, excellent H_1-antihistamine efficacy with accompanying lower plasma concentrations for up to 24 h compared to conventional o/w cream formulations in a rabbit model.

A number of future studies are proposed after consideration of the results from the present studies:

Compared to a control formulation such as Glaxal Base, the peripheral H_1-antihistaminic activity and the systemic absorption of hydroxyzine or cetirizine from liposome formulations will need to be evaluated after storage of liposomes for up to 24 months at 10±2°C, 25±3°C and 37±0.1°C. This study needs to be conducted to evaluate if changes in liposome size by fusion and/or aggregation or by loss of outer lamellas will affect the peripheral H_1-antihistaminic activity and the systemic absorption of hydroxyzine and cetirizine even though PETH or PEC is unchanged.

Compared to a control formulation such as Glaxal Base, skin concentrations of hydroxyzine and cetirizine from liposome formulations will need to be determined in the rabbit or other animal model by sacrificing the animal and using skin strips or biopsy samples or by the skin stripping method in live

animals. Also the metabolism of hydroxyzine to cetirizine in the skin from liposome formulations will need to be determined in the rabbit or other animal model by sacrificing the animal then using a skin biopsy technique, or by the skin stripping method.

Compared to a control formulation such as Glaxal Base, peripheral H_1-antihistaminic activity using the histamine skin test (128, 129) and accompanying plasma concentrations of hydroxyzine or cetirizine from HPC–MLV will need to be evaluated in healthy adult participants.

Compared to a control formulation such as Glaxal Base, peripheral H_1-antihistaminic activity using the histamine skin test or allergen test and accompanying plasma concentrations of hydroxyzine or cetirizine from HPC–MLV in adults and children with allergic skin disorders (114) will need to be evaluated.

Once the above future studies have been completed, more extensive studies on humans will be required before the recommendation of once daily application of HPC-MLV containing cetirizine for treatment of allergic skin disorders in adult and pediatric patients could be approved. This recommendation might help to improve the patient compliance, reduce the frequent application of conventional ointment or cream formulations and decrease the discomfort resulting from systemic adverse effects.

Table 1: HPLC Calibration of Hydroxyzine in Aqueous Solution

Concentration of Hydroxyzine (ng/mL)	Mean Peak Area Ratio	% C.V.
0	0.00	0.0
100	0.08	1.3
200	0.18	1.6
400	0.41	0.5
600	0.59	0.2
800	0.80	0.1

Table 2: HPLC Calibration of Cetirizine in Aqueous Solution

Concentration of Cetirizine (ng/mL)	Mean Peak Area Ratio	% C.V.
0	0.00	0.00
100	0.27	7.40
200	0.54	5.50
400	1.10	3.60
600	1.55	2.60
800	2.20	0.90
1000	2.70	0.40

n= 8

% C.V. = percent coefficient of variation

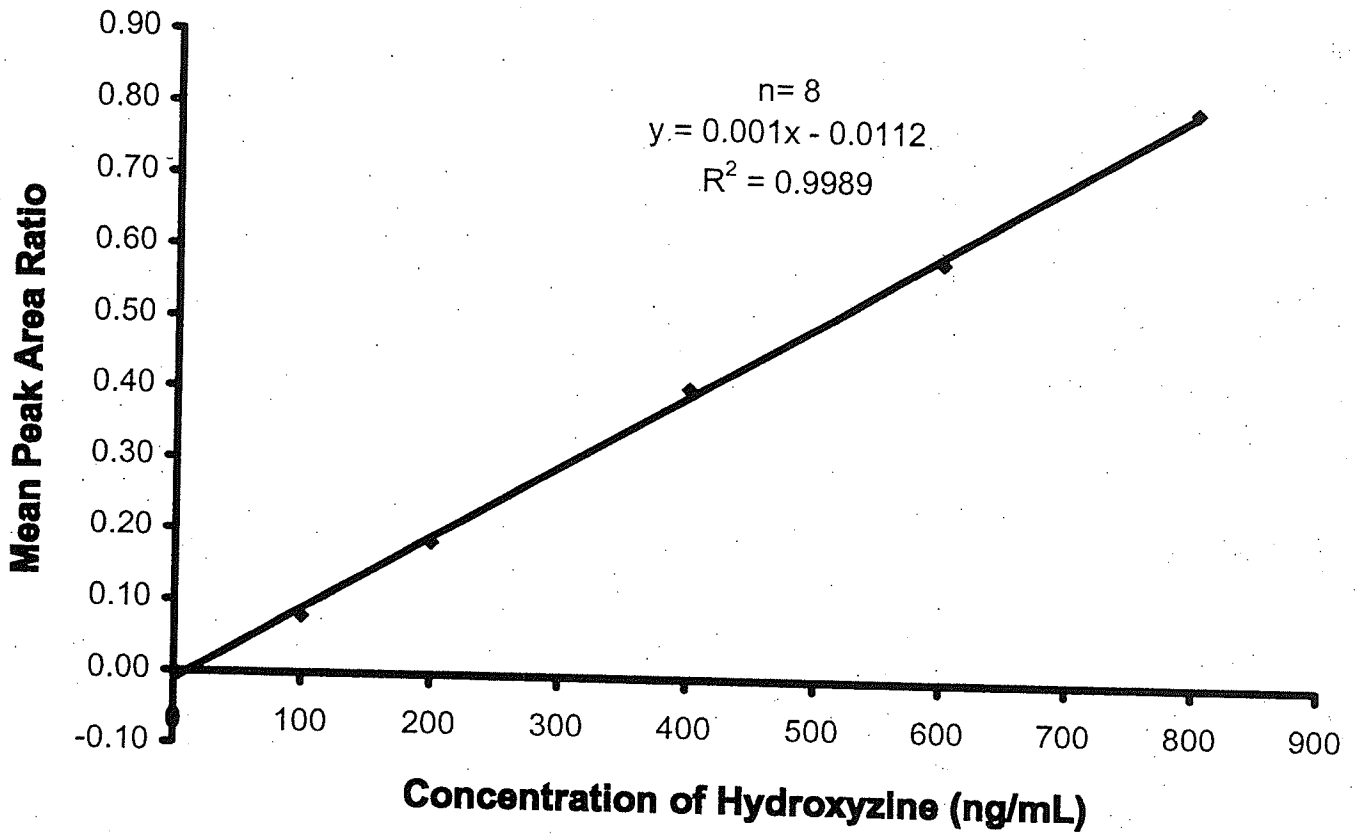

Figure 1: HPLC Calibration of Hydroxyzine in Aqueous Solution

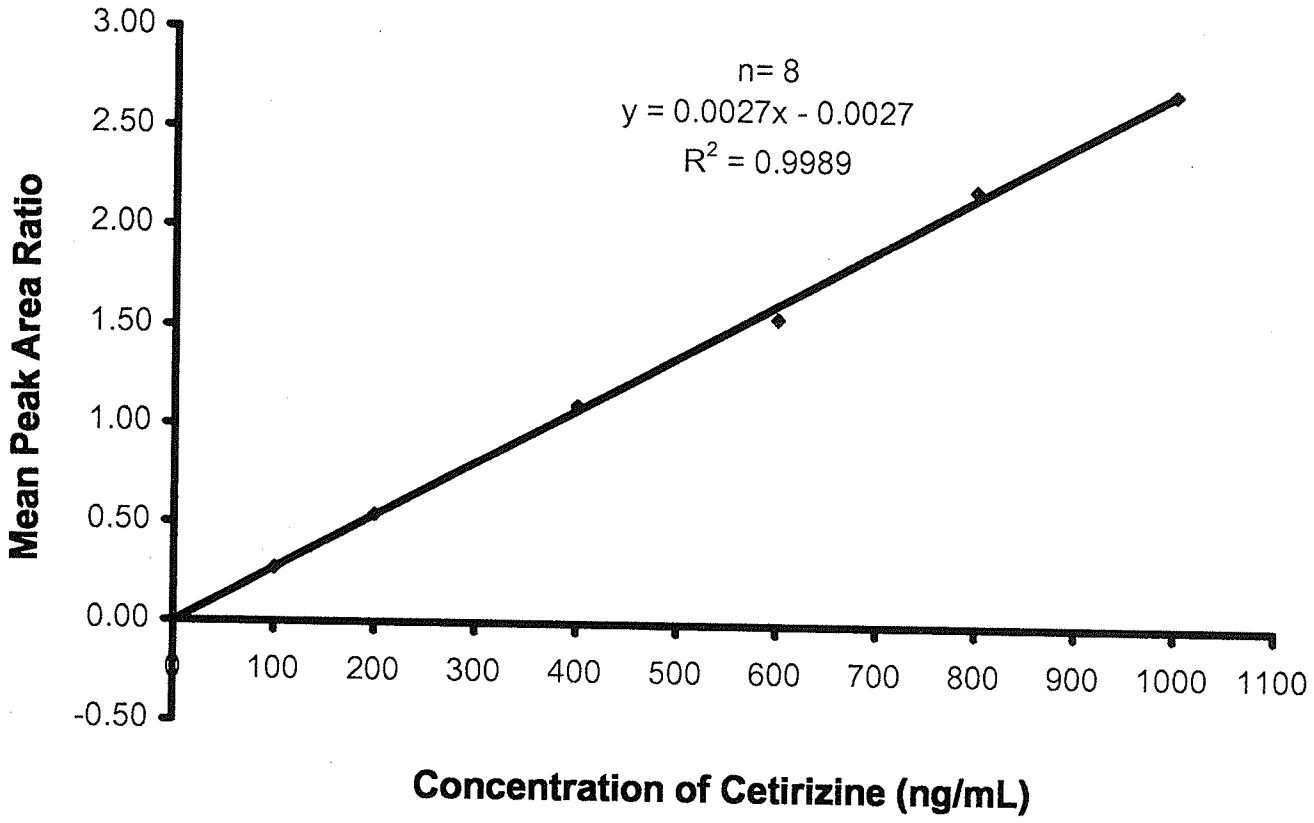

Figure 2: HPLC Calibration of Cetirizine in Aqueous Solution

Table 3: Effect of Preparation Methods on the Percent Entrapment of Hydroxyzine (PETH) in PC-MLV, pH 7, at Initial Formulation and after Storage at 10°C

Condition of the Experiments* / Time (months)	A	B	C	D	E	CONTROL
	Mean Percent Entrapment of Hydroxyzine					
0	94.8	94.9	95.0	95.3	94.8	94.3
1	94.5	94.0	95.5	95.5	94.0	92.7
2	93.2	96.1	96.1	95.7	96.1	92.0
3	95.7	94.0	95.5	95.7	95.5	93.0
4	96.7	96.1	95.7	95.7	93.2	92.7
5	96.7	95.5	95.5	96.1	94.0	92.6
6	93.2	92.1	96.1	96.7	95.5	93.6
7	94.0	96.7	95.7	96.7	93.2	93.0
8	93.2	95.7	95.5	96.7	94.0	92.2
9	96.7	94.0	96.1	95.7	95.5	92.7
10	95.5	95.6	96.0	97.0	95.5	94.0
11	93.2	92.1	96.1	96.7	95.5	91.9
12	95.0	95.4	95.2	95.4	94.3	91.8
18	96.7	96.1	95.7	95.7	93.2	92.0
24	96.5	96.0	95.5	96.0	95.7	91.8
Physical Appearance/Months (m)	**	***	**	**	**	***

n= 3

PC-MLV = multilamellar vesicles (MLV) prepared using L-α-phosphatidylcholine (PC)

**discoloration at 4m

***No change/ 24m

*Condition of the Experiments

Hydration Time	Freezing and Thawing (5 cycles after hydration)	
	No	Yes
1h	Control	Batch A
24 h	Batch B	Batch C
48 h	Batch D	Batch E

In stability study samples resulting in no loss of Percent Entrapment of Hydroxyzine (PETH) over 24 months, intermediate time PETH values that were > ± 5% of initial PETH values were considered as outliers and not included in the data analysis

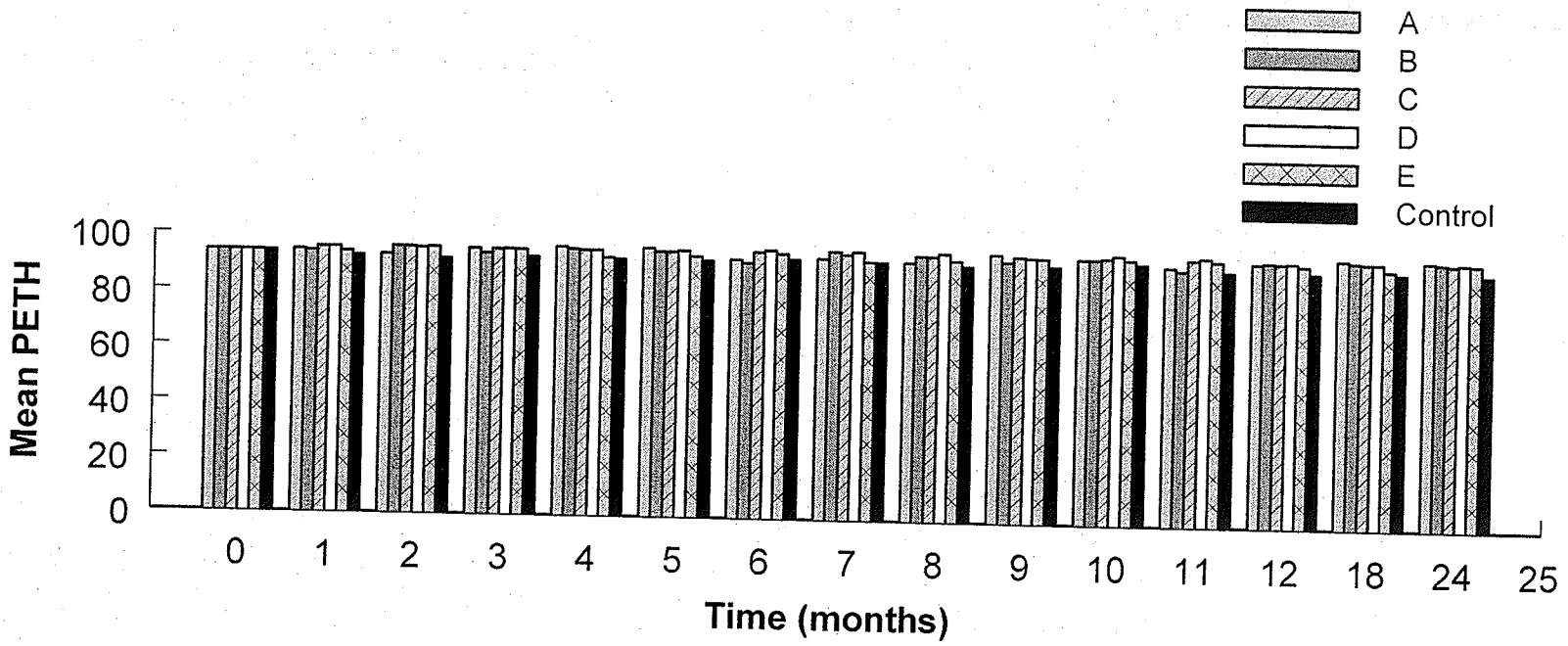

Figure 3: Effect of Preparation Methods on the Percent Entrapment of Hydroxyzine (PETH) in PC-MLV, pH 7, at Initial Formulation and after Storage at 10°C.

n=3

PC-MLV = multilamellar vesicles (MLV) prepared using L-∝-phosphatidylcholine (PC)

Conditions of the Experiments:

Hydration Time	Freezing and Thawing (5 cycles after hydration)	
	No	Yes
1h	Control Batch	Batch A
24 h	Batch B	Batch C
48 h	Batch D	Batch E

In stability study samples resulting in no loss of PETH over 24 months, intermediate time PETH values that were > ± 5% of initial PETH values were considered as outliers and not included in the data analysis

Table 4: Effect of Preparation Methods on the Percent Entrapment of Hydroxyzine (PETH) in PC-MLV, pH 7, at Initial Formulation and after Storage at 37°C

Condition of the Experiments* / Time (months)	A	B	C	D	E	CONTROL
	Mean Percent Entrapment of Hydroxyzine					
0	94.8	94.9	95.0	95.3	94.8	94.3
1	13.2	27.6	12.6	43.0	15.1	26.5
Physical Appearance/Months (m)	Discoloration from white into buff and droplets on the surface					

n= 3

PC-MLV = multilamellar vesicles (MLV) prepared using L-α-phosphatidylcholine (PC)

*Condition of the Experiments:

Hydration Time	Freezing and Thawing (5 cycles after hydration)	
	No	Yes
1h	Control	Batch A
24 h	Batch B	Batch C
48 h	Batch D	Batch E

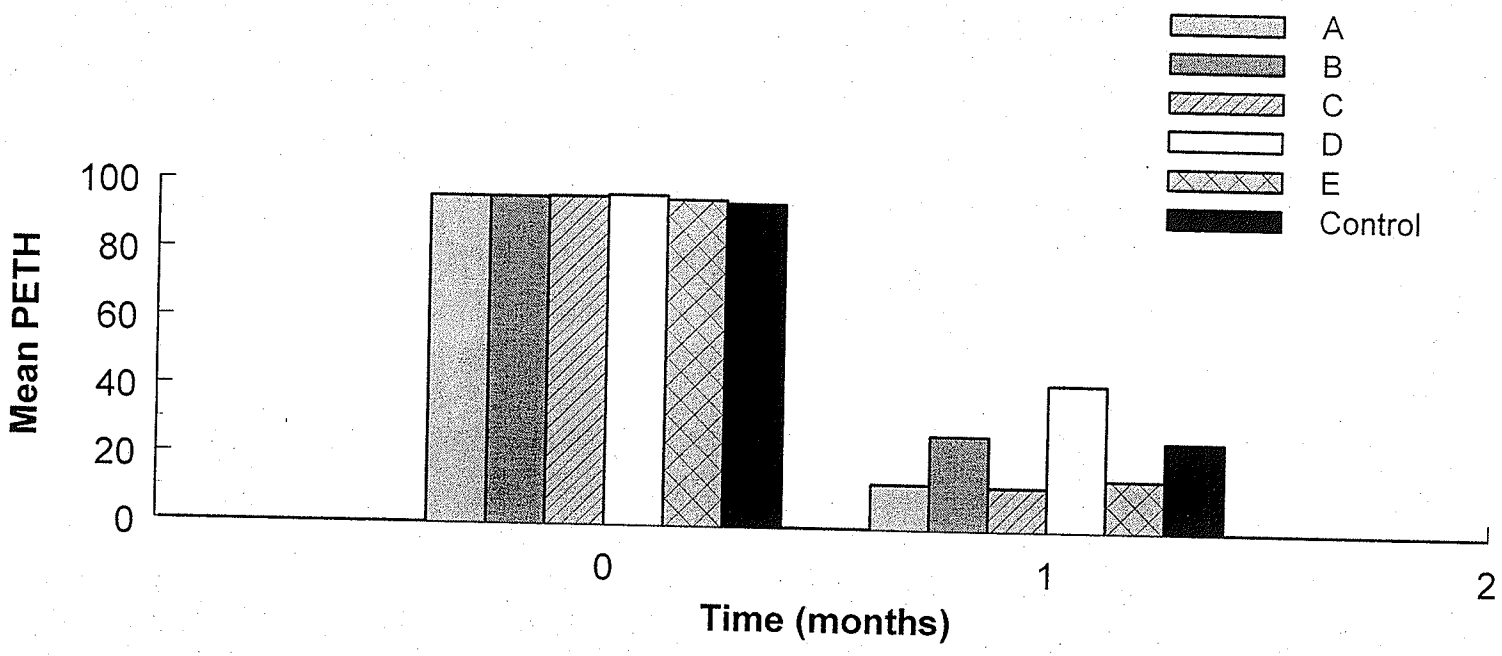

Figure 4: Effect of Preparation Methods on the Percent Entrapment of Hydroxyzine (PETH) in PC-MLV, pH 7, at Initial Formulation and after Storage at 37°C.

n=3

PC-MLV = multilamellar vesicles (MLV) prepared using L-∝-phosphatidylcholine (PC)

Conditions of the Experiments:

Hydration Time	Freezing and Thawing (5 cycles after hydration)	
	No	Yes
1h	Control Batch	Batch A
24 h	Batch B	Batch C
48 h	Batch D	Batch E

Table 5: Effect of Preparation Methods on the Percent Entrapment of Hydroxyzine (PETH) in PC Liposomes, pH 7, at Initial Formulation and after Storage at 37°C

Condition of the Experiments* / Time (months)	SUV	MLV
	Mean Percent Entrapment of Hydroxyzine	
0	94.0	94.3
1	27.1	26.5
Physical Appearance	discoloration **	discoloration***

n= 3
PC = L-α-Phosphatidylcholine
SUV = small unilamellar vesicles
MLV = multilamellar vesicles
* SUV prepared using ethanol injection method
* MLV prepared using lipid film hydration method
*hydration time = 1 h, and no freezing and thawing
** from white into buff and no droplets on the surface
***from white into buff and droplets on the surface

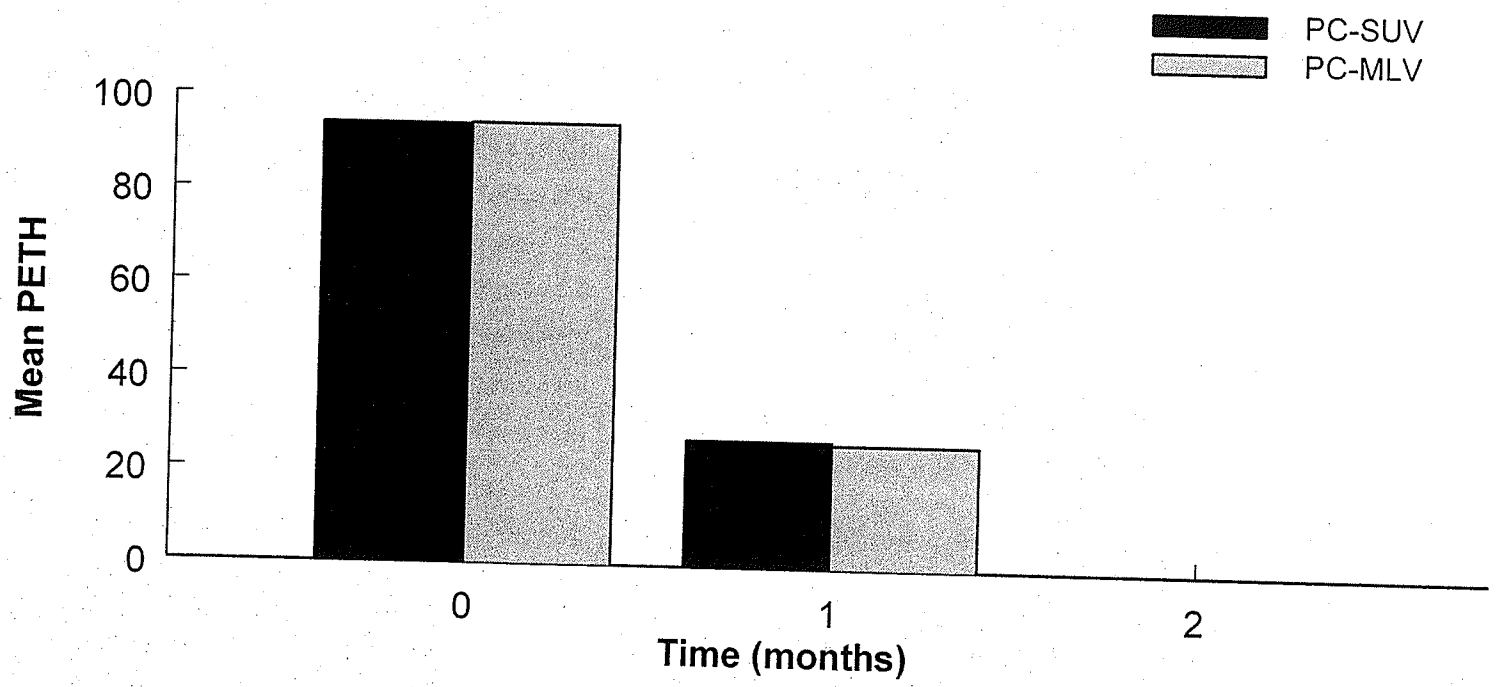

Figure 5: Effect of Preparation Methods on the Percent Entrapment of Hydroxyzine (PETH) in PC Liposomes, pH 7, at Initial Formulation and after Storage at 37°C.

n=3

PC-SUV = small unilamellar vesicles (SUV) prepared using L-α-phosphatidylcholine (PC),

PC-MLV = multilamellar vesicles (MLV) prepared using L-α-phosphatidylcholine (PC),

Conditions of the Experiments: hydration time for 1 h, no freezing and thawing, SUV prepared using ethanol injection method, MLV prepared using lipid film hydration method

Table 6: Effect of Preparation Methods on the Percent Entrapment of Hydroxyzine (PETH) in PC Liposomes, pH 6.5, at Initial Formulation and after Storage at 37°C

Condition of the Experiments* / Time (months)	SUV	MLV
	Mean Percent Entrapment of Hydroxyzine	
0	86.0	94.3
1	27.1	61.8
Physical Appearance	discoloration **	discoloration***

n= 3
PC = L-α-Phosphatidylcholine
SUV = small unilamellar vesicles
MLV = multilamellar vesicles
* SUV prepared using ethanol injection method
* MLV prepared using lipid film hydration method
*hydration time = 1 h, and no freezing and thawing
** from white into buff and no droplets on the surface
***from white into buff and droplets on the surface

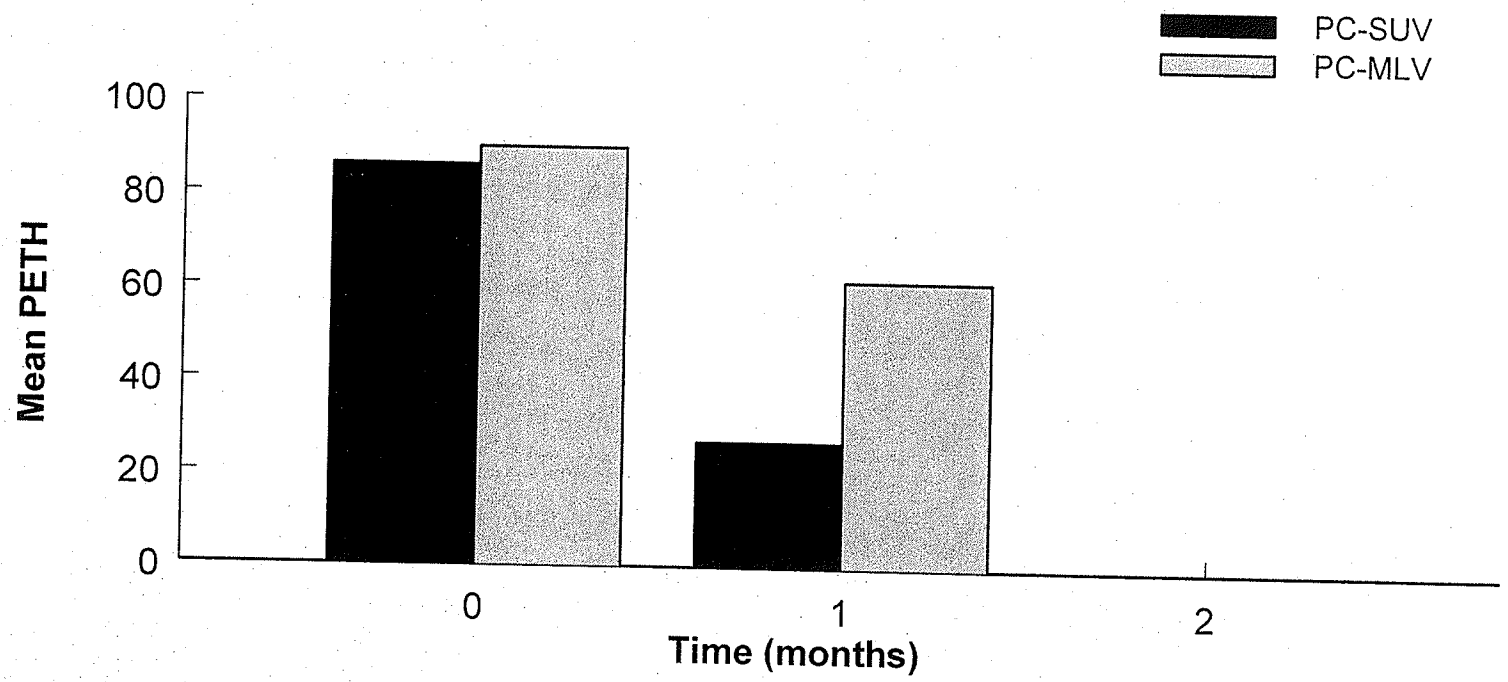

Figure 6: Effect of Preparation Methods on the Percent Entrapment of Hydroxyzine (PETH) in PC Liposomes, pH 6.5, at Initial Formulation and after Storage at 37°C.

n=3

PC-SUV = small unilamellar vesicles (SUV) prepared using L-α-phosphatidylcholine (PC),

PC-MLV = multilamellar vesicles (MLV) prepared using L-α-phosphatidylcholine (PC),

Conditions of the Experiments: hydration time for 1 h, no freezing and thawing, SUV prepared using ethanol injection method, MLV prepared using lipid film hydration method

Table 7: Effect of Preparation Methods on the Percent Entrapment of Hydroxyzine (PETH) in PC Liposomes, pH 6.5, at Initial Formulation and after Storage for 7 days at 37°C

Condition of the Experiments* / Time (days)	SUV	MLV
	Mean Percent Entrapment of Hydroxyzine	
1	86.0	94.3
2	92.0	91.0
3	93.0	89.0
4	94.0	87.0
5	94.0	86.5
6	91.0	80.0
7	82.0	82.0
Physical Appearance	slight discoloration**	discoloration**

n= 3
PC = L-α-Phosphatidylcholine
SUV = small unilamellar vesicles
MLV = multilamellar vesicles
* SUV prepared using ethanol injection method
* MLV prepared using lipid film hydration method
**after 6 days

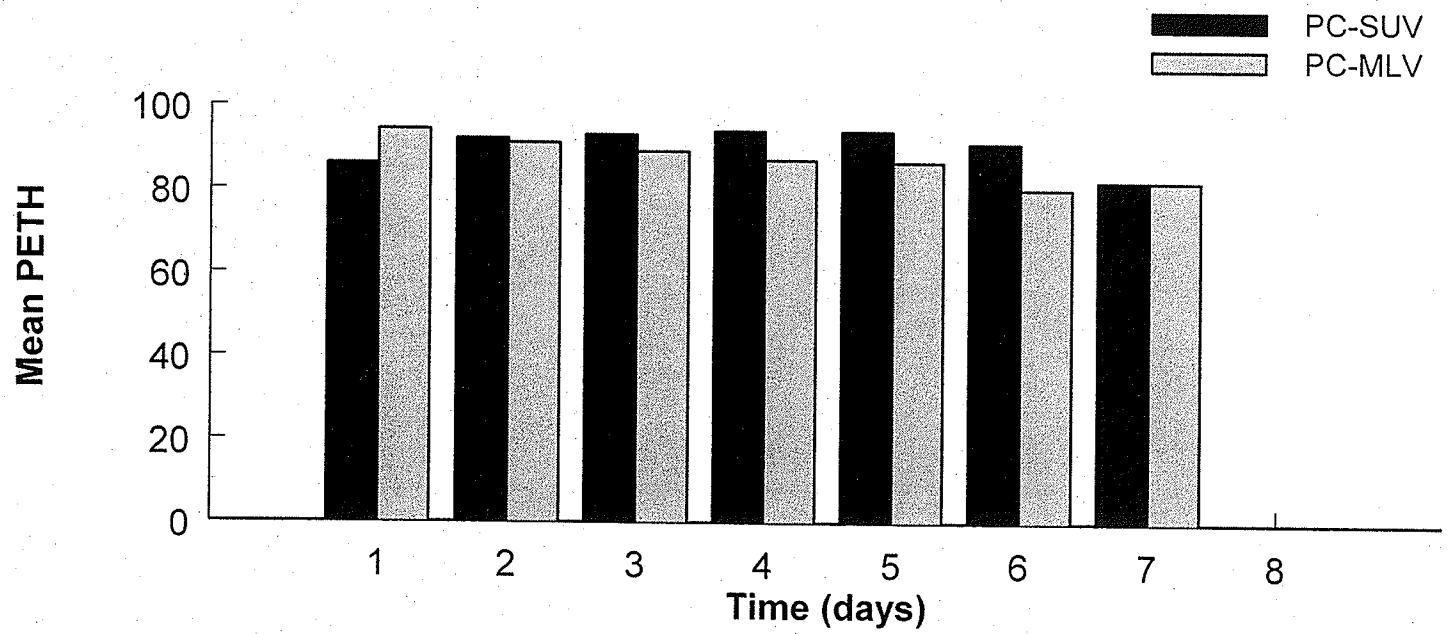

Figure 7: Effect of Preparation Methods on the Percent Entrapment of Hydroxyzine (PETH) in PC Liposomes, pH 6.5, at Initial Formulation and after Storage for 7 days at 37°C.

n=3

PC-SUV = small unilamellar vesicles (SUV) prepared using L-α-phosphatidylcholine (PC),

PC-MLV = multilamellar vesicles (MLV) prepared using L-α-phosphatidylcholine (PC),

Conditions of the Experiments: hydration time for 1 h, no freezing and thawing, SUV prepared using ethanol injection method, MLV prepared using lipid film hydration method

Table 8: Effect of Preparation Methods on the Percent Entrapment of Cetirizine (PEC) in PC Liposomes, pH 6.5, at Initial Formulation and after Storage for 7 days at 37°C

Condition of the Experiments* / Time (days)	SUV	MLV
	Mean Percent Entrapment of Cetirizine	
1	92.0	92.0
2	94.1	93.6
3	92.9	91.3
4	92.8	88.8
5	93.6	93.9
6	93.6	91.9
7	91.3	91.8
Physical Appearance	slight discoloration**	slight discoloration**

n= 3
PC = L-α-Phosphatidylcholine
SUV = small unilamellar vesicles
MLV = multilamellar vesicles
* SUV prepared using ethanol injection method
* MLV prepared using lipid film hydration method
**after 6 days

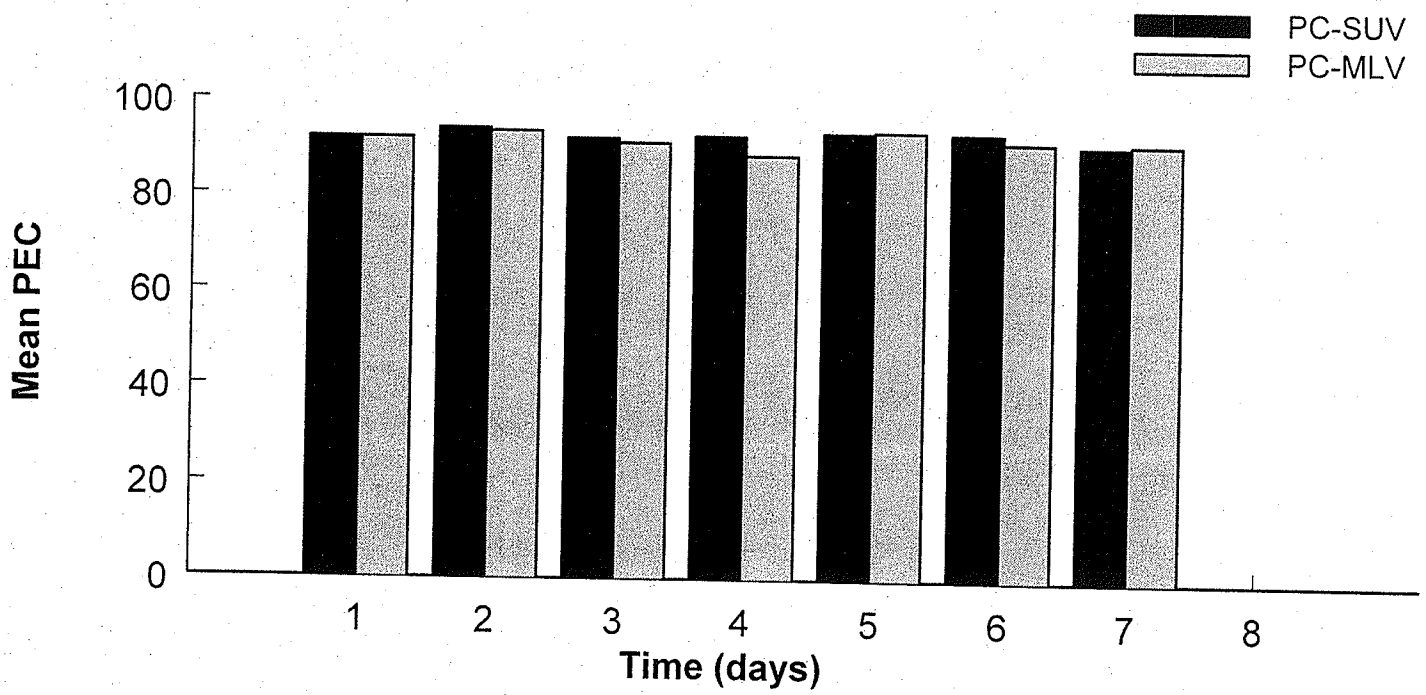

Figure 8: Effect of Preparation Methods on the Percent Entrapment of Cetirizine (PEC) in PC Liposomes, pH 6.5, at Initial Formulation and after Storage for 7 days at 37°C.

n=3

PC-SUV = small unilamellar vesicles (SUV) prepared using L-α-phosphatidylcholine (PC),

PC-MLV = multilamellar vesicles (MLV) prepared using L-α-phosphatidylcholine (PC),

Conditions of the Experiments: hydration time for 1 h, no freezing and thawing, SUV prepared using ethanol injection method, MLV prepared using lipid film hydration method

Table 9: Effect of Changing pH on the Percent Entrapment of Hydroxyzine (PETH) in PC-SUV, pH 6.5, at Initial Formulation and after Storage at 10°C

Hydrating Buffer pH	5.0	5.5	6.0	6.5	7.0
Time (months)	Mean Percent Entrapment of Hydroxyzine				
0	53.0	84.0	86.0	86.0	94.0
1	50.0	85.0	86.0	88.6	93.0
2	51.0	82.0	85.0	87.5	92.0
3	53.0	82.0	84.0	87.5	91.0
4	50.0	83.0	84.0	88.0	90.0
5	50.0	84.0	82.0	86.5	90.0
6	45.0	80.0	79.0	85.0	85.0
7	48.0	79.0	80.0	87.5	90.0
8	46.0	80.0	82.0	87.0	89.0
9	45.0	80.0	81.0	88.0	92.0
10	39.0	82.0	83.0	85.0	90.0
11	50.1	82.0	85.0	87.0	85.0
12	30.0	83.0	85.0	87.5	91.0
18	50.0	82.0	85.0	87.0	95.0
24	52.0	80.0	83.0	85.0	92.0
Physical Appearance	No change				

n= 3

PC-SUV = small unilamellar vesicles (SUV) prepared using L-α-phosphatidylcholine (PC)

In stability study samples resulting in no loss of Percent Entrapment of Hydroxyzine (PETH) over 24 months, intermediate time PETH values that were > ± 5% of initial PETH values were considered as outliers and not included in the data analysis

Table 10: Effect of Changing pH on the Percent Entrapment of Hydroxyzine (PETH) in PC-MLV, pH 6.5, at Initial Formulation and after Storage at 10°C

Hydrating Buffer pH / Time (months)	5.0	5.5	6.0	6.5	7.0
	Mean Percent Entrapment of Hydroxyzine				
0	82.0	82.0	86.0	94.3	94.3
1	80.0	81.0	83.0	92.7	92.0
2	79.0	80.0	84.0	92.0	93.0
3	80.0	79.0	87.0	93.0	94.0
4	81.0	82.0	85.0	92.7	91.0
5	83.0	83.0	86.0	92.6	93.0
6	80.0	83.0	81.0	93.6	90.0
7	79.0	84.0	80.0	93.0	80.0
8	78.0	82.0	83.0	92.2	82.0
9	80.0	80.0	82.0	92.7	90.0
10	81.0	81.0	81.0	94.0	91.0
11	79.3	80.0	82.0	91.9	89.2
12	80.0	79.0	80.0	91.8	93.0
18	82.0	80.0	79.0	92.0	90.0
24	79.0	80.0	83.0	91.8	91.0
Physical Appearance	No change				

n= 3

PC-MLV = multilamellar vesicles (MLV) prepared using L-α-phosphatidylcholine (PC)

In stability study samples resulting in no loss of Percent Entrapment of Hydroxyzine (PETH) over 24 months, intermediate time PETH values that were > ± 5% of initial PETH values were considered as outliers and not included in the data analysis

Table 11: Effect of Changing pH on the Percent Entrapment of Cetirizine (PEC) in PC-SUV, pH 6.5, at Initial Formulation and after Storage at 10°C

Hydrating Buffer pH / Time (months)	5.0	5.5	6.0	6.5
	Mean Percent Entrapment of Cetirizine			
0	94.5	93.0	91.0	92.0
12	90.0	81.0	83.0	88.1
24	89.0	80.0	84.0	90.1
Physical Appearance	no change			

n= 3

PC-SUV = small unilamellar vesicles (SUV) prepared using L-α-phosphatidylcholine (PC)

Table 12: Effect of Changing pH on the Percent Entrapment of Cetirizine (PEC) in PC-MLV, pH 6.5, at Initial Formulation and after Storage at 10°C

Hydrating Buffer pH / Time (months)	5.0	5.5	6.0	6.5
	Mean Percent Entrapment of Cetirizine			
0	92.0	93.5	92.5	92.0
12	80.0	81.0	83.0	84.3
24	79.0	80.0	84.0	74.3
Physical Appearance	slight discoloration*			

n= 3
PC-MLV = multilamellar vesicles (MLV) prepared using L-α-phosphatidylcholine (PC)
*after 4 months increased with time

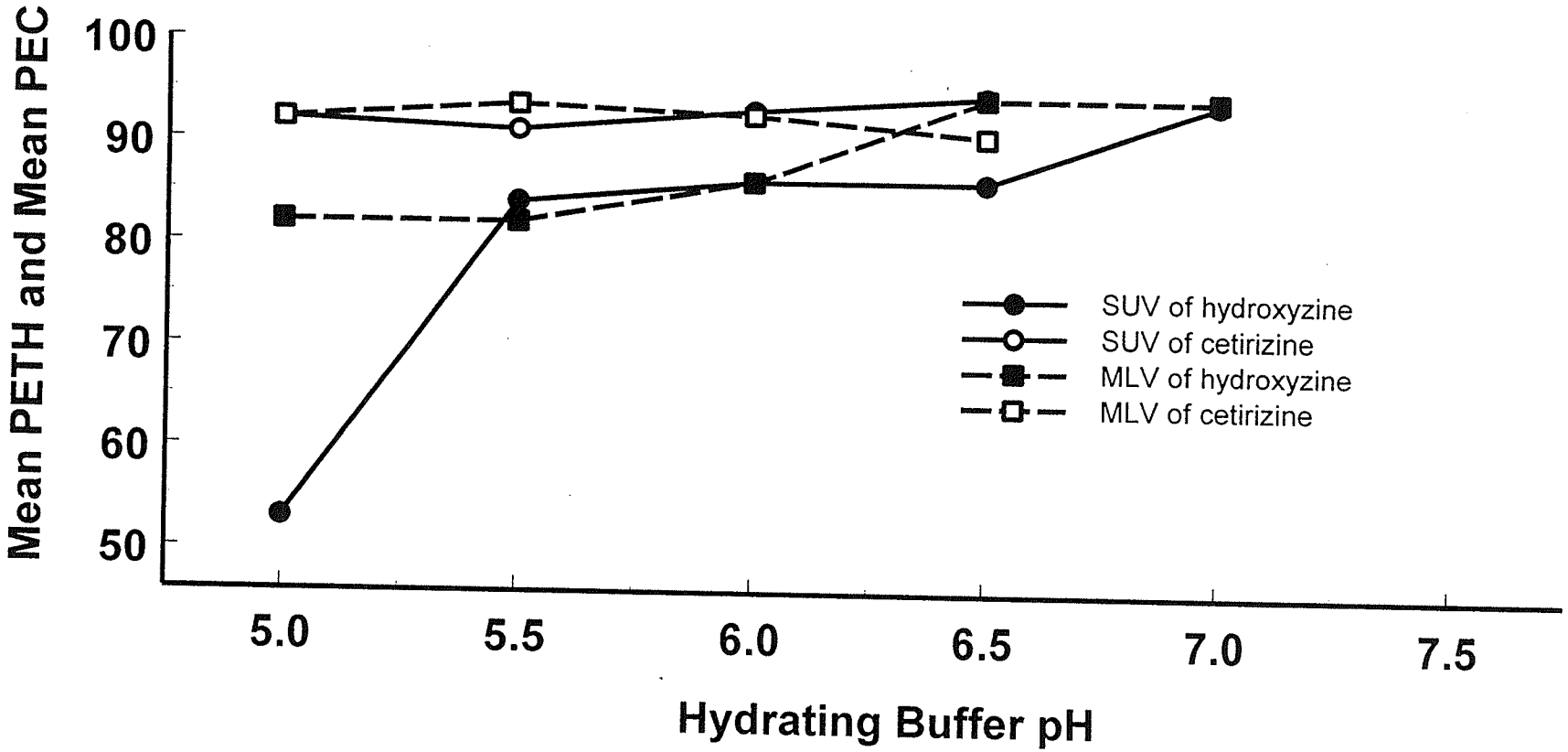

Figure 9: Effect of Changing pH on the Initial Percent Entrapment of Hydroxyzine (PETH) or Cetirizine (PEC) in PC-SUV or PC-MLV.

n=3

PC-SUV = small unilamellar vesicles (SUV) prepared using L-α-phosphatidylcholine (PC),

PC-MLV = multilamellar vesicles (MLV) prepared using L-α-phosphatidylcholine (PC)

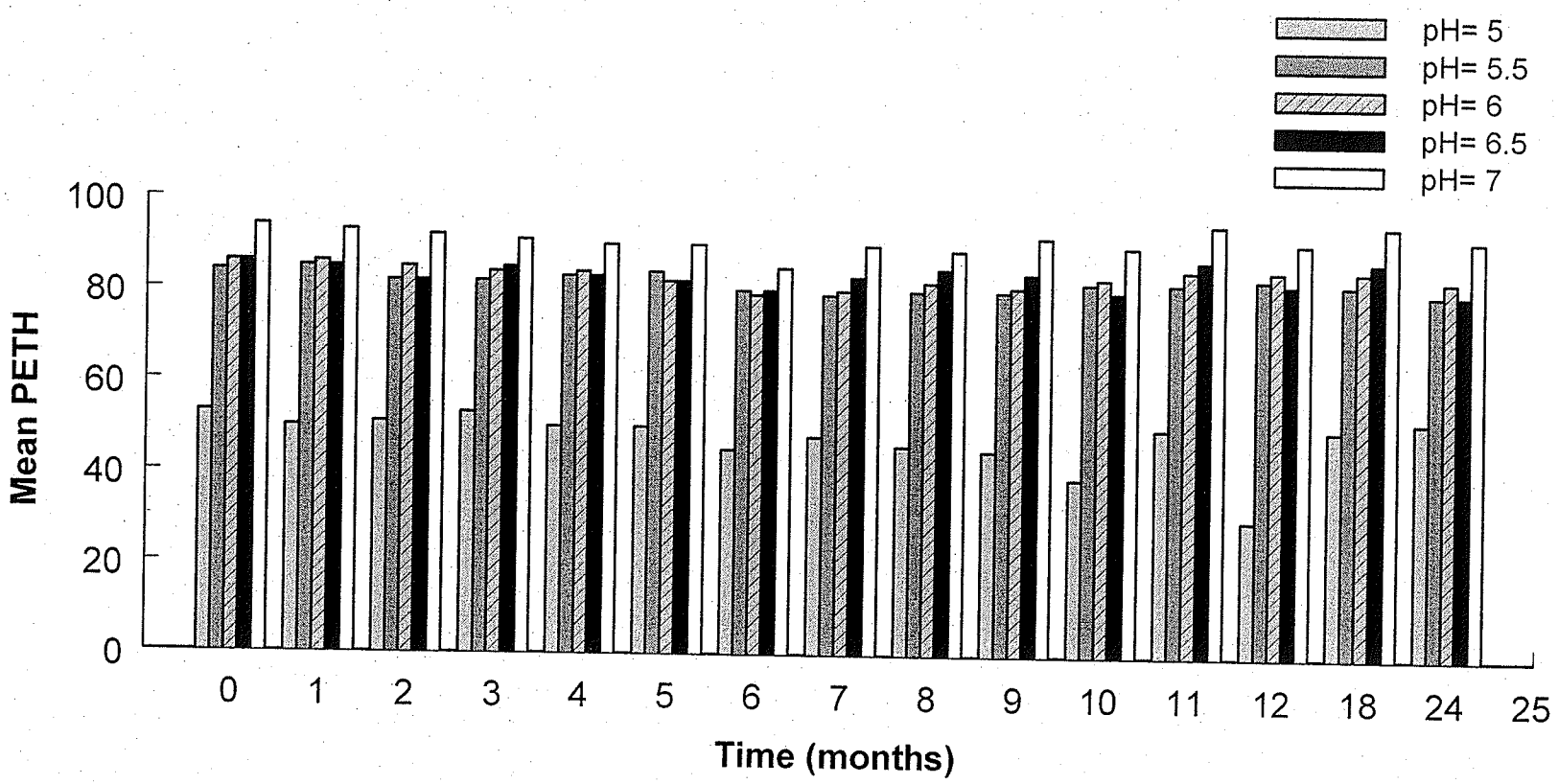

Figure 10: Effect of Changing pH on the Percent Entrapment of Hydroxyzine (PETH) in PC-SUV at Initial Formulation and after Storage at 10°C.

n=3

PC-SUV = small unilamellar vesicles (SUV) prepared using L-α-phosphatidylcholine (PC)

In stability study samples resulting in no loss of PETH over 24 months, intermediate time PETH values that were > ± 5% of initial PETH values were considered as outliers and not included in the data analysis

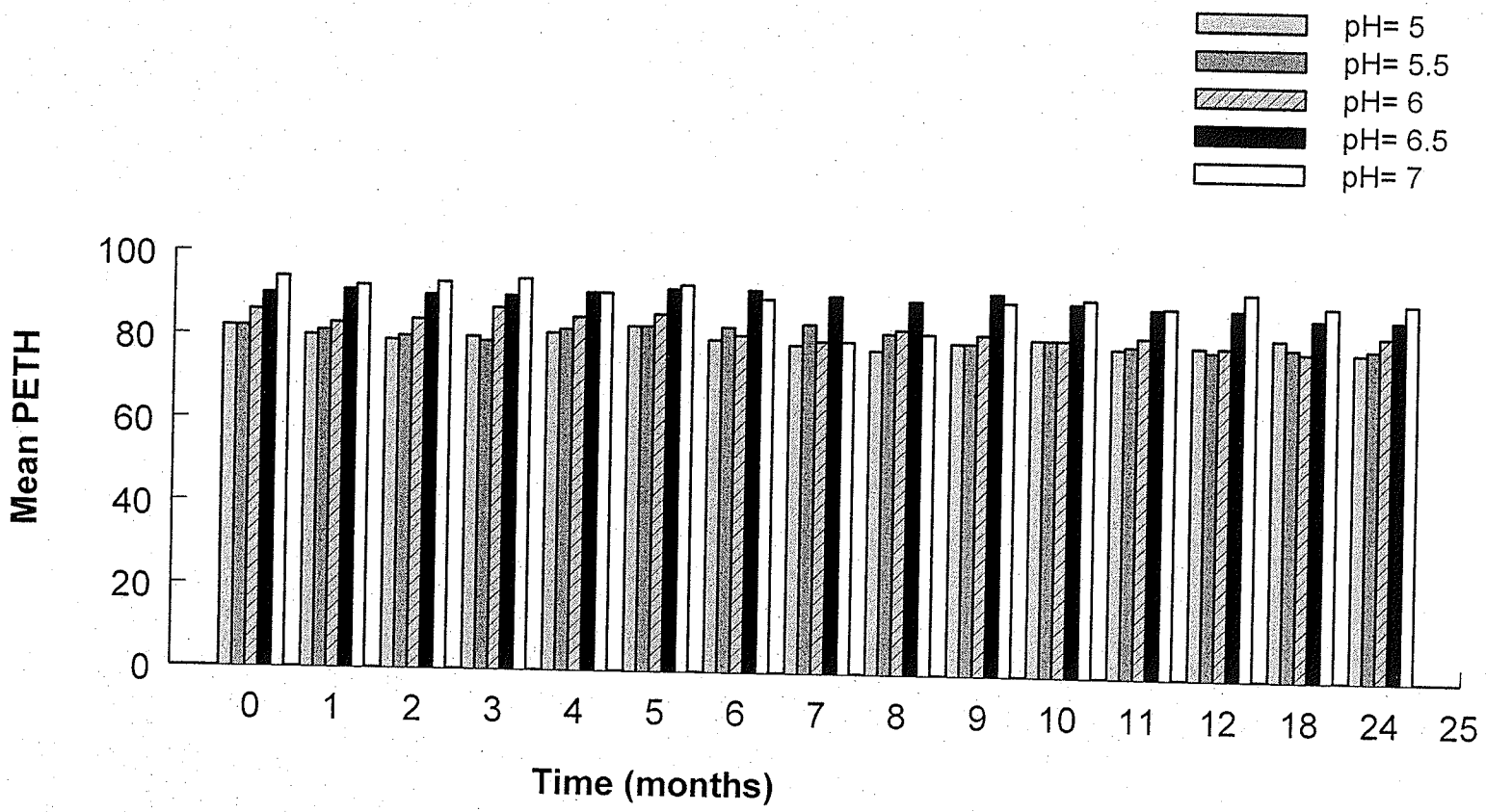

Figure 11: Effect of Changing pH on the Percent Entrapment of Hydroxyzine (PETH) in PC-MLV at Initial Formulation and after Storage at 10°C.

n=3

PC-MLV = multilamellar vesicles (MLV) prepared using L-α-phosphatidylcholine (PC)

In stability study samples resulting in no loss of PETH over 24 months, intermediate time PETH values that were > ± 5% of initial PETH values were considered as outliers and not included in the data analysis

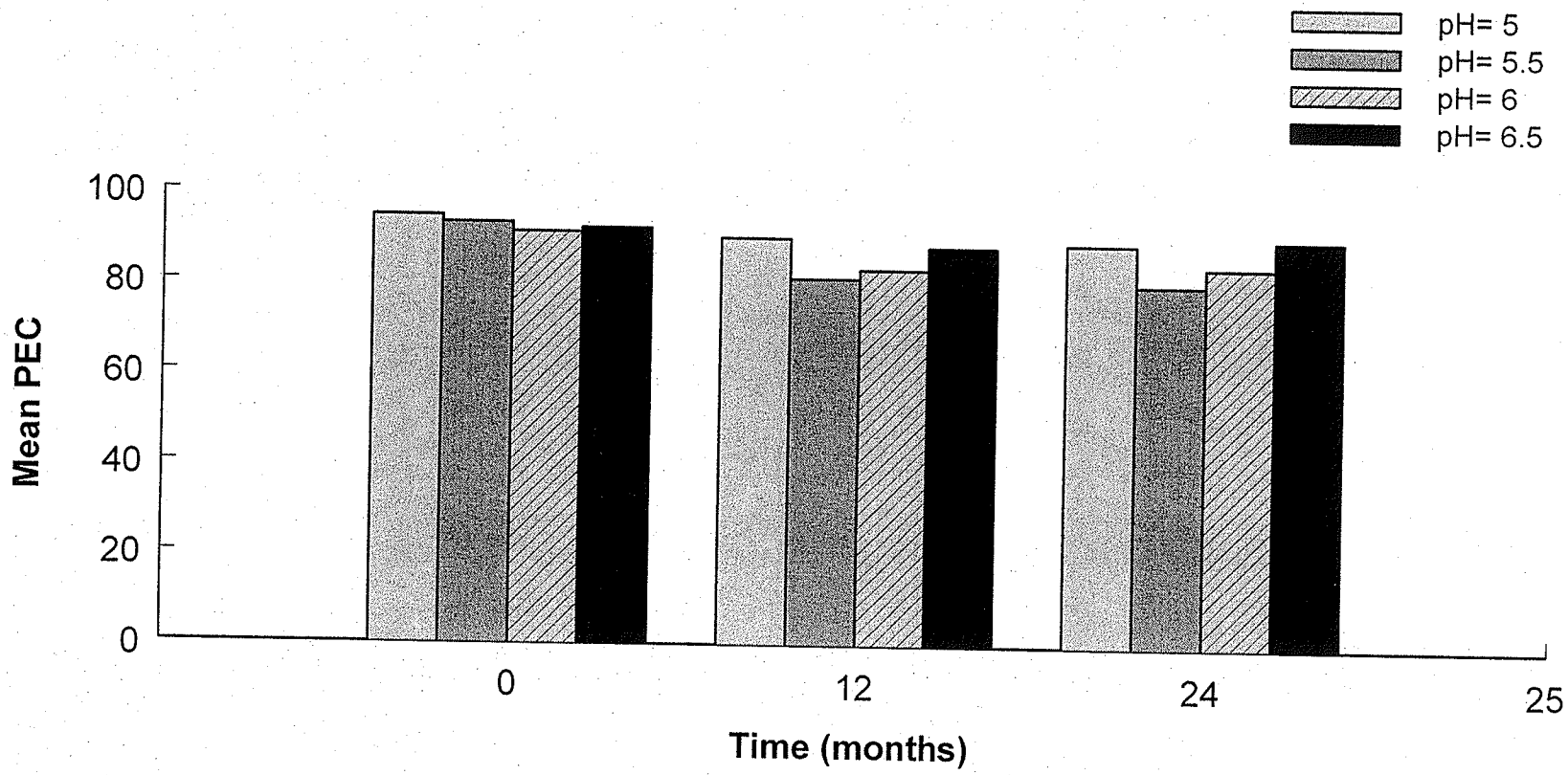

Figure 12: Effect of Changing pH on the Percent Entrapment of Cetirizine (PEC) in PC-SUV at Initial Formulation and after Storage at 10°C.

n=3

PC-SUV = small unilamellar vesicles (SUV) prepared using L-α-phosphatidylcholine (PC)

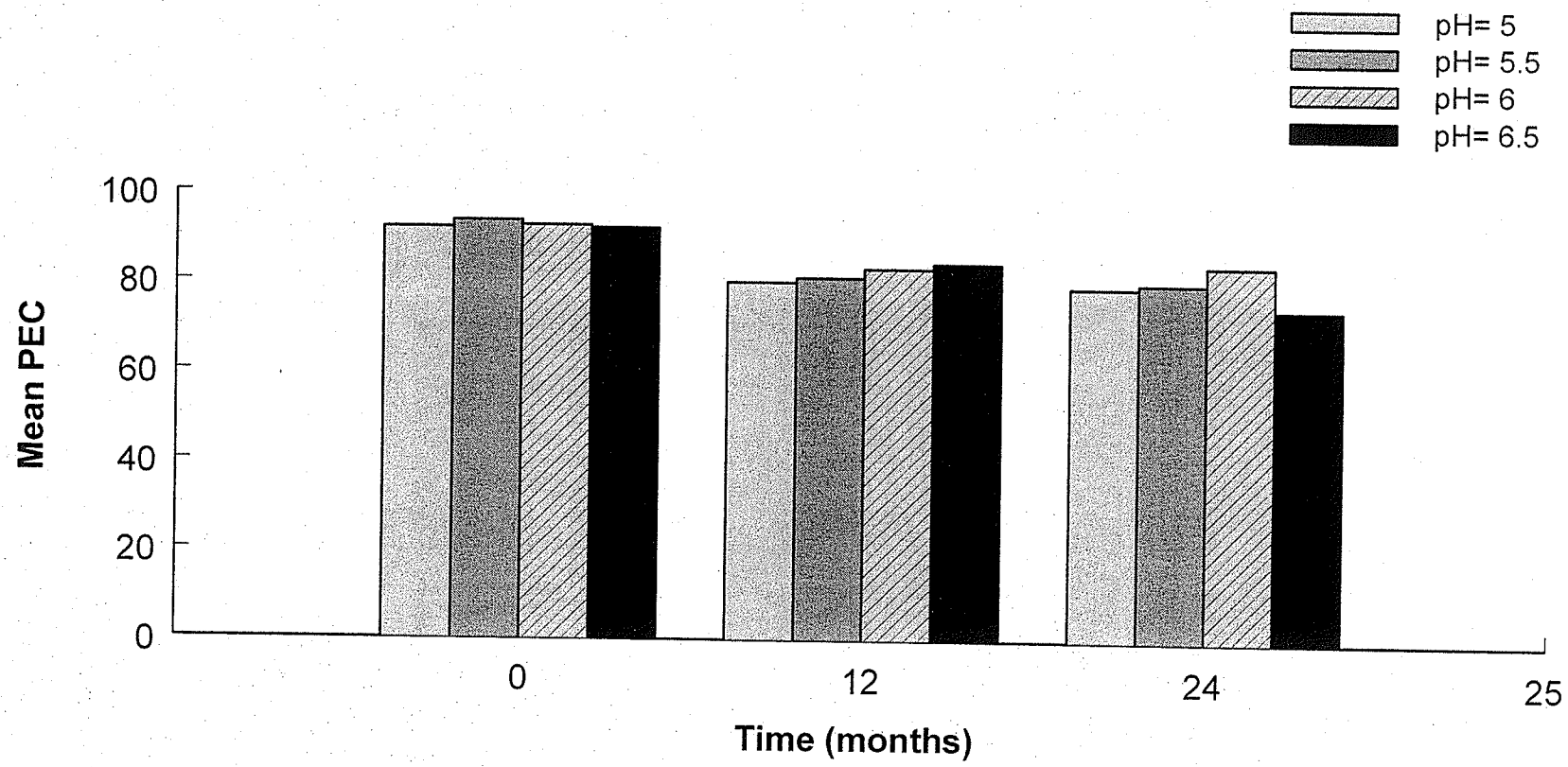

Figure 13: Effect of Changing pH on the Percent Entrapment of Cetirizine (PEC) in PC-MLV at Initial Formulation and after Storage at 10°C.

n=3

PC-MLV = multilamellar vesicles (MLV) prepared using L-α-phosphatidylcholine (PC)

Table 13: Effect of Changing Phospholipids on the Percent Entrapment of Hydroxyzine (PETH) in SUV, pH 6.5, at Initial Formulation and after Storage at 37°C

Phospholipids / Time (months)	PC	PS
	Mean Percent Entrapment of Hydroxyzine	
0	86.0	91.0
1	27.1	90.0
2	n.a.	89.0
3	n.a.	90.0
4	n.a.	90.0
5	n.a.	90.0
6	n.a.	86.0
7	n.a.	89.0
8	n.a.	88.0
9	n.a.	90.0
10	n.a.	91.0
11	n.a.	80.0
12	n.a.	89.0
18	n.a.	99.0
24	n.a.	94.0
Physical Appearance	unstable *	discoloration**

n= 3
PC = L-α-Phosphatidylcholine
PS = L-α-Phosphatidylserine
SUV = small unilamellar vesicles
* after 1 month
** after 4 months increased with time
n.a.= not available
In stability study samples resulting in no loss of Percent Entrapment of Hydroxyzine (PETH) over 24 months, intermediate time PETH values that were > ± 5% of initial PETH values were considered as outliers and not included in the data analysis

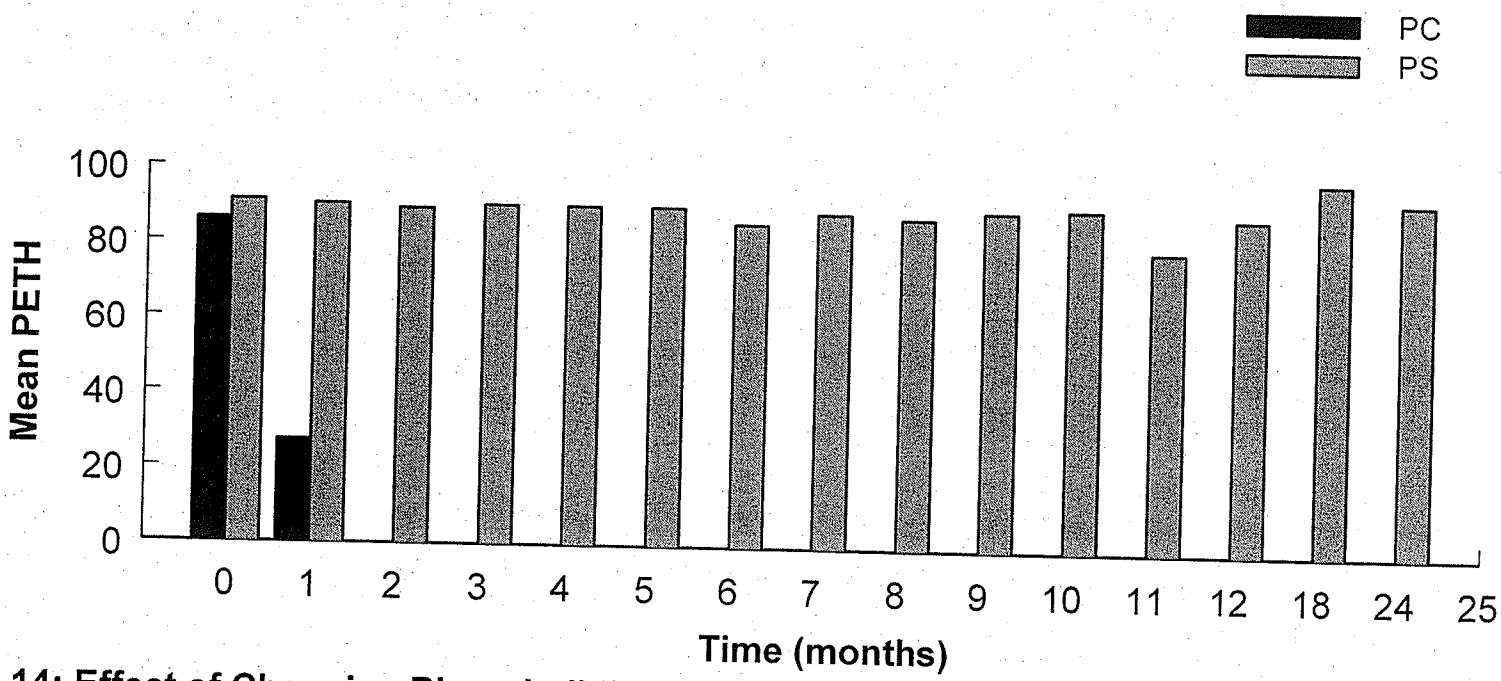

Figure 14: Effect of Changing Phospholipids on the Percent Entrapment of Hydroxyzine (PETH) in SUV, pH= 6.5, at Initial Formulation and after Storage at 37°C.

n=3

PC = L-α-Phosphatidylcholine, PS = L-α-Phosphatidylserine, SUV = small unilamellar vesicles

In stability study samples resulting in no loss of PETH over 24 months, intermediate time PETH values that were > ± 5% of initial PETH values were considered as outliers and not included in the data analysis

Table 14: Effect of Changing Phospholipids on the Percent Entrapment of Hydroxyzine (PETH) in MLV, pH 6.5, at Initial Formulation and after Storage at 37°C

Phospholipids / Time (months)	PC	HPC	PS
	Mean Percent Entrapment of Hydroxyzine		
0	94.3	91.0	94.3
1	61.8	94.0	97.0
2	n.a.	92.0	96.0
3	n.a.	93.0	98.0
4	n.a.	95.0	98.0
5	n.a.	91.0	92.0
6	n.a.	90.0	93.0
7	n.a.	92.0	95.0
8	n.a.	91.0	95.0
9	n.a.	91.0	94.0
10	n.a.	90.0	95.0
11	n.a.	89.0	93.0
12	n.a.	90.0	92.0
18	n.a.	92.0	n.a.
24	n.a.	91.0	n.a.
Physical Appearance	unstable*	no change	unstable**

n= 3
PC = L-α-Phosphatidylcholine
HPC = L-α-Phosphatidylcholine hydrogenated
PS = L-α-Phosphatidylserine
MLV = multilamellar vesicles
* after 4 months increased with time
** after 13 months increased with time
n.a.= not available
In stability study samples resulting in no loss of Percent Entrapment of Hydroxyzine (PETH) over 24 months, intermediate time PETH values that were > ± 5% of initial PETH values were considered as outliers and not included in the data analysis

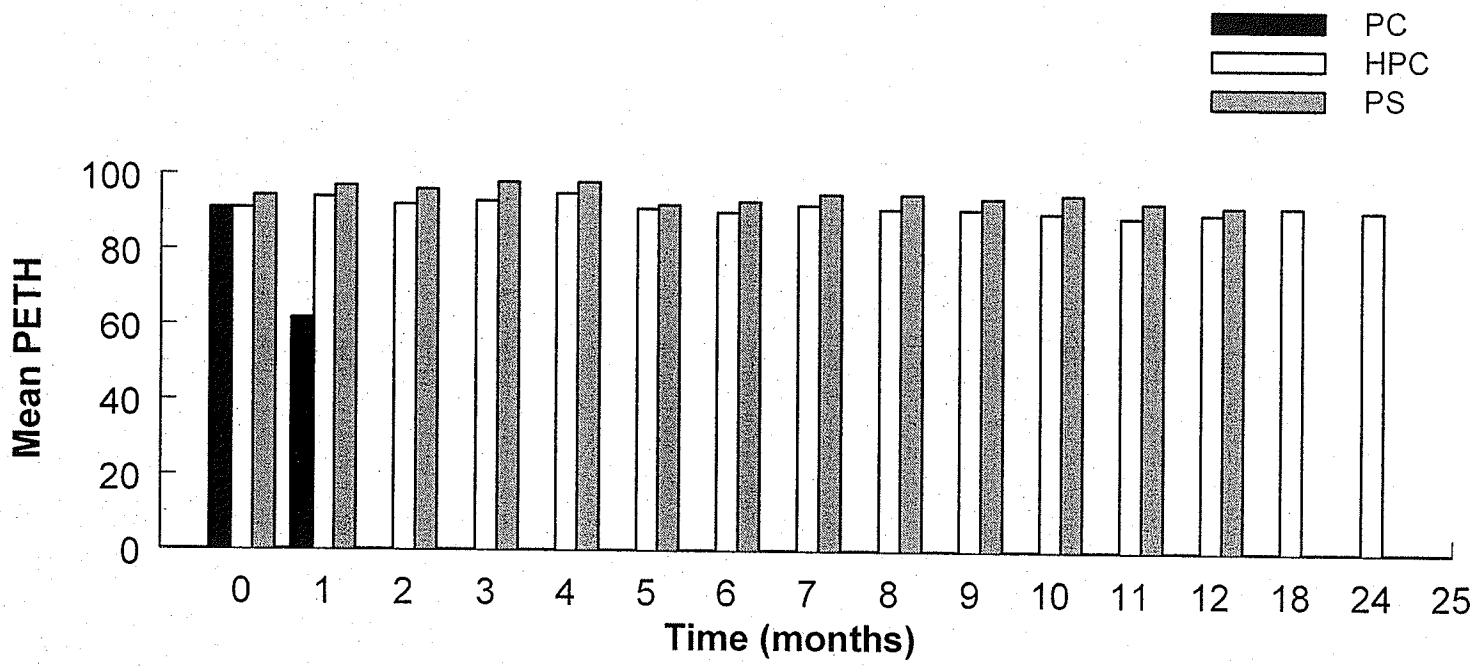

Figure 15: Effect of Changing Phospholipids on the Percent Entrapment of Hydroxyzine (PETH) in MLV, pH= 6.5, at Initial Formulation and after Storage at 37°C.

n=3

PC = L-α-Phosphatidylcholine, HPC = L-α-Phosphatidylcholine hydrogenated, PS = L-α-Phosphatidylserine, MLV = multilamellar vesicles

In stability study samples resulting in no loss of PETH over 24 months, intermediate time PETH values that were > ± 5% of initial PETH values were considered as outliers and not included in the data analysis

Table 15: Effect of Changing Phospholipids on the Percent Entrapment of Hydroxyzine (PETH) in SUV, pH 6.5, at Initial Formulation and after Storage at 25°C

Phospholipids / Time (months)	PC	PS
	Mean Percent Entrapment of Hydroxyzine	
0	86.0	91.0
1	85.0	94.0
2	86.0	92.0
3	83.0	95.0
4	84.0	93.0
5	83.0	90.0
6	82.0	92.0
7	80.0	91.0
8	78.0	92.0
9	75.0	89.0
10	82.0	90.0
11	80.0	92.0
12	81.0	91.0
18	80.0	98.0
24	80.3	80.0
Physical Appearance	discoloration*	discoloration*

n= 3
PC = L-α-Phosphatidylcholine
PS = L-α-Phosphatidylserine
SUV = small unilamellar vesicles
* after 4 months increased with time
In stability study samples resulting in no loss of Percent Entrapment of Hydroxyzine (PETH) over 24 months, intermediate time PETH values that were > ± 5% of initial PETH values were considered as outliers and not included in the data analysis

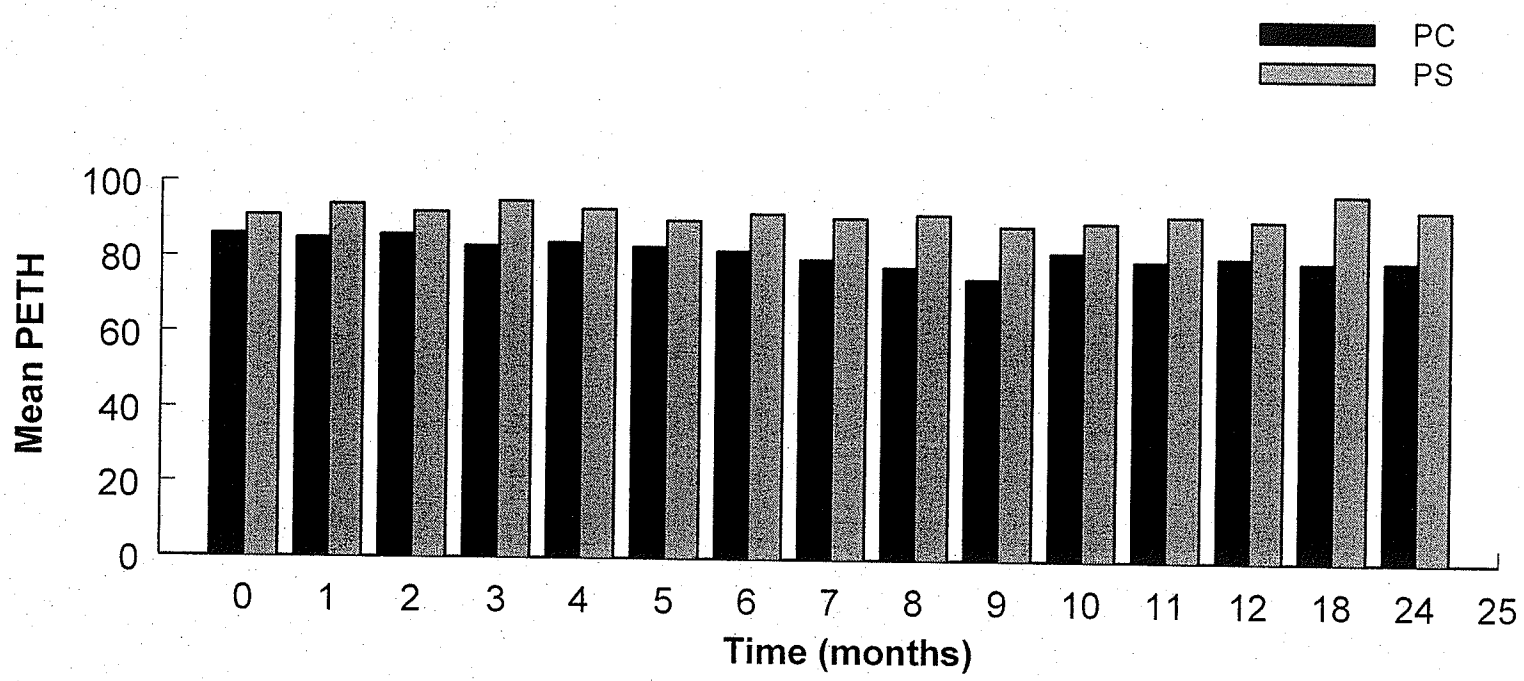

Figure 16: Effect of Changing Phospholipids on the Percent Entrapment of Hydroxyzine (PETH) in SUV, pH 6.5, at Initial Formulation and after Storage at 25°C.

n=3

PC = L-α-Phosphatidylcholine, PS = L-α-Phosphatidylserine, SUV = small unilamellar vesicles

In stability study samples resulting in no loss of PETH over 24 months, intermediate time PETH values that were > ± 5% of initial PETH values were considered as outliers and not included in the data analysis

Table 16: Effect of Changing Phospholipids on the Percent Entrapment of Hydroxyzine (PETH) in MLV, pH 6.5, at Initial Formulation and after Storage at 25°C

Phospholipids / Time (months)	PC	HPC	PS
	Mean Percent Entrapment of Hydroxyzine		
0	94.3	91.0	94.3
1	90.0	92.0	97.0
2	91.0	93.0	98.0
3	91.0	90.0	97.0
4	93.0	90.0	98.0
5	90.0	90.0	95.0
6	89.0	89.0	94.0
7	90.0	92.0	96.0
8	88.0	93.0	92.0
9	89.0	90.0	94.0
10	90.0	89.0	95.0
11	92.0	90.0	90.0
12	89.0	91.0	91.0
18	87.0	90.0	97.0
24	n.a.	92.0	94.0
Physical Appearance	discoloration*	no change	discoloration*

n= 3
PC = L-α-Phosphatidylcholine
HPC = L-α-Phosphatidylcholine hydrogenated
PS = L-α-Phosphatidylserine
MLV = multilamellar vesicles
* after 4 months increased with time
n.a. = not available
In stability study samples resulting in no loss of Percent Entrapment of Hydroxyzine (PETH) over 24 months, intermediate time PETH values that were > ± 5% of initial PETH values were considered as outliers and not included in the data analysis

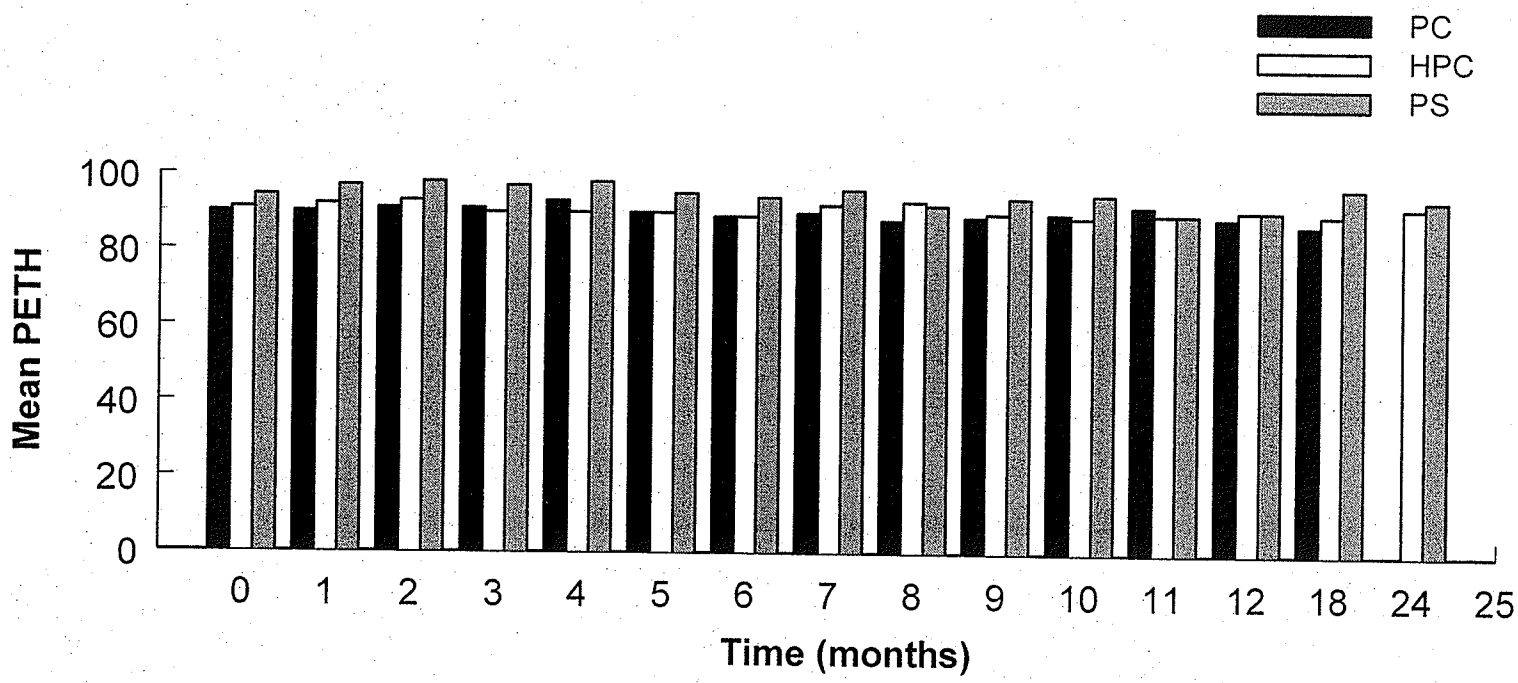

Figure 17: Effect of Changing Phospholipids on the Percent Entrapment of Hydroxyzine (PETH) in MLV, pH 6.5, at Initial Formulation and after Storage at 25°C.

n=3

PC = L-α-Phosphatidylcholine, HPC = L-α-Phosphatidylcholine hydrogenated, PS = L-α-Phosphatidylserine, MLV = multilamellar vesicles

In stability study samples resulting in no loss of PETH over 24 months, intermediate time PETH values that were > ± 5% of initial PETH values were considered as outliers and not included in the data analysis

Table 17: Effect of Changing Phospholipids on the Percent Entrapment of Hydroxyzine (PETH) in SUV, pH 6.5, at Initial Formulation and after Storage at 10°C

Phospholipids / Time (months)	PC	HPC	PS
	Mean Percent Entrapment of Hydroxyzine		
0	86.0	93.0	91.0
1	88.6	90.0	90.0
2	87.5	89.0	94.0
3	87.5	90.1	92.0
4	88.0	89.9	95.0
5	86.5	90.5	93.0
6	85.0	89.5	95.0
7	87.5	n.a.	94.0
8	87.0	n.a.	90.0
9	88.0	n.a.	91.0
10	85.0	n.a.	92.0
11	90.5	n.a.	90.0
12	87.5	88.1	93.0
18	92.5	86.9	97.0
24	85.0	88.1	94.0
Physical Appearance	no change	no change	slight discoloration*

n= 3
PC = L-α-Phosphatidylcholine
HPC = L-α-Phosphatidylcholine hydrogenated
PS = L-α-Phosphatidylserine
SUV = small unilamellar vesicles
* after 4 months increased with time
n.a. = not available
In stability study samples resulting in no loss of Percent Entrapment of Hydroxyzine (PETH) over 24 months, intermediate time PETH values that were > ± 5% of initial PETH values were considered as outliers and not included in the data analysis

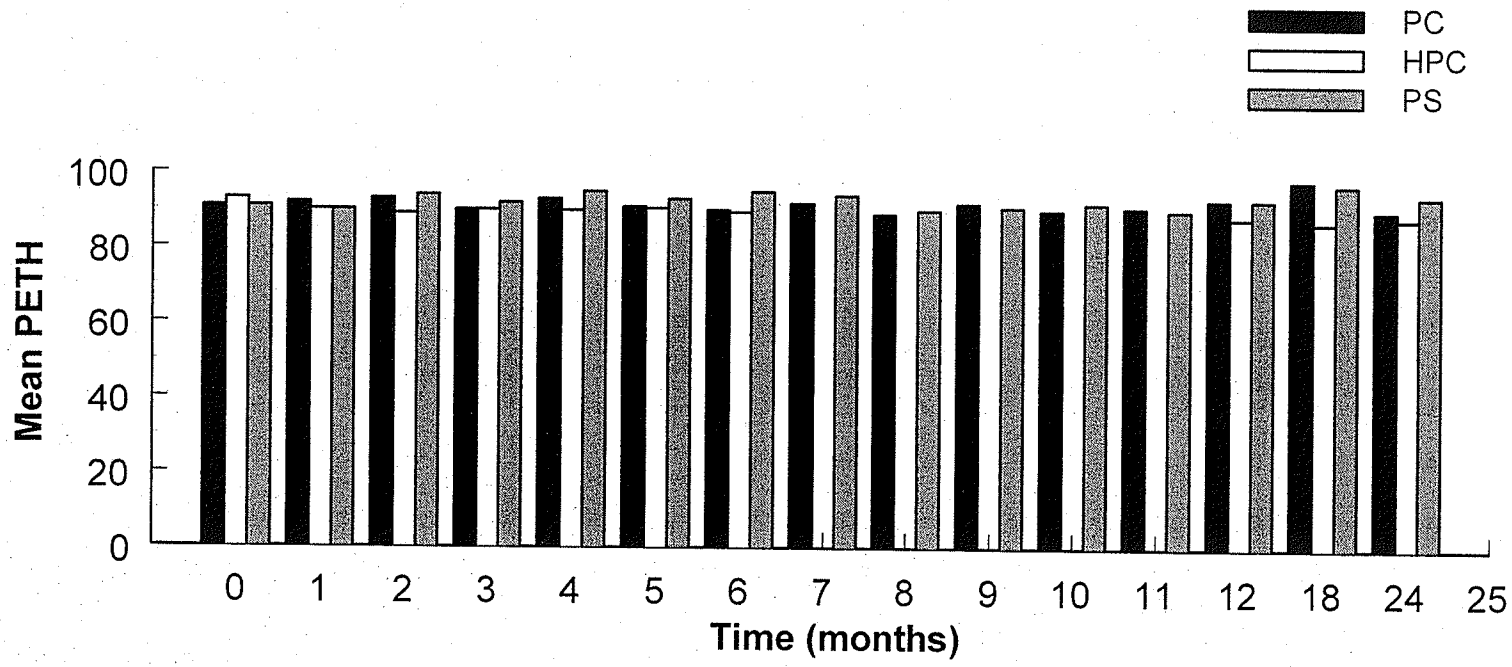

Figure 18: Effect of Changing Phospholipids on the Percent Entrapment of Hydroxyzine (PETH) in SUV, pH= 6.5, at Initial Formulation and after Storage at 10°C.

n=3

PC = L-α-Phosphatidylcholine, HPC = L-α-Phosphatidylcholine hydrogenated, PS = L-α-Phosphatidylserine,

SUV = small unilamellar vesicles

In stability study samples resulting in no loss of PETH over 24 months, intermediate time PETH values that were > ± 5% of initial PETH values were considered as outliers and not included in the data analysis

Table 18: Effect of Changing Phospholipids on the Percent Entrapment of Hydroxyzine (PETH) in MLV, pH 6.5, at Initial Formulation and after Storage at 10°C

Phospholipids / Time (months)	PC	HPC	PS
	Mean Percent Entrapment of Hydroxyzine		
0	94.3	94.0	93.0
1	92.7	97.0	95.0
2	92.0	96.0	97.0
3	93.0	98.0	98.0
4	92.7	98.0	91.0
5	92.6	94.0	95.0
6	93.6	95.0	90.0
7	93.0	94.0	94.0
8	92.2	93.0	93.0
9	92.7	94.0	92.0
10	94.0	93.0	92.0
11	91.9	92.0	90.0
12	91.8	94.0	91.0
18	92.0	89.0	97.0
24	91.8	90.0	95.0
Physical Appearance	no change	no change	slight discoloration

n= 3

PC = L-α-Phosphatidylcholine HPC = L-α-Phosphatidylcholine hydrogenated

PS = L-α-Phosphatidylserine MLV = multilamellar vesicles

* after 4 months increased with time

In stability study samples resulting in no loss of Percent Entrapment of Hydroxyzine (PETH) over 24 months, intermediate time PETH values that were > ± 5% of initial PETH values were considered as outliers and not included in the data analysis

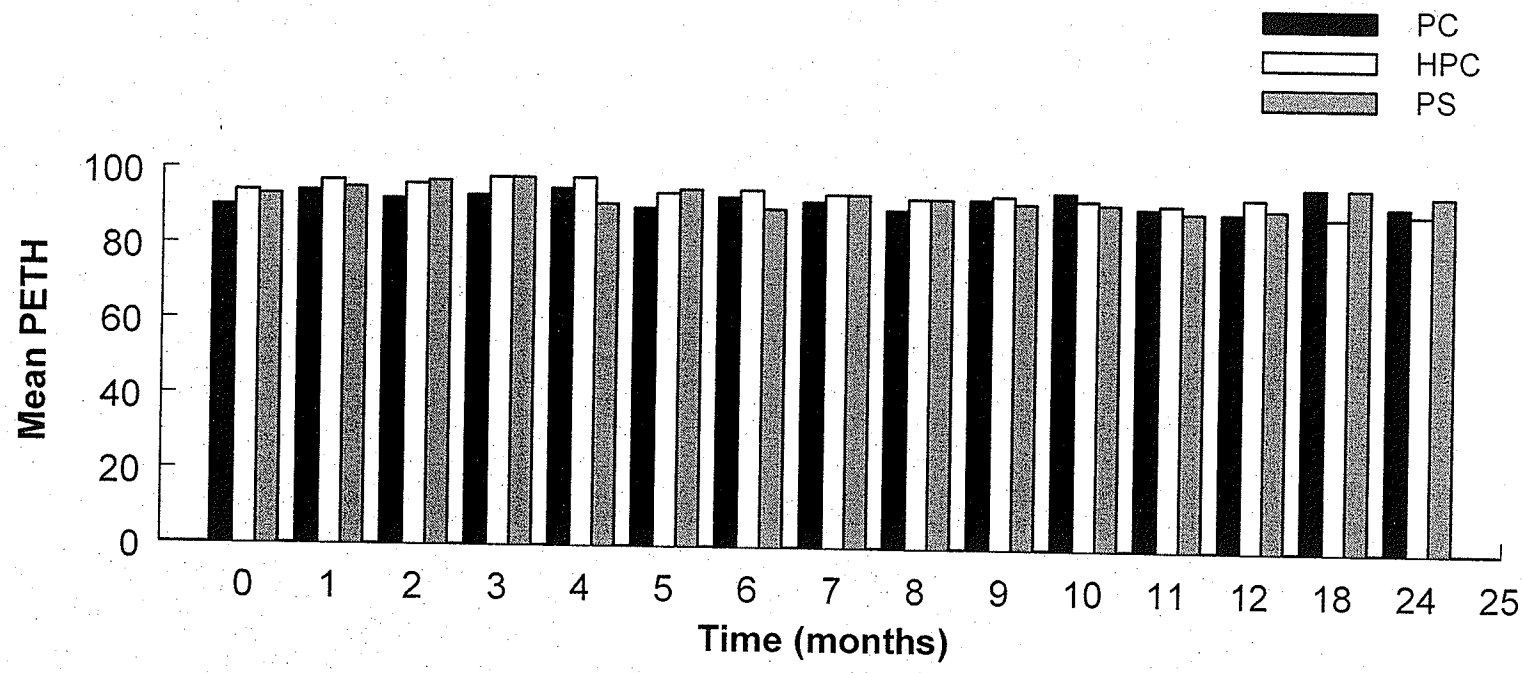

Figure 19: Effect of Changing Phospholipids on the Percent Entrapment of Hydroxyzine (PETH) in MLV, pH 6.5, at Initial Formulation and after Storage at 10°C.

n=3

PC = L-α-Phosphatidylcholine, HPC = L-α-Phosphatidylcholine hydrogenated, PS = L-α-Phosphatidylserine,

MLV = multilamellar vesicles

In stability study samples resulting in no loss of PETH over 24 months, intermediate time PETH values that were > ± 5% of initial PETH values were considered as outliers and not included in the data analysis

Table 19: Effect of Changing Phospholipids on the Percent Entrapment of Cetirizine (PEC) in SUV, pH 6.5, at Initial Formulation and after Storage at 10°C

Phospholipids / Time (months)	PC	HPC	PS
	Mean Percent Entrapment of Cetirizine		
0	92.0	92.8	93.4
12	88.1	91.0	92.1
24	90.1	89.3	92.1
Physical Appearance	no change	no change	slight discoloration**

n= 3
PC = L-α-Phosphatidylcholine
HPC = L-α-Phosphatidylcholine hydrogenated
PS = L-α-Phosphatidylserine
SUV = small unilamellar vesicles
* *after 4 months increased with time

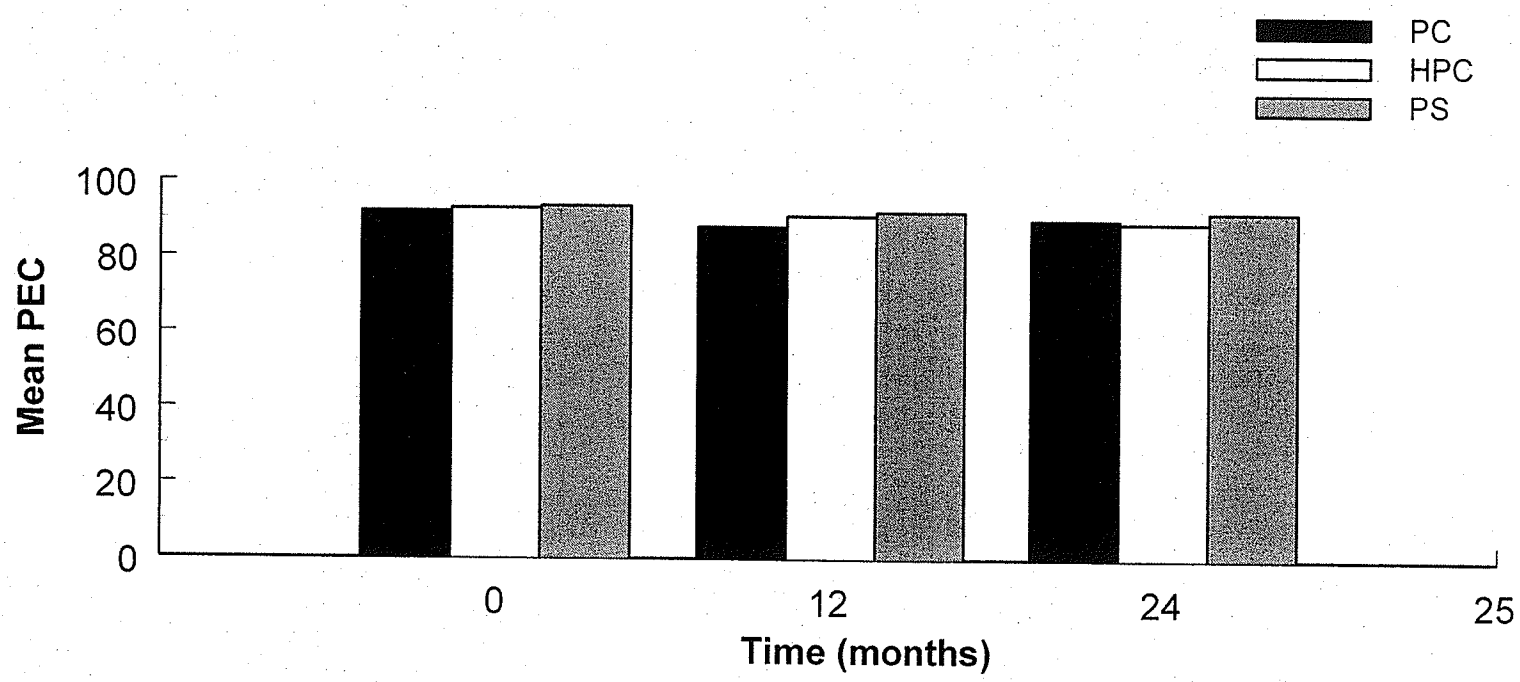

Figure 20: Effect of Changing Phospholipids on the Percent Entrapment of Cetirizine (PEC) in SUV, pH 6.5, at Initial Formulation and after Storage at 10°C.

n=3

PC = L-α-Phosphatidylcholine, HPC = L-α-Phosphatidylcholine hydrogenated, PS = L-α-Phosphatidylserine, SUV = small unilamellar vesicles

Table 20: Effect of Changing Phospholipids on the Percent Entrapment of Cetirizine (PEC) in MLV, pH 6.5, at Initial Formulation and after Storage at 10°C

Phospholipids / Time (months)	PC	HPC	PS
	Mean Percent Entrapment of Cetirizine		
0	92.0	89.7	90.7
12	84.3	89.5	70.8
24	74.3	87.5	69.8
Physical Appearance	slight discoloration*	no change	slight discoloration*

n= 3
PC = L-α-Phosphatidylcholine
HPC = L-α-Phosphatidylcholine hydrogenated
PS = L-α-Phosphatidylserine
MLV = multilamellar vesicles
*after 4 months increased with time

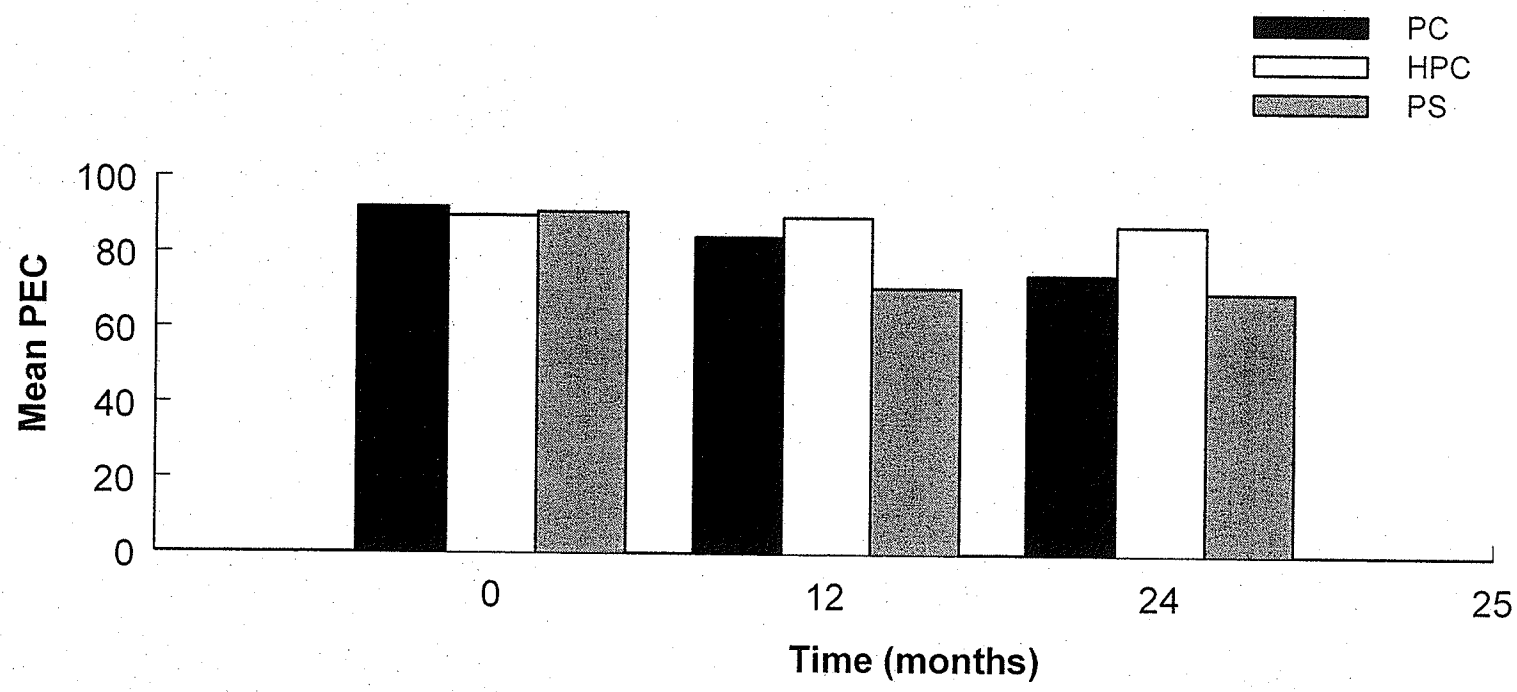

Figure 21: Effect of Changing Phospholipids on the Percent Entrapment of Cetirizine (PEC) in MLV, pH 6.5, at Initial Formulation and after Storage at 10°C.

n=3

PC = L-α-Phosphatidylcholine, HPC = L-α-Phosphatidylcholine hydrogenated, PS = L-α-Phosphatidylserine, MLV = multilamellar vesicles

Table 21: Effect of Changing Phospholipids: the Mean Particle Diameters of Initial and Stored Hydroxyzine or Cetirizine Liposomes, pH = 6.5, Stored at 10°C

Liposomes	Hydroxyzine			Cetirizine			F (%)	Time (m)
	*PSA (μm)	**PSA (nm)	***PSA (nm)	*PSA (μm)	**PSA (nm)	***PSA (nm)		
PC-SUV	**0.26 ± 0.2**	**51.7 ± 7.9**	**174.0 ± 82.1**	**0.17 ± 0.09**	**153.5 ± 17.8**	**109.0 ± 17.9**	**100.0**	**0**
PC-SUV	2.7 ± 0.36	n.d.	265.2 ± 100.2	1.52 ± 0.24	n.d.	222.0 ± 60.5	96.8	20
HPC-SUV	**2.58 ± 0.37**	**n.d.**	**120.0 ± 43.2**	**1.96 ± 0.28**	**40.0 ± 4**	**180.0 ± 89.0**	**98.0**	**0**
HPC-SUV	n.d.	n.d.	n.d.	n.d.	n.d.	n.d.	n.d.	20
PS-SUV	**0.13 ± 0.06**	**102.5 ± 4.8**	**171.6 ± 64.3**	**0.10± 0.04**	**204.5 ± 11.1**	**100.9 ± 40.3**	**100.0**	**0**
PS-SUV	2.18 ± 0.34	n.d.	300 ± 50.1	1.75 ± 0.25	n.d.	306.1 ± 58.1	91.0	20
PC-MLV	**4.87 ± 0.65**	**264 ± 22.3**	**1020 ± 70.1**	**3.47 ± 0.53**	**358.3 ± 22.0**	**1000.5 ± 100.1**	**91.7**	**0**
PC-MLV	2.73 ± 0.34	n.d.	n.d.	1.7 ± 0.23	n.d.	798.5 ± 50.1	99.7	20
HPC-MLV	**9.46 ± 0.96**	**162 ± 22.9**	**834.0 ± 30.2**	**11.16 ± 1.28**	**296.0 ± 27.1**	**2300.1 ± 54.2**	**95.0**	**0**
HPC-MLV	2.65 ± 0.81	n.d.	1093.2 ± 40.5	14.51 ± 10.08	n.d.	1740.0 ± 100.5	100.0	20
PS-MLV	**5.97± 0.60**	**271.4 ± 39.1**	**996.2 ± 100.1**	**2.65 ± 0.81**	**162.5 ± 22.9**	**1099.6 ± 105.1**	**86.3**	**0**
PS-MLV	2.18 ± 0.33	n.d.	958.8 ± 90.5	1.51 ± 0.19	n.d.	772.8 ± 60.1	100.0	20

n= 3 m = months SD = Standard deviation F = % volume of the sample analyzed
* PSA = Mean particle size ± SD measured using Submicron Particle Sizer n.d. = not determined or the TEM was out of focus
** PSA = Mean particle diameters ± SEM measured from Transmission Electron Micrograph (TEM)
*** PSA = Mean particle diameters ± SEM measured from Micrograph of Optical Microscope (MOM) connected to video camera and computer
PC-SUV = small unilamellar vesicles (SUV) prepared using L-α-phosphatidylcholine (PC)
PC-MLV = multilamellar vesicles (MLV) prepared using L-α-phosphatidylcholine (PC)
HPC-SUV = small unilamellar vesicles (SUV) prepared using L-α-phosphatidylcholine hydrogenated (HPC)
HPC-MLV = multilamellar vesicles (MLV) prepared using L-α-phosphatidylcholine hydrogenated (HPC)
PS-SUV = small unilamellar vesicles (SUV) prepared using L-α-phosphatidylserine (PS)
PS-MLV = multilamellar vesicles (MLV) prepared using L-α-phosphatidylserine (PS)

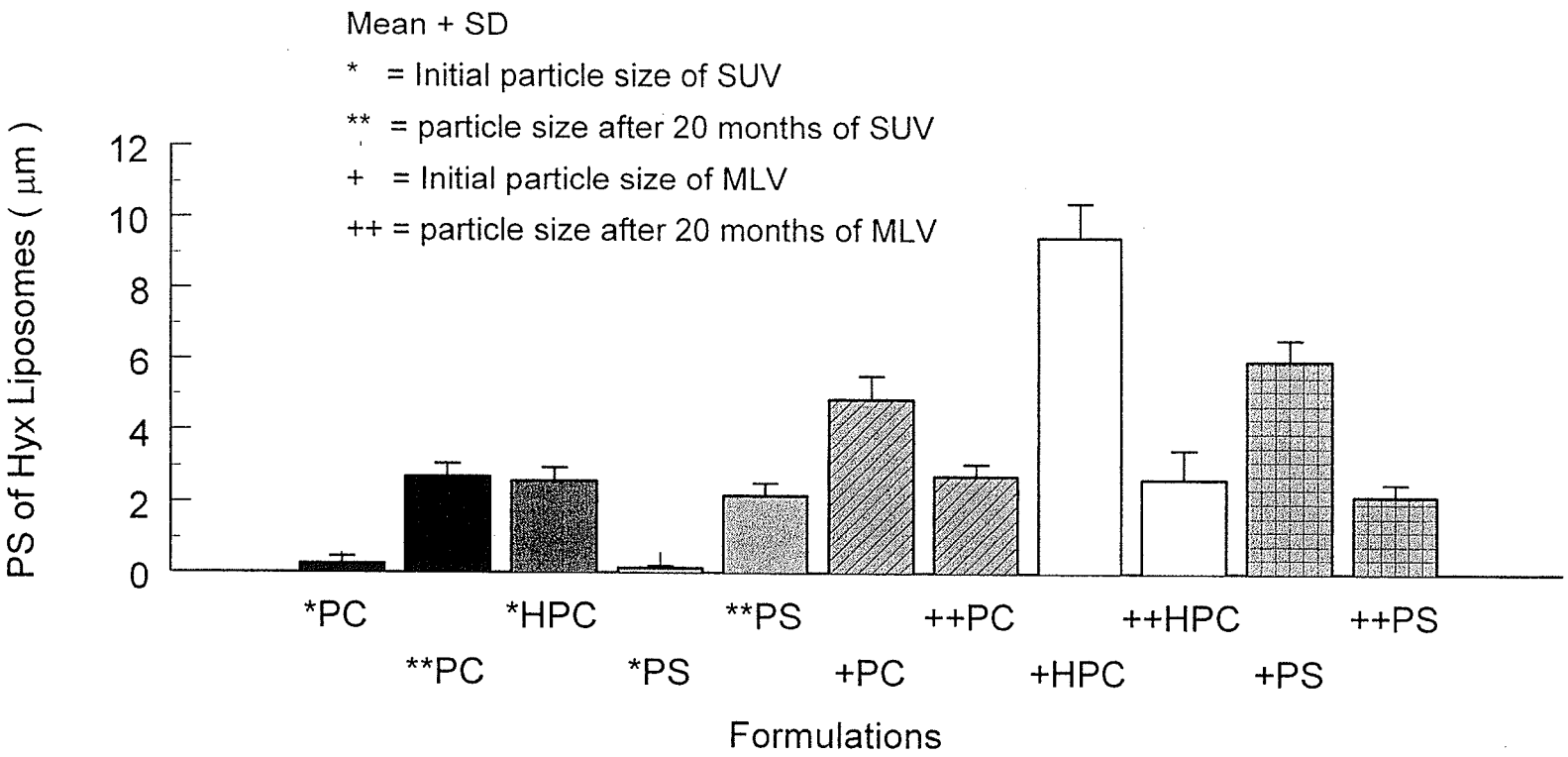

Figure 22a: Effect of Changing Phospholipids on the Initial and Long Term Particle Size of Hydroxyzine Liposomes Measured Using Submicron Particle Sizer, pH= 6.5, Stored at 10°C

n=3

PC = L-α-Phosphatidylcholine, HPC = L-α-Phosphatidylcholine hdrogenated, PS = L-α-Phosphatidylserine, SUV = small unilamellar vesicles, MLV = multilamellar vesicles, Hyx= Hydroxyzine

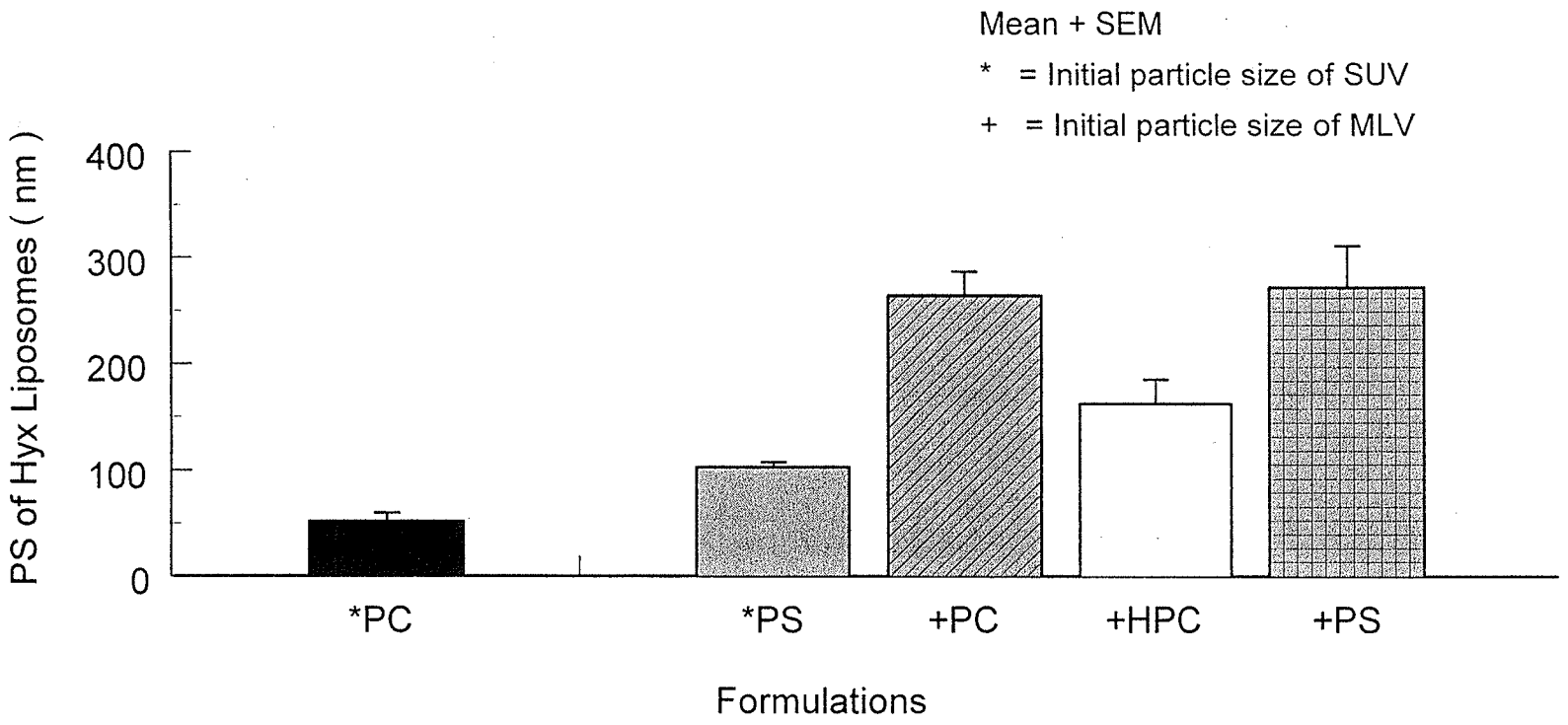

Figure 22b: Effect of Changing Phospholipids on the Initial Particle Size of Hydroxyzine Liposomes Measured from Transmission Electron Micrograph, pH= 6.5

n=3

PC = L-α-Phosphatidylcholine, HPC = L-α-Phosphatidylcholine hdrogenated, PS = L-α-Phosphatidylserine, SUV = small unilamellar vesicles, MLV = multilamellar vesicles, Hyx= Hydroxyzine

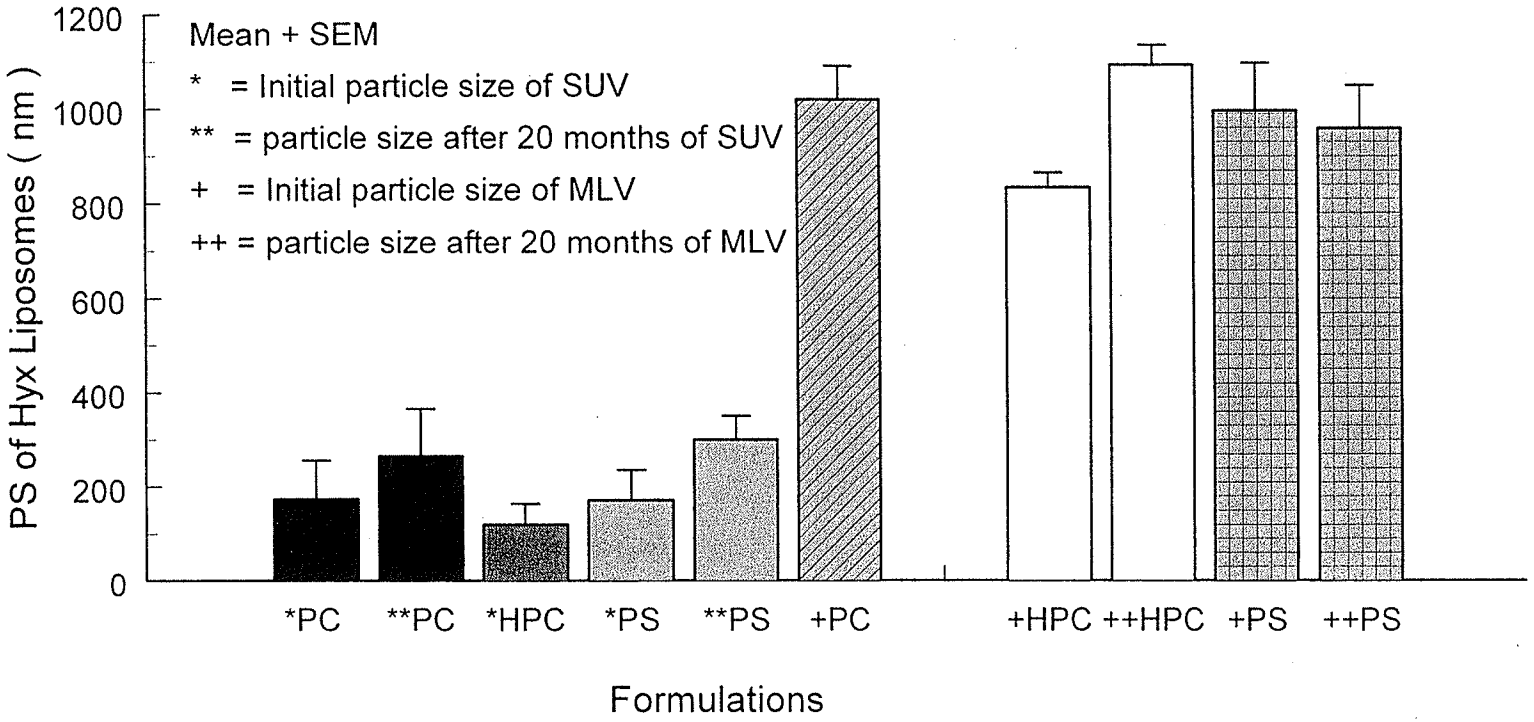

Figure 22c: Effect of Changing Phospholipids on the Initial and Long Term Particle Size of Hydroxyzine Liposomes Measured Using Optical Microscope Connected with Video Camera and Computer, pH= 6.5, Stored at 10°C

n= 6

PC = L-α-Phosphatidylcholine, HPC = L-α-Phosphatidylcholine hdrogenated, PS = L-α-Phosphatidylserine, SUV = small unilamellar vesicles, MLV = multilamellar vesicles, Hyx= Hydroxyzine

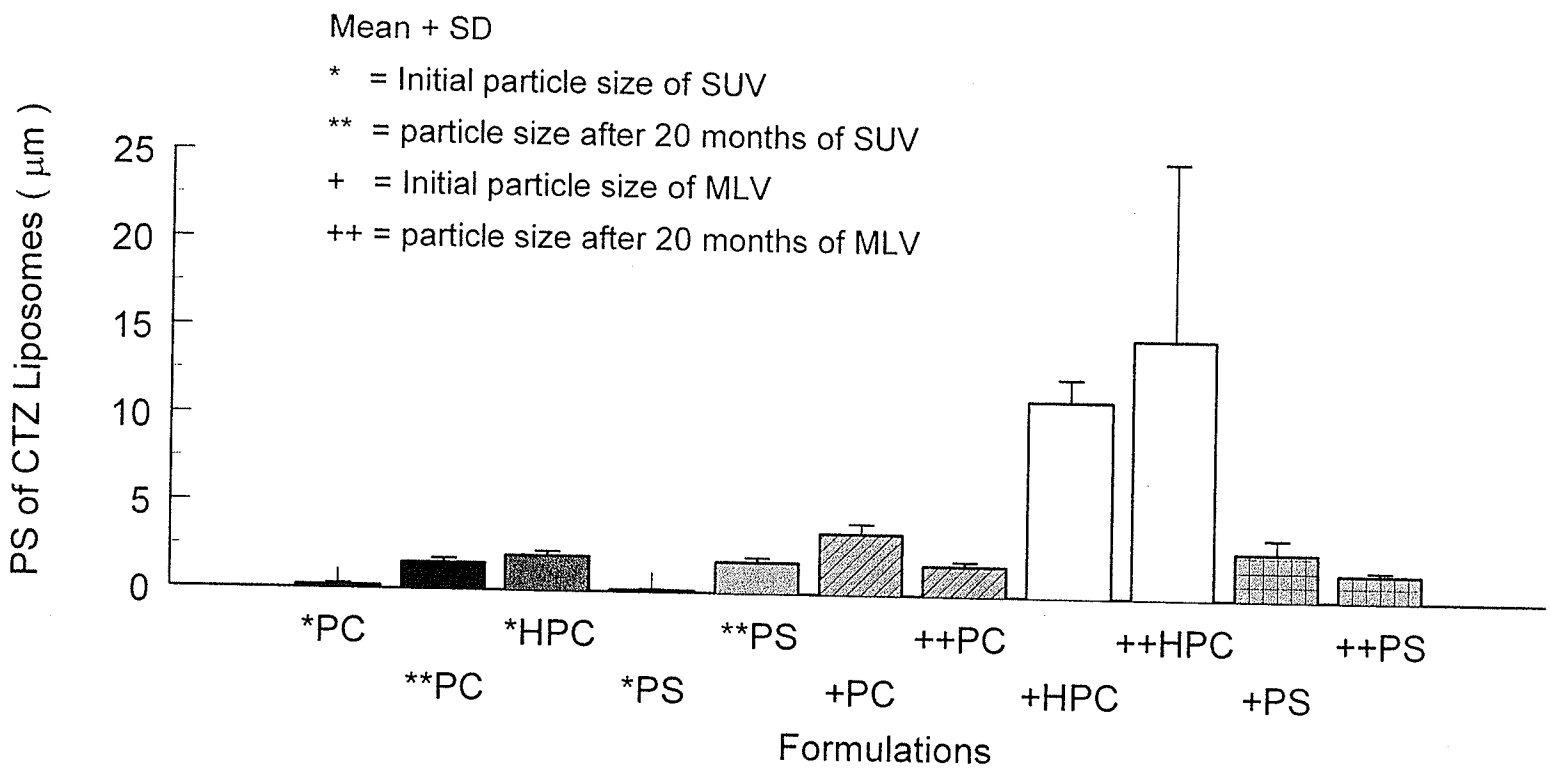

Figure 23a: Effect of Changing Phospholipids on the Initial and Long Term Particle Size of Cetirizine Liposomes Measured Using Submicron Particle Sizer, pH= 6.5, Stored at 10°C

n=3

PC = L-α-Phosphatidylcholine, HPC = L-∝-Phosphatidylcholine hdrogenated, PS = L-∝-Phosphatidylserine, SUV = small unilamellar vesicles, MLV = multilamellar vesicles, CTZ= Cetirizine

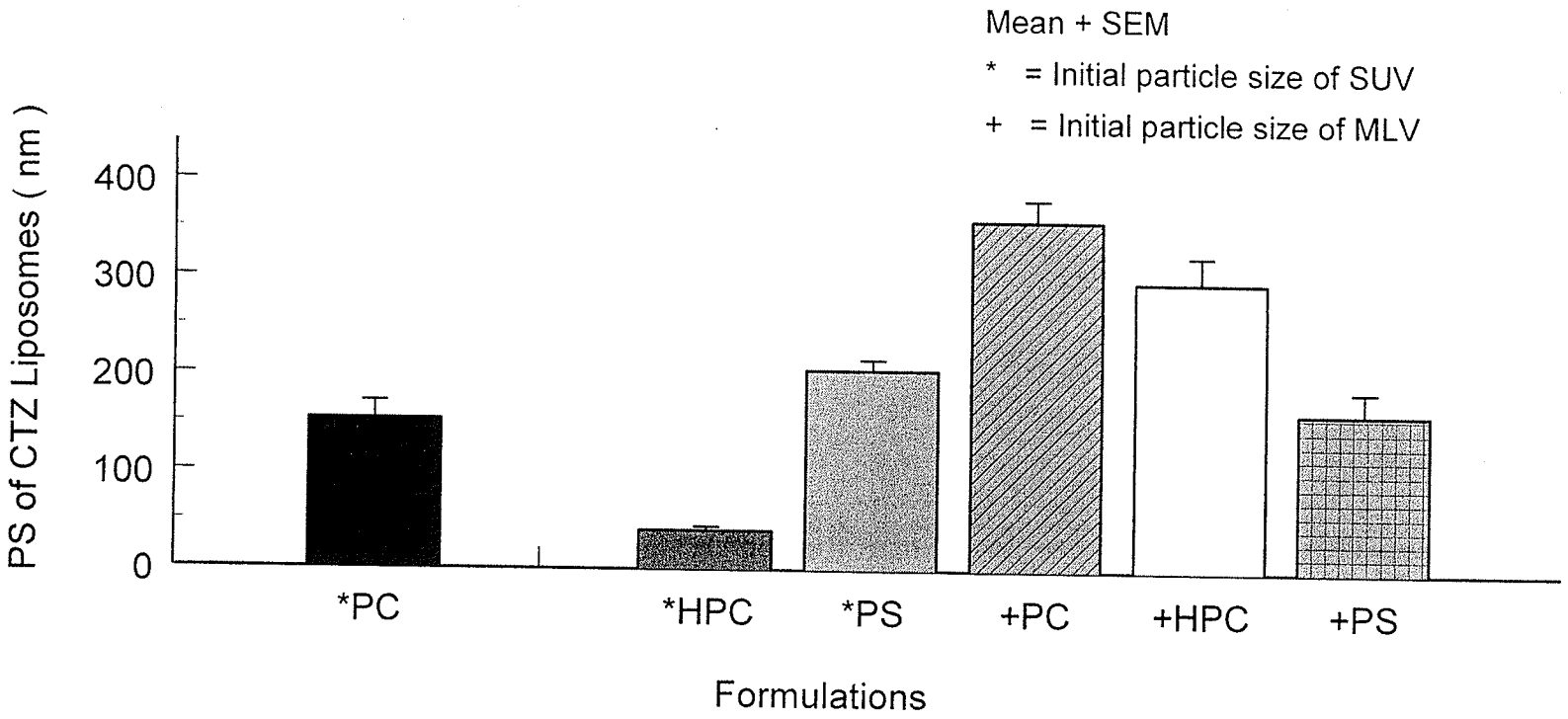

Figure 23b: Effect of Changing Phospholipids on the Initial Particle Size of Cetirizine Liposomes Measured from Transmission Electron Micrograph, pH= 6.5

n=3

PC = L-α-Phosphatidylcholine, HPC = L-α-Phosphatidylcholine hdrogenated, PS = L-α-Phosphatidylserine, SUV = small unilamellar vesicles, MLV = multilamellar vesicles, CTZ= Cetirizine

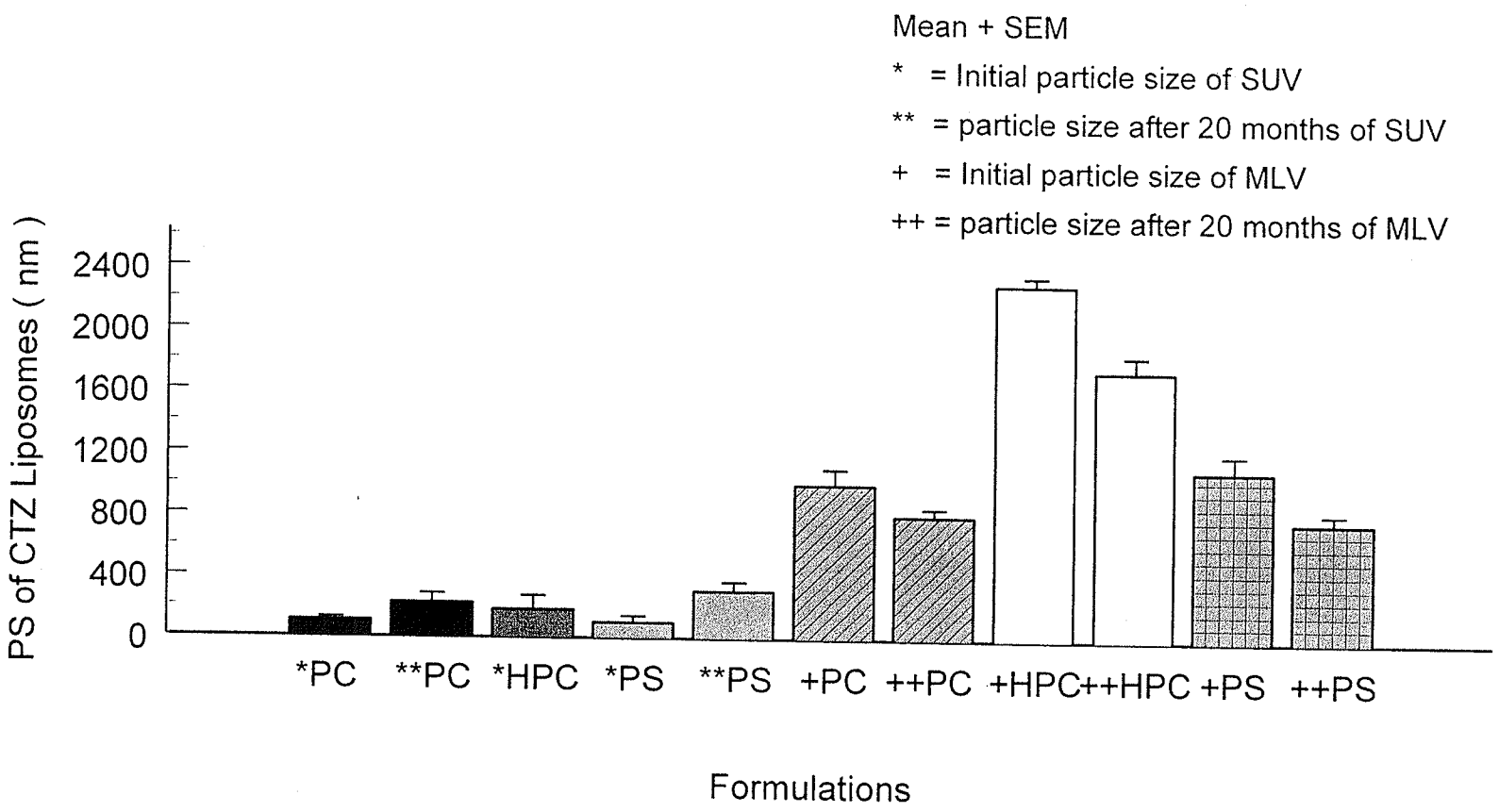

Figure 23c: Effect of Changing Phospholipids on the Initial and Long Term Particle Size of Cetirizine Liposomes Measured Using Optical Microscope Connected with Video Camera and Computer, pH= 6.5, Stored at 10°C

n= 6

PC = L-α-Phosphatidylcholine, HPC = L-α-Phosphatidylcholine hdrogenated, PS = L-α-Phosphatidylserine, SUV = small unilamellar vesicles, MLV = multilamellar vesicles, CTZ= Cetirizine

Table 22: Histamine-Induced Wheal Areas on Shaved Backs of Rabbits after the Topical Application of Non-Medicated PC-SUV

Time (h) / Rabbit Code	Wheal Area (cm^2)					
	0	0.5	1	2	3	4
1	1.13	1.16	1.12	1.38	1.14	0.95
3	1.09	1.06	1.63	1.63	1.37	1.03
6	1.30	1.10	1.24	1.38	1.40	1.36
Mean	1.18	1.11	1.33	1.46	1.30	1.11
SEM	0.07	0.03	0.15	0.08	0.08	0.13

n= 3

PC-SUV = small unilamellar vesicles (SUV) prepared using L-α-phosphatidylcholine (PC)

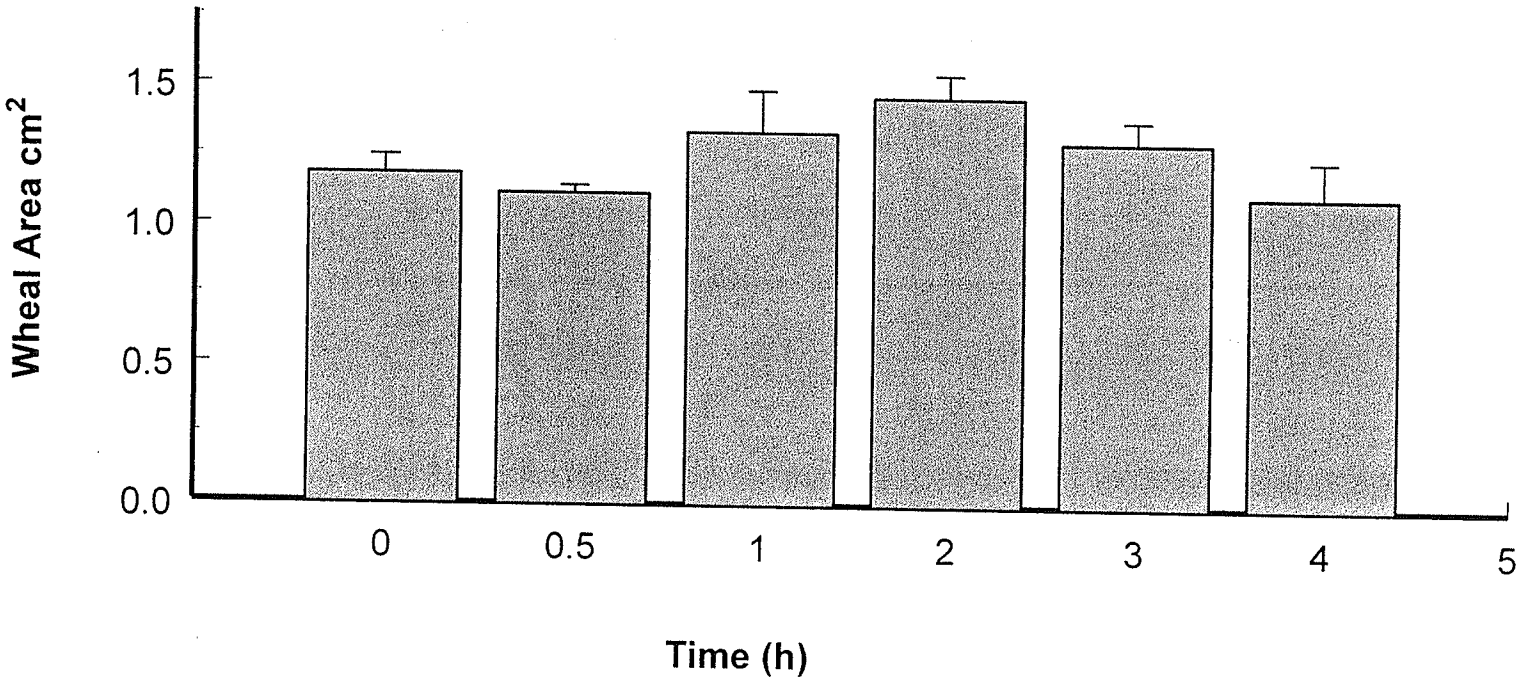

Figure 24: Mean ± SEM Wheal Areas of Histamine-Induced Wheal on Shaved Backs of Rabbits after the Topical Application of of Non-Medicated PC-SUV.

n=3

PC-SUV = small unilamellar vesicles (SUV) prepared using L-α-phosphatidylcholine (PC)

Table 23: HPLC Calibration of Hydroxyzine in Plasma

Concentration of Hydroxyzine (ng/mL)	Mean Peak Area Ratio	% C.V.
0	0.00	0.00
20	0.14	1.43
40	0.26	1.15
60	0.40	0.50
80	0.54	0.19
100	0.70	0.43

Table 24: HPLC Calibration of Cetirizine in Plasma

Concentration of Cetirizine (ng/mL)	Mean Peak Area Ratio	% C.V.
0	0.000	0.000
20	0.25	0.005
40	0.50	0.007
60	0.78	0.007
80	1.10	0.012
100	1.30	0.009

n= 8
% C.V. = percent coefficient of variation

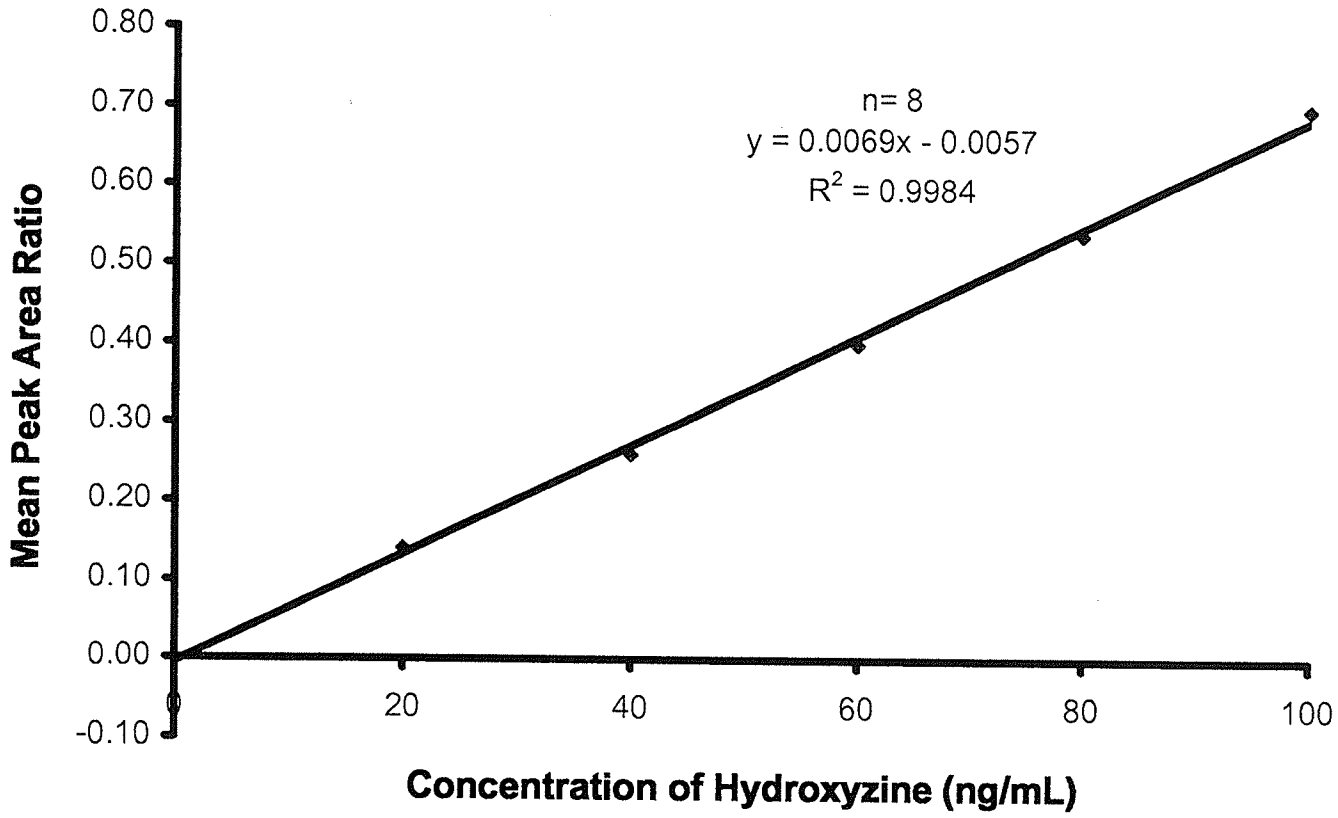

Figure 25: HPLC Calibration of Hydroxyzine in Plasma

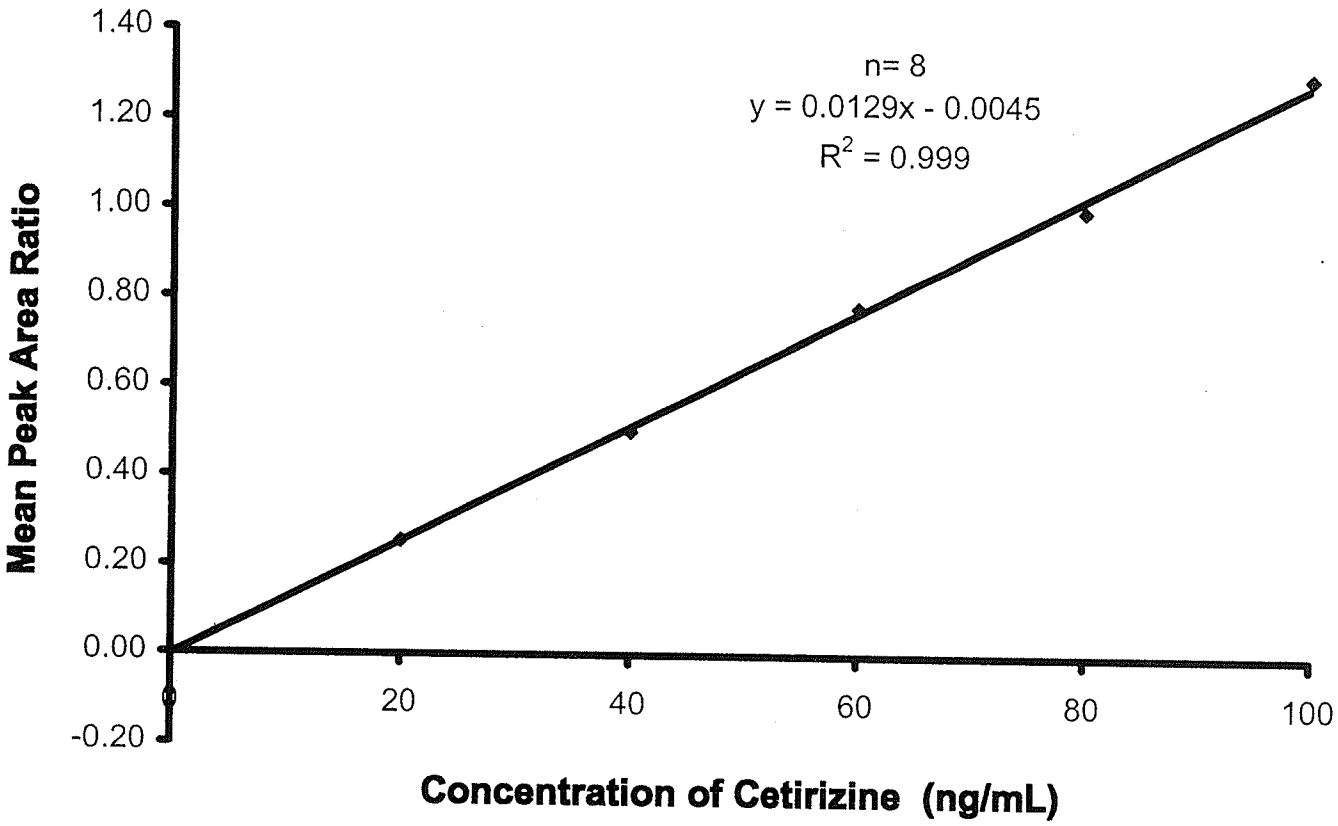

Figure 26: HPLC Calibration of Cetirizine in Plasma

Table 25: Histamine-Induced Wheal Areas on the Shaved Backs of Rabbits Before and After the Topical Application of 10 mg Hydroxyzine from GB

PD Parameter	Wheal Area (cm^2)										
Time (h) / Rabbit Code	0	0.5	1	2	3	4	5	6	8	10	24
1	0.91	0.00	0.00	0.07	0.33	0.20	0.14	0.04	0.08	0.15	0.17
2	0.86	0.14	0.10	0.05	0.19	0.18	0.16	0.00	0.06	0.27	0.48
3	0.70	0.22	0.08	0.37	0.77	0.71	0.55	0.52	0.48	0.11	0.20
4	0.84	0.09	0.30	0.33	0.14	0.13	0.28	0.17	0.15	0.28	0.51
5	1.06	0.36	0.44	0.28	0.60	0.60	0.55	0.31	0.32	0.29	0.20
6	1.12	0.54	0.43	0.32	0.00	0.00	0.25	0.18	0.44	0.246	0.41
Mean	0.92	0.22	0.23	0.24	0.34	0.30	0.32	0.20	0.25	0.25	0.33
SEM	0.06	0.08	0.08	0.06	0.12	0.12	0.08	0.08	0.08	0.04	0.06

n= 6
PD = Pharmacodynamic
GB = Glaxal Base

Table 26: Histamine-Induced Wheal Areas on the Shaved Backs of Rabbits Before and After the Topical Application of 10 mg Hydroxyzine from PC-SUV

PD Parameter	Wheal Area (cm^2)										
Time (h) / Rabbit Code	0	0.5	1	2	3	4	5	6	8	10	24
1	0.72	0.06	0.00	0.00	0.08	0.28	0.13	0.17	0.61	0.14	0.00
2	0.81	1.04	0.67	0.25	0.55	0.04	0.17	0.00	0.00	0.29	0.27
3	1.11	0.57	0.11	0.22	0.11	0.11	0.21	0.07	0.17	0.15	0.35
4	0.79	0.05	0.00	0.00	0.14	0.26	0.20	0.16	0.49	0.15	0.00
5	0.94	0.16	0.18	0.00	0.00	0.00	0.00	0.00	0.21	0.19	0.24
6	1.18	0.44	0.11	0.00	0.00	0.00	0.00	0.15	0.00	0.29	0.39
Mean	0.92	0.39	0.18	0.08	0.15	0.11	0.12	0.09	0.25	0.20	0.21
SEM	0.08	0.16	0.10	0.05	0.08	0.05	0.04	0.03	0.10	0.03	0.07

n= 6
PD = Pharmacodynamic
PC-SUV = small unilamellar vesicles (SUV) prepared using L-α-phosphatidylcholine (PC)

Table 27: Histamine-Induced Wheal Areas on the Shaved Backs of Rabbits Before and After the Topical Application of 10 mg Hydroxyzine from PC-MLV

PD Parameter	Wheal Area (cm^2)										
Time (h) / Rabbit Code	0	0.5	1	2	3	4	5	6	8	10	24
1	0.79	0.35	0.17	0.06	0.00	0.00	0.10	0.09	0.10	0.08	0.16
2	1.04	0.29	0.11	0.15	0.07	0.12	0.09	0.08	0.05	0.04	0.00
3	1.02	0.34	0.23	0.34	0.06	0.19	0.30	0.00	0.11	0.44	0.44
4	1.18	0.18	0.16	0.03	0.00	0.11	0.00	0.00	0.58	0.12	0.37
5	0.55	0.46	0.10	0.16	0.15	0.00	0.18	0.08	0.18	0.45	0.54
6	1.06	0.12	0.07	0.00	0.00	0.00	0.00	0.00	0.03	0.09	0.07
Mean	0.94	0.29	0.14	0.12	0.05	0.07	0.11	0.04	0.17	0.20	0.26
SEM	0.09	0.05	0.02	0.05	0.02	0.03	0.05	0.02	0.08	0.08	0.09

n= 6
PD = Pharmacodynamic
PC-MLV = multilamellar vesicles (MLV) prepared using L-α-phosphatidylcholine (PC)

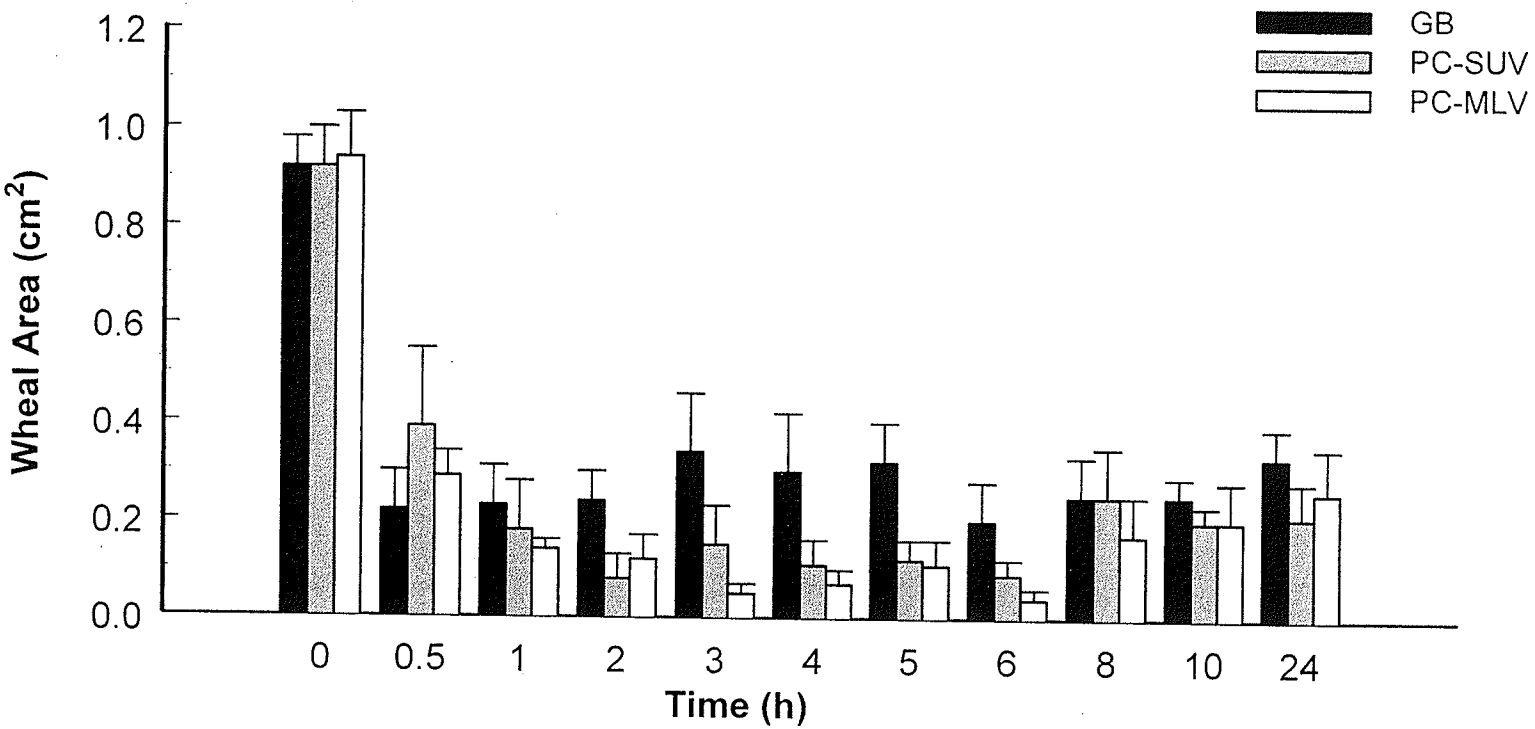

Figure 27: Mean ± SEM Wheal Areas of Histamine-Induced Wheal on the Shaved Backs of Rabbits after the Topical Application of 10 mg Hydroxyzine from GB or PC-SUV, or PC-MLV

n=6

GB = Glaxal Base,

PC-SUV = small unilamellar vesicles (SUV) prepared using L-α-phosphatidylcholine (PC),

PC-MLV = multilamellar vesicles (MLV) prepared using L-α-phosphatidylcholine (PC)

Table 28: Percent Suppression of Histamine-Induced Wheal Formation on the Shaved Backs of Rabbits after the Topical Application of 10 mg Hydroxyzine from GB

PD Parameter	Percent Wheal Suppression									
Time (h) / Rabbit Code	0.5	1	2	3	4	5	6	8	10	24
1	100.0	100.0	92.6	63.9	77.9	84.3	96.1	91.5	83.1	80.9
2	84.1	88.3	94.6	77.5	79.5	82.0	100.0	93.6	68.3	44.6
3	68.6	88.1	46.6	0.0	0.0	21.3	25.6	31.4	83.7	72.0
4	89.9	64.1	60.8	83.2	84.1	67.1	80.4	82.3	66.9	39.5
5	66.0	58.1	73.2	43.2	43.4	48.5	70.5	69.5	72.8	80.9
6	51.9	61.7	71.8	100.0	100.0	77.6	83.7	60.8	67.0	63.6
Mean	76.8	76.7	73.3	61.3	64.2	63.5	76.1	71.5	73.6	63.6
SEM	7.2	7.2	7.5	14.5	14.9	10.0	11.0	9.5	3.2	7.3

n= 6
PD = Pharmacodynamic
GB = Glaxal Base

Table 29: Percent Suppression of Histamine-Induced Wheal Formation on the Shaved Backs of Rabbits after the Topical Application of 10 mg Hydroxyzine from PC-SUV

PD Parameter	Percent Wheal Suppression									
Time (h) / Rabbit Code	0.5	1	2	3	4	5	6	8	10	24
1	91.5	100.0	100.0	88.9	60.7	81.8	76.3	15.4	80.8	100.0
2	0.0	16.4	69.0	31.5	95.3	79.0	100.0	100.0	64.1	67.1
3	48.8	90.6	80.4	89.8	90.3	81.2	93.7	85.0	86.5	68.6
4	93.4	100.0	100.0	81.8	67.6	74.9	80.0	37.7	81.5	100.0
5	82.7	81.3	100.0	100.0	100.0	100.0	100.0	77.1	79.7	74.3
6	63.0	90.4	100.0	100.0	100.0	100.0	87.5	100.0	75.5	66.9
Mean	63.2	79.8	91.6	82.0	85.6	86.2	89.6	69.2	78.0	79.5
SEM	14.5	13.0	5.5	10.5	7.0	4.5	4.1	14.3	3.1	6.6

n= 6
PD = Pharmacodynamic
PC-SUV = small unilamellar vesicles (SUV) prepared using L-α-phosphatidylcholine (PC)

Table 30: Percent Suppression of Histamine-Induced Wheal Formation on the Shaved Backs of Rabbits after the Topical Application of 10 mg Hydroxyzine from PC-MLV

PD Parameter	Percent Wheal Suppression									
Time (h) / Rabbit Code	0.5	1	2	3	4	5	6	8	10	24
1	55.9	79.2	93.1	100.0	100.0	87.4	89.3	87.8	89.8	80.0
2	71.8	89.5	86.1	93.8	88.1	91.3	92.3	95.0	96.2	100.0
3	66.3	77.1	66.9	94.3	81.6	70.4	100.0	89.3	56.7	57.1
4	84.4	86.2	97.2	100.0	90.5	100.0	100.0	50.8	90.0	68.8
5	16.6	82.1	71.8	72.7	100.0	67.8	85.6	67.4	18.2	2.2
6	88.9	93.7	100.0	100.0	100.0	100.0	100.0	97.1	91.1	93.3
Mean	64.0	84.7	85.8	93.5	93.4	86.1	94.5	81.2	73.7	66.9
SEM	10.7	2.6	5.6	4.3	3.2	5.8	2.6	7.5	12.5	14.4

n= 6
PD = Pharmacodynamic
PC-MLV = multilamellar vesicles (MLV) prepared using L-α-phosphatidylcholine (PC)

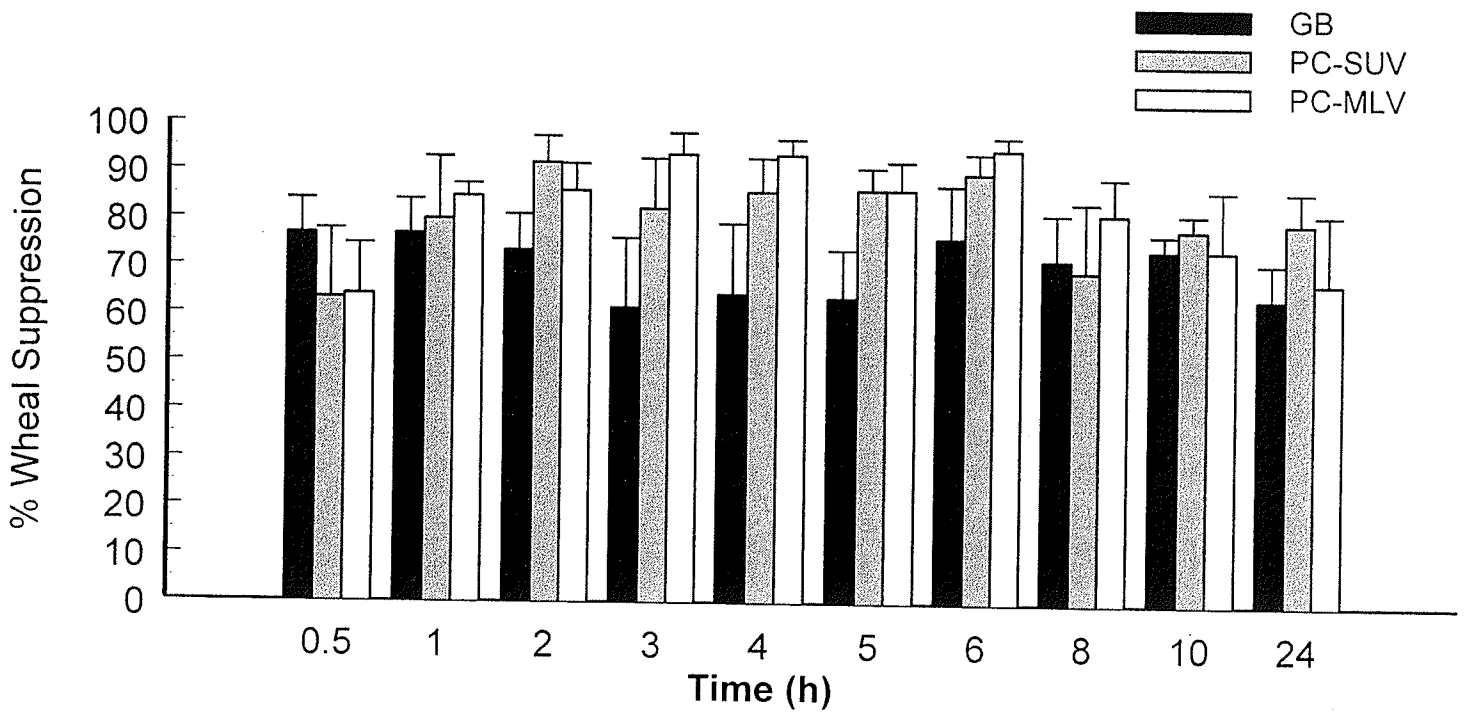

Figure 28: Mean ± SEM Percent Suppression of Histamine-Induced Wheal Formation on the Shaved Backs of Rabbits after the Topical Application of 10 mg Hydroxyzine from GB or PC-SUV, or PC-MLV.

n=6

GB = Glaxal Base,

PC-SUV = small unilamellar vesicles (SUV) prepared using L-α-phosphatidylcholine (PC),

PC-MLV = multilamellar vesicles (MLV) prepared using L-α-phosphatidylcholine (PC)

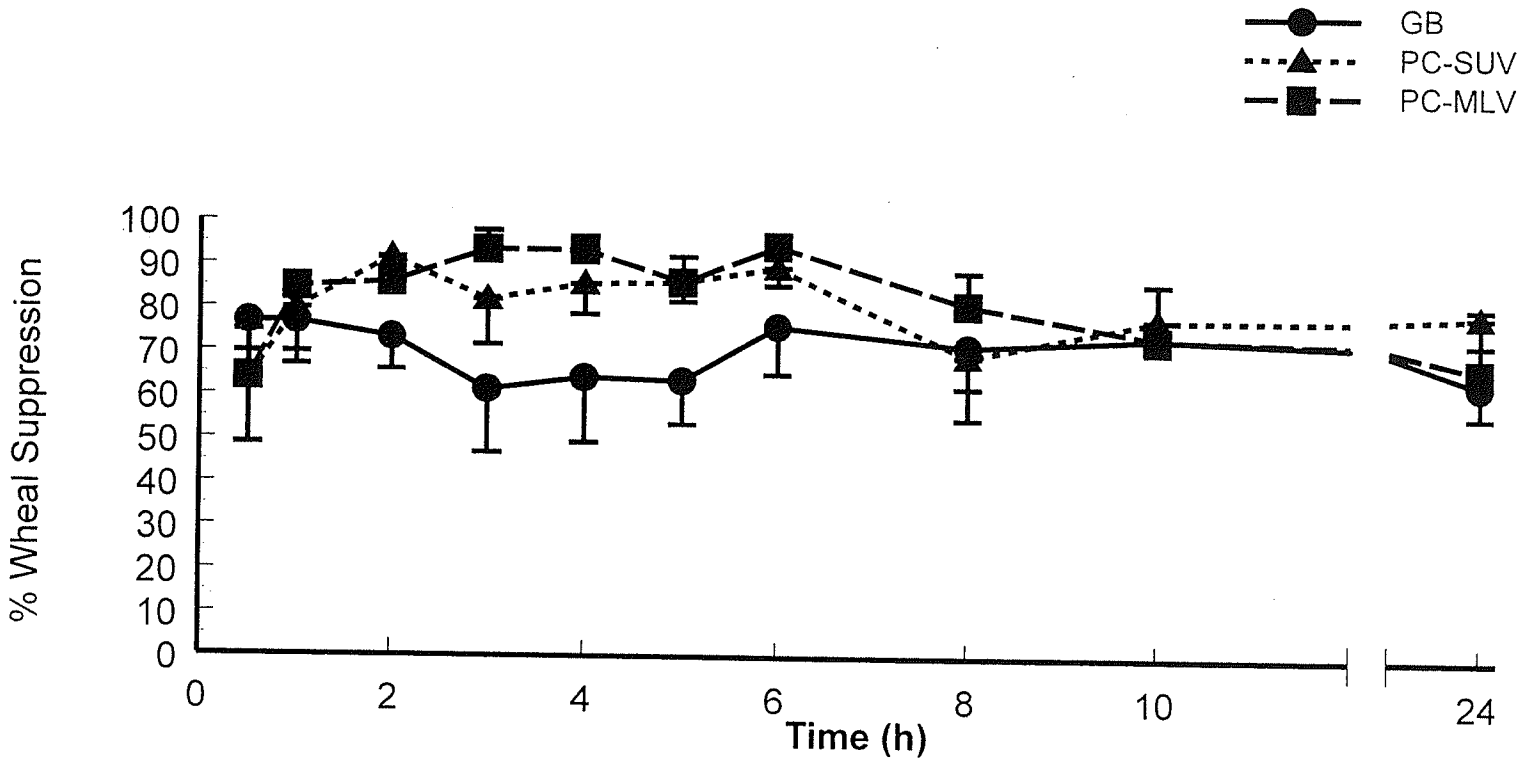

Figure 28a: Mean ± SEM Percent Suppression of Histamine-Induced Wheal Formation on the Shaved Backs of Rabbits after the Topical Application of 10 mg Hydroxyzine from GB or PC-SUV, or PC-MLV.

n=6

GB = Glaxal Base,

PC-SUV = small unilamellar vesicles (SUV) prepared using L-α-phosphatidylcholine (PC),

PC-MLV = multilamellar vesicles (MLV) prepared using L-α-phosphatidylcholine (PC)

Table 31: Hydroxyzine Plasma Concentrations after the Topical Application of 10 mg Hydroxyzine from GB on the Shaved Backs of Rabbits

PK Parameter	Hydroxyzine Plasma Concentration (ng/mL)										
Time (h) / Rabbit Code	0	0.5	1	2	3	4	5	6	8	10	24
1	0.0	41.5	36.9	35.7	35.7	25.3	13.8	11.5	6.8	11.5	5.7
2	0.0	110.9	358.3	285.5	55.4	56.6	147.9	36.9	25.3	18.4	6.8
3	0.0	67.0	30.0	23.0	51.9	0.0	5.7	2.2	23.0	8.0	34.6
4	0.0	4.5	5.7	9.2	13.8	10.3	12.6	12.6	10.3	9.2	8.0
5	0.0	68.1	41.5	3.4	10.3	38.1	14.9	2.2	8.0	23.0	11.5
6	0.0	18.4	19.6	26.5	20.7	26.5	24.2	20.7	17.2	13.8	4.5
Mean	0.0	51.7	82.0	63.9	31.3	26.1	36.5	14.4	15.1	14.0	11.9
SEM	0.0	15.8	55.5	44.6	7.9	8.2	22.4	5.3	3.2	2.4	4.6

n= 6

PK = Pharmacokinetics

GB = Glaxal Base

Table 32: Hydroxyzine Plasma Concentrations after the Topical Application of 10 mg Hydroxyzine from PC-SUV on the Shaved Backs of Rabbits

PK Parameter	Hydroxyzine Plasma Concentration (ng/mL)										
Time (h) / Rabbit Code	0	0.5	1	2	3	4	5	6	8	10	24
1	0.0	14.9	19.6	20.7	21.9	9.2	6.8	9.2	2.2	2.2	1.1
2	0.0	50.8	16.1	4.5	1.1	1.1	0.0	5.7	0.0	9.2	0.0
3	0.0	0.0	8.0	0.0	2.2	4.5	9.2	3.4	4.5	2.2	2.2
4	0.0	2.2	4.5	5.7	0.0	12.6	10.3	16.1	5.7	4.5	2.2
5	0.0	5.7	3.4	2.2	9.2	2.2	0.0	4.5	0.0	0.0	0.0
6	0.0	0.0	3.4	4.5	2.2	1.1	3.4	1.1	0.0	0.0	0.0
Mean	0.0	12.3	9.2	6.3	6.1	5.1	4.9	6.7	2.1	3.0	0.9
SEM	0.0	8.0	2.9	3.0	3.4	2.0	1.8	2.2	1.0	1.4	0.4

n= 6

PK = Pharmacokinetics

PC-SUV = small unilamellar vesicles (SUV) prepared using L-α-phosphatidylcholine (PC)

Table 33: Hydroxyzine Plasma Concentrations after the Topical Application of 10 mg Hydroxyzine from PC-MLV on the Shaved Backs of Rabbits

PK Parameter	Hydroxyzine Plasma Concentration (ng/mL)										
Time (h) / Rabbit Code	0	0.5	1	2	3	4	5	6	8	10	24
1	0.0	0.0	2.2	11.5	13.8	12.6	4.5	5.7	4.5	2.2	1.1
2	0.0	72.7	67.0	33.4	14.9	13.8	1.1	4.5	0.0	0.0	0.0
3	0.0	0.0	0.0	0.0	0.0	0.0	0.0	0.0	0.0	0.0	0.0
4	0.0	0.0	11.5	0.0	6.8	12.6	0.0	17.2	0.0	6.8	12.6
5	0.0	2.3	0.0	0.0	0.0	8.0	2.2	10.3	0.0	0.0	0.0
6	0.0	0.0	0.0	3.4	0.0	0.0	0.0	0.0	0.0	0.0	0.0
Mean	0.0	12.5	13.4	8.0	5.9	7.8	1.3	6.3	0.8	1.5	2.3
SEM	0.0	12.1	10.9	5.4	2.9	2.6	0.7	2.7	0.8	1.1	2.1

n= 6

PK = Pharmacokinetics

PC-MLV = multilamellar vesicles (MLV) prepared using L-α-phosphatidylcholine (PC)

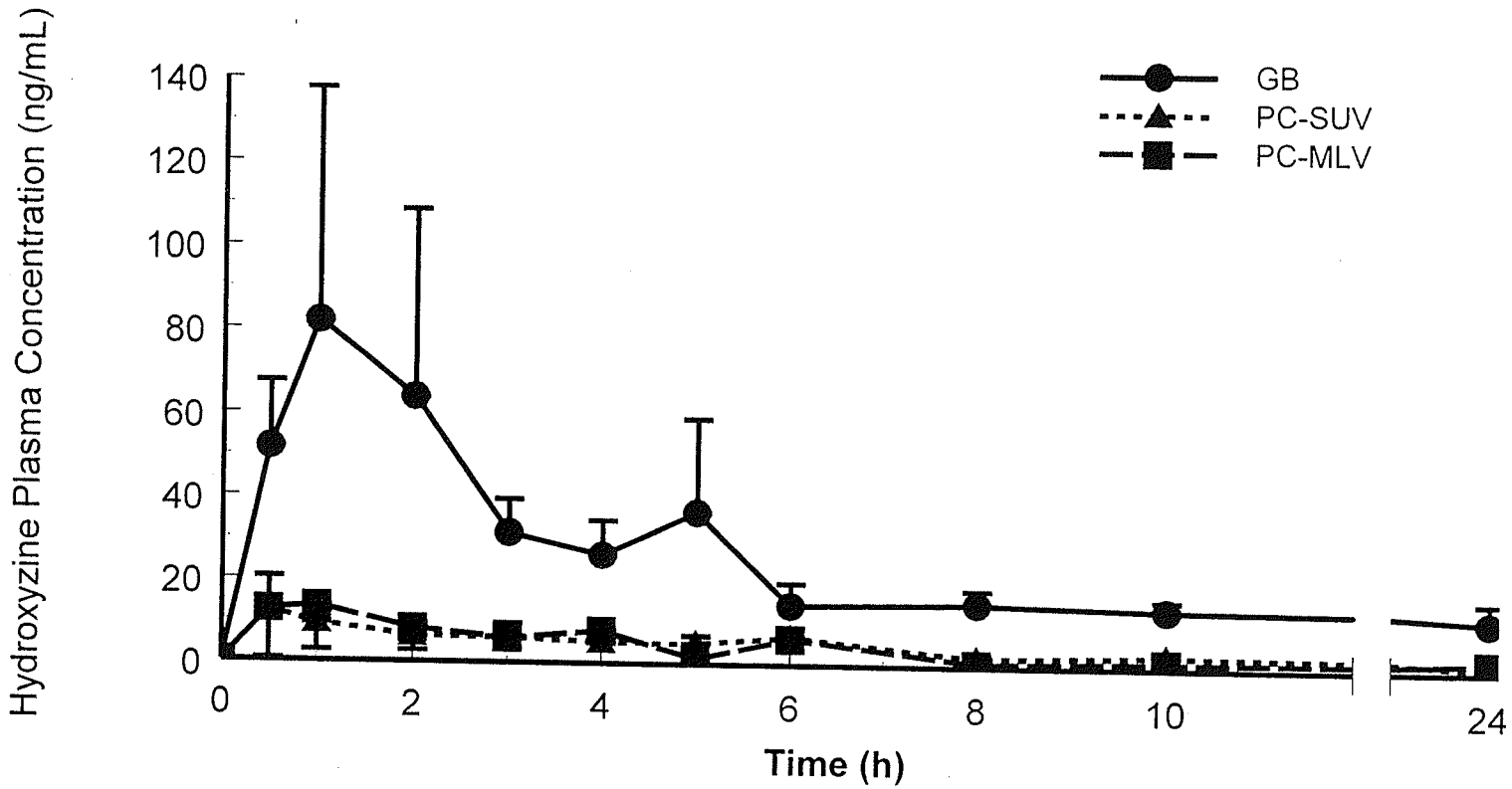

Figure 29: Mean ± SEM Hydroxyzine Plasma Concentrations after the Topical Application of 10 mg Hydroxyzine From GB or PC-SUV or PC-MLV on the Shaved Backs of Rabbits.

n=6

GB = Glaxal Base,

PC-SUV = small unilamellar vesicles (SUV) prepared using L-α-phosphatidylcholine (PC),

PC-MLV = multilamellar vesicles (MLV) prepared using L-α-phosphatidylcholine (PC)

Table 34: Cetirizine Plasma Concentrations after the Topical Application of 10 mg Hydroxyzine from GB on the Shaved Backs of Rabbits

PK Parameter	Cetirizine Plasma Concentration (ng/mL)										
Time (h) / Rabbit Code	0	0.5	1	2	3	4	5	6	8	10	24
3	0.0	29.0	34.0	n.a.	34.0	n.a.	48.1	n.a.	n.a.	93.5	64.7
4	0.0	17.3	24.8	43.1	37.3	17.3	72.7	67.2	93.0	58.1	58.1
5	0.0	12.1	54.8	31.5	88.9	n.a.	29.8	n.a.	n.a.	34.0	37.3
6	0.0	15.3	18.2	22.3	57.3	n.a.	62.2	33.1	25.7	23.2	n.a.
Mean	0.0	18.4	32.9	32.3	54.4	17.3	53.2	50.2	59.3	52.2	53.4
SEM	0.0	3.7	8.0	6.0	12.6	0.0	9.3	17.0	33.7	15.6	8.3

PK = Pharmacokinetics
GB = Glaxal Base
n.a.= not available

Table 35: Cetirizine Plasma Concentrations after the Topical Application of 10 mg Hydroxyzine from PC-SUV on the Shaved Backs of Rabbits

PK Parameter	Cetirizine Plasma Concentration (ng/mL)										
Time (h) / Rabbit Code	0	0.5	1	2	3	4	5	6	8	10	24
3	0.0	29.0	26.5	n.a.	33.1	16.5	40.6	26.5	39.9	17.3	43.1
4	0.0	20.7	40.4	n.a.	37.3	29.0	45.6	20.7	43.6	29.0	53.9
5	0.0	26.1	25.3	27.4	35.3	47.6	69.8	12.1	n.a.	19.8	61.3
6	0.0	24.7	14.9	30.7	31.1	29.9	n.a.	29.5	26.1	26.1	36.9
Mean	0.0	25.1	26.8	29.0	34.2	30.7	52.0	22.2	36.5	23.1	48.8
SEM	0.0	1.7	5.2	1.7	1.3	6.4	9.0	3.8	5.3	2.7	5.4

PK = Pharmacokinetics
PC-SUV = small unilamellar vesicles (SUV) prepared using L-α-phosphatidylcholine (PC)
n.a.= not available

Table 36: Cetirizine Plasma Concentrations after the Topical Application of 10 mg Hydroxyzine from PC-MLV on the Shaved Backs of Rabbits

PK Parameter	Cetirizine Plasma Concentration (ng/mL)										
Time (h) / Rabbit Code	0	0.5	1	2	3	4	5	6	8	10	24
3	0.0	12.8	2.4	56.5	69.6	64.4	68.5	61.5	55.7	81.4	43.2
4	0.0	23.6	61.9	22.8	88.3	27.0	41.1	36.5	n.a.	36.9	69.6
5	0.0	23.9	n.a.	n.a.	51.9	8.3	34.9	48.2	56.3	88.5	24.6
6	0.0	n.a.	30.3	n.a.	n.a.	38.6	42.8	27.0	30.3	n.a.	37.8
Mean	0.0	20.1	31.5	39.6	70.0	34.6	46.8	43.3	47.4	69.0	43.8
SEM	0.0	3.6	17.2	16.8	10.5	11.7	7.4	7.5	8.6	16.1	9.5

PK = Pharmacokinetics
PC-MLV = multilamellar vesicles (MLV) prepared using L-α-phosphatidylcholine (PC)
n.a.= not available

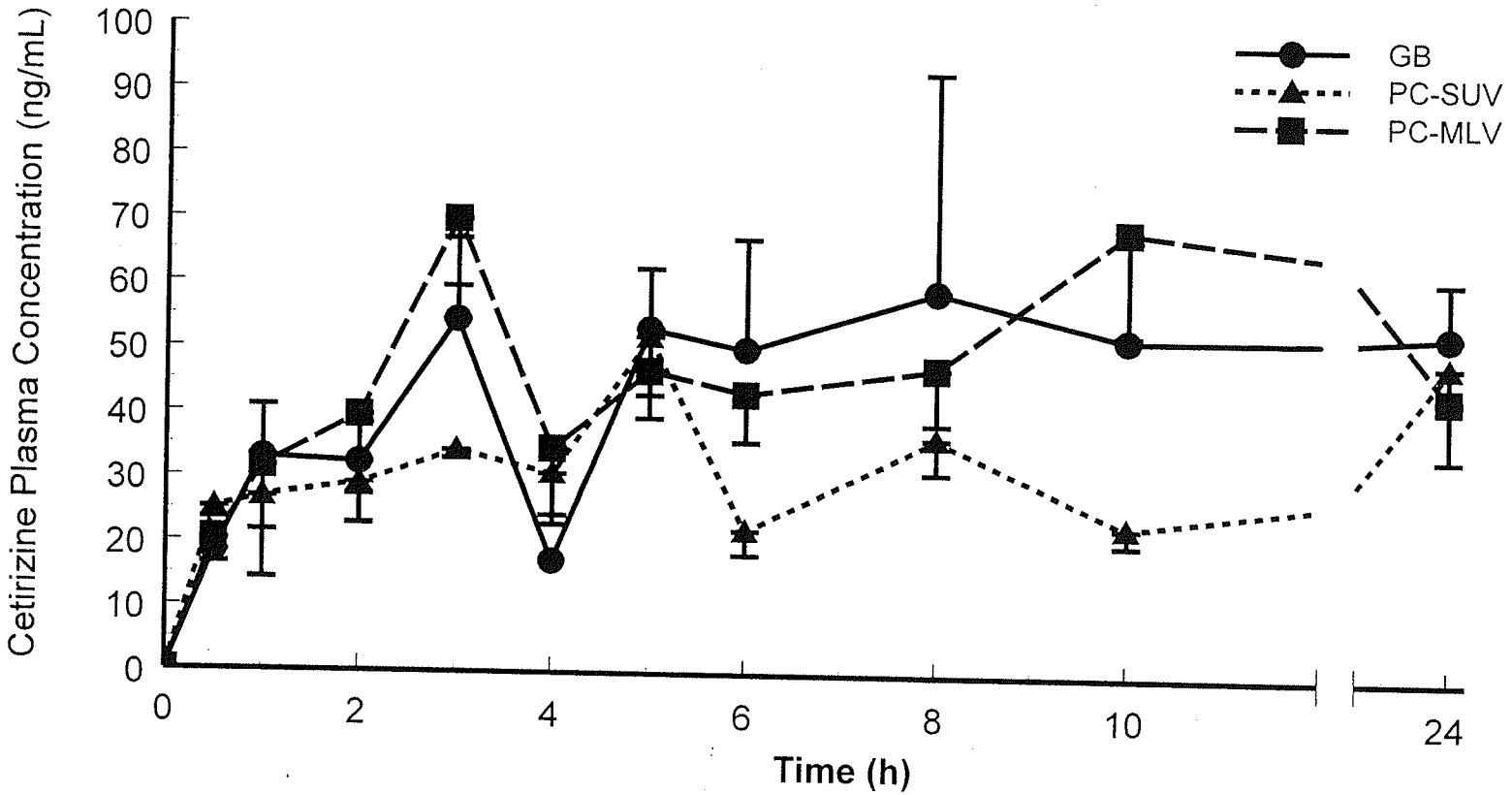

Figure 30: Mean ± SEM Cetirizine Plasma Concentrations after the Topical Application of 10 mg Hydroxyzine From GB or PC-SUV or PC-MLV on the Shaved Backs of Rabbits.

n= or > 3

GB = Glaxal Base,

PC-SUV = small unilamellar vesicles (SUV) prepared using L-α-phosphatidylcholine (PC),

PC-MLV = multilamellar vesicles (MLV) prepared using L-α-phosphatidylcholine (PC)

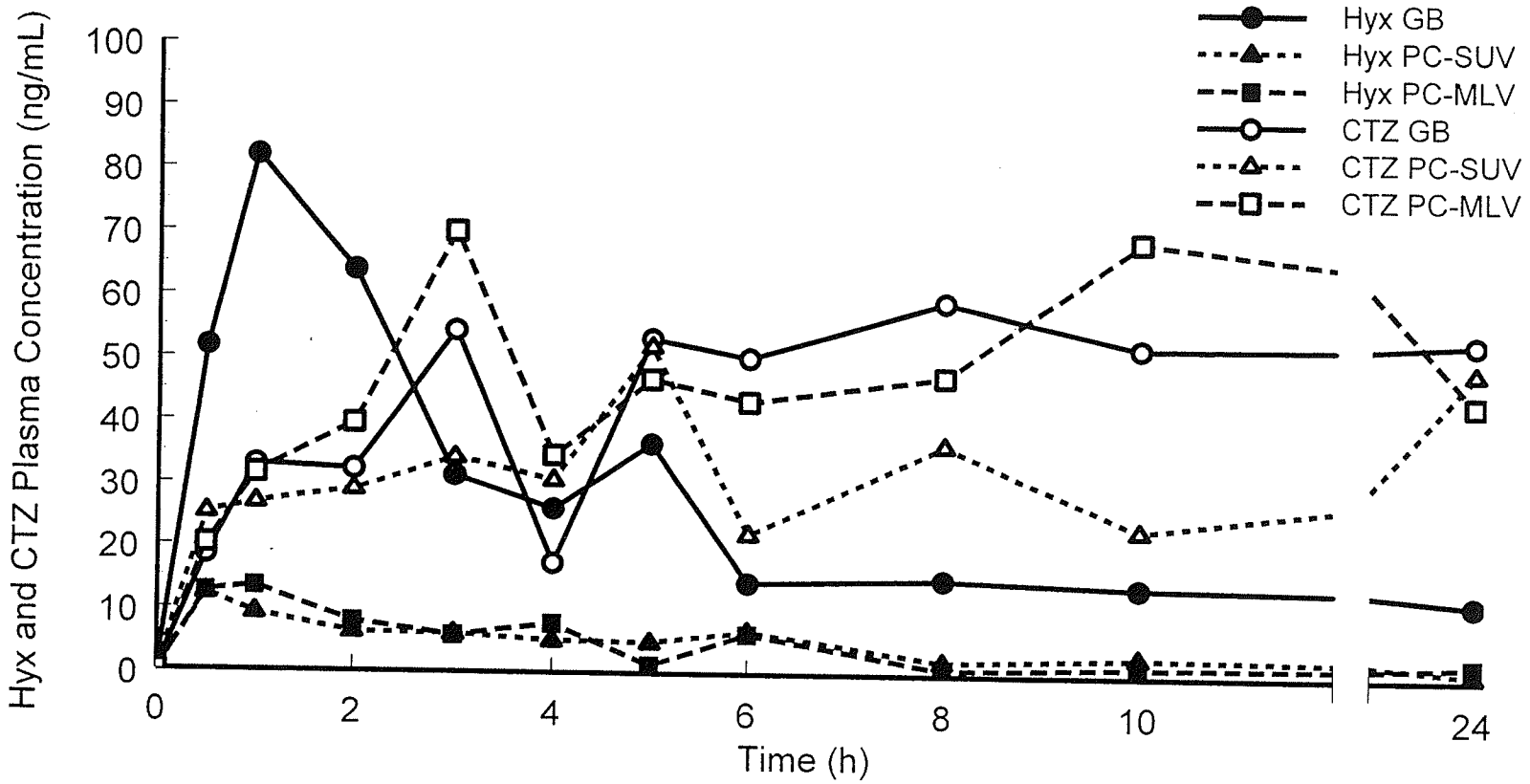

Figure 30a: Mean Hydroxyzine and Cetirizine Plasma Concentrations after the Topical Application of 10 mg Hydroxyzine From GB or PC-SUV or PC-MLV on the Shaved Backs of Rabbits.

n= or > 3

GB = Glaxal Base,

PC-SUV = small unilamellar vesicles (SUV) prepared using L-α-phosphatidylcholine (PC),

PC-MLV = multilamellar vesicles (MLV) prepared using L-α-phosphatidylcholine (PC), Hyx = Hydroxyzine, CTZ = Cetirizine

Table 37: Mean ± SEM Percent of Hydroxyzine Dose Remaining on the Shaved Backs of Rabbits at 24 hours after the Topical Application of 10 mg Hydroxyzine from GB or PC-SUV or PC-MLV

Formulations	Percent of Hydroxyzine Remaining Mean ± SEM
GB	0.06 ± 0.02
PC-SUV	0.02 ± 0.01
PC-MLV	0.04 ± 0.01

n= 6
GB = Glaxal Base
PC-SUV = small unilamellar vesicles (SUV) prepared using L-α-phosphatidylcholine (PC)
PC-MLV = multilamellar vesicles (MLV) prepared using L-α-phosphatidylcholine (PC)

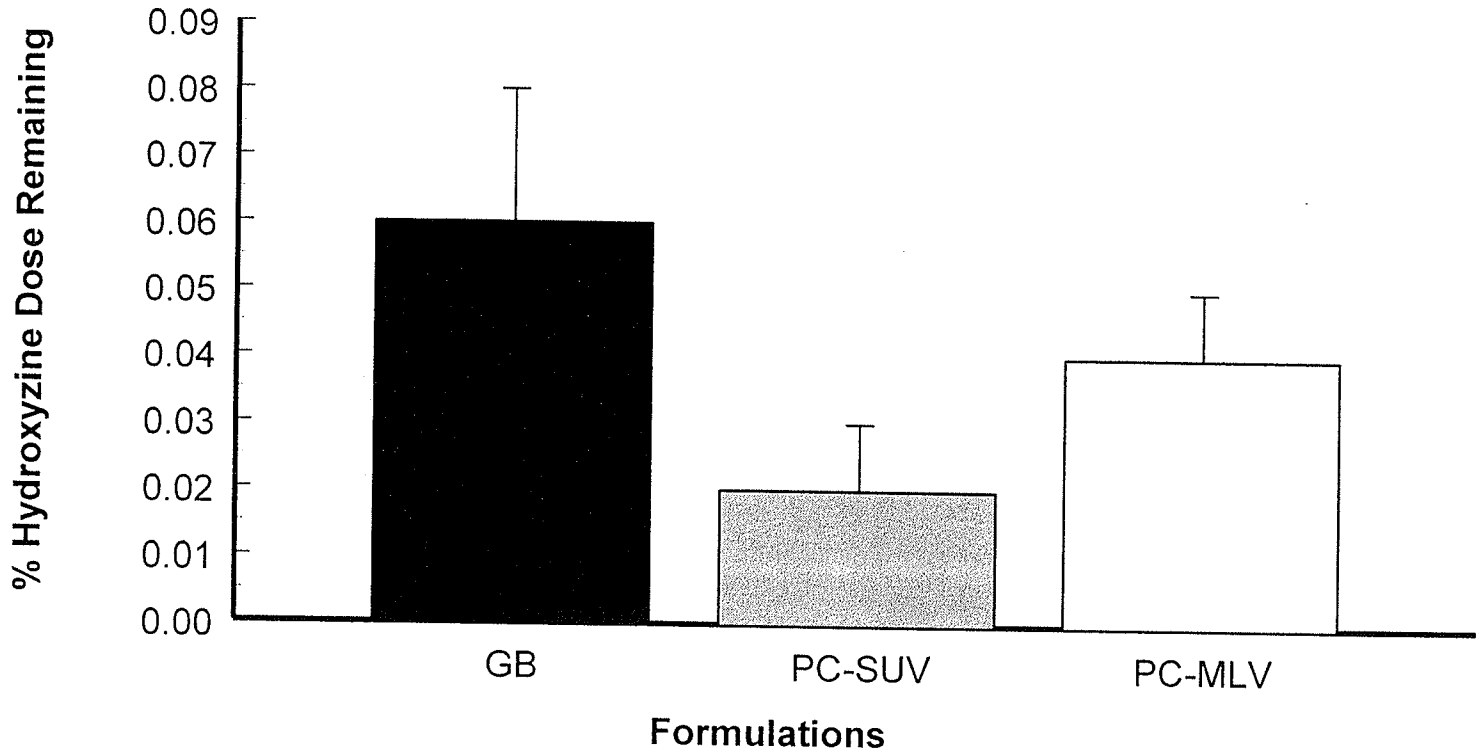

Figure 31: Mean ± SEM Percent of Hydroxyzine Dose Remaining on the Shaved Backs of Rabbits at 24 hours after the Topical Application of 10 mg Hydroxyzine from GB or PC-SUV or PC-MLV.

n= 6

GB = Glaxal Base,

PC-SUV = small unilamellar vesicles (SUV) prepared using L-α-phosphatidylcholine (PC),

PC-MLV = multilamellar vesicles (MLV) prepared using L-α-phosphatidylcholine (PC)

Table 38: Histamine-Induced Wheal Areas on the Shaved Backs of Rabbits Before and After the Topical Application of 10 mg Cetirizine from GB

PD Parameter	Wheal Area (cm^2)										
Time (h) / Rabbit Code	0	0.5	1	2	3	4	5	6	8	10	24
1	0.91	0.49	0.82	0.91	0.89	0.25	0.21	0.10	0.08	0.30	0.51
2	0.92	0.47	0.68	0.28	0.46	0.23	0.17	0.16	0.09	0.44	0.54
3	1.38	0.50	0.47	0.63	0.50	0.17	0.77	0.93	0.68	0.74	0.59
4	0.64	0.22	0.40	0.27	0.33	0.15	0.15	0.35	0.16	0.37	0.53
5	1.13	0.52	0.53	0.40	0.49	0.38	0.46	0.27	0.42	0.25	0.58
6	1.28	0.49	0.53	0.25	0.69	0.50	0.45	0.25	0.69	0.65	0.70
Mean	1.04	0.45	0.57	0.46	0.56	0.28	0.37	0.34	0.35	0.46	0.57
SEM	0.11	0.05	0.06	0.11	0.08	0.05	0.10	0.12	0.12	0.08	0.03

n= 6
PD = Pharmacodynamic
GB = Glaxal Base

Table 39: Histamine-Induced Wheal Areas on the Shaved Backs of Rabbits Before and After the Topical Application of 10 mg Cetirizine from PC-SUV

PD Parameter	Wheal Area (cm^2)										
Time (h) / Rabbit Code	0	0.5	1	2	3	4	5	6	8	10	24
1	1.13	0.34	0.22	0.09	0.26	0.29	0.10	0.00	0.14	0.30	0.58
2	1.20	0.50	0.17	0.16	0.08	0.21	0.27	0.07	0.20	0.10	0.55
3	1.02	0.14	0.61	0.45	0.49	0.25	0.09	0.00	0.00	0.18	0.30
4	0.91	0.55	0.39	0.16	0.57	0.33	0.34	0.08	0.08	0.21	0.22
5	0.89	0.42	0.17	0.31	0.28	0.25	0.07	0.05	0.04	0.18	0.31
6	1.11	0.80	1.05	1.13	0.74	0.28	0.81	0.38	0.08	0.39	0.41
Mean	1.04	0.46	0.43	0.38	0.40	0.27	0.28	0.10	0.09	0.23	0.40
SEM	0.05	0.09	0.14	0.16	0.10	0.02	0.11	0.06	0.03	0.04	0.06

n= 6
PD = Pharmacodynamic
PC-SUV = small unilamellar vesicles (SUV) prepared using L-α-phosphatidylcholine (PC)

Table 40: Histamine-Induced Wheal Areas on the Shaved Backs of Rabbits Before and After the Topical Application of 10 mg Cetirizine from PC-MLV

PD Parameter	Wheal Area (cm^2)										
Time (h) / Rabbit Code	0	0.5	1	2	3	4	5	6	8	10	24
1	0.78	0.45	0.32	0.21	0.18	0.06	0.20	0.06	0.00	0.18	0.31
2	1.09	0.36	0.29	0.36	0.33	0.11	0.07	0.00	0.08	0.13	0.08
3	1.20	0.60	0.68	0.27	0.41	0.31	0.00	0.00	0.03	0.20	0.51
4	1.17	0.49	0.23	0.21	0.17	0.08	0.00	0.05	0.09	0.34	0.63
5	1.07	1.07	0.51	0.44	0.13	0.09	0.12	0.00	0.08	0.31	0.43
6	1.10	0.42	0.29	0.08	0.10	0.12	0.05	0.00	0.00	0.09	0.07
Mean	1.07	0.57	0.39	0.26	0.22	0.13	0.07	0.02	0.05	0.21	0.34
SEM	0.06	0.11	0.07	0.05	0.05	0.04	0.03	0.01	0.02	0.04	0.09

n= 6
PD = Pharmacodynamic ,
PC-MLV = multilamellar vesicles (MLV) prepared using L-α-phosphatidylcholine (PC)

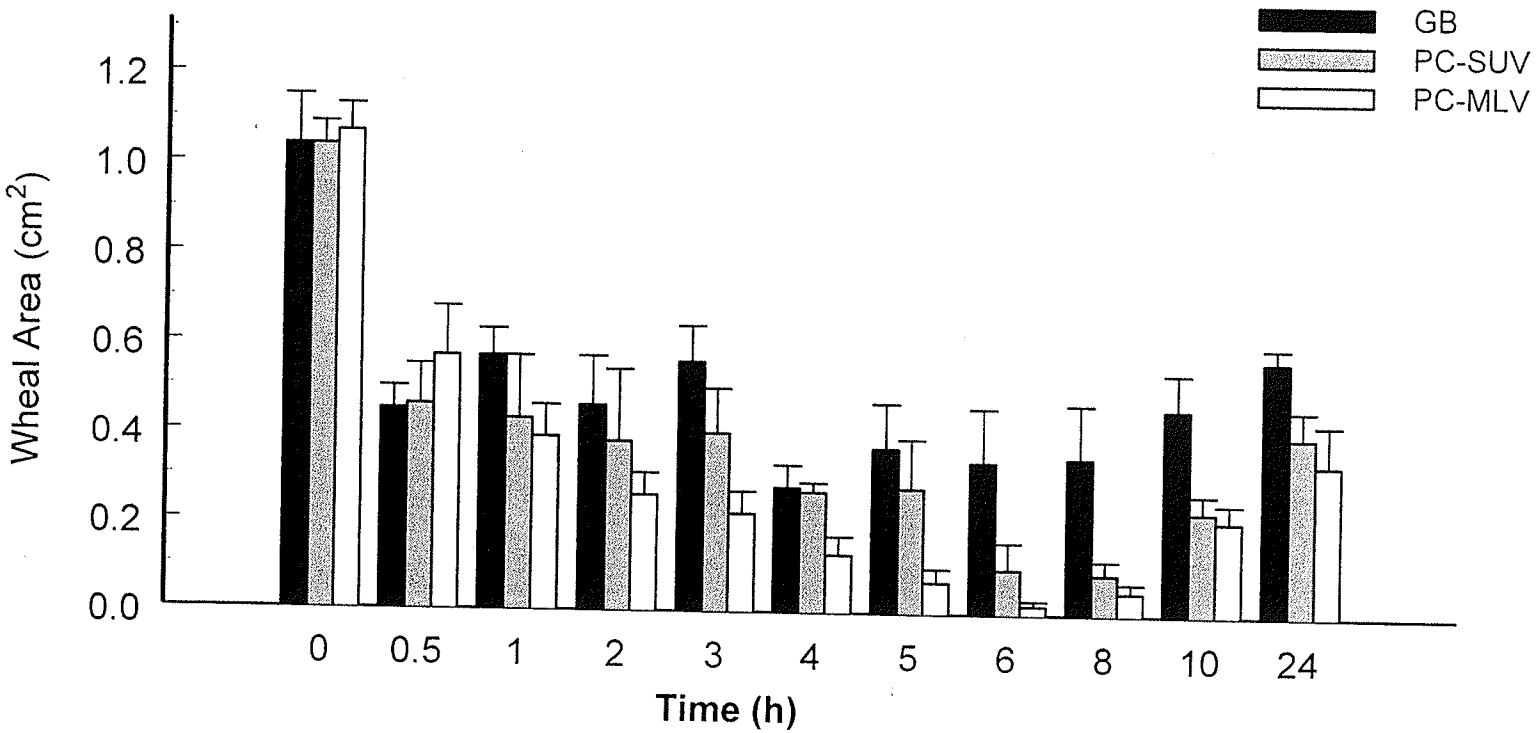

Figure 32: Mean ± SEM Wheal Areas of Histamine-Induced Wheal on the Shaved Backs of Rabbits after the Topical Application of 10 mg Cetirizine from GB or PC-SUV, or PC-MLV.

n=6

GB = Glaxal Base,

PC-SUV = small unilamellar vesicles (SUV) prepared using L-α-phosphatidylcholine (PC),

PC-MLV = multilamellar vesicles (MLV) prepared using L-α-phosphatidylcholine (PC)

Table 41: Percent Suppression of Histamine-Induced Wheal Formation on the Shaved Backs of Rabbits after the Topical Application of 10 mg Cetirizine from GB

PD Parameter	Percent Wheal Suppression									
Time (h) / Rabbit Code	0.5	1	2	3	4	5	6	8	10	24
1	45.6	9.8	0.0	1.8	72.5	76.8	89.2	91.2	66.6	44.2
2	45.4	21.1	67.4	47.0	72.9	80.4	81.8	89.3	48.8	37.1
3	29.1	33.3	9.6	28.3	75.6	0.0	0.0	2.7	0.0	16.1
4	73.7	52.1	67.9	60.8	81.8	81.9	59.0	81.5	55.6	37.6
5	50.9	50.2	62.1	53.8	63.8	56.3	74.9	60.8	76.2	45.6
6	56.4	52.3	77.8	38.8	55.3	59.5	77.3	38.3	41.9	37.4
Mean	50.2	36.5	47.5	38.4	70.3	59.2	63.7	60.6	48.2	36.3
SEM	6.0	7.4	13.7	8.7	3.8	12.6	13.4	14.2	10.9	4.3

n= 6
PD = Pharmacodynamic
GB = Glaxal Base

Table 42: Percent Suppression of Histamine-Induced Wheal Formation on the Shaved Backs of Rabbits after the Topical Application of 10 mg Cetirizine from PC-SUV

PD Parameter	Percent Wheal Suppression									
Time (h) / Rabbit Code	0.5	1	2	3	4	5	6	8	10	24
1	52.2	69.3	87.5	63.8	59.9	85.6	100.0	80.0	58.8	19.6
2	37.8	79.5	80.0	90.7	74.2	67.1	90.8	75.7	87.5	31.4
3	87.5	45.6	59.9	56.0	77.4	92.0	100.0	100.0	84.0	72.8
4	29.9	50.1	79.2	27.8	58.7	56.5	89.9	90.0	73.2	72.0
5	55.6	81.8	66.4	69.9	73.6	93.0	95.2	95.3	80.5	66.6
6	32.2	11.2	3.9	37.3	76.7	31.7	67.9	92.9	66.6	65.6
Mean	49.2	56.3	62.8	57.6	70.1	71.0	90.6	89.0	75.1	54.7
SEM	8.8	10.9	12.5	9.3	3.5	9.8	4.9	3.8	4.5	9.4

n= 6

PD = Pharmacodynamic

PC-SUV = small unilamellar vesicles (SUV) prepared using L-α-phosphatidylcholine (PC)

Table 43: Percent Suppression of Histamine-Induced Wheal Formation on the Shaved Backs of Rabbits after the Topical Application of 10 mg Cetirizine from PC-MLV

PD Parameter	Percent Wheal Suppression									
Time (h) / Rabbit Code	0.5	1	2	3	4	5	6	8	10	24
1	43.3	59.2	73.3	77.2	92.2	74.6	92.6	100.0	77.2	60.7
2	65.8	72.4	65.7	68.5	89.0	92.9	100.0	92.3	87.9	92.0
3	40.7	33.6	73.8	60.1	69.4	100.0	100.0	97.2	80.6	50.0
4	58.2	80.8	82.5	85.9	93.0	100.0	95.5	92.2	71.0	46.2
5	0.0	6.9	19.5	75.8	84.3	77.8	100.0	85.8	43.5	21.7
6	60.6	72.7	92.1	90.7	88.7	95.2	100.0	100.0	91.1	93.6
Mean	44.8	54.3	67.8	76.3	86.1	90.1	98.0	94.6	75.2	60.7
SEM	9.8	11.6	10.3	4.6	3.6	4.6	1.3	2.3	7.0	11.4

n= 6
PD = Pharmacodynamic
PC-MLV = multilamellar vesicles (MLV) prepared using L-α-phosphatidylcholine (PC)

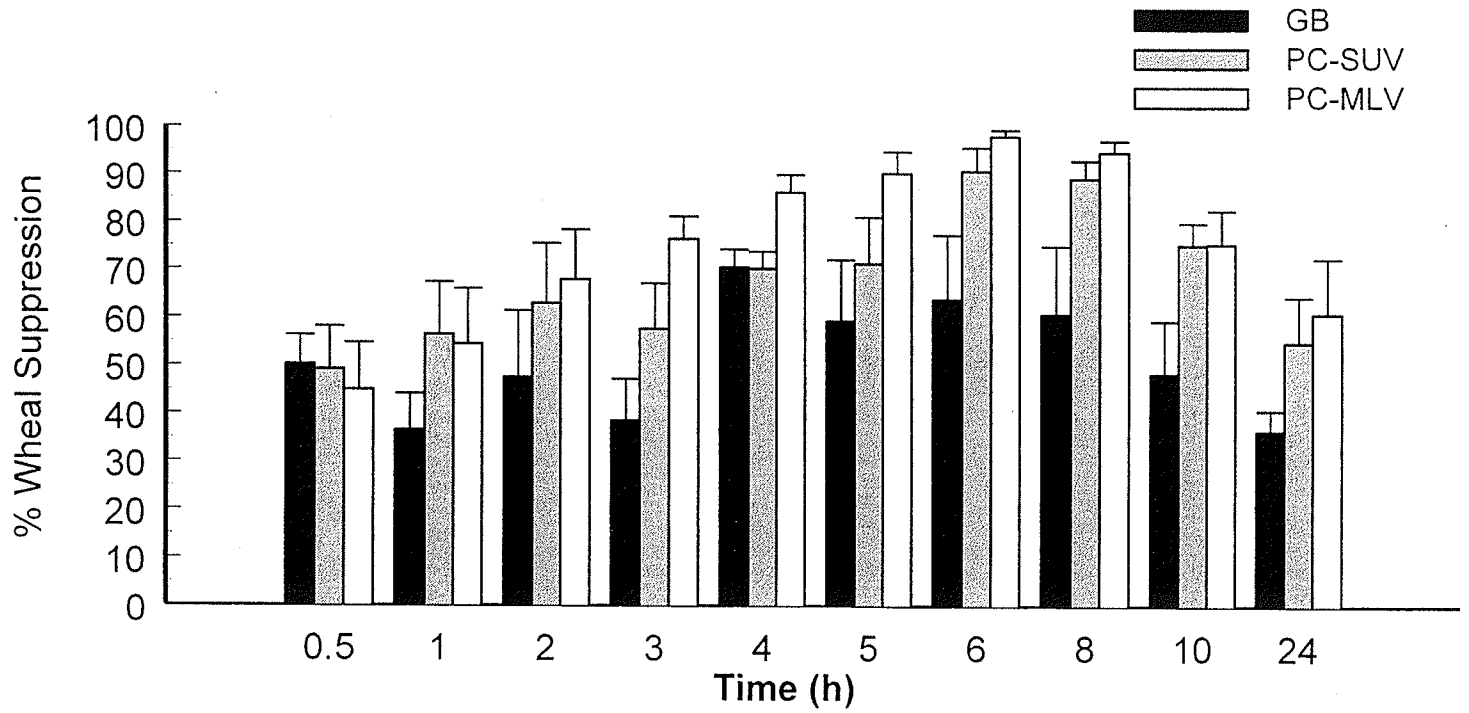

Figure 33: Mean ± SEM Percent Suppression of Histamine-Induced Wheal Formation on the Shaved Backs of Rabbits after the Topical Application of 10 mg Cetirizine from GB or PC-SUV, or PC-MLV.

n=6

GB = Glaxal Base,

PC-SUV = small unilamellar vesicles (SUV) prepared using L-α-phosphatidylcholine (PC),

PC-MLV = multilamellar vesicles (MLV) prepared using L-α-phosphatidylcholine (PC)

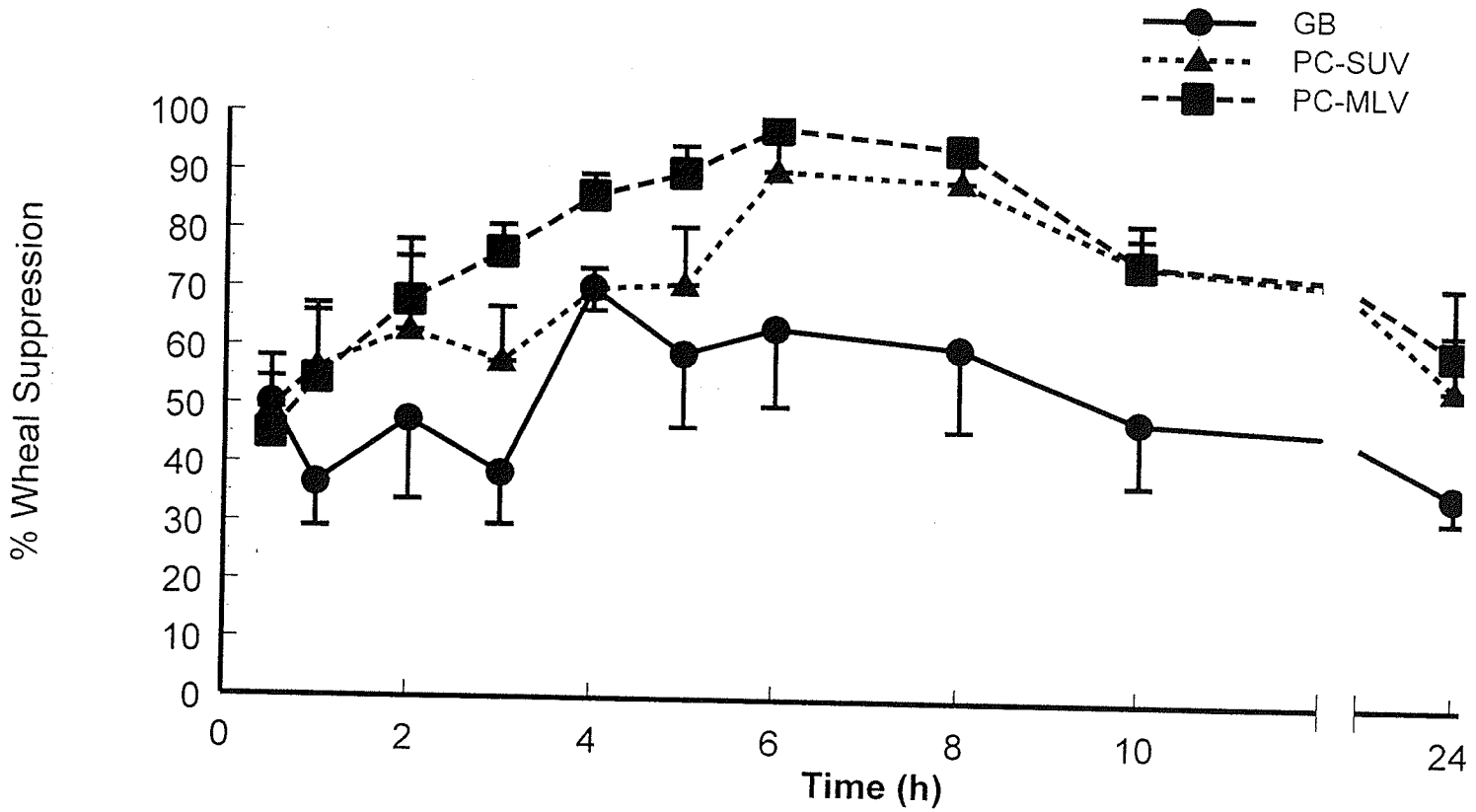

Figure 33a: Mean ± SEM Percent Suppression of Histamine-Induced Wheal Formation on the Shaved Backs of Rabbits after the Topical Application of 10 mg Cetirizine from GB or PC-SUV, or PC-MLV.

n=6

GB = Glaxal Base,

PC-SUV = small unilamellar vesicles (SUV) prepared using L-α-phosphatidylcholine (PC),

PC-MLV = multilamellar vesicles (MLV) prepared using L-α-phosphatidylcholine (PC)

Table 44: Cetirizine Plasma Concentrations after the Topical Application of 10 mg Cetirizine from GB on the Shaved Backs of Rabbits

PK Parameter	Cetirizine Plasma Concentration (ng/mL)										
Time (h) / Rabbit Code	0	0.5	1	2	3	4	5	6	8	10	24
1	0.0	55.2	74.4	41.9	46.5	22.0	17.8	43.2	44.8	4.1	0.0
2	0.0	79.8	65.6	31.1	27.8	32.0	7.4	6.6	0.0	1.2	0.0
3	0.0	45.7	45.7	26.5	12.8	44.4	9.9	24.1	66.5	17.8	7.4
4	0.0	64.4	56.1	31.1	21.1	6.6	4.9	11.6	7.0	6.6	3.7
5	0.0	59.4	46.5	49.8	45.3	13.7	3.3	0.0	0.0	0.0	0.0
6	0.0	46.5	36.1	29.5	41.5	17.8	60.2	13.7	4.1	2.8	0.0
Mean	0.0	58.5	54.1	35.0	32.5	22.7	17.3	16.5	20.4	5.4	1.9
SEM	0.0	5.2	5.8	3.7	5.7	5.5	8.8	6.2	11.5	2.7	1.3

n= 6

PK = Pharmacokinetics

GB = Glaxal Base

Table 45: Cetirizine Plasma Concentrations after the Topical Application of 10 mg Cetirizine from PC-SUV on the Shaved Backs of Rabbits

PK Parameter	Cetirizine Plasma Concentration (ng/mL)										
Time (h) / Rabbit Code	0	0.5	1	2	3	4	5	6	8	10	24
1	0.0	8.3	8.3	25.3	23.2	10.3	12.0	11.6	21.6	10.7	0.0
2	0.0	17.4	16.2	26.5	28.6	30.3	27.8	36.1	29.0	23.2	7.8
3	0.0	14.5	19.9	16.6	12.4	21.1	17.0	7.8	14.9	10.3	10.3
4	0.0	27.0	19.1	12.4	12.4	19.9	11.6	20.7	22.4	13.2	13.2
5	0.0	14.1	14.5	22.0	19.1	24.1	10.3	16.6	22.4	30.3	32.8
6	0.0	3.7	25.7	9.5	33.2	32.4	35.3	34.0	34.5	27.4	20.7
Mean	0.0	14.1	17.3	18.7	21.5	23.0	19.0	21.1	24.1	19.2	14.2
SEM	0.0	3.3	2.4	2.9	3.5	3.2	4.2	4.8	2.8	3.6	4.6

n= 6

PK = Pharmacokinetics

PC-SUV = small unilamellar vesicles (SUV) prepared using L-α-phosphatidylcholine (PC)

Table 46: Cetirizine Plasma Concentrations after the Topical Application of 10 mg Cetirizine from PC-MLV on the Shaved Backs of Rabbits

PK Parameter	Cetirizine Plasma Concentration (ng/mL)										
Time (h) / Rabbit Code	0	0.5	1	2	3	4	5	6	8	10	24
1	0.0	0.0	0.0	0.0	0.0	0.0	0.0	78.9	15.3	10.0	85.6
2	0.0	35.3	6.2	6.2	64.0	60.2	48.6	49.4	93.5	78.1	51.9
3	0.0	14.5	19.5	4.9	4.1	16.2	41.1	41.5	69.8	51.9	12.8
4	0.0	28.6	10.3	15.7	14.5	60.2	59.8	93.9	63.6	45.3	29.5
5	0.0	19.1	16.6	22.0	14.5	10.7	24.5	12.8	13.2	19.1	9.1
6	0.0	24.9	24.5	17.0	64.0	67.3	36.9	23.6	20.3	30.3	7.8
Mean	0.0	20.4	12.8	11.0	26.8	35.8	35.2	50.0	45.9	39.1	32.8
SEM	0.0	5.0	3.7	3.5	12.0	12.2	8.5	12.8	13.9	10.1	12.6

n= 6

PK = Pharmacokinetics

PC-MLV = multilamellar vesicles (MLV) prepared using L-α-phosphatidylcholine (PC)

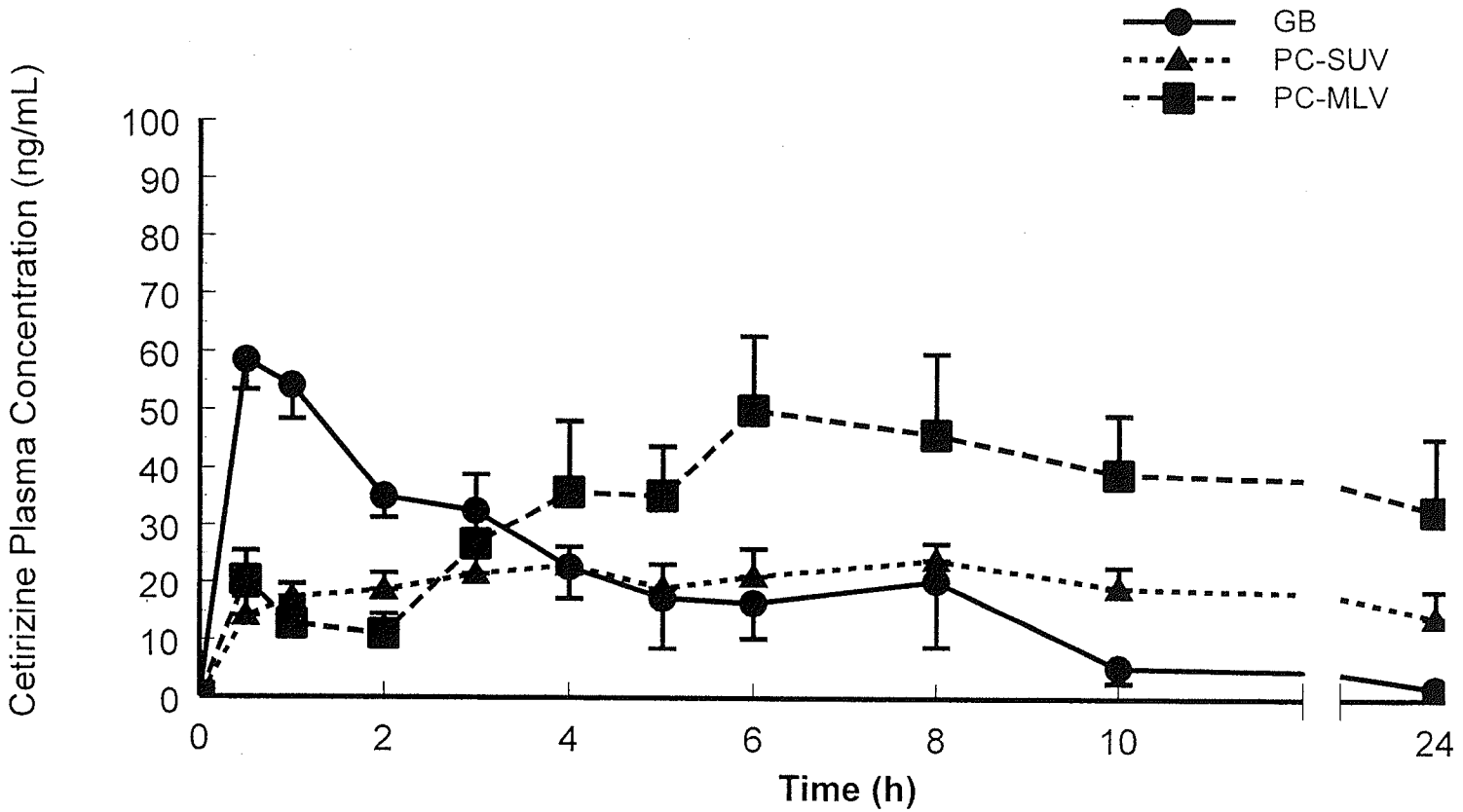

Figure 34: Mean ± SEM Cetirizine Plasma Concentrations after the Topical Application of 10 mg Cetirizine From GB or PC-SUV or PC-MLV on the Shaved Backs of Rabbits.

n=6

GB = Glaxal Base,

PC-SUV = small unilamellar vesicles (SUV) prepared using L-α-phosphatidylcholine (PC),

PC-MLV = multilamellar vesicles (MLV) prepared using L-α-phosphatidylcholine (PC)

Table 47: Mean ± SEM Percent of Cetirizine Dose Remaining on the Shaved Backs of Rabbits at 24 hours after the Topical Application of 10 mg Cetirizine from GB or PC-SUV or PC-MLV

Formulations	Percent of Cetirizine Remaining Mean ± SEM
GB	17.4 ± 3.6
PC-SUV*+	9.9 ± 1.5
PC-MLV	32 ± 9.2

n= 6

* Significantly different from GB $p \leq 0.05$

+ Significantly different from MLV $p \leq 0.05$

GB = Glaxal Base

PC-SUV = small unilamellar vesicles (SUV) prepared using L-α-phosphatidylcholine (PC)

PC-MLV = multilamellar vesicles (MLV) prepared using L-α-phosphatidylcholine (PC)

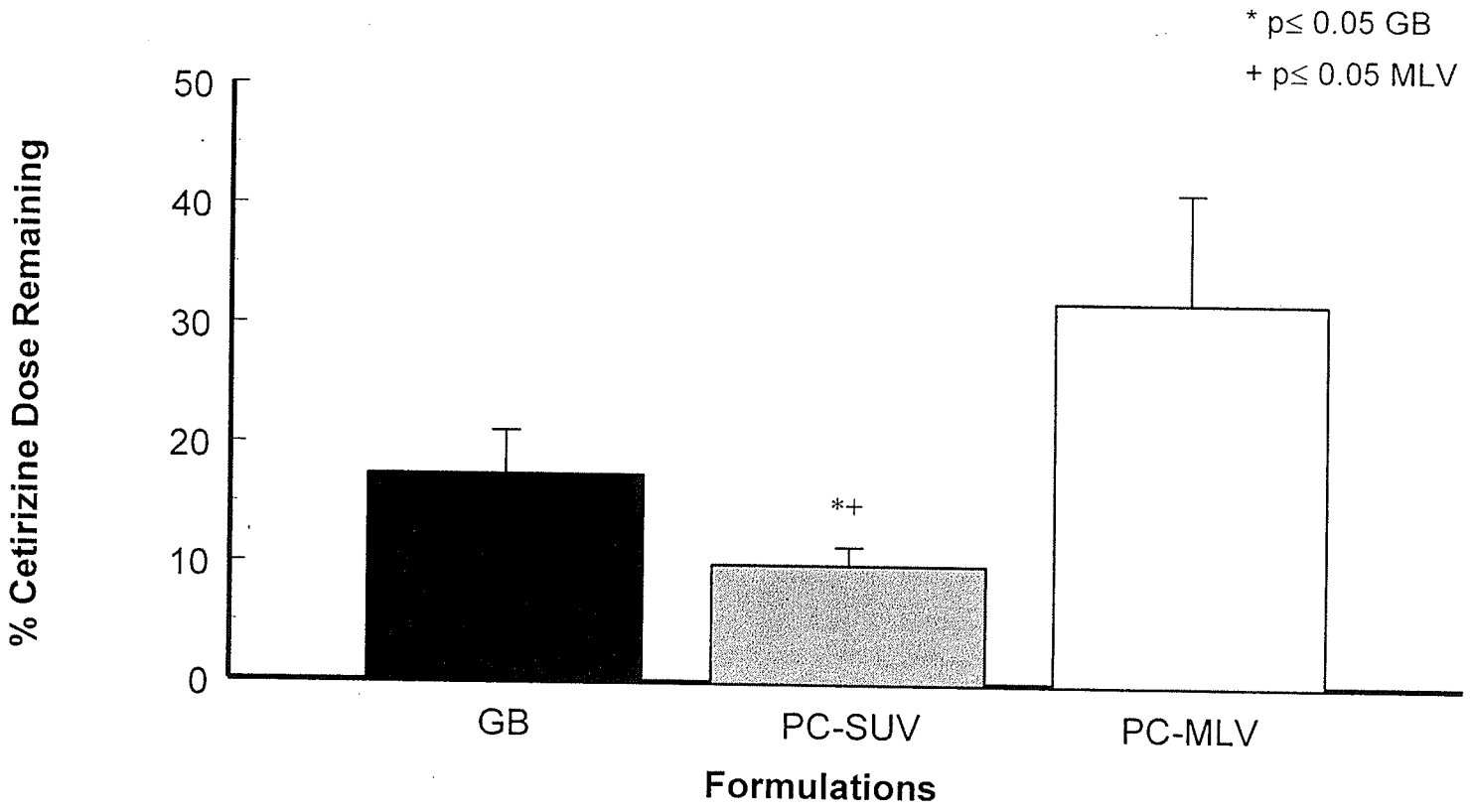

Figure 35: Mean ± SEM Percent of Cetirizine Dose Remaining on the Shaved Backs of Rabbits at 24 hours after the Topical Application of 10 mg Cetirizine from GB or PC-SUV or PC-MLV.

n=6

GB = Glaxal Base,

PC-SUV = small unilamellar vesicles (SUV) prepared using L-α-phosphatidylcholine (PC),

PC-MLV = multilamellar vesicles (MLV) prepared using L-α-phosphatidylcholine (PC)

Table 48: Histamine-Induced Wheal Areas on the Shaved Backs of Rabbits Before and After the Topical Application of 10 mg Cetirizine from HPC-SUV

PD Parameter	Wheal Area (cm^2)										
Time (h) / Rabbit Code	0	0.5	1	2	3	4	5	6	8	10	24
3	1.22	0.75	0.75	0.80	0.74	0.75	0.94	1.13	1.03	0.40	0.14
4	1.13	1.07	1.07	1.03	0.51	0.99	1.02	0.68	0.75	1.03	0.27
5	0.99	0.90	0.74	0.70	0.40	0.50	0.40	0.30	0.30	0.31	0.00
6	1.21	1.01	1.01	0.86	1.17	0.75	1.03	0.55	0.58	0.56	0.00
Mean	1.13	0.93	0.89	0.85	0.71	0.75	0.85	0.67	0.67	0.58	0.10
SEM	0.05	0.07	0.09	0.07	0.17	0.10	0.15	0.17	0.15	0.16	0.06

n= 4
PD = Pharmacodynamic
HPC-SUV= small unilamellar vesicles (SUV) prepared using L-α-phosphatidylcholine hydrogenated (HPC)

Table 49: Histamine-Induced Wheal Areas on the Shaved Backs of Rabbits Before and After the Topical Application of 10 mg Cetirizine from HPC-MLV

PD Parameter	Wheal Area (cm^2)										
Time (h) / Rabbit Code	0	0.5	1	2	3	4	5	6	8	10	24
3	1.22	0.75	0.06	0.19	0.46	0.01	0.05	0.02	0.03	0.11	0.29
4	1.13	0.26	0.02	n.a.	n.a.	n.a.	n.a.	n.a.	n.a.	n.a.	n.a.
5	1.20	0.21	0.14	0.02	0.10	0.02	0.02	0.09	0.07	0.28	0.42
6	1.64	1.21	0.10	0.53	0.51	0.08	0.28	0.17	0.14	0.21	0.20
Mean	1.30	0.61	0.08	0.25	0.36	0.04	0.12	0.09	0.08	0.20	0.30
SEM	0.12	0.24	0.03	0.15	0.13	0.02	0.08	0.04	0.03	0.05	0.06

n= 4
PD = Pharmacodynamic
HPC-MLV= multilamellar vesicles (MLV) prepared using L-α-phosphatidylcholine hydrogenated (HPC)
n.a. = not available

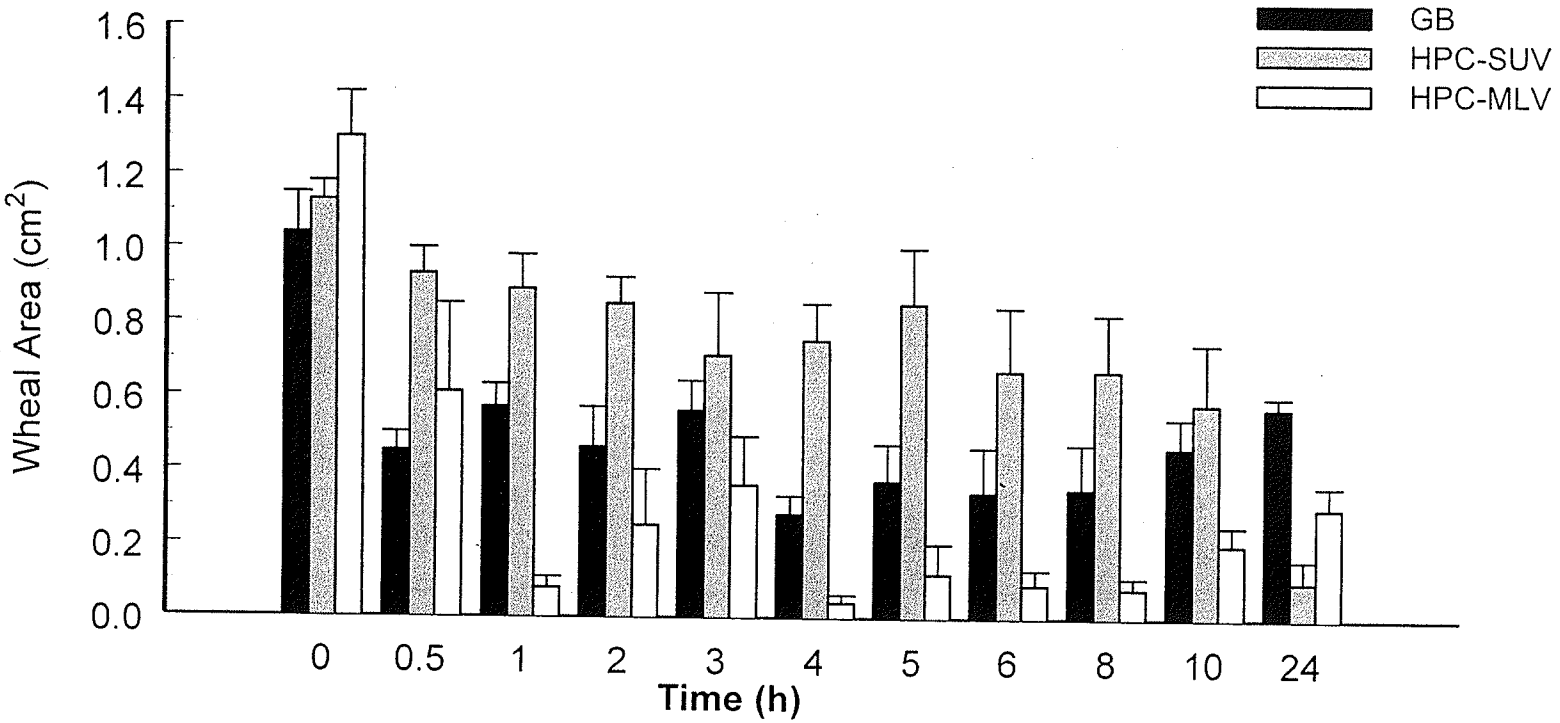

Figure 36: Mean ± SEM Wheal Areas of Histamine-Induced Wheal on the Shaved Backs of Rabbits after the Topical Application of 10 mg Cetirizine from GB or HPC-SUV, or HPC-MLV.

n= or > 3

GB = Glaxal Base,

HPC-SUV = small unilamellar vesicles (SUV) prepared using L-α-phosphatidylcholine hydrogenated (HPC),

HPC-MLV = multilamellar vesicles (MLV) prepared using L-α-phosphatidylcholine hydrogenated (HPC)

Table 50: Percent Suppression of Histamine-Induced Wheal Formation on the Shaved Backs of Rabbits after the Topical Application of 10 mg Cetirizine from HPC-SUV

PD Parameter	Percent Wheal Suppression									
Time (h) / Rabbit Code	0.5	1	2	3	4	5	6	8	10	24
3	38.5	38.5	34.4	39.1	38.3	23.0	7.0	15.2	67.1	88.2
4	14.1	14.1	17.3	59.2	20.6	18.4	45.6	40.0	17.6	78.6
5	9.1	24.9	29.0	59.4	49.3	59.1	69.4	69.3	68.4	100.0
6	16.5	16.7	28.8	3.1	37.9	14.4	54.5	52.0	53.6	100.0
Mean	19.6	23.6	27.4	40.2	36.5	28.7	44.1	44.1	51.7	91.7
SEM	6.5	5.5	3.6	13.2	5.9	10.3	13.3	11.3	11.8	5.2

n= 4
PD = Pharmacodynamic
HPC-SUV= small unilamellar vesicles (SUV) prepared using L-α-phosphatidylcholine hydrogenated (HPC)

Table 51: Percent Suppression of Histamine-Induced Wheal Formation on the Shaved Backs of Rabbits after the Topical Application of 10 mg Cetirizine from HPC-MLV

PD Parameter	Percent Wheal Suppression									
Time (h) / Rabbit Code	0.5	1	2	3	4	5	6	8	10	24
3	38.5	95.3	84.8	62.0	99.3	95.7	98.7	97.2	91.1	76.6
4	76.7	98.2	n.a.	n.a.	n.a.	n.a.	n.a.	n.a.	n.a.	n.a.
5	82.8	88.0	98.1	92.0	98.3	98.3	92.5	94.5	76.3	64.8
6	24.2	93.7	66.7	68.3	94.8	82.4	89.6	91.4	87.2	87.3
Mean	55.6	93.8	83.2	74.1	97.5	92.1	93.6	94.4	84.9	76.2
SEM	14.3	2.2	9.1	9.1	1.4	4.9	2.7	1.7	4.4	6.5

n= 3
PD = Pharmacodynamic
HPC-MLV= multilamellar vesicles (MLV) prepared using L-α-phosphatidylcholine hydrogenated (HPC)
n.a. = not available

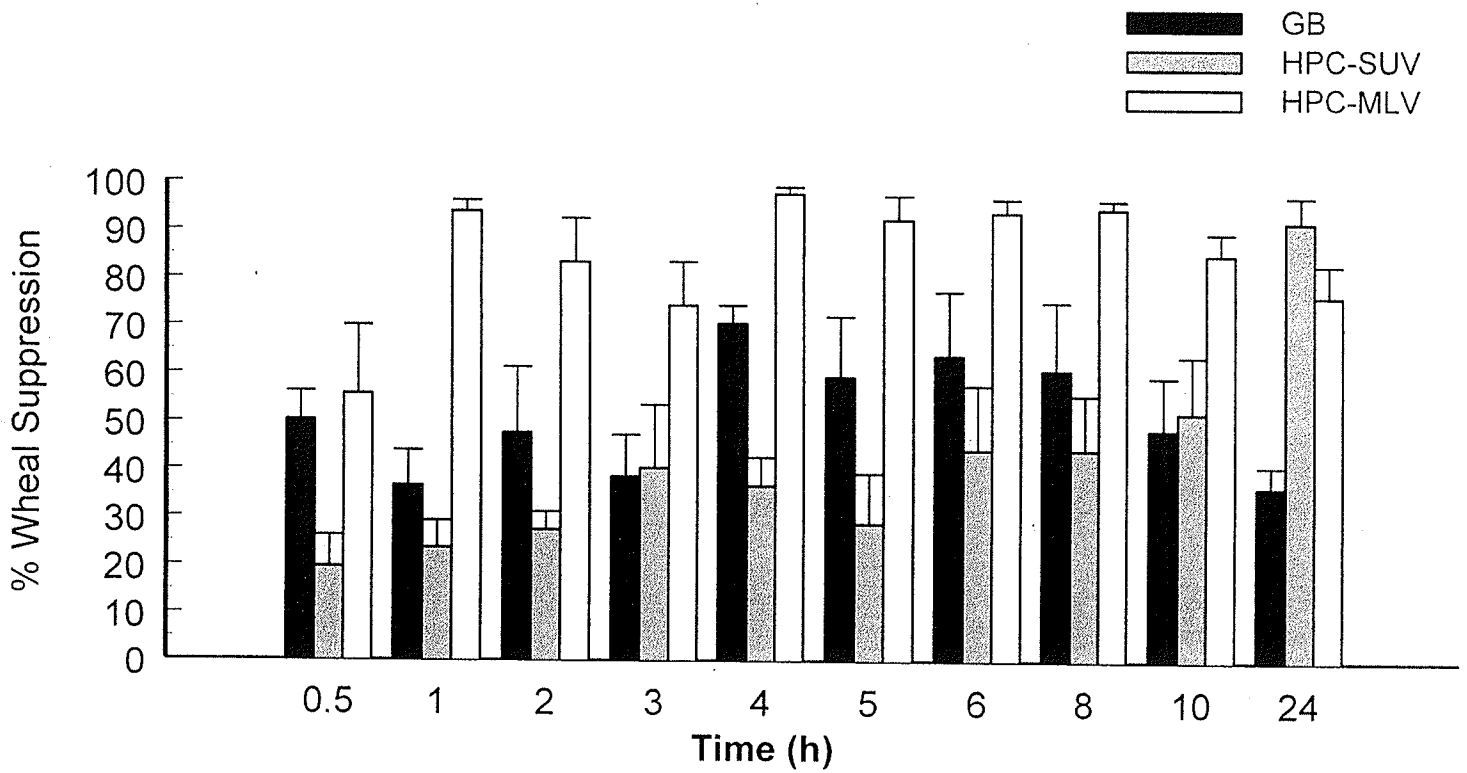

Figure 37: Mean ± SEM Percent Suppression of Histamine-Induced Wheal Formation on the Shaved Backs of Rabbits after the Topical Application of 10 mg Cetirizine from GB or HPC-SUV, or HPC-MLV.

n= or > 3

GB = Glaxal Base,

HPC-SUV = small unilamellar vesicles (SUV) prepared using L-α-phosphatidylcholine hydrogenated (HPC),

HPC-MLV = multilamellar vesicles (MLV) prepared using L-α-phosphatidylcholine hydrogenated (HPC)

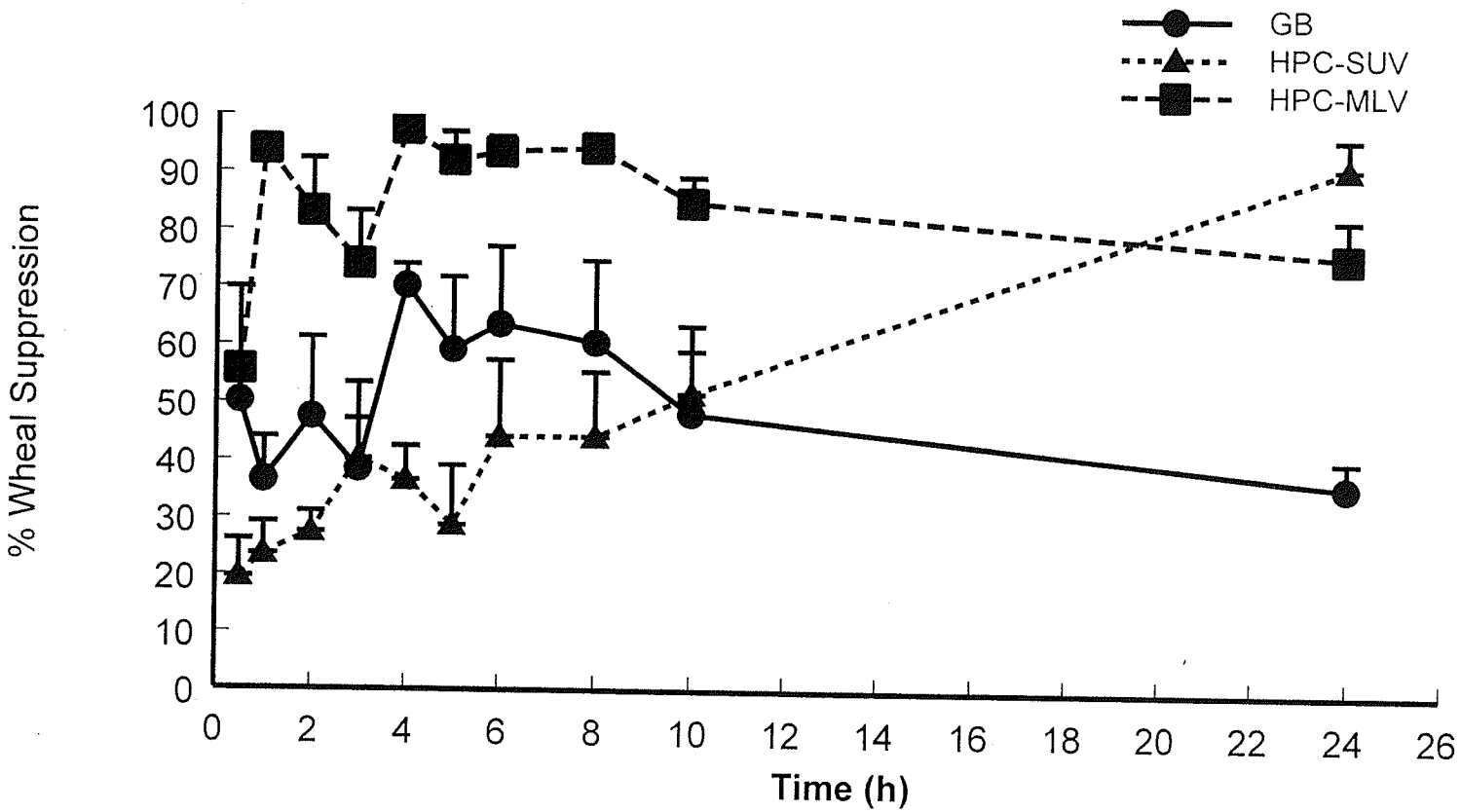

Figure 37a: Mean ± SEM Percent Suppression of Histamine-Induced Wheal Formation on the Shaved Backs of Rabbits after the Topical Application of 10 mg Cetirizine from GB or HPC-SUV, or HPC-MLV.

n= or > 3

GB = Glaxal Base,

HPC-SUV = small unilamellar vesicles (SUV) prepared using L-α-phosphatidylcholine hydrogenated (HPC),

HPC-MLV = multilamellar vesicles (MLV) prepared using L-α-phosphatidylcholine hydrogenated (HPC)

Table 52: Cetirizine Plasma Concentrations after the Topical Application of 10 mg Cetirizine from HPC-SUV on the Shaved Backs of Rabbits

PK Parameter	Cetirizine Plasma Concentration (ng/mL)										
Time (h) / Rabbit Code	0	0.5	1	2	3	4	5	6	8	10	24
1	0.0	7.4	4.5	5.8	4.1	4.5	4.1	6.2	9.9	6.6	3.7
3	0.0	10.3	6.6	8.3	8.7	7.8	8.7	7.0	9.9	6.2	5.8
5	0.0	11.6	9.9	9.9	4.9	2.0	7.0	7.0	7.8	7.0	2.0
6	0.0	6.2	4.9	6.2	6.2	7.4	5.8	6.2	4.1	6.6	4.9
Mean	0.0	8.9	6.5	7.5	6.0	5.4	6.4	6.6	7.9	6.6	4.1
SEM	0.0	1.3	1.2	1.0	1.0	1.4	1.0	0.2	1.4	0.2	0.8

n= 4

PK = Pharmacokinetics

HPC-SUV= small unilamellar vesicles (SUV) prepared using L-α-phosphatidylcholine hydrogenated (HPC)

Table 53: Cetirizine Plasma Concentrations after the Topical Application of 10 mg Cetirizine from HPC-MLV on the Shaved Backs of Rabbits

PK Parameter	Cetirizine Plasma Concentration (ng/mL)										
Time (h) / Rabbit Code	0	0.5	1	2	3	4	5	6	8	10	24
3	0.0	8.7	3.3	2.8	29.5	16.6	27.4	42.8	46.5	17.4	12.4
4	0.0	43.6	26.5	54.4	n.a.	n.a.	n.a.	n.a.	n.a.	n.a.	n.a.
5	0.0	0.0	42.3	17.8	30.7	32.4	28.2	39.9	22.8	28.6	37.8
6	0.0	44.8	34.9	26.1	22.8	35.7	23.6	6.6	48.6	19.1	5.8
Mean	0.0	24.3	26.8	25.3	27.7	28.2	26.4	29.7	39.3	21.7	18.6
SEM	0.0	11.7	8.5	10.8	2.5	5.9	1.4	11.6	8.3	3.5	9.8

n= 3

PK = Pharmacokinetics

HPC-MLV= multilamellar vesicles (MLV) prepared using L-α-phosphatidylcholine hydrogenated (HPC)

n.a. = not available

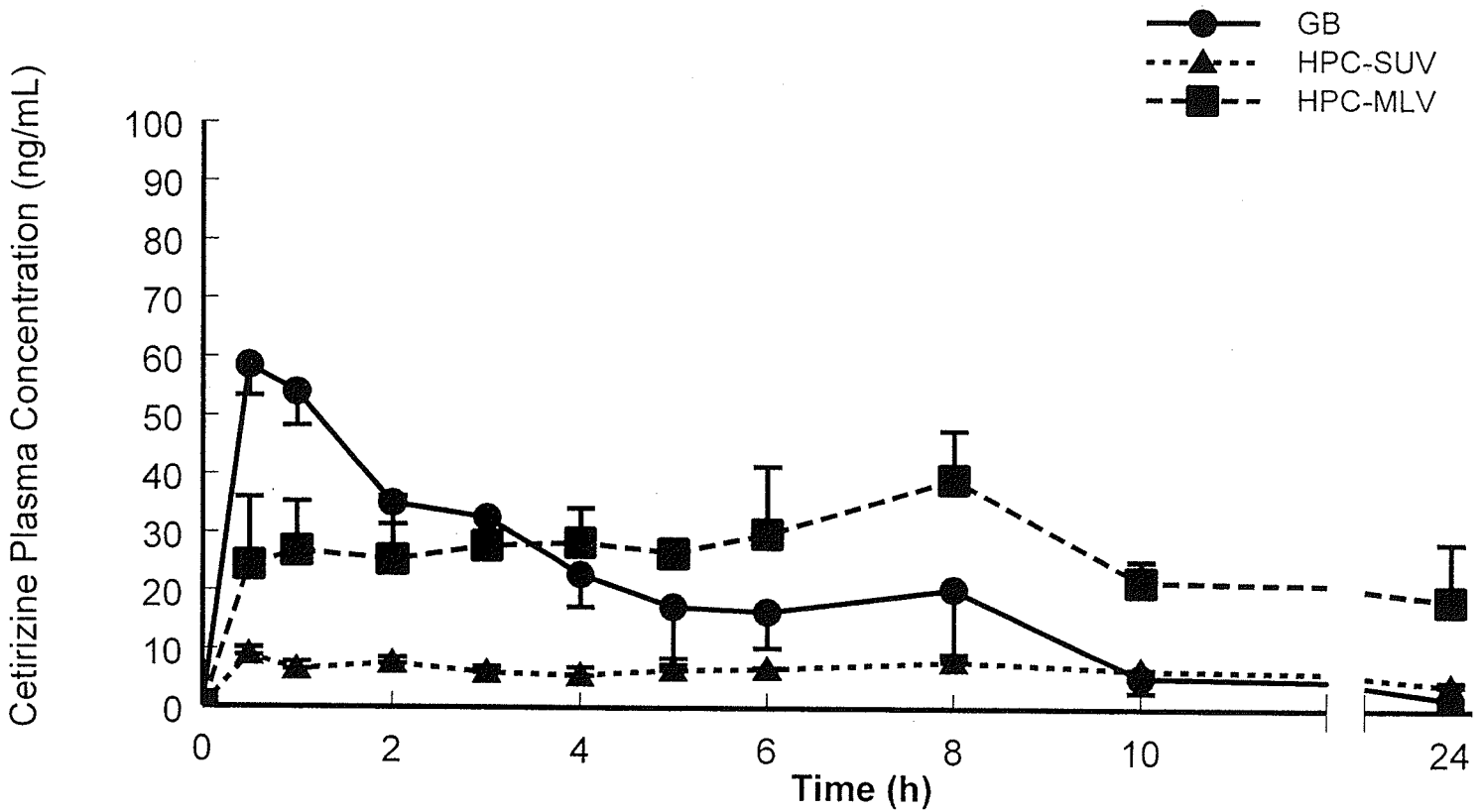

Figure 38: Mean ± SEM Cetirizine Plasma Concentrations after the Topical Application of 10 mg Cetirizine From GB or HPC-SUV or HPC-MLV on the Shaved Backs of Rabbits.

n= or > 3

GB = Glaxal Base,

HPC-SUV = small unilamellar vesicles (SUV) prepared using L-α-phosphatidylcholine hydrogenated (HPC),

HPC-MLV = multilamellar vesicles (MLV) prepared using L-α-phosphatidylcholine hydrogenated (HPC)

Table 54: Mean ± SEM Percent of Cetirizine Dose Remaining on the Shaved Backs of Rabbits at 24 hours after the Topical Application of 10 mg Cetirizine from GB or HPC-SUV or HPC-MLV

Formulations	Percent of Cetirizine Remaining Mean ± SEM
GB	17.4 ± 3.6
HPC-SUV*+	5.9 ± 0.7
HPC-MLV	19.2 ± 4.0

n= 3

* Significantly different from GB $p \leq 0.05$

+ Significantly different from MLV $p \leq 0.05$

GB = Glaxal Base

HPC-SUV= small unilamellar vesicles (SUV) prepared using L-α-phosphatidylcholine hydrogenated (HPC)

HPC-MLV= multilamellar vesicles (MLV) prepared using L-α-phosphatidylcholine hydrogenated (HPC)

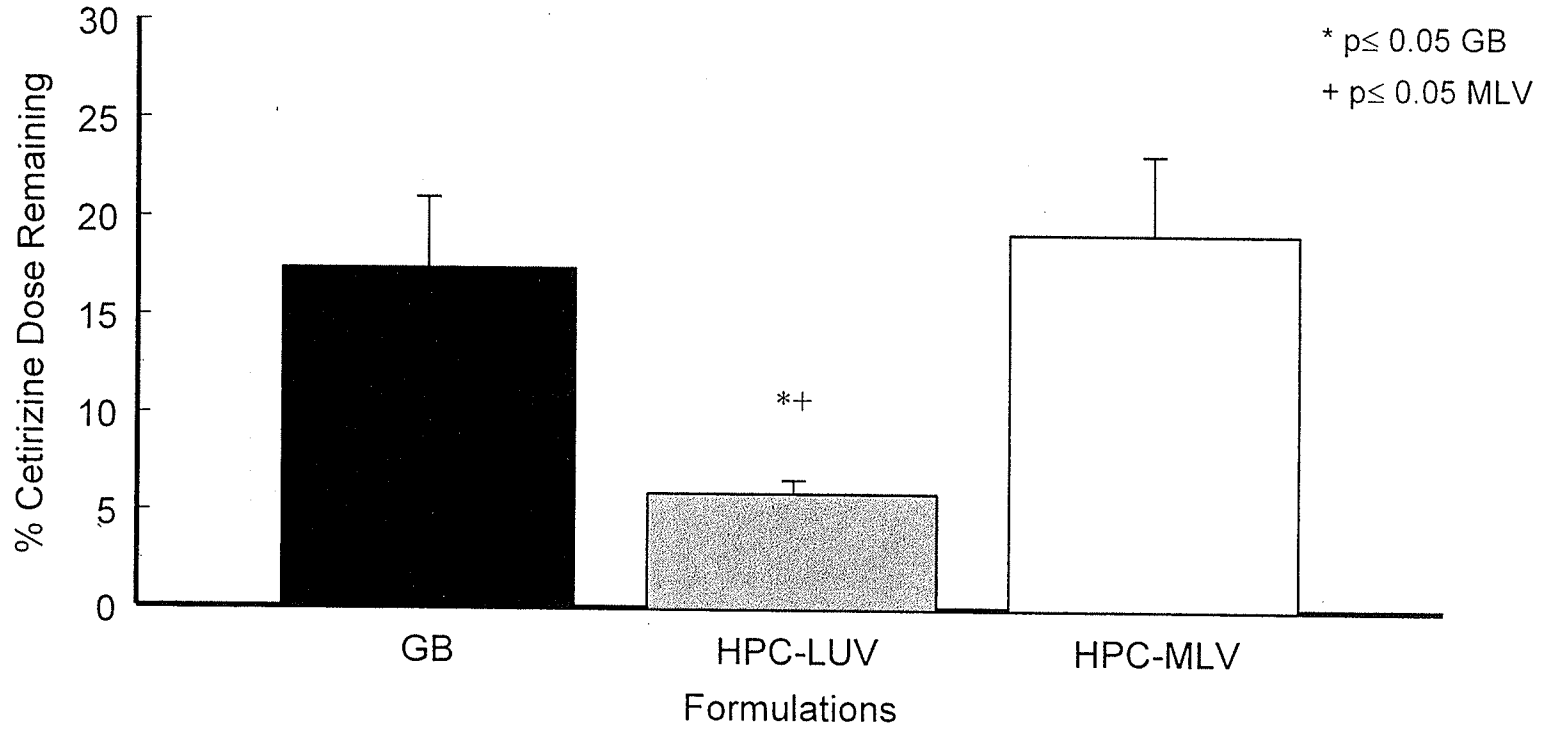

Figure 39: Mean ± SEM Percent of Cetirizine Dose Remaining on the Shaved Backs of Rabbits at 24 hours after the Topical Application of 10 mg Cetirizine from GB or HPC-SUV or HPC-MLV.

n= or > 3

GB = Glaxal Base,

HPC-SUV = small unilamellar vesicles (SUV) prepared using L-α-phosphatidylcholine hydrogenated (HPC),

HPC-MLV = multilamellar vesicles (MLV) prepared using L-α-phosphatidylcholine hydrogenated (HPC)

REFERENCES

1. Reinert M, Wiest R, Barth L, Andres R, Ozdoba C, Seiler R. Transdermal nitroglycerin in patients with subarachnoid hemorrhage. *Neurol Res* 2004 ;26: 435-439.
2. Billich A, Aschauer H, Aszodi A, Stuetz A. Percutaneous absorption of drugs used in atopic eczema: pimecrolimus permeates less through skin than corticosteroids and tacrolimus. *Int J Pharm* 2004; **269**:29-35.
3. Mealey KL, Peck KE, Bennett BS, Sellon RK, Swinney GR, Melzer K, Gokhale, Krone TM. Systemic absorption of amitriptyline and buspirone after oral and transdermal administration of healthy cats. *J Vet Intern Med* 2004; **18**: 43-46.
4. Bodde HE, Verhoeven J, Driel LM JV. The skin compliance of transdermal drug delivery system. *Crit Rev Ther Drug Carrier Syst* 1989; **6**: 87-115.
5. Kanitakis J. Anatomy, histology and immunohistochemistry of normal human skin. *Eur J Dermatol* 2002; **12**:1-13.
6. Lynch DH, Roberts LK. Immunology of the skin. *In Topical Drug Delivery Formulations,* Osborne DW, Amann AH (eds). Marcel Dekker: New York, 1990; 89.
7. Wertz PW. Epidermal lipids. *Semin Dermatol* 1992; **11**:106-113.
8. Montagna W, Kligman AM, Carlisle KS. *Atlas of Normal Human Skin*. Springer-Verlag: New York, 1992; 30-34.

9. Roberts MS, Cross SE, Anissimov. Factors affecting the formulation of a reservoir for topically applied solutes. *Skin Pharmacol Physiol* 2004; **17**: 3-16.

10. Wertz PW. Lipids and barrier function of the skin. *Acta Derm Venereol Suppl (Stockh)* 2000; **208**: 7-11.

11. Yourick JJ, Koenig ML, Yourick DL, Bronaugh RL. Fate of chemicals in skin after dermal application: does the in vitro skin reservoir affect the estimate of systemic absorption?. *Toxicol Appl Pharmacol* 2004; **195** :309-320.

12. Sheth NV, Mckeough MB, Spruance SL. Measurement of the stratum corneum drug reservoir to predict the therapeutic efficacy of topical Iododeoxyuridine for herpes simplex virus infection. *J Invest Dermatol* 1989; **6**: 598-602.

13. Krishna DR, Klotz U. Extrahepatic metabolism of drugs in humans. *Clin Pharmacokinet* 1994; **26**: 144-160.

14. Steinstrasser I, Merkle HP. Dermal metabolism of topically applied drugs: pathways and models reconsidered. *Pharm Acta Helv* 1995; **70**: 3-24.

15. Bashir SJ, Maibach HI. Cutaneous metabolism of xenobiotics. *In Topical Absorption of Dermatological Products*. Bronaugh RL, Maibach HI (eds). Marcel Dekker: New York, 2002; 77-91.

16. Ademola JI, Wester RC, Maibach HI. Cutaneous metabolism of theophylline by the human skin. *J Invest Dermatol* 1992; **98**: 310-314.

17. Higo N, Hinz RS, Lau DTW, Benet LZ, Guy RH. Cutaneous metabolism of nitroglycerin *in-vitro*. I. Homogenized versus intact skin. *Pharm Res* 1992; **9**: 187-190.

18. Higo N, Hinz RS, Lau DTW, Benet LZ, Guy RH. Cutaneous metabolism of nitroglycerin *in-vitro*. II. Effects of skin condition and penetration enhancement. *Pharm Res* 1992; **9**: 303-306.

19. Guy RH, Hadgraft J. Percutaneous penetration enhancement: physicochemical considerations and implications for prodrug design. *In Prodrugs,* Sloan KB (ed). Marcel Dekker: New York, 1992; 2-3.

20. Otberg N, Richter H, Schaefer H, Blume-Peytavi U, Sterry W, Lademann J. Variations of hair follicle size and distribution in different body sites. *J Invest Dermatol* 2004; **122**: 14-19.

21. Lauer AC. Percutaneous drug delivery to the hair follicle. *In Topical Absorption of Dermatological Products,* Bronaugh RL, Kraeling MEK, Yourick J, Hood HL (eds). Marcel Dekker: New York, 2002; 93-113.

22. Schäfer P, Bewick-Sonntag C, Capri MG, Berardesca E. Physiology changes in skin barrier function in relation to occlusion level, exposure time and climatic conditions. *Skin Pharmacol Appl Skin Physiol* 2002; **15**: 7-19.

23. Franz TJ, Lehman PA, Feldman SR, Spellman MC. Bioavailability of clobetasol propionate in different vehicles. *Skin Pharmacol Appl Skin Physiol* 2003; **16**: 212-216.

24. Ladenheim D, Martin GP, Marriott C, Hollingsbee DA, Brown MB. An in-vitro study of the effect of hydrocolloid patch occlusion on the penetration of triamcinolone acetonide through skin in man. *J Pharm Pharmacol* 1996; **48**: 806-811.

25. Rudy SJ, Pamela C, Vetter P. Percutaneous absorption of topically applied medication. *Dermatol Nursing* 2003; **15**: 145-152.

26. Meuling WJ, Franssen AC, Brouwer DH, van Hemmen JJ. The influence of skin moisture on the dermal absorption of propoxur in human volunteers: a consideration for biological monitoring practices. *Sci Total Environ* 1997; **199**: 165-172.

27. Chiou YB, Blume-Petytavi U. Stratum corneum maturation. *Skin Pharmacol Physiol* 2004; **17**:57-66.

28. Barrett DA, Rutter N. Transdermal delivery and the premature neonate. Crit Rev Ther Drug Carrier Syst 1994; **11**: 1-30.

29. Behne MJ, Barry NP, Hanson KM, Aronchik I, Clegg RW, Gratton E, Feingold K, Holleran WM, Elias PM, Mauro TM. Neonatal development of stratum corneum pH gradient: localization and mechanisms leading to emergence of optimal barrier function. *J Invest Dermatol* 2003; **120**: 998-1006.

30. Roskos KV, Maibach HI. Percutaneous absorption and age: Implications for therapy. *Drugs Aging* 1992; **2**: 432-449.

31. Murphy M, Carmichael AJ. Transdermal drug delivery systems and skin sensitivity reactions: Incidence and management. *Am J Clin Dermatol* 2000; **1**: 361-368.

32. Warner KS, Li SK, He N, Suhonen TM, Chantasart D, Bolikal D, Higuchi WI. Structure-activity relationship for chemical skin permeation enhancers: probing the chemical microenvironment of the site of action. *J Pharm Sci* 2003; **92**:1305-1322.

33. Jackson JA, Diliberto JJ, Birnbaum LS. Estimation of octanol-water partition coefficients and correlation with dermal absorption for several polyhalogenated aromatic hydrocarbons. *Fundam Appl Toxicol* 1993; **21**: 334-344.

34. Tayar N, Tsai RS, Testa B, Carrupt PA, Hansch C, Leo A. Percutaneous penetration of drugs: a quantitative structure-permeability relationship study. *J Pharm Sci* 1991; **80**: 744-749.

35. Gorukanti SR, Li L, Kim KH. Transdermal delivery of antiparkinsonian agent, benztropine. I. Effect of vehicles on skin permeation. *Int J Pharm* 1999 ; **192**:159-172.

36. Sintov AC, Krymberk I, Gavrilov V, Gorodischer R. Transdermal delivery of paracetamol for paediatric use: effects of vehicle formulations on the percutaneous penetration. *J Pharm Pharmacol* 2003; **55**:911-919.

37. Siddiqui O. Physicochemical, physiological, and mathematical considerations in optimizing percutaneous absorption of drugs. *Crit Rev Ther Drug Carrier Syst* 1989; **6**: 1-38.

38. Barry BW. Vehicle effects: What is an enhancer. *In Topical Drug Bioavailability, Bioequivalence and Penetration.* Shah VP, Maibach HI (eds). Plenum press: New York, 1993; 269.

39. Williams AC, Barry BW. Penetration enhancers. *Adv Drug Deliv Rev* 2004; **56**:603-618.

40. Yamashita F, Hashida M. Mechanistic and empirical modeling of skin permeation of drugs. *Adv Drug Deliv Rev* 2003; **55**:1185-1199.

41. Monteiro-Riviere NA, Inman AO, Mak V, Wertz P, Riviere JE. Effect of selective lipid extraction from different body regions on epidermal barrier function. *Pharm Res* 2001; **18**: 992-1011.

42. Kanikkannan N, Singh M. Skin permeation enhancement effect and skin irritation of saturated fatty alcohols. *Int J Pharm* 2002; **248**:219-228.

43. Guy RH. Current status and future prospects of transdermal drug delivery. *Pharm Res*. 1996; **13**: 1765-1769.

44. Patil S, Singh P, Platzer CS, Maibach H. Epidermal enzymes as penetration enhancers in transdermal drug delivery. *J Pharm Sci* 1996; **85**: 249-252.

45. Tsai J-C, Guy RH, Thornfeldt CR, Gao WN, Feingold KR, Elias PM. Metabolic approaches to enhance transdermal drug delivery I. Effect of lipid synthesis inhibitors. *J Pharm Sci* 1996; **85**: 643-648.

46. Cevc G. Lipid vesicles and other colloids as drug carriers on the skin. *Adv Drug Deliv Rev* 2004; **56**: 675-711.

47. King MJ, Michel D, Foldvari M. Evidence for lymphatic transport of insulin by topically applied biphasic vesicles. *J Pharm Pharmacol* 2003; **55**:1339-1344.

48. Boinpally RR, Zhou SL, Poondru S, Devraj G, Jasti BR. Lecithin vesicles for topical delivery of diclofenac. *Eur J Pharm Biopharm* 2003; **56**:389-392.

49. Ogiso T, Yamaguchi T, Iwaki M, Tanino T, Miyake Y. Effect of positively and negatively charged liposomes on skin permeation of drugs. *J Drug Target* 2001; **9**: 49-59.

50. Kulkarni SB, Betageri GV, Singh M. Factors affecting microencapsulation of drugs in liposomes. *J Microencapsul* 1995 ;**12** :229-246.

51. Ostro MJ, Cullis PR. Use of liposomes as injectable-drug delivery systems. *Am J Hosp Pharm* 1989; **46**:1576-1587.

52. Foldvari M. Effect of vehicle on topical liposomal drug delivery: petrolatum bases. *J Microencapsul* 1996;**13**: 589-600.

53. Mezei M, Gulasekharam V. Liposomes--a selective drug delivery system for the topical route of administration. Lotion dosage form. *Life Sci* 1980; **26**:1473-1477.

54. Foong WC, Harsany BB, Mezei M. Biodisposition and histological evaluation of topically applied retinoic acid in liposomal, cream and gel dosage forms. *In Phospholipids*, Hanin I, Pepeu G (eds). Plenum Press: New York, 1990; 279-282.

55. Posner R. Liposomes. *J Drugs Dermatol* 2002; **1**:161-164.

56. Agarwal R, Katare OP, Vyas SP. Preparation and *in vitro* evaluation of liposomal/niosomal delivery systems for antipsoriatic drug dithranol. *Int J Pharm* 2001; **228**: 43-52.

57. Yarosh D, Klein J, O'Connor A, Hawk J, Rafal E, Wolf P. Effect of topically applied T4 endonuclease V in liposomes on skin cancer in xeroderma pigmentosum: a randomised study. Xeroderma Pigmentosum Study Group. *Lancet* 2001; **357**: 926-929.

58. Both DM, Goodtzova K, Yarosh DB, Brown DA. Liposome-encapsulated ursolic acid increases ceramides and collagen in human skin cells. *Arch Dermatol Res* 2002; **293**: 569-75.

59. Bouwstra JA, Honeywell-Nguyen PL. Skin structure and mode of action of vesicles. *Adv Drug Deliv Rev* 2002; **54** Suppl 1:S41-55.

60. Price CI, Horton WJ, Baxter CR. Liposome delivery of aminoglycosides in burn wounds. *Surg Gynecol Obstet* 1992; **174**: 414-418.

61. Price CI, Horton WJ, Baxter CR. Topical liposomal delivery of antibiotics in soft tissue infection. *J Surg Res* 1990; **49**: 174-178.

62. Erdogan M, Wright JR Jr, McAlister VC. Liposomal tacrolimus lotion as a novel topical agent for treatment of immune-mediated skin disorders: experimental studies in a murine model. *Br J Dermatol* 2002;**146** :964-967.

63. Niemiec SM, Latta JM, Ramachandran C, Weiner ND, Roessler BJ. Perifollicular transgenic expression of human Interleukin-1 receptor antagonist protein following topical application of novel liposome-plasmid DNA formulations *in vivo. J Pharm Sci* 1997; **86**: 701-708.

64. Fleisher D, Niemiec SM, Oh CK, Hu Z, Ramachandran C, Weiner N. Topical delivery of growth hormone releasing peptide using liposomal systems: An *in vitro* study using hairless mouse skin. *Life Sci* 1995; **57**: 1293-1297.

65. Egbaria K, Ramachandran C, Kittayanond D, Weiner N. Topical delivery of liposomally encapsulated interferon evaluated by *in vitro* diffusion studies. *Antimicrob Agents Chemother* 1990; **34**: 107-110.

66. Mezei M. Liposomes in the topical application of drugs: a review. *In Liposomes as Drug Carriers, Recent Trends and Progress,* Gregoriadis G (ed). John Wily and Sons: New York, Toronto, 1988; 664.

67. Verma DD, Verma S, Blume G, Fahr A. Liposomes increase skin penetration of entrapped and non-entrapped hydrophilic substances into human skin: a skin

penetration and confocal laser scanning microscopy study. *Eur J Pharm Biopharm* 2003; **55**: 271-277.

68. Ferreira LS, Ramaldes GA, Nunan EA, Ferreira LA. In vitro skin permeation and retention of paromomycin from liposomes for topical treatment of the cutaneous leishmaniasis. *Drug Dev Ind Pharm* 2004; **30**: 289-96.
69. El Ridy MS, Khalil RM. Free versus liposome-encapsulated lignocaine hydrochloride topical applications. *Pharmazie* 1999; **54**: 682-684.
70. Bonowitz A, Schaller M, Laude J, Reimer K, Korting HC. Comparative therapeutic and toxic effects of different povidone iodine (PVP-I) formulations in a model of oral candidosis based on in vitro reconstituted epithelium. *J Drug Target* 2001; **9**: 75-83.
71. Li L, Hoffman RM. The feasibility of targeted selective gene therapy of the hair follicle. Nat Med 1995; **1**: 705-706.
72. Perugini P, Genta I, Pavanetto F, Conti B, Scalia S, Baruffini A. Study on glycolic acid delivery by liposomes and microspheres. *Int J Pharm* 2000; **196**: 51-61.
73. Betageri GV, Kulkarni SB. Preparation of liposomes. *In Microspheres, Microcapsules and Liposomes: Preparation and Chemical Applications,* Arshady R (ed). Citus Books: London, United Kingdom, 1999; 489-521.
74. Lichtenberg D, Barenholz Y. Liposomes: preparation, characterization, and preservation. *Methods Biochem Anal* 1988; **33:**337-462.
75. Egerdie RB, Reid G, Trachtenberg J. The effect of liposome encapsulated antineoplastic agents on transitional cell carcinoma in tissue culture. *J Urol* 1989; **142**: 390-398.

76. Keough KMW, Giffin B, Kariel N. The influence of unsaturation on the phase transition temperatures of a series of heteroacid phosphatidylcholines containing twenty-carbon chains. *Biochim Biophys Acta* 1987; **902**: 1-10.

77. http://www.lipidat.chemistry.ohio-state.edu/ Dec 1st , 2000.

78. Avanti Polar Lipids, INC., *Products Catalog Edition VI Revision II*, 46,47,51,54.

79. Rowe RC, Sheskey PJ, Weller PJ. *Handbook of Pharmaceutical Excipients.* The Pharmaceutical Press and the American Pharmaceutical Association: London, UK & Chicago, USA, 2003; 340-342.

80. Fiume Z. Final report on the safety assessment of Lecithin and Hydrogenated Lecithin. *Int J Toxicol* 2001; **20** Suppl 1:21-45.

81. Roger RC New. Influence of liposome characteristics on their properties and fate. *In Liposomes as Tools in Basic Research and Industry*, Philippot JR, Schuber F (eds). CRC Press Inc: London, UK, 1995; 3-20.

82. Yarosh DB. Liposomes in investigative dermatology. *Photodermatol Photoimmunol Photomed* 2001; **17**: 203-212.

83. Fang JY, Hong CT, Chiu WT, Wang YY. Effect of liposomes and niosomes on skin permeation of enoxacin. *Int J Pharm* 2001; **219**:61-72.

84. Demel RA, De Kruyff B. The function of sterols in membranes. *Biochem Biophys Acta* 1976; **457**:109-132.

85. Coderch L, Fonollosa J, De Pera M, Estelrich J, De La Maza A, Parra JL. Influence of cholesterol on liposome fluidity by EPR. Relationship with percutaneous absorption. *J Control Release* 2000; **68**: 85-95.

86. Veatch SL, Keller SL. Separation of liquid phases in giant vesicles of ternary mixtures of phospholipids and cholesterol. *Biophys J* 2003; **85**: 3074-83.

87. Simons FER, Johnston L, Gu X, Simons KJ. Suppression of the early and late cutaneous allergic response using fexofenadine and montelukast. *Ann Allergy Asthma Immunol* 2001; **86**: 44-50.

88. Friday GA, Fireman P. In *Atlas of Allergies,* Fireman P, Slavin RG (eds). Gower Medical Publishing: New York, London, 1991; 4.2-4.10.

89. Church MK, Clough GF. Human skin mast cells: *in vitro* and *in vivo* studies. *Ann Allergy Asthma Immunol* 1999; **83**: 471-475.

90. Smith Pease CK, Basketter DA, Patlewicz GY. Contact allergy: the role of skin chemistry and metabolism. *Clin Exp Dermatol* 2003; **28**:177-183.

91. Fireman P. In *Atlas of Allergies,* Fireman P, Slavin RG (eds). Gower Medical Publishing: New York, London, 1991; 1.2-1.24.

92. Foreman JC. Neuropeptides and the pathogenesis of allergy. *Allergy* 1987; **42**: 1-11.

93. Berman BA, Ross RN, Sly RM. Conversation on allergy and Immunology: Urticaria. *Cutis* 1982; **30**: 696-700.

94. Duc J, Pécoud A. Successful treatment of idiopathic cold urticaria with the association of H_1 and H_2 antagonists: A case report. *Ann Allergy* 1986; **56**: 355-357.

95. Tokura Y, Takigawa M, Yamauchi T, Yamada M. Solar Urticara: A case with good therapeutic response to cimetidine. *Dermatol* 1986; **173**: 224-228.

96. Rebhun J. Hypothetical role of H_2 blockers in chronic urticaria. *Ann Allergy* 1981; **47**: 440-442.

97. Loden M. The skin barrier and use of Moisturizers in atopic dermatitis. *Clin Dermatol* 2003; **21**:145-157.

98. Wüthrich B. Clinical aspects, epidemiology, and prognosis of atopic dermatitis. *Ann Allergy Asthma Immunol* 1999; **83**: 464-470.

99. Leung DYM. Atopic dermatitis: New insights and opportunities for therapeutic intervention. *J Allergy Clin Immunol* 2000; **105**: 860-876.

100. Stuttgen G. The present status of anti-inflammatory agents in dermatology. *Drugs* 1988; **36**: 43-48.

101. Ortonne JP. Clinical potential of topical corticosteroids. *Drugs* 1988; **36**: 38 - 42.

102. Goa KL. Clinical pharmacology and pharmacokinetic properties of topically applied corticosteroids. *Drugs* 1988; **36**: 51-61.

103. Bos JD. Non-steroidal topical immunomodulators provide skin-selective, self-limiting treatment in atopic dermatitis. *Eur J Dermatol* 2003;**13**: 455-461.

104. Brown ES, Khan DA, Nejtek VA. The psychiatric side effects of corticosteroids. *Ann Allergy Asthma Immunol* 1999; **83**: 495-504.

105. Theoharides TC. Histamine$_2$ (H_2)-Receptor antagonists in the treatment of urticaria. *Drugs* 1989; **37**: 345-355.

106. Mayumi H, Kimura S, Asano M, Shimokawa T, Au-Yong TF, Yayama T. Intravenous cimetidine as an effective treatment for systemic anaphylaxis and acute allergic skin reactions. *Ann Allergy* 1987; **58**: 447-450.

107. Farnam J, Grant JA, Guernsey BG, Jorrizo JL, Petrusa ER. Successful treatment of chronic idiopathic urticaria and angioedema with cimetidine alone. *J Allergy Clin Immunol* 1984; **73**: 842-845.

108. Sahasrabudhe DM, McCune CS, O'Donnell RW, Henshaw EC. Inhibition of suppressor T lymphocytes (Ts) by cimetidine. *J Immunol* 1987; **138**: 2760-2763.

109. Bakker RA, Timmerman H, Leurs R. Histamine receptors: Specific ligands, receptor biochemistry, and signal tranduction. *In Histamine and H_1-antihistamines in Allergic Disease,* Simons FER (ed). Marcel Dekker Inc: New York, 2002; 27-64.

110. Chen X, Simons FE, Simons KJ. Effect of the H_2-receptor antagonist cimetidine, on the pharmacokinetics and pharmacodynamics of the H_1-receptor antagonists hydroxyzine and cetirizine in rabbits. *Pharm Res* 1994;11 :295-300.

111. Simons FER, Murray HE, Simons KJ. Quantitation of H_1 - receptor antagonists in skin and serum. *J Allergy Clin Immunol* 1995; **95**: 759-764.

112. Tasaka K, Kamei C, Akagi M, Mio M, Izushi K, Yoshida T, Nakamura S. Effect of loratadine on immediate and delayed type hypersensitivity reactions. . *Arzneimittelforschung* 1995; **45**: 796-804.

113. Amichai B, Grunwald MH, Brenner L. Fexofenadine hydrochloride – A new anti-histaminic drug. *IMAJ* 2001; **3**: 207-209.

114. Simons FER, Simons KJ, Becker AB, Haydey RP. Pharmacokinetics and antipruritic effects of hydroxyzine in children with atopic dermatitis. *J Pediatr* 1984; **104**:123-127.

115. Simons KJ, Simons FER. Clinical pharmacology of H_1-antihistamines. *In Histamine and H_1-antihistamines in Allergic Disease,* Simons FER (ed). Marcel Dekker Inc: New York, 2002; 141-178.

116. Reynolds JEF (ed). *Martindale the Extra Pharmacopoeia 13^{ed}*. The Pharmaceutical Press: London, UK, 1993; 926.

117. Balen GPV, Caron G, Ermondi G, Pagliara A, Grandi T, Bouchard G, Fruttero R, Carrupt P-A, Testa B. Lipophilicity behaviour of the zwitterionic antihistamine cetirizine in phosphatidylcholine liposomes/water systems. *Pharm Res* 2001; **18**: 694-701.

118. Portnoy JM, Dinakar C. Review of cetirizine hydrochloride for the treatment of allergic disorders. *Expert Opin Pharmacother* 2004; 5: 125-35.

119. Wellington K, Jarvis B. Cetirizine/Pseudoephedrine. *Drugs* 2001; **61**: 2231-2240.

120. Pfizer Inc Website. http://www.pfizer.com/hml/pi's/zyrtecpi.html. [26 Sep. 2003].

121. Rihoux JP. Therapeutic index of H_1-antihistamines: example of cetirizine. *Ann Allergy Asthma Immunol* 1999; **83**: 489-491.

122. Canonica GW, Ciprandi G. Minimal persistent inflammation may be controlled by cetirizine. *Ann Allergy Asthma Immunol* 1999; **83**: 445-448.

123.Simons FER. H_1-receptor antagonists: safety issues. *Ann Allergy Asthma Immunol* 1999; **83**: 481-488.

124. Black AK, Greaves MW. Antihistamines in Urticaria and Angioedema. *In Histamine and H_1-antihistamines in Allergic Disease,* Simons FER (ed). Marcel Dekker Inc: New York, 2002; 249-286.

125. Huston RL, Cypcar D, Cheng GS, Foulds DM. Toxicity from topical administration of diphenhydramine in children. *Clin Pediatr* 1990; **29**: 542-545

126. Bawati MJ. *Evaluation of the Disposition and Efficacy of Hydroxyzine in Liposome Formulations Applied Topically to Rabbits*. Master Thesis, University of Manitoba 1999.

127. Personal communication, Information Center, Avanti Polar Lipids Inc., Alabaster, AL, USA. Jan. 2000.

128. Simons FE, Simons KJ, and Frith EM. The pharmacokinetics and antihistaminic of the H_1 receptor antagonist hydroxyzine. *J Allergy Clin Immunol* 1984; **73**: 69-75.

129. Watson WTA, Simons KJ, Chen XY, Simons FE R. Cetirizine: A pharmacokinetic and pharmacodynamic evaluation in children with seasonal allergic rhinitis. *J Allergy Clin Immunol* 1989; **84**: 457-64.

130. Chatterjee S, Banerjee DK. Preparation, isolation, and characterization of liposomes containing natural and synthetic lipids. *Methods Mol Biol* 2002; **199**: 3-16.

131. Betz G, Nowbakhat P, Imboden R, Imanidis G. Heparin penetration into and permeation through human skin from aqueous and liposomal formulations in vitro. *Int J Pharm* 2001; **228**: 47-59.

132. Peters H, Moll F. Pharmacodynamics of a liposomal preparation for local anaesthesia. *Arzneimittelforschung* 1995; **45**: 253-256.

133. Batzri S, Korn ED. Single bilayer liposomes prepared without sonication. *Biochim Biophys Acta* 1973; **298**:1015-1019.

134. Avanti Polar Lipids, INC., Products Catalog Edition VI Revision II, p. 185.

135. Ammar HO, El-Ridy MS, Ghorab M, Ghorab MM. Evaluation of the antischistosomal effect of praziquantel in a liposomal delivery system in mice. *Int J Pharm* 1994; **103**: 237-241.

136. Nagarsenker MS, Londhe VY, Nadkarni GD. Preparation and evaluation of liposomal formulations of tropicamide for ocular delivery. *Int J Pharm* 1999; **190**: 63-71.

137. Bangham AD, Standish MM, Watkins JC. Diffusion of univalent ions across the lamellae of swollen phospholipids. *J Mol Biol* 1965; **13**: 238-252.

138. Joshi M, Misra A. Dry powder inhalation of liposomal Ketotifen fumarate: formulation and characterization. *Int J Pharm* 2001; **223**: 5-27.

139. Bhalerao SS, Harshal AR. Preparation, optimization, characterization, and stability studies of salicylic acid liposomes. *Drug Dev Ind Pharm* 2003; **29**: 451-467.

140. Hayat MA. *Principle and Techniques of Electron Microscopy:Biological Applications*. Van Nostrand Reinhold company: NEW York, 1970; 101-143.

141. Schaller M, Steinle R, Korting HC. Light and electron microscopic findings in human epidermis reconstructed in vitro upon topical application of liposomal tretinoin. *Acta Derm Venereol* 1997; **77**: 122-126.

142. Simons FE, Watson WT, Minuk GY, Simons KJ. Cetirizine pharmacokinetics and pharmacodynamics in primary biliary cirrhosis. *J Clin Pharmacol* 1993 ;**33**:949-954.

143. Gu X, Simons FE, Simons KJ. Epinephrine absorption after different routes of administration in an animal model. *Biopharm Drug Dispos* 1999; **20**: 401-405.

144. Wester RC, Maibach HI. Animal models for percutaneous absorption. *In Topical Drug Bioavailability Bioequivalence and Penetration,* Shah VP, Maibach HI (eds). Plenum Press: New York and London, 1993; 338.

145. Harkness JE, Wagner JE. *The Biology and Medicine of Rabbits and Rodents.* Lea and Febiger: Philadelphia and London, 1989; 11, 73.

146. Simons FE, Silver NA, Gu X, Simons KJ. Skin concentrations of H_1-receptor antagonists. *J Allergy Clin Immunol* 2001; **107**: 526-530.

147. Schubert R, Joos M, Deicher M, Magerle R, Lasch J. Destabilization of egg lecithin liposomes on the skin after topical application measured by perturbed ϒϒ angular correlation spectroscopy (PAC) with ^{111}In. *Biochimica Biophysica Acta.* 1993;**1150**:162-164.

148. Patel VB, Misra AN. Encapsulation and stability of clofazimine liposomes. *J Microencapsul* 1999; **16**: 357-367.

149. Valenta C, Cladera J, O'shea P, Hadgraft J. Effect of phloretin on the percutaneous absorption of lignocaine across human skin. *J Pharm Sci* 2001; **90**: 485-491.

150. Betageri GV. Liposomal encapsulation and stability of dideoxyinosine triphosphate. *Drug Dev Ind Pharm* 1993; **19**: 531-539.

151. Mezei M, Gulasekharam V. Liposomes-A selective drug delivery system for the topical route of administration: gel dosage form. *J Pharm Pharmacol* 1982; **34**: 473-474.

152. Nicoli S, Cappellazzi M, Colombo P, Santi P. Characterization of the permselective properties of rabbit skin during transdermal iontophoresis. *J Pharm Sci* 2003; **92**:1482-1488.

153.Anigbogu A, Patil S, Singh P, Liu P, Dinh S, Maibach H. An in vivo investigation of the rabbit skin responses to transdermal iontophoresis. *Int J Pharm* 2000 ;**200**:195-206.

154. Bensley BA. *Practical Anatomy of Rabbit.* The University of Toronto Press: Toronto 1931; 21.

155. Kaplan HM. *The Rabbit in Experimental Physiology.* Scholars Library: New York, 1962; 55.

156. Simons FE, Silver NA, Gu X, Simons KJ. Clinical pharmacology of H_1-antihistamines in the skin. *J Allergy Clin Immunol* 2002; **110**: 777-783.

157. Bashir SJ, Maibach HI. Cutaneous Metabolism during in vitro percutaneous absorption. *In Topical Absorption of Dermatological Products,* Bronaugh RL, Kraeling MEK, Yourick J, Hood HL (eds). Marcel Dekker: New York, 2002; 77-81.

158.Simons KJ, Watson WTA, Chen X Y, Simons FER. Pharmacokinetic and pharmacodynamic studies of the H_1-receptor antagonist hydroxyzine in the elderly. *Clin Pharmacol Ther* 1989; **45**: 9-14.

159. Mezei M. Liposomes and the skin. *In Liposomes in Drug Delivery*, Gregoriadis G, Florence AT, Patel HM (eds). Harwood Academic Publishers: Switzerland, 1993; 125-135.

160. Foldvari M, Gesztes A, Mezei M. Dermal drug delivery by liposome encapsulation: Clinical and electron microscopic studies. *J Microencapsul* 1990; **7:** 479-489.

161. Wohlrab W, Lasch J. Penetration Kinetics of liposomal hydrocortisone in human skin. *Dermatologica* 1987; **174**: 18-22.

162. Wohlrab W, Lasch J. The effect of liposomal incorporation of topically applied hydrocortisone on its serum concentration and urinary excretion. *Dermatol Mon schr* 1989; **175**: 348-352.

163. Harsanyi BB, Hilchie JC, Mezei M. Liposomes as drug carriers for oral ulcers. *J Dent Res* 1986; **65**: 1133-1141.

164. Nielsen PN, Skov PS, Poulsen LK, Schmelz M, Petersen LJ. Cetirizine inhibits skin reactions but not mediator release in immediate and developing late-phase allergic cutaneous reactions. A double-blind, placebo-controlled study. *Clin Exp Allergy*. 2001; **31**:1378-1384.

165. Ogiso T, Yamaguchi T, Iwaki M, Tanino T, Miyake Y. Effect of positively and negatively charged liposomes on skin permeation of drugs. *J Drug Target* 2001; **9**: 49-59.

166. Bernard E, Dubois JL, Wepierre J. Importance of sebaceous glands in cutaneous penetration of an antiandrogen: Target effect of liposomes. *J Pharm Sci* 1997; **86**: 573-578.

167. Tschan T, Steffen H, Supersaxo A. Sebaceous-gland deposition of isotretinoin after topical application: An in vitro study using human facial skin. *Skin Pharmacol* 1997; **10**: 126-134.

168. Honzak L, Sentjure M, Swartz HM. In vivo EPR of topical delivery of a hydrophilic substance ancapsulated in multilamellar liposomes applied to the skin of hairless and normal mice. *J Control Release* 2000; **66**: 221-228.

169. Patel HM. Liposomes as a controlled-release system. *Biochem Soc Trans* 1985; **13**: 513-516.

170. Williams AC. Transdermal and Topical Drug Delivery. London, UK: Pharmaceutical Press; 2003.

171. Unger E, Fritz T, Shen DK, Wu G. Manganese-based liposomes: comparative approach. *Invest Radiol* 1993; 28: 933-938.

172. Egbaria K, Ramachandran C, Weiner N. Topical delivery of ciclosporin: Evaluation of various formulations using in vitro diffusion studies in hairless mouse skin. *Skin Pharmacol* 1990; **3**: 21-28.

173. Egbaria K, Ramachandran C, Weiner N. Topical application of liposomally entrapped ciclosporin evaluated by in vitro diffusion studies with human skin. *Skin Pharmacol* 1991; **4**: 21-28.

174. Fisher R, Murphy M, Hung O, Mezei M, Stewart R. Absorption of liposome-encapsulated tetracaine versus nonliposome-encapsulated tetracaine from open wounds in rabbits. *Am J Emerg Med* 1994; **12**: 521-523.

175. Mezei M. liposomes as penetration promoters and localizers of topically applied drugs. In Hsieh D (ed), Drug Permeation Enhancement: Theory and Applications. New York, NY, Marcel Dekker Inc, 1994, pp171-198.

176. Mezei M. Biodisposition of liposome encapsulated active ingredients applied to the skin. In Liposome Dermatics, Braun-Falco O, Korting HC, Mailbach HI (ed),. Berlin: Springer-Verlag, 1992, pp117-127.

177. Elzainy AAW, Gu X, Simons FER, Simons KJ. Hydroxyzine form topical phospholipid liposomal formulations: evaluation of peripheral antihistaminic activity and systemic absorption in a rabbit model. *AAPS Journal* 2003; **5**(4): 1-8 (Article 28:http://www.aapsj.org)

178. Elzainy AAW, Gu X, Simons FER, Simons KJ. Cetirizine from topical phosphatidylcholine liposomes: evaluation of peripheral antihistaminic activity and systemic absorption in a rabbit model. *Biopharm and Drug Dispos* 2004 (in press).

179. Elzainy AAW, Gu X, Simons FER, Simons KJ. Cetirizine from topical phosphatidylcholine-hydrogenated liposomes: evaluation of peripheral antihistaminic activity and systemic absorption in a rabbit model. *AAPS Journal* 2004; **6**(3): 1-7 (Article 18: http://www.aapsj.org).

Appendix A

Figure 1: HPLC Chromatogram of Hydroxyzine

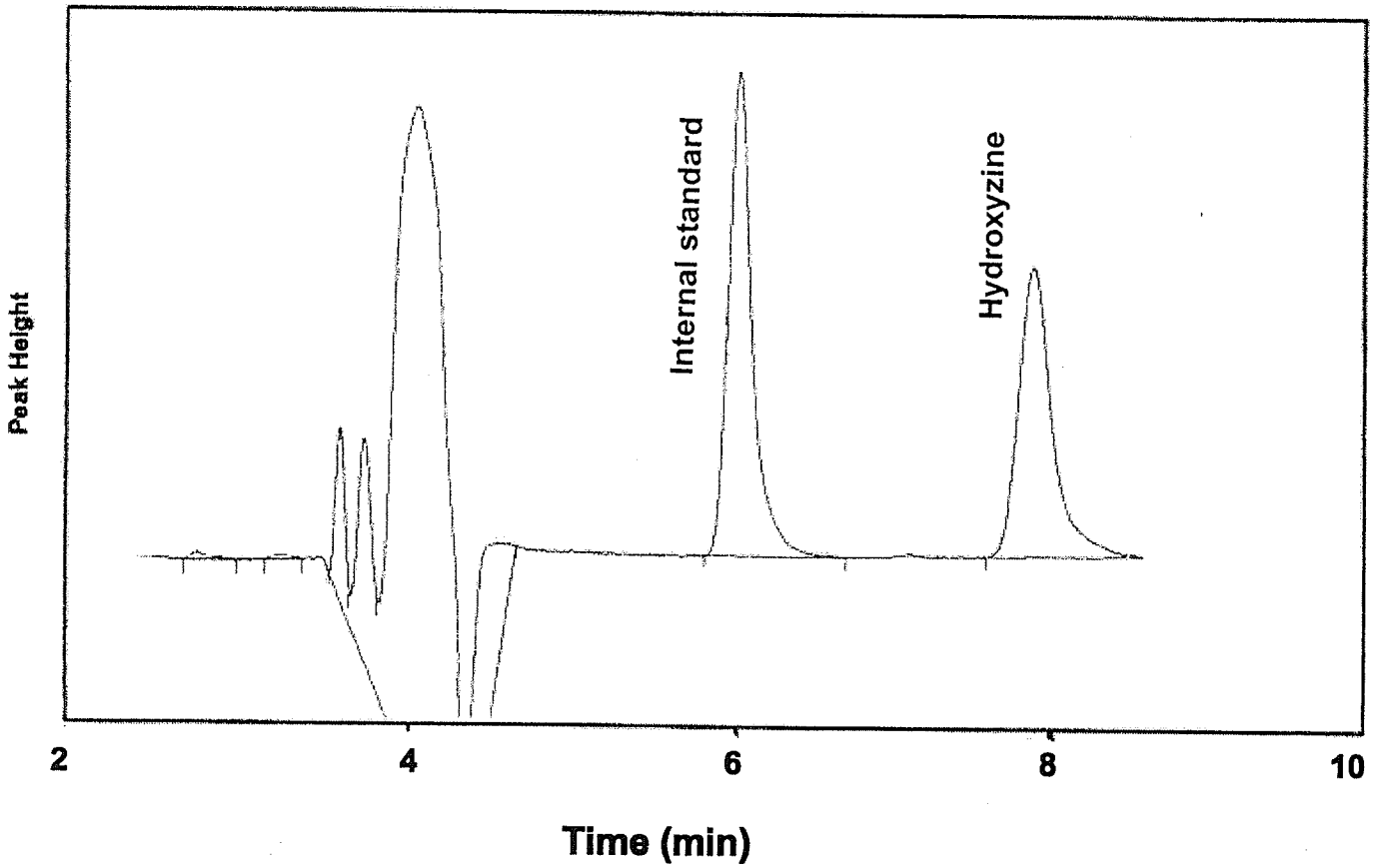

Figure 2: HPLC Chromatogram of Cetirizine

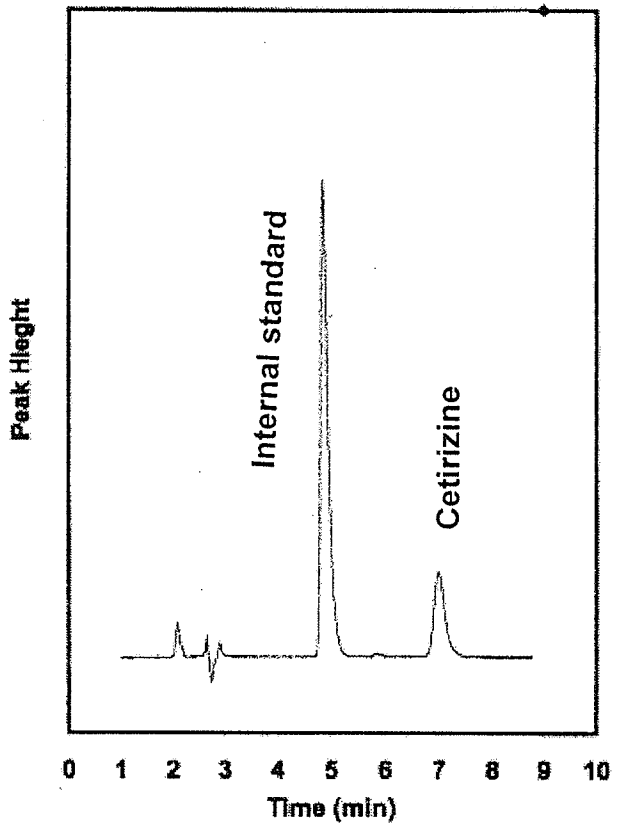

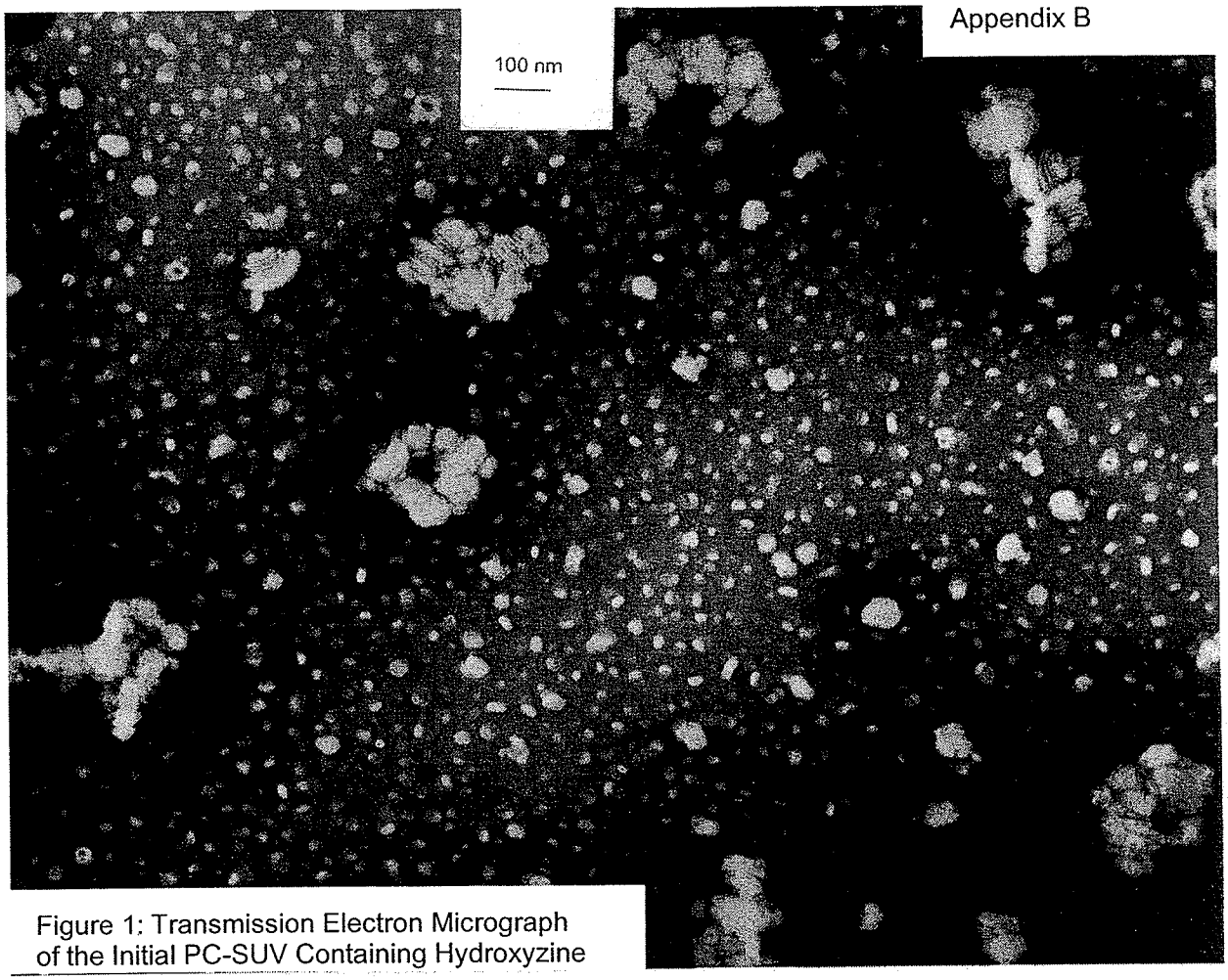

Figure 1: Transmission Electron Micrograph of the Initial PC-SUV Containing Hydroxyzine

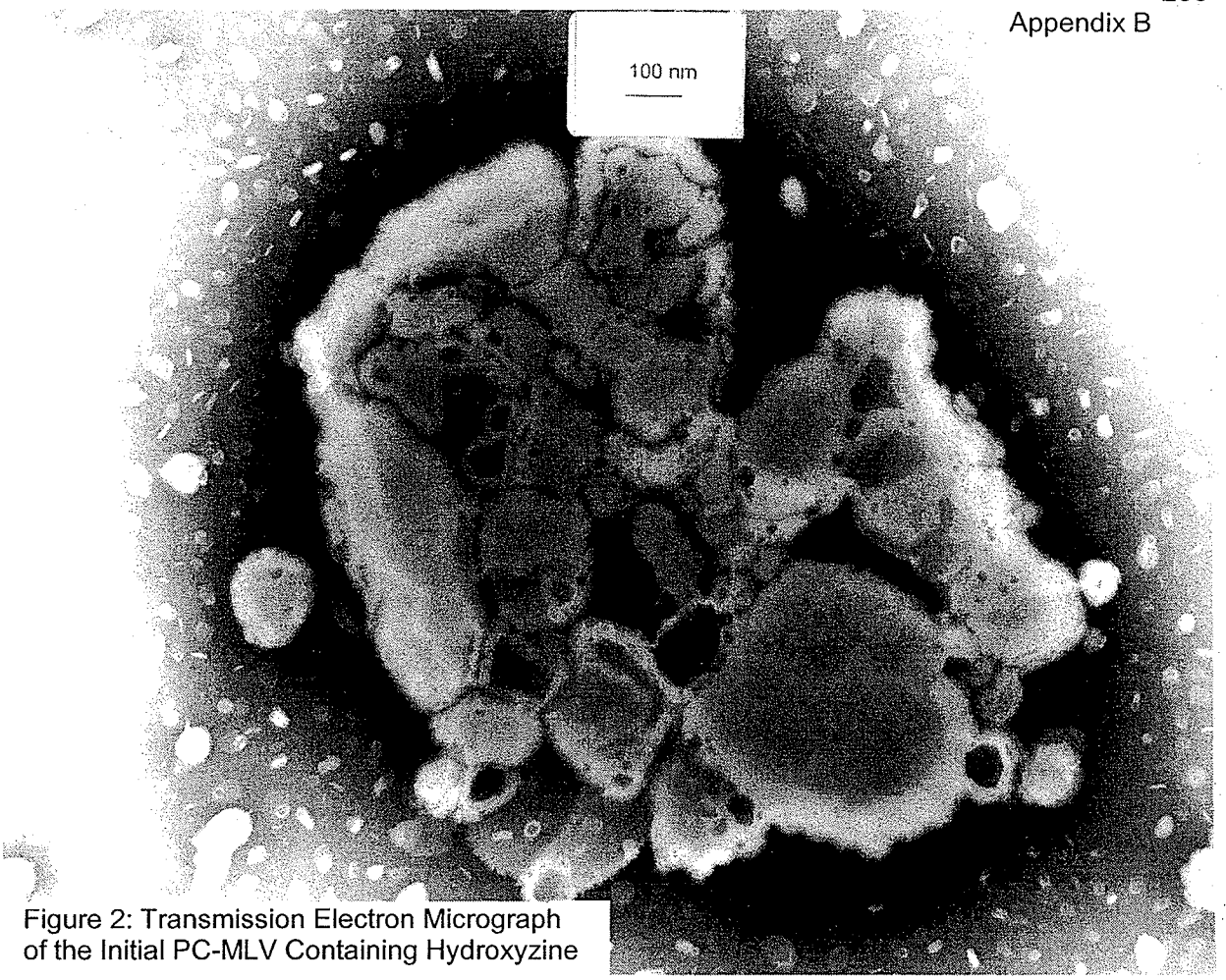

Figure 2: Transmission Electron Micrograph
of the Initial PC-MLV Containing Hydroxyzine

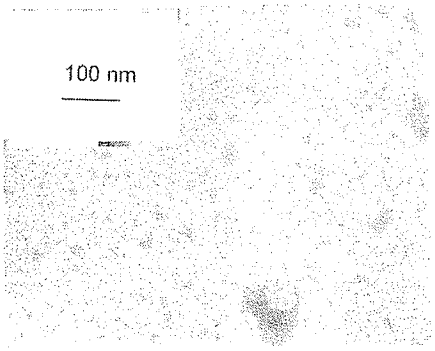

Figure 3: Transmission Electron Micrograph
of the Initial HPC-SUV Containing Hydroxyzine

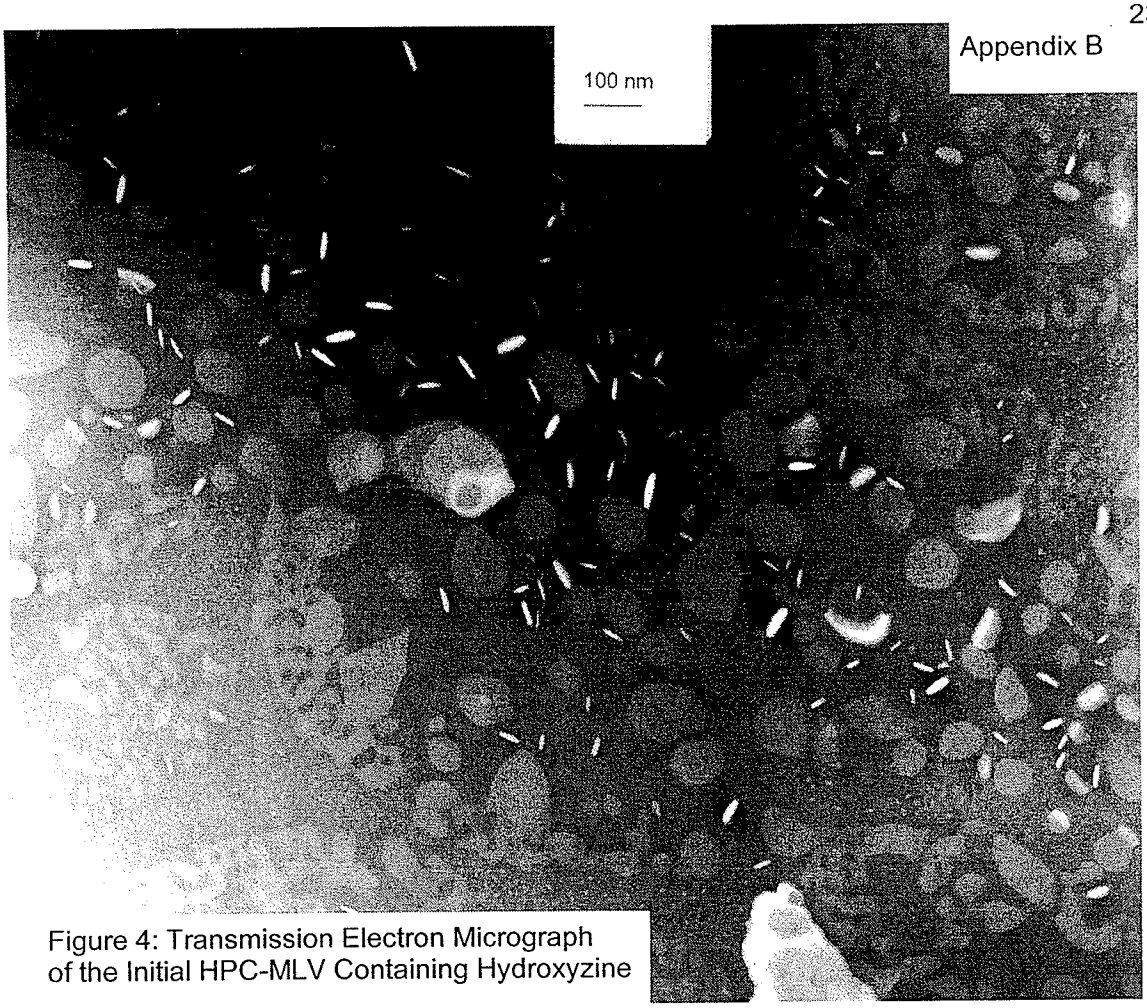

Figure 4: Transmission Electron Micrograph
of the Initial HPC-MLV Containing Hydroxyzine

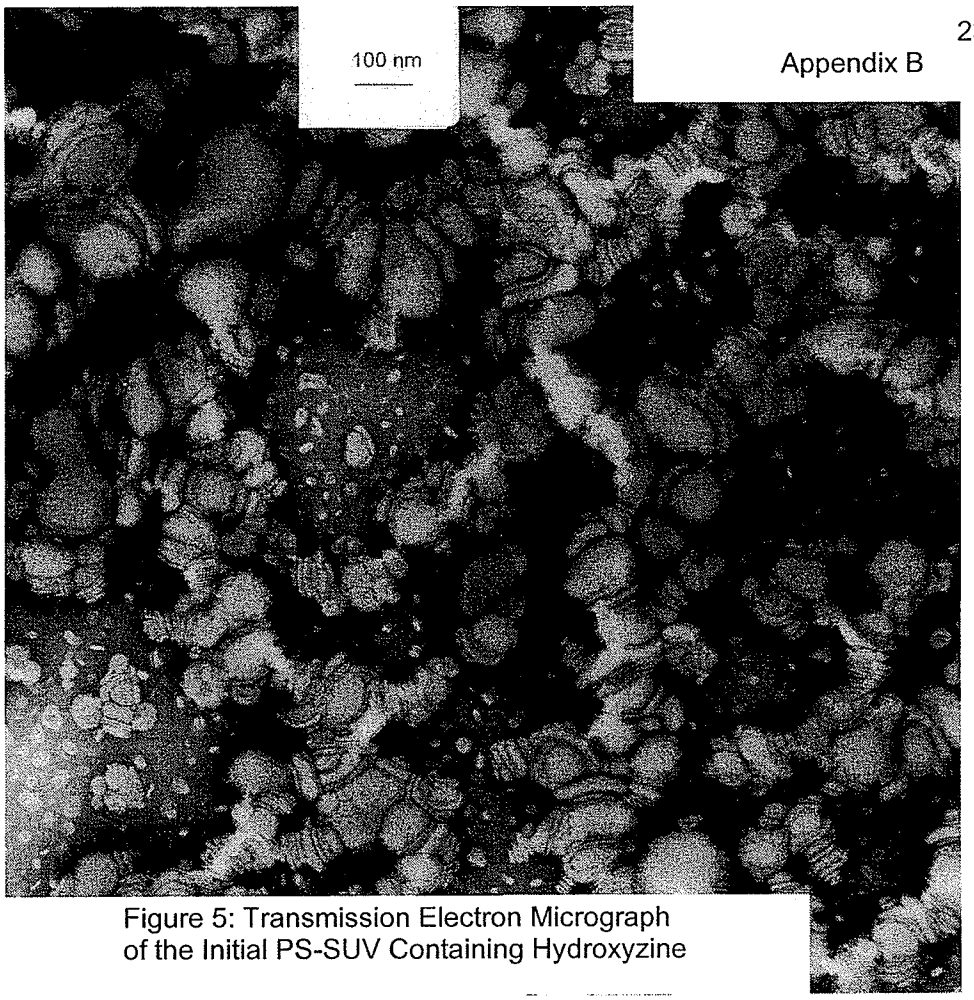

Figure 5: Transmission Electron Micrograph
of the Initial PS-SUV Containing Hydroxyzine

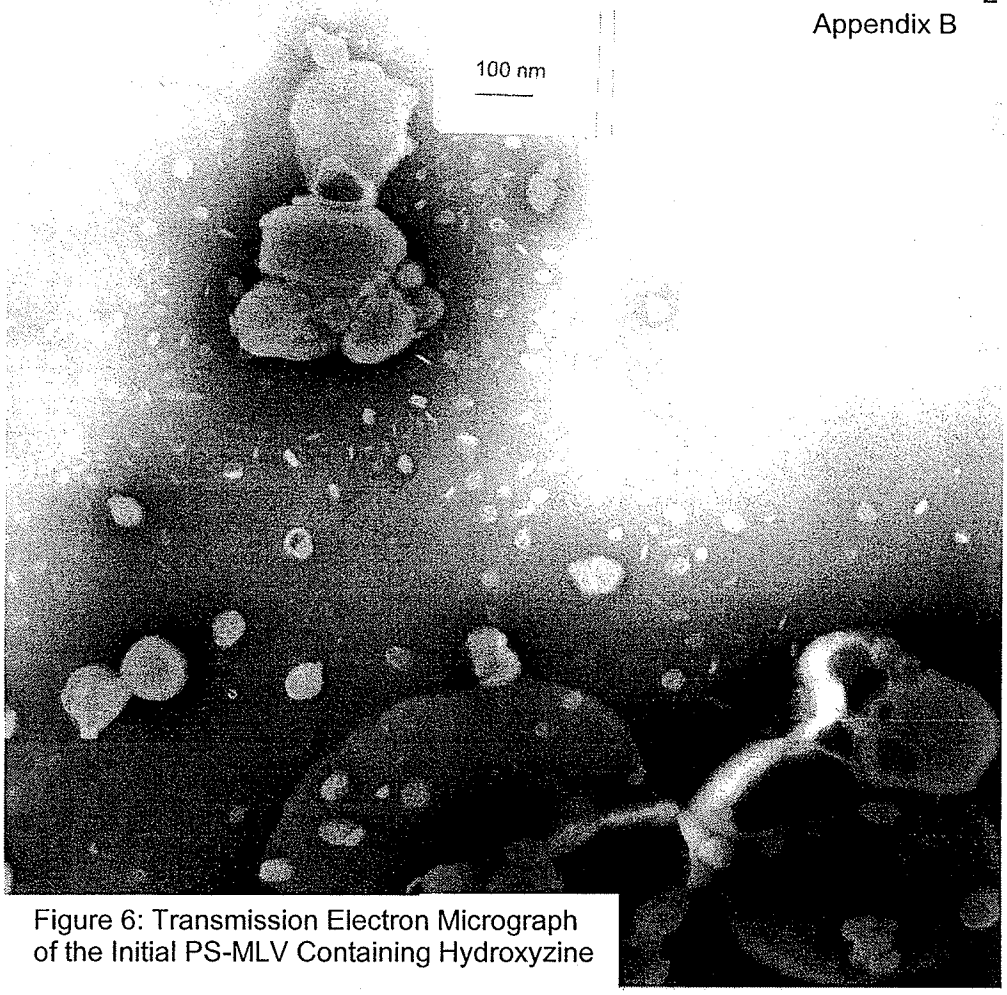

Figure 6: Transmission Electron Micrograph of the Initial PS-MLV Containing Hydroxyzine

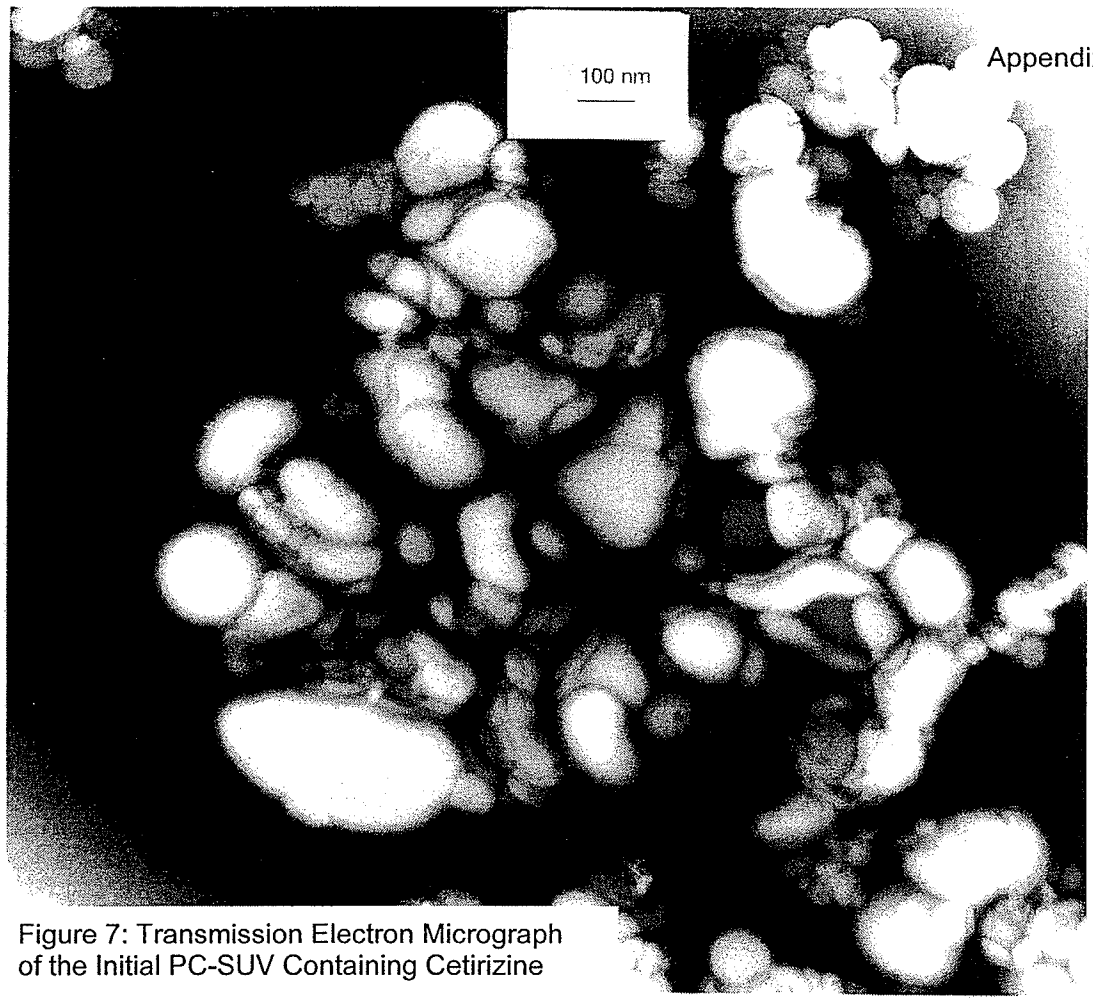

Figure 7: Transmission Electron Micrograph of the Initial PC-SUV Containing Cetirizine

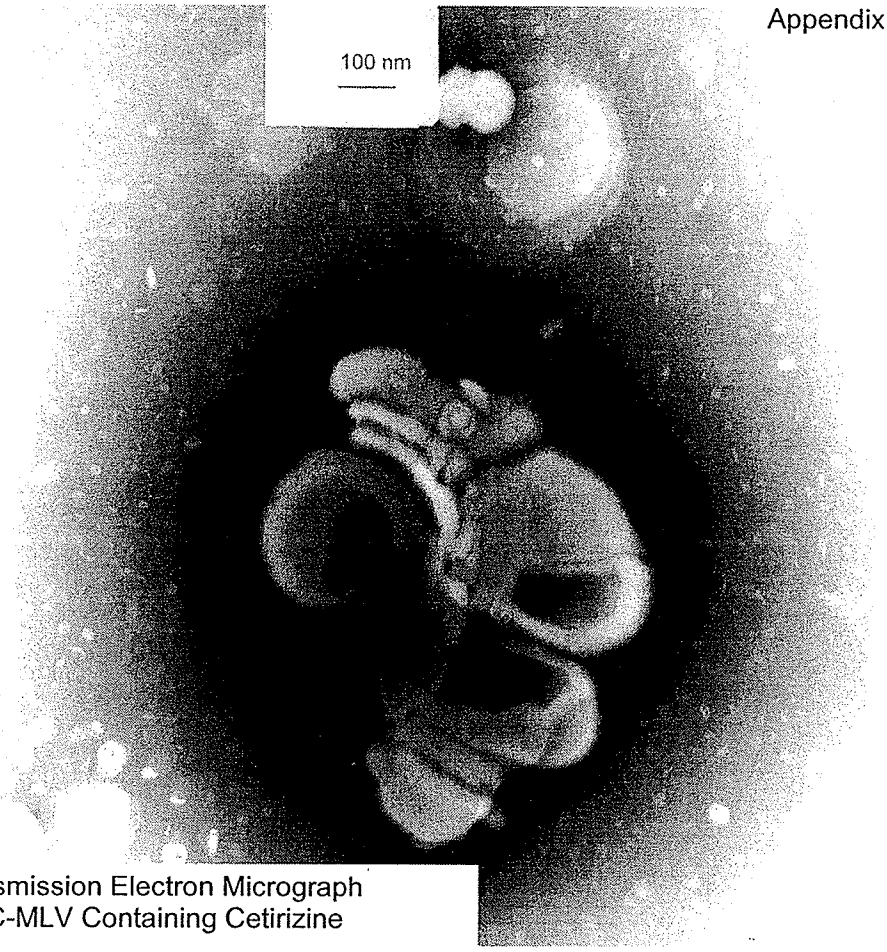

Figure 8: Transmission Electron Micrograph
of the Initial PC-MLV Containing Cetirizine

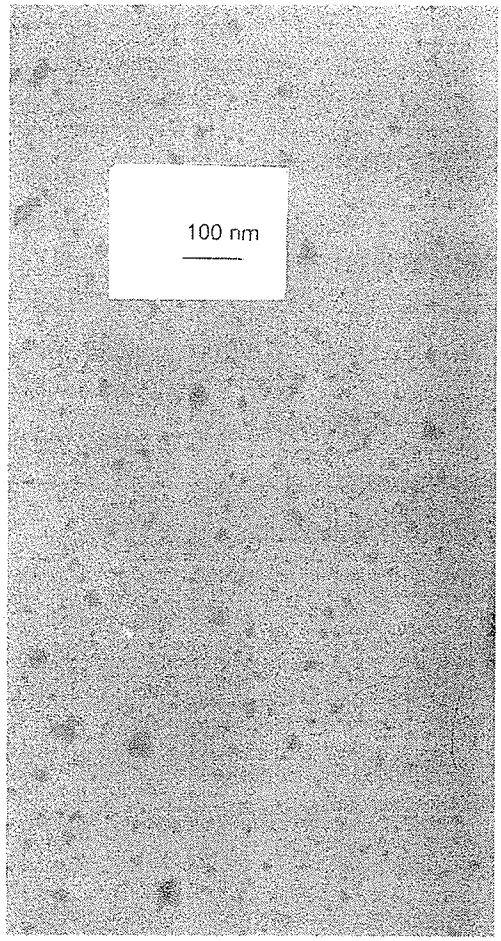

Figure 9: Transmission Electron Micrograph of the Initial HPC-SUV Containing Cetirizine

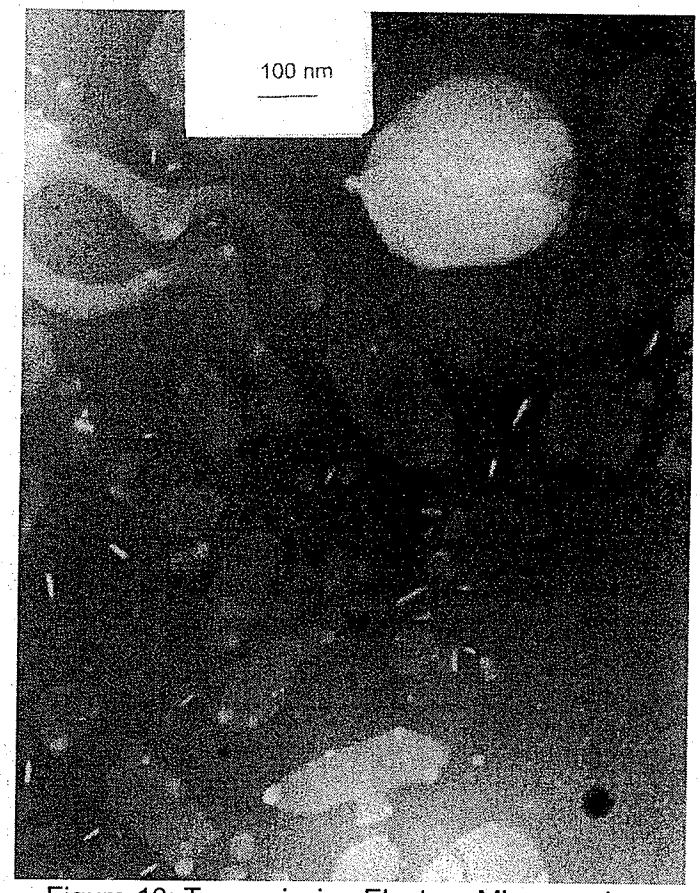

Figure 10: Transmission Electron Micrograph
of the Initial HPC-MLV Containing Cetirizine

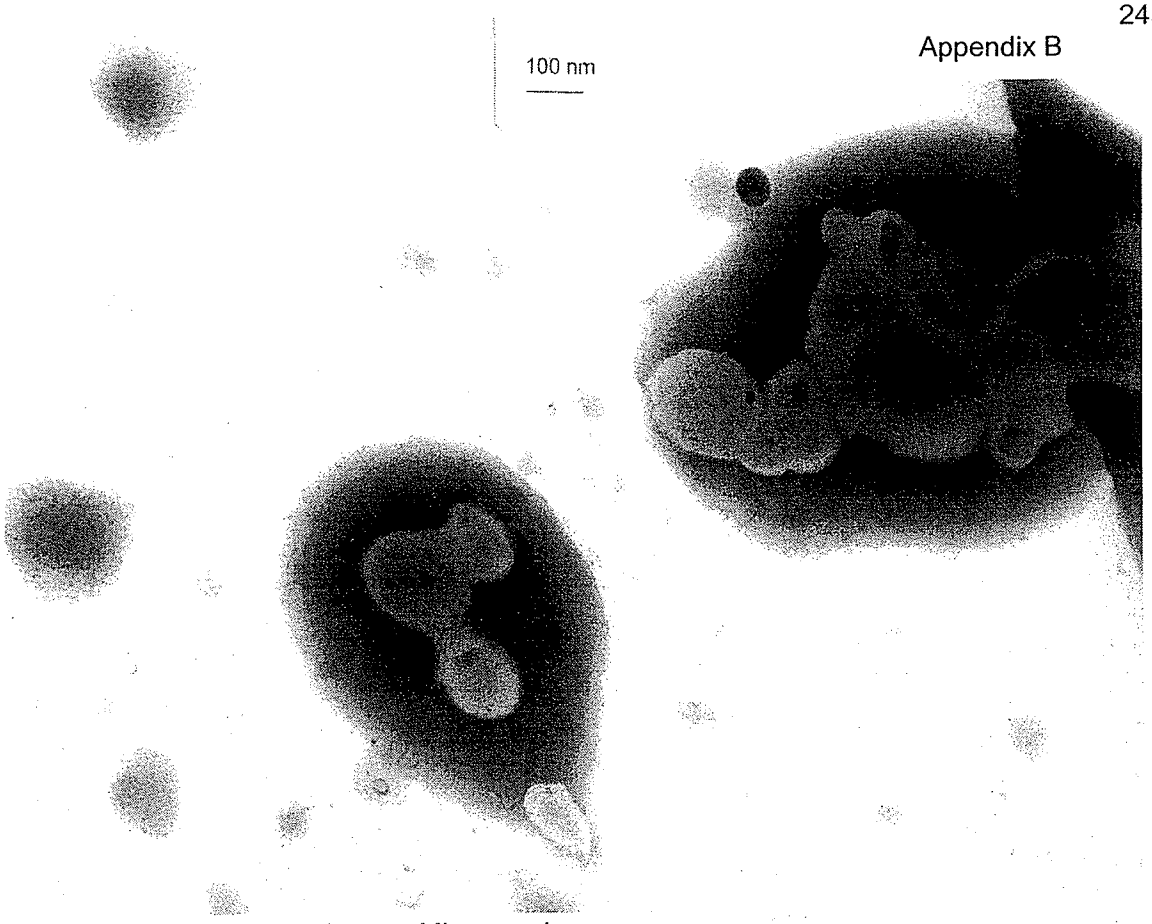

Figure 11: Transmission Electron Micrograph
of the Initial PS-SUV Containing Cetirizine

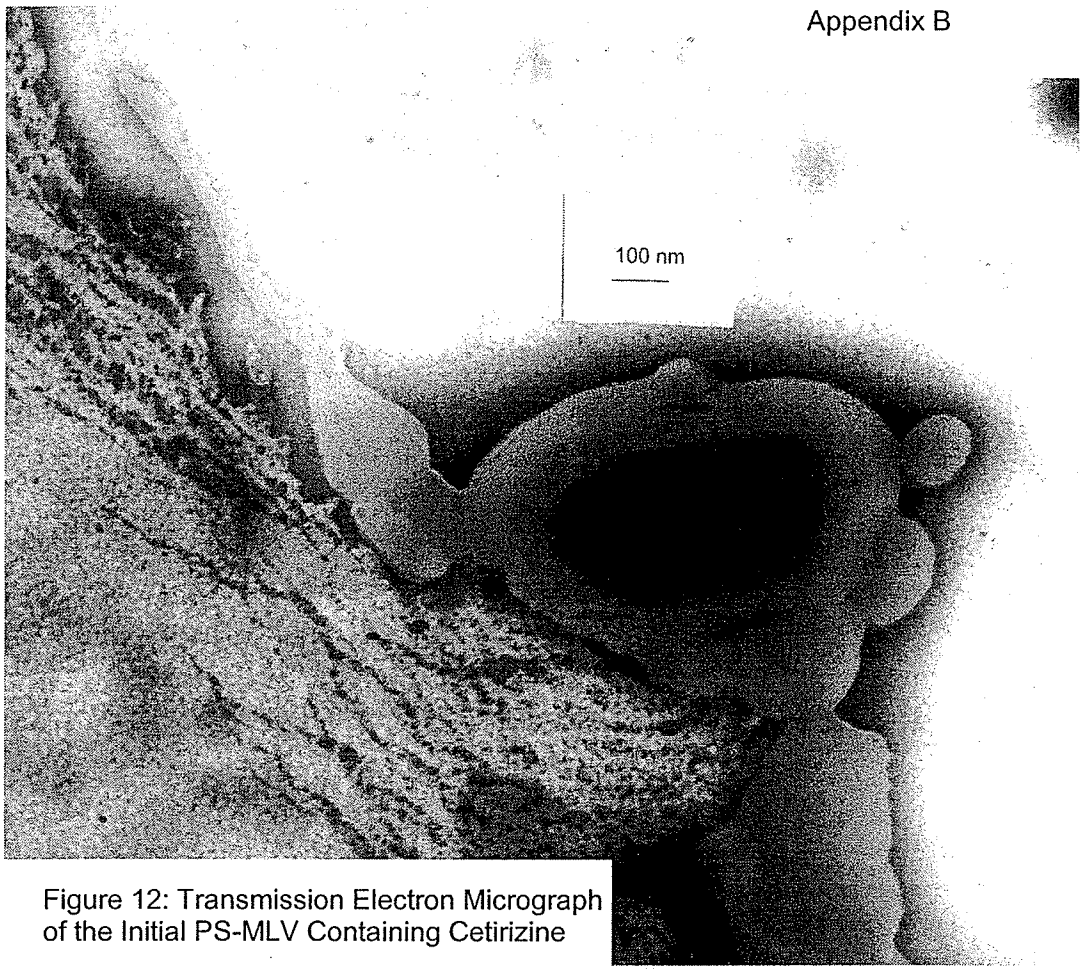

Figure 12: Transmission Electron Micrograph of the Initial PS-MLV Containing Cetirizine

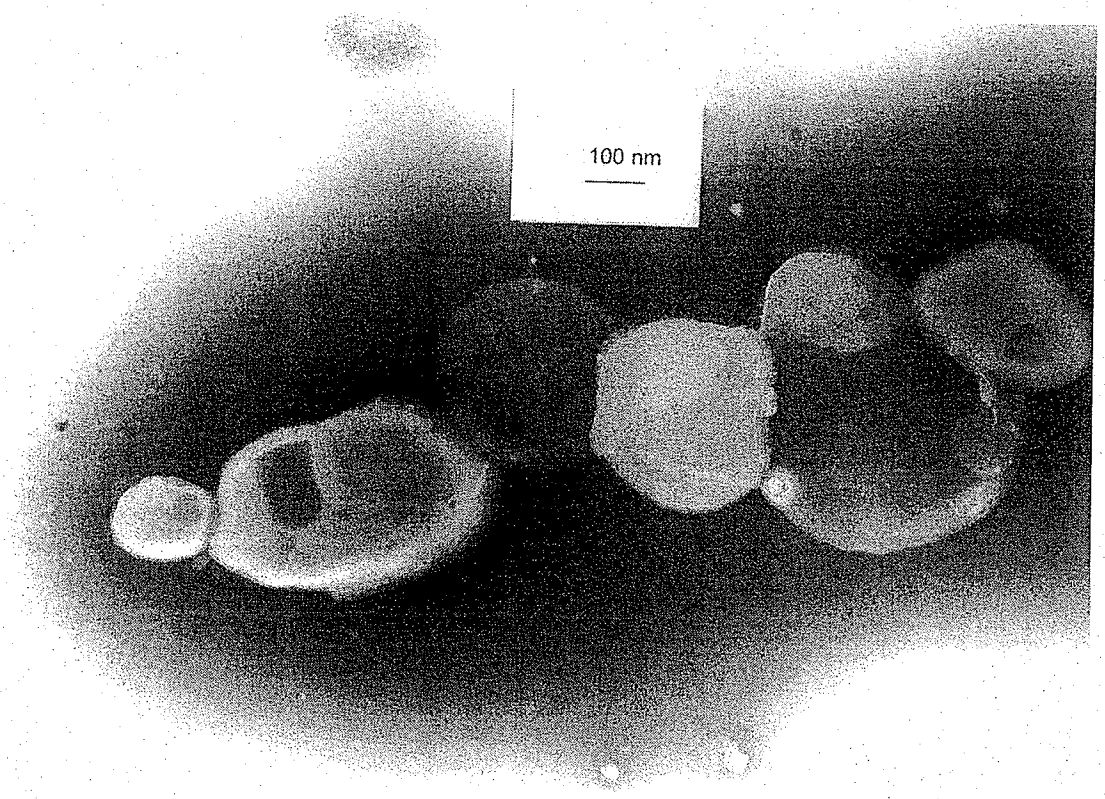

Figure 13: Transmission Electron Micrograph of HPC-MLV Containing Cetirizine Stored at 10C for 12 Months

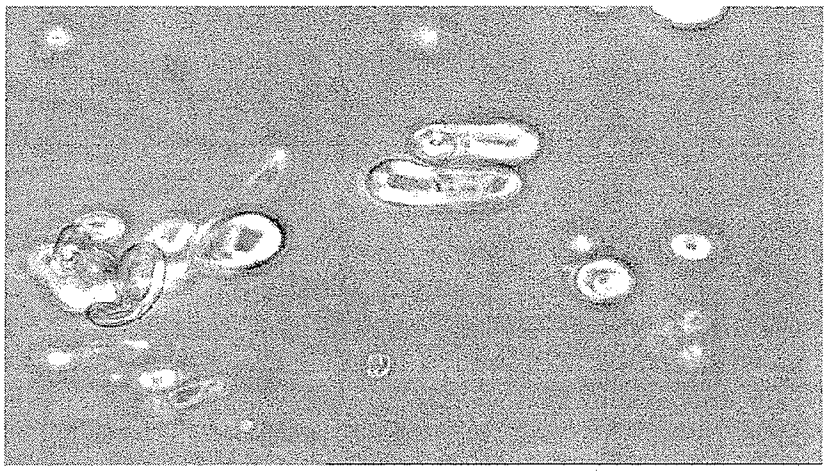

Figure 14: Micrograph from Optical Microscope of HPC-MLV Containing Hydroxyzine Stored at 10°C for 12 Months. (834.0 ± 30.2 nm)

Appendix C

Figure 1: Particle Size Distribution of Initial PC-SUV Containing Hydroxyzine Determined by Submicron Particle Sizer

VOLUME-Weighted GAUSSIAN DISTRIBUTION Analysis (Vesicle)

GAUSSIAN SUMMARY:

Mean Diameter	= 263.6 nm	Chi Squared	= 359734.250
Stnd. Deviation	= 196.1 nm (74.4 %)	Baseline Adj.	= 1.104 %
Coeff. of Var'n	= 0.744	Mean Diff. Coeff.	= 1.76E-008 cm2/s

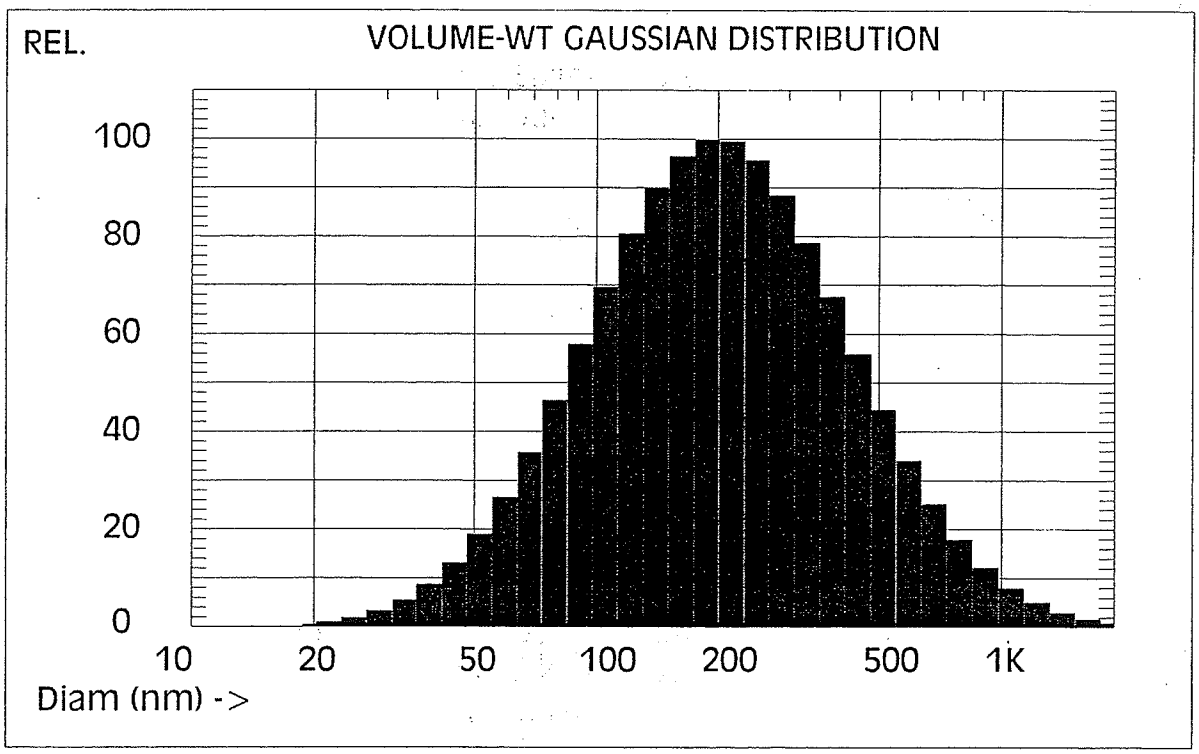

Cumulative Result:

25 % of distribution < 112.5 nm
50 % of distribution < 185.9 nm
75 % of distribution < 307.3 nm
90 % of distribution < 482.2 nm
99 % of distribution < 1024.1 nm

Run Time	= 0 Hr 40 Min 47 Sec	Wavelength	= 632.8 nm
Count Rate	= 187 KHz	Temperature	= 23 deg C
Channel #1	= 7840.8 K	Viscosity	= 0.933 cp
Channel Width	= 25.0 uSec	Index of Ref.	= 1.333

Appendix C

Figure 2: Particle Size Distribution of Initial PC-MLV Containing Hydroxyzine Determined by Submicron Particle Sizer

VOLUME-Weighted NICOMP DISTRIBUTION Analysis (Vesicle)

NICOMP SUMMARY:

Peak #1: Mean Diam.= 329.3 nm, S.Dev.= 39.3 nm (11.9%) Vol= 8.3 %
Peak #2: Mean Diam.= 4870.3 nm, S.Dev.= 648.0 nm (13.3%) Vol= 91.7 %

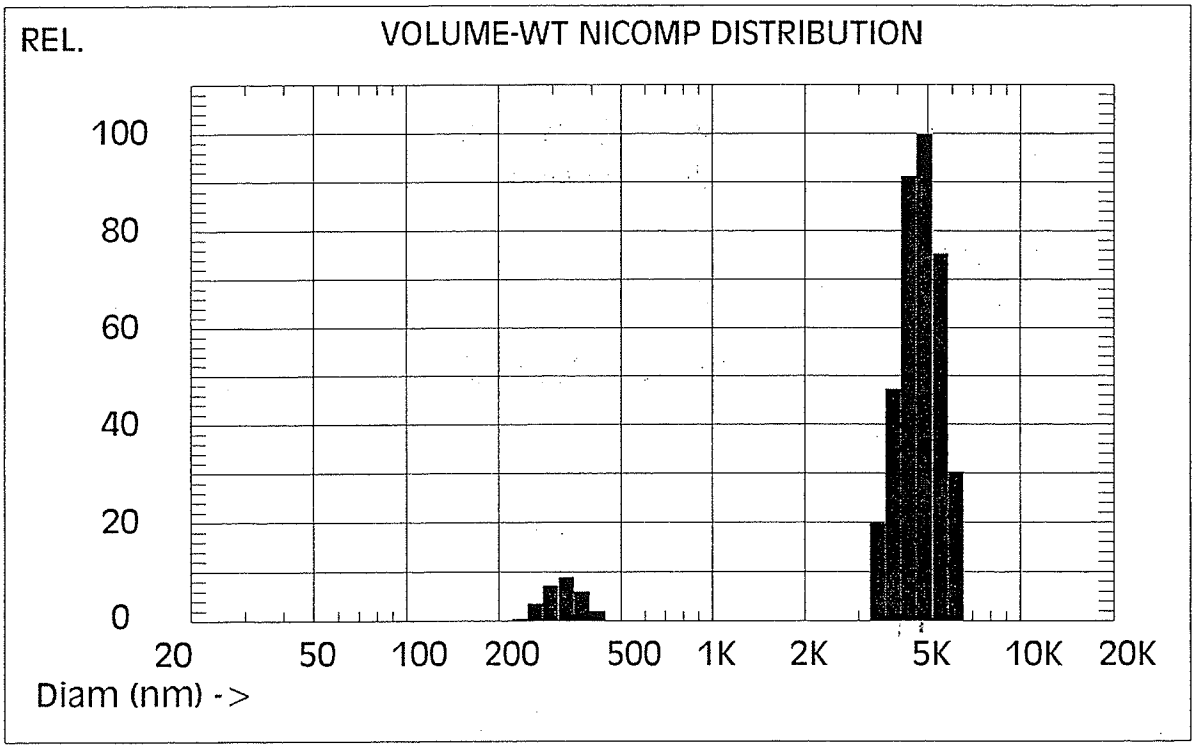

Mean Diameter = 4467.9 nm Fit Error = 108.703 Residual = 0.000

NICOMP SCALE PARAMETERS:

Min. Diam. = 20 nm Plot Size = 60
Smoothing = 3 Plot Range = 1000

GAUSSIAN SUMMARY:

Mean Diameter = 1721.9 nm Chi Squared = 75798.852
Stnd. Deviation = 1121.0 nm (65.1 %) Baseline Adj. = 0.978 %
Coeff. of Var'n = 0.651 Mean Diff. Coeff. = 2.70E-009 cm2/s

Run Time = 0 Hr 37 Min 44 Sec Wavelength = 632.8 nm
Count Rate = 214 KHz Temperature = 23 deg C
Channel #1 = 7259.1 K Viscosity = 0.933 cp
Channel Width = 250.0 uSec Index of Ref. = 1.333

Appendix C

Figure 3: Particle Size Distribution of Initial HPC-SUV Containing Hydroxyzine Determined by Submicron Particle Sizer

VOLUME-Weighted NICOMP DISTRIBUTION Analysis (Vesicle)

NICOMP SUMMARY:

Peak #1: Mean Diam.= 61.4 nm, S.Dev.= 7.4 nm (12.0%) Vol= 0.2 %
Peak #2: Mean Diam.= 276.9 nm, S.Dev.= 33.2 nm (12.0%) Vol= 1.8 %
Peak #3: Mean Diam.= 2584.5 nm, S.Dev.= 367.9 nm (14.2%) Vol= 98.0 %

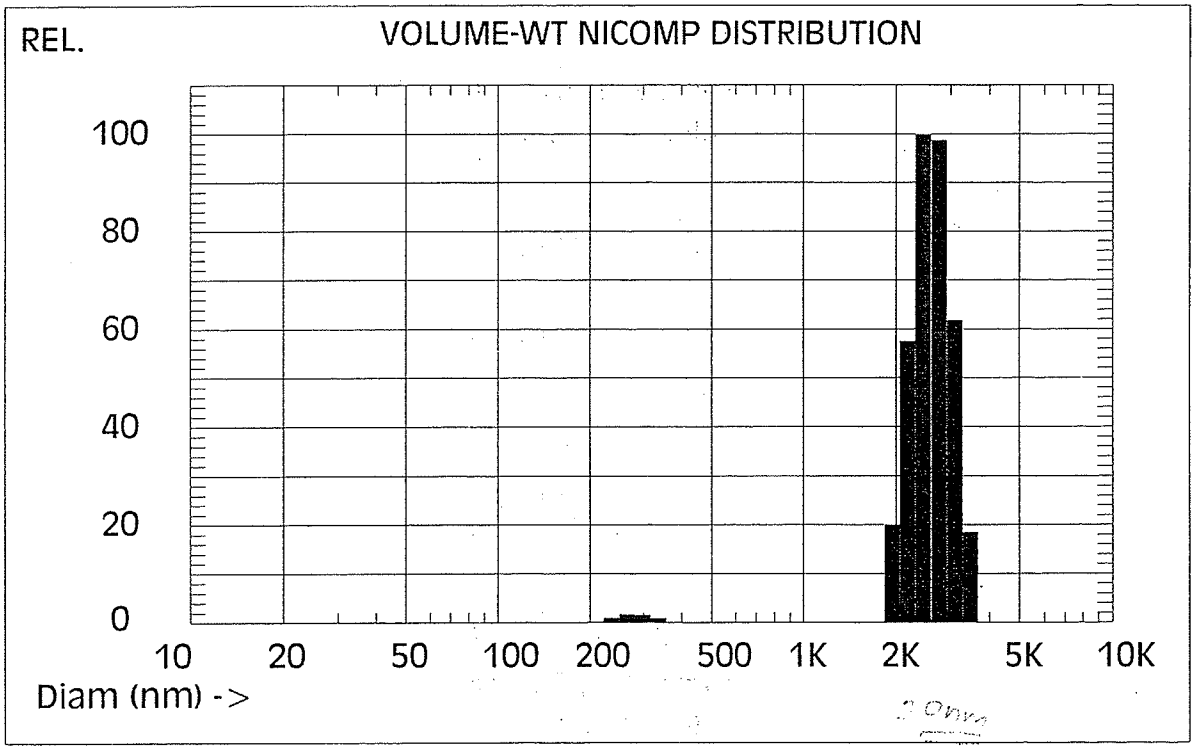

Mean Diameter = 2591.7 nm Fit Error = 7.702 Residual = 0.000

NICOMP SCALE PARAMETERS:

Min. Diam. = 10 nm Plot Size = 60
Smoothing = 3 Plot Range = 1000

GAUSSIAN SUMMARY:

Mean Diameter = 2716.7 nm Chi Squared = 7959.390
Stnd. Deviation = 2119.0 nm (78.0 %) Baseline Adj. = 0.000 %
Coeff. of Var'n = 0.780 Mean Diff. Coeff. = 1.71E-009 cm2/

Run Time	= 0 Hr 35 Min 10 Sec		Wavelength	= 632.8	nm
Count Rate	= 168	KHz	Temperature	= 23	deg C
Channel #1	= 7160.4	K	Viscosity	= 0.933	cp
Channel Width	= 120.0	uSec	Index of Ref.	= 1.333	

Appendix C

Figure 4: Particle Size Distribution of Initial HPC-MLV Containing Hydroxyzine Determined by Submicron Particle Sizer

VOLUME-Weighted NICOMP DISTRIBUTION Analysis (Vesicle)

NICOMP SUMMARY:

Peak #1: Mean Diam.= 116.0 nm, S.Dev.= 11.2 nm (9.6%) Vol= 5.0 %

Peak #2: Mean Diam.= 9463.9 nm, S.Dev.= 959.5 nm (10.1%) Vol= 95.0 %

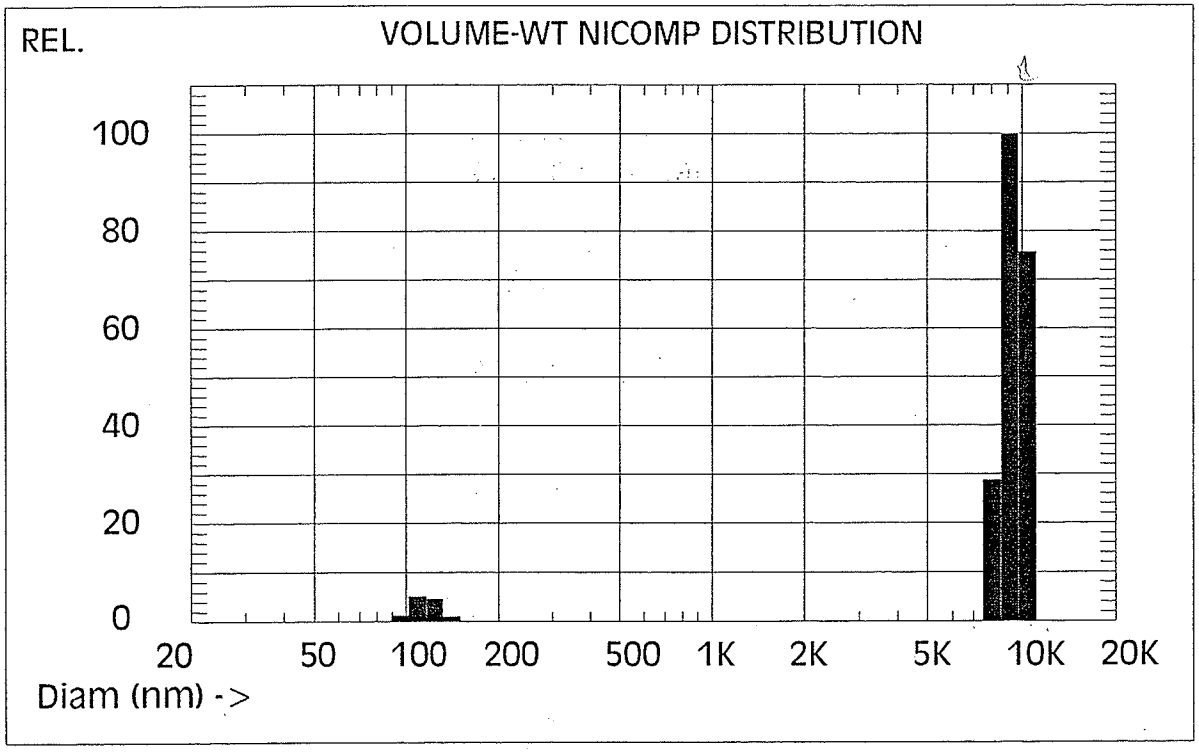

Sample

Mean Diameter = 8934.1 nm Fit Error = 288.552 Residual = 0.000

NICOMP SCALE PARAMETERS:

Min. Diam. = 20 nm Plot Size = 54

Smoothing = 2 Plot Range = 1000

GAUSSIAN SUMMARY:

Mean Diameter = 3221.7 nm Chi Squared = 17454.721

Stnd. Deviation = 2728.8 nm (84.7 %) Baseline Adj. = 0.000 %

Coeff. of Var'n = 0.847 Mean Diff. Coeff. = 1.44E-009 cm2/

Run Time	= 0 Hr 6 Min 33 Sec		Wavelength	= 632.8	nm
Count Rate	= 238	KHz	Temperature	= 23	deg C
Channel #1	= 810.1	K	Viscosity	= 0.933	cp
Channel Width	= 250.0	uSec	Index of Ref.	= 1.333	

Appendix C

Figure 5: Particle Size Distribution of Initial PS-SUV Containing Hydroxyzine Determined by Submicron Particle Sizer

VOLUME-Weighted GAUSSIAN DISTRIBUTION Analysis (Vesicle)

GAUSSIAN SUMMARY:

Mean Diameter	= 134.4 nm	Chi Squared	= 70.952
Stnd. Deviation	= 60.7 nm (45.2 %)	Baseline Adj.	= 0.000 %
Coeff. of Var'n	= 0.452	Mean Diff. Coeff.	= 3.46E-008 cm2

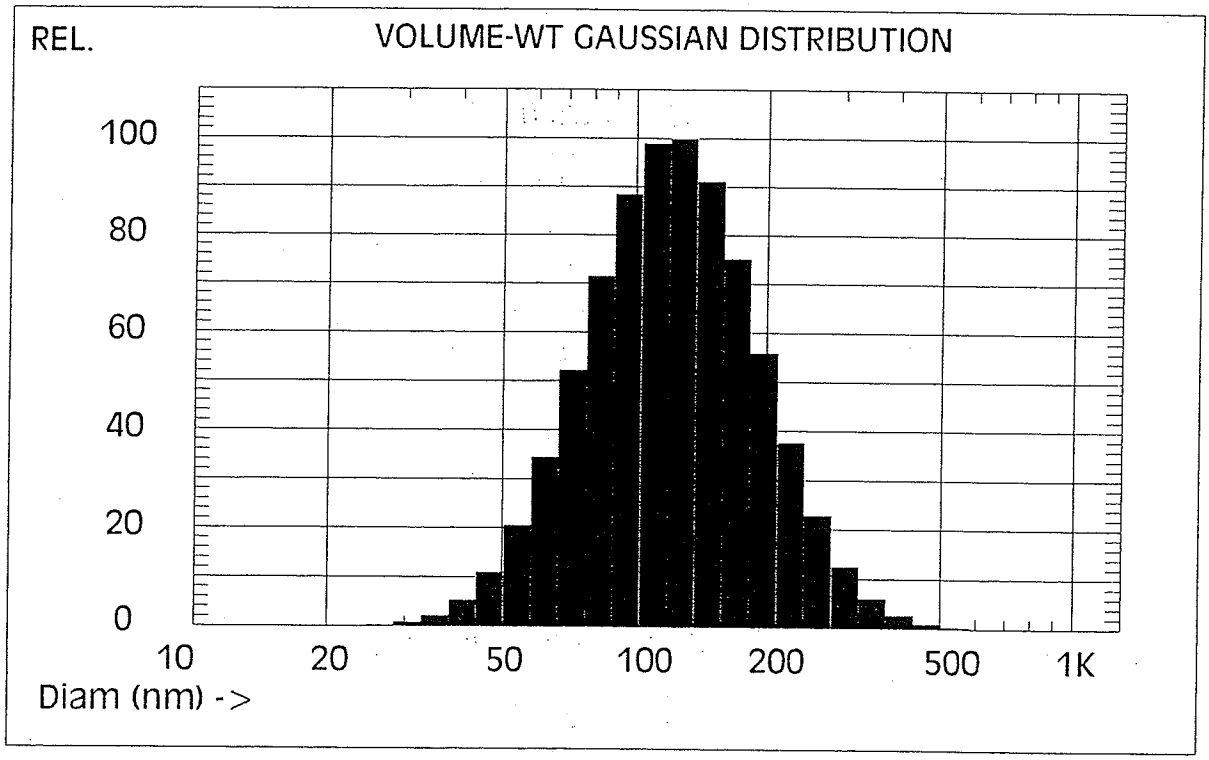

Cumulative Result:

25 % of distribution <	83.3 nm
50 % of distribution <	112.9 nm
75 % of distribution <	153.3 nm
90 % of distribution <	201.4 nm
99 % of distribution <	324.4 nm

Run Time	= 0 Hr 20 Min 34 Sec	Wavelength	= 632.8 nm
Count Rate	= 275 KHz	Temperature	= 23 deg C
Channel #1	= 1230.5 K	Viscosity	= 0.933 cp
Channel Width	= 15.0 uSec	Index of Ref.	= 1.333

Appendix C

Figure 6: Particle Size Distribution of Initial PS-MLV Containing Hydroxyzine Determined by Submicron Particle Sizer

VOLUME-Weighted NICOMP DISTRIBUTION Analysis (Vesicle)

NICOMP SUMMARY:

Peak #1: Mean Diam.= 499.0 nm, S.Dev.= 55.0 nm (11.0%) Vol= 13.7 %
Peak #2: Mean Diam.= 5969.1 nm, S.Dev.= 600.3 nm (10.1%) Vol= 86.3 %

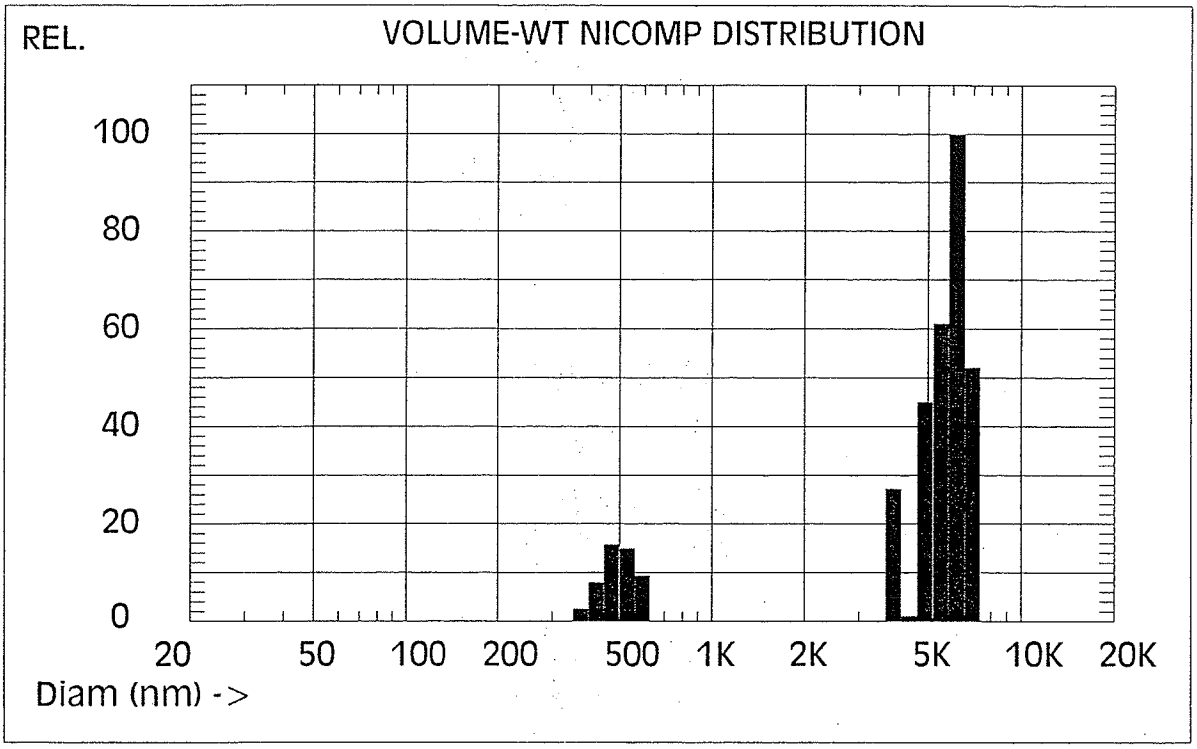

Mean Diameter = 4972.1 nm Fit Error = 98.295 Residual = 0.000

NICOMP SCALE PARAMETERS:

Min. Diam. = 20 nm Plot Size = 60
Smoothing = 3 Plot Range = 1000

GAUSSIAN SUMMARY:

Mean Diameter = 1065.6 nm Chi Squared = 2727.216
Stnd. Deviation = 628.7 nm (59.0 %) Baseline Adj. = 0.357 %
Coeff. of Var'n = 0.590 Mean Diff. Coeff. = 4.36E-009 cm2/

Run Time = 0 Hr 16 Min 54 Sec Wavelength = 632.8 nm
Count Rate = 200 KHz Temperature = 23 deg C
Channel #1 = 2992.8 K Viscosity = 0.933 cp
Channel Width = 160.0 uSec Index of Ref. = 1.333